

**Effect of polyphenols on sugar transport by human GLUT2,
GLUT5 and GLUT7**

Julia Sandrin Gauer

Submitted in accordance with the requirements for the degree of Doctor of
Philosophy

The University of Leeds
School of Food Science and Nutrition

August 2017

The candidate confirms that the work submitted is her own and that appropriate credit has been given where reference has been made to the work of others.

This copy has been supplied on the understanding that it is copyright material and that no quotation from the thesis may be published without proper acknowledgement.

The right of Julia Sandrin Gauer to be identified as Author of this work has been asserted by her in accordance with the Copyright, Designs and Patents Act 1988.

© 2017 The University of Leeds and Julia Sandrin Gauer

The contribution of the candidate and the other authors to this work has been explicitly indicated below. The candidate confirms that appropriate credit has been given within the thesis where reference has been made to the work of others. Further details of the work from jointly authored publications/submitted manuscripts and the contributions of the candidate and the other authors to the work are included below.

Chapters 3 and 4 contains work which has also been used in the publication

Jose Villa-Rodriguez, Ebru Aydin, Julia S. Gauer, Alison Pyner, Gary Williamson, and Asimina Kerimi (2017). Green and chamomile teas, but not acarbose, attenuate glucose and fructose transport via inhibition of GLUT2 and GLUT5. *Accepted by the Journal of Molecular Nutrition & Food Research (2017)*

Asimina Kerimi, Hilda Nyambe, Alison Pyner, Ebum Oladele, Julia S. Gauer, Yala Stevens and Gary Williamson (2017). Blunting post-prandial glucose spikes by oleuropein is through inhibition of sucrose hydrolysis and of sugar transport. *Submitted to the European Journal of Nutrition (2017)*

Chapter 4 contains work which has also been used in the publication

Asimina Kerimi, Hilda Nyambe-Silavwe, Julia S. Gauer, Francisco A. Tomás-Barberán, and Gary Williamson (2017). Pomegranate juice, but not an extract, confers a lower glyceemic response on a high GI food: randomized, crossover, controller trials in healthy subjects. *Accepted by the American Journal of Clinical Nutrition (2017)*

Chapters 3-6 contains work which has also been used in the publication

Julia S. Gauer, Samantha Gardner, Sarka Tumova, Asimina Kerimi, Jonathan Lippiat, and Gary Williamson (2017). Differential patterns of inhibition of the sugar transporters GLUT2, GLUT5 and GLUT7 by flavonoids. *Manuscript in preparation; planned submission to Biochemical Pharmacology*

Conference abstracts

A. Kerimi, J. S. Gauer and G. Williamson (2017). Effect of orange juice and its constituents on intestinal glucose and fructose transport through GLUT2 and GLUT5.

International Conference on Polyphenols and Health (ICPH) 2017 – Quebec, Canada

J. S. Gauer, J. Lippiat, A. Kerimi, S. Tumova, S. Gardner, L. McKeown, G. Williamson (2017). Effect of polyphenols on sugar transport by GLUT2, GLUT5 and GLUT7.

Experimental Biology – Chicago, USA

Selected as a finalist for ASN's Emerging Leaders in Nutrition Science Poster Competition.

J. S. Gauer, J. Lippiat, A. Kerimi, S. Tumova, S. Gardner, L. McKeown, G. Williamson (2016). Effect of (poly)phenols on fructose transport by GLUT transporters.

Food Bioactives and Health Conference – Norwich, UK

J. S. Gauer, J. Lippiat, A. Kerimi, S. Tumova, S. Gardner, L. McKeown, G. Williamson (2015). The effects of polyphenols on fructose transport by GLUT5.

2nd PhD Student Conference – Leeds, UK

J. S. Gauer, J. Lippiat, A. Kerimi, S. Tumova, S. Gardner, L. McKeown, G. Williamson. (2015). The effects of polyphenols on fructose transport by GLUT5.

International Conference on Polyphenols and Health (ICPH) – Tours, France

J. S. Gauer, J. Lippiat, A. Kerimi, S. Tumova, L. McKeown, G. Williamson (2014). The chronic effects of dietary polyphenols on fructose absorption by GLUT5.

1st PhD Student Conference – Leeds, UK

J. S. Gauer, J. Lippiat, A. Kerimi, S. Tumova, L. McKeown, G. Williamson (2014). The chronic effects of dietary polyphenols on fructose absorption by GLUT5.

INFOGEST PhD Training School "Food Digestion and Human Health"–
Budapest, Hungary

Acknowledgements

First and foremost, my sincere gratitude to my supervisor Professor Gary Williamson, for giving me the opportunity to conduct this research, sharing his expertise, and for always taking the time to help me whenever I needed. Your guidance throughout this process has been crucial.

Thanks to Dr. Lynn McKeown for helping me from the very beginning with the plasmid constructs and for the continuous supply of invaluable advice over the years. Also, many thanks to Dr. Jonathan Lippiat, who kindly welcomed me into his laboratory and allowed me to use the microinjector for my experiments throughout the whole duration of my project.

A most heartfelt thank you to my amazing post-docs Dr. Asimina Kerimi and Dr. Sarka Tumova, for their patience, kindness, optimism and many delicious baked goods. You both have always selflessly allocated time to help me. I am immensely appreciative of all your technical assistance with conducting this project, and for your personal contribution to my achievements.

Special thanks to Dr. Samantha Gardner for assisting me in tackling all the hurdles encountered with the molecular biology techniques, and for being a great rowing coach. My gratefulness to Dr. Laszlo Abranko for his support with the HPLC and delightful tales of his lovely daughter's mischiefs. Many thanks to Dr. Aleksandra Konic Ristic for all the insightful conversations, and for all her kindness and cheerfulness. My gratitude to all FS&N members of staff for their willingness to help.

Thank you to my dear friends and fellow PhD students, Michael, Ali, Pepe, Hilda, Idolo, Yuanlu, Heidi and Evelien. All the good times we had together outweigh the hard times. Many thanks, also, to my charming housemates Erin, Hollie, Neil and Arlo, for so kindly sharing their home with me and for always making me smile. I am so happy to have met you all and wish you nothing but happiness for the future. Special thanks to Chris, and all the other wonderful people and friends I have been so lucky to meet throughout this journey. Thanks to Andrea, Nico, and all other old friends for sticking by me.

Lastly, I would like to thank my incredible family for their consistent and unconditional support, both financially and emotionally. My eternal gratitude to my lovely sisters, Joana and Luane, and amazing parents, Laura and Hugo. The person I am, and all I have accomplished, is because of you.

Abstract

Background: High dietary sugar intake is controversially associated with an increase in prevalence of type 2 diabetes globally. This has been attributed to the impact that sugars have in the development of disease risk factors linked to diabetes, cardiovascular disease and others. (Poly)phenols present in our daily diet may affect these processes by multiple mechanisms, including effects on the digestion, uptake and post-prandial distribution of glucose and fructose.

Aim: Study the expression of GLUT7 in Caco-2/TC7 intestinal cells and identify novel inhibitors of sugar transporters by determining the direct impact of specific (poly)phenols and extracts on fructose and glucose uptake by GLUT2 and GLUT7 transporters, as well as their effect on sugar uptake by the fructose specific transporter GLUT5.

Methods: The Caco-2/TC7 cell model was used to investigate GLUT7 expression. For sugar transport studies, *X. laevis* oocytes were injected with the relevant transporter mRNA. After protein expression, oocytes were incubated in a ¹⁴C-glucose/fructose solution containing individual (poly)phenols and extracts. Automated capillary Western blotting (Wes) confirmed protein expression on oocyte membranes and uptake of internalised ¹⁴C-glucose/fructose was observed by liquid scintillation counting.

Results: The presence of fructose led to a significant increase in GLUT7 expression, as determined by mRNA (13% increase, $p \leq 0.001$) and protein (2.7-fold increase, $p \leq 0.05$) analysis of the Caco-2/TC7 cell model. GLUT5-mediated fructose transport was significantly inhibited by German chamomile extract (IC₅₀ of

0.73±0.18 mg/ml), sugar-free pomegranate extract (0.48 ± 0.22 mg/ml), apigenin (IC₅₀ = 40 ± 4 µM), (-)-epigallocatechin-gallate (EGCG) (IC₅₀= 72 ± 13 µM) and hesperidin (IC₅₀ = 264 ± 72 µM). GLUT2-mediated glucose transport was significantly inhibited by various compounds and extracts, including quercetin (IC₅₀ = 7 ± 1 µM), EGCG (IC₅₀ = 72 ± 13 µM) and apigenin (IC₅₀ = 27 ± 4 µM). These three compounds also significantly inhibited fructose transport by GLUT2; IC₅₀ = 8 ± 2 µM for quercetin, 93 ± 16 µM for EGCG and 28 ± 10 µM for apigenin. In addition, apigenin significantly decreased the uptake of both glucose (IC₅₀ = 38 ± 2 µM) and fructose (IC₅₀ = 16 ± 12 µM) by GLUT7.

Conclusions: The quantitative model used to investigate the molecular mechanism of GLUT2, GLUT5 and GLUT7 inhibition by specific (poly)phenols, achieved through over-expression of transporters in *X. laevis* oocytes, identified novel inhibitors for each of these individual transporters. In addition, apigenin was shown to be a potent inhibitor of sugar transport by all three GLUTs investigated. Moreover, fructose was shown to modulate expression of GLUT7 in the Caco-2/TC7 model. Further characterisation of the lesser known GLUT7, sharing 58% sequence similarity to GLUT5, will help highlight any role it may play in regulation of sugar uptake. Overall these results suggest that some of these compounds or extracts may have potential in interventions aimed at the control of post-prandial blood sugar levels in both healthy volunteers and diabetic patients.

Table of contents

Acknowledgements	i
Abstract	iii
Table of contents	v
List of tables	x
List of figures	xi
List of abbreviations	xv
Chapter 1 Introduction and research objectives	1
1.1 Overview	1
1.2 The health burden of diabetes mellitus and associated diseases.....	2
1.2.1 The role of glucose in the development of diabetes mellitus...3	
1.2.2 The role of fructose in the development of risk factors associated with diabetes mellitus	5
1.3 Sugar uptake by GLUTs	11
1.3.1 Sugar transport by GLUT2, GLUT5 and GLUT7	14
1.4 Overview of (poly)phenols	19
1.4.1 Bioavailability in humans	22
1.4.2 Attenuation of disease risk factors by (poly)phenol rich extracts and pure compounds	24
1.4.3 Effect of (poly)phenols on postprandial glycaemia	27
1.4.4 Effect of (poly)phenols on sugar uptake by GLUTs	29
1.5 Research models	31
1.5.1 Caco-2/TC7 intestinal cell model.....	31
1.5.2 <i>Xenopus laevis</i> oocytes	31
1.6 Research rationale, aims and objectives	34
1.6.1 Research rationale and purpose	34
1.6.2 Project aims	35
1.6.3 Project objectives	36
Chapter 2 General Methods	39
2.1 Extracts and pure compounds used in inhibition studies	39
2.1.1 Materials	39
2.1.2 Preparation of Eucalyptus Leaf Extract (ELE) by reflux extraction of eucalyptus leaves	43

2.1.3	Defatting of dark chocolate product for extract preparation ..	43
2.1.4	Preparation of dark chocolate extract	44
2.1.5	HPLC-FLD protocol for chocolate extract analysis	44
2.2	General methods applied to Caco-2 and Caco-2/TC7 cell model ..	46
2.2.1	Materials	46
2.2.2	Caco-2 and Caco-2/TC7 basic cell culturing	47
2.2.3	GLUT7 gene expression analysis	48
2.2.4	Immunofluorescence staining	50
2.2.5	Cell surface protein biotinylation	51
2.2.6	Protein analysis	53
2.2.7	Statistical analysis	54
2.3	Molecular biology	54
2.3.1	Materials	54
2.3.2	Propagation of pBF expression vector and human GLUT2, 5 and 7 gene containing vectors	57
2.3.3	Design of plasmid constructs by insertion of human GLUT genes into pBF expression vector	59
2.3.4	Confirmation of G7pGEM-HE plasmid sequence	63
2.3.5	Isolation of mRNA encoding hGLUT2, hGLUT5 and hGLUT7 genes	63
2.4	Microinjection of mRNA into oocytes and sugar uptake experiments	65
2.4.1	Materials	65
2.4.2	Preparation of <i>Xenopus laevis</i> oocytes for microinjection and expression of recombinant hGLUT2, hGLUT5 and hGLUT7	66
2.4.3	[¹⁴ C] Fructose uptake by GLUT5	68
2.4.4	[¹⁴ C] Fructose and [¹⁴ C] Glucose uptake by GLUT2	69
2.4.5	[¹⁴ C] Deoxy-D-glucose, [¹⁴ C] Fructose and [¹⁴ C] Glucose uptake by GLUT7	69
2.4.6	Protein analysis of <i>X. laevis</i> membrane extracts by Western blot	69
2.4.7	Protein analysis of <i>X. laevis</i> membrane extracts by Wes	70
2.4.8	Statistical analysis	71
Chapter 3 Characterization of hGLUT2, hGLUT5 and hGLUT7 using the Caco-2/TC7 cell culture model		73
3.1	Abstract	73
3.2	Introduction	74

3.3	Determination of location of GLUTs on cellular membranes by immunostaining	76
3.4	Characterization of hGLUT7 through quantitative protein and mRNA analysis	82
3.4.1	Quantification of hGLUT7 mRNA following cell differentiation in the presence of different sugars.....	82
3.4.2	Quantification of total and cell surface hGLUT7 protein expression following cell differentiation in the presence of different sugars	86
3.5	Summary and discussion of results.....	91
Chapter 4 Fructose uptake inhibition of heterologously expressed hGLUT5 by (poly)phenols.....		97
4.1	Abstract	97
4.2	Introduction.....	98
4.3	Validation of GLUT5pBF plasmid construct functionality	102
4.3.1	Confirmation of adequate placement of hGLUT5 gene in expression vector	102
4.3.2	Confirmation of specificity and quality of mRNA product.....	107
4.4	Validation of <i>X. laevis</i> model functionality.....	109
4.4.1	Fructose uptake by GLUT5-expressing oocytes and inhibition by known specific inhibitors	109
4.4.2	Determination of expression of recombinant hGLUT5 on oocyte membrane extracts	114
4.5	Uptake experiment results and discussion	118
4.5.1	Effect of extracts on fructose uptake by GLUT5.....	120
4.5.2	Effect of pure compounds on fructose uptake by GLUT5....	128
4.5.3	Summary of results from fructose uptake experiments	134
Chapter 5 Glucose and fructose uptake inhibition of heterologously expressed hGLUT2 by (poly)phenols		141
5.1	Abstract	141
5.2	Introduction.....	142
5.3	Validation of GLUT2pBF plasmid construct functionality.....	146
5.3.1	Confirmation of adequate placement of hGLUT2 gene in expression vector	146
5.3.2	Confirmation of specificity and quality of mRNA product.....	151
5.4	Validation of <i>X. laevis</i> model functionality.....	154
5.4.1	Glucose uptake by GLUT2-expressing oocytes and inhibition by known specific inhibitors	154

5.4.2	Determination of expression of recombinant hGLUT2 on oocyte membrane extracts.....	157
5.5	Uptake experiment results and discussion	159
5.5.1	Effect of extracts on glucose uptake by GLUT2	161
5.5.2	Effect of pure compounds on glucose uptake by GLUT2 ...	164
5.5.3	Comparison of effect of pure compounds on glucose and fructose uptake by GLUT2.....	167
5.5.4	Summary of results from glucose and fructose uptake experiments.....	171
Chapter 6 Glucose and fructose inhibition of heterologously expressed hGLUT7 by (poly)phenols		177
6.1	Abstract	177
6.2	Introduction	178
6.3	Validation of GLUT7pBF and GLUT7pGEM-HE plasmid construct functionality.....	180
6.3.1	Confirmation of adequate placement of hGLUT7 gene in expression vector	180
6.3.2	Confirmation of specificity and quality of mRNA product	188
6.4	Validation of <i>X. laevis</i> model functionality	194
6.4.1	Sugar uptake by GLUT7-expressing oocytes and inhibition by known specific inhibitors	194
6.4.2	Determination of expression of recombinant hGLUT7 on oocytes membrane extracts.....	198
6.5	Uptake experiment results and discussion	202
6.5.1	Effect of extracts on glucose uptake by GLUT7	203
6.5.2	Effect of pure compounds on glucose and fructose uptake by GLUT7.....	205
6.5.3	Summary of results from glucose and fructose uptake experiments.....	213
Chapter 7 Summary discussion, future perspectives and conclusions		218
7.1	Research rationale and objectives.....	218
7.1.1	The role of (poly)phenols in CVD and T2DM prevention	218
7.1.2	Effect of (poly)phenols on carbohydrate uptake and digestion	220
7.2	Discussion of research outcomes and novelty of findings	221
7.2.1	Characterization of hGLUT7.....	221
7.2.2	Sugar uptake experiments.....	223

7.3	Future research perspectives	228
7.3.1	Cell culture studies.....	228
7.3.2	Human intervention studies.....	229
7.4	Overall conclusion	231
References	233
Appendix A	pBF plasmid sequence	253
Appendix B	GLUT5pBF sequence.....	254
Appendix C	GLUT2pBF sequence.....	255
Appendix D	GLUT7pBF sequence.....	256
Appendix E	GLUT7pGEM-HE sequence	257
Appendix F	Confocal images of GLUT2 with WGA.....	258
Appendix G	Confocal images of GLUT7 with WGA	259

List of tables

Table 1-1 Examples of disease factor attenuation by (poly)phenolic extracts	26
Table 1-2 GLUT2 and GLUT5 inhibition by (poly)phenolic compounds and (poly)phenol rich extracts	30
Table 2-1 List of extracts used in inhibition studies, including the supplier and main (poly)phenolic composition.....	41
Table 2-2 Specific conditions of the mobile phase during the full length of the run.....	46
Table 2-3 List of universal primers, and their sequence, used for sequencing reactions of each vector.	56
Table 2-4 List of customized primers, and their sequence, used for sequencing reactions of each vector.	57
Table 4-1 Compounds/extracts used in GLUT5-mediated fructose uptake inhibition studies described in this chapter	119
Table 4-2 Compounds and their respective inhibition on fructose uptake by GLUT5	137
Table 4-3 Extracts and their respective inhibition on fructose uptake by GLUT5. Experimental condition was 0.1 mM fructose for 5 mins at 25 °C	138
Table 5-1 Compounds/ extracts used in GLUT2-mediated glucose/fructose uptake inhibition studies described in this chapter	160
Table 5-2 Compounds and their respective inhibition on sugar uptake by GLUT2	172
Table 5-3 Extracts and their respective inhibition on glucose uptake by GLUT2.	173
Table 6-1 Compounds/ extracts used in GLUT2-mediated glucose/fructose uptake inhibition studies described in this chapter	203
Table 6-2 Structure of apigenin and its inhibition of GLUT7 sugar uptake	217
Table 7-1 Summary of inhibition of GLUT2-, GLUT5- and GLUT7-mediated sugar uptake by pure compounds apigenin, quercetin and EGCG227	

List of figures

Figure 1-1 Metabolic effects of fructose on liver.....	10
Figure 1-2 Radial tree representative of the structural alignment of the extended glucose transporter family (GLUT).....	12
Figure 1-3 Schematic illustration of the structure of classes 1 and 2 of the GLUT family.....	13
Figure 1-4 Illustration of the transport of sugars across the enterocyte by three GLUT transporters (GLUTs 2, 5 and 7) and sodium dependent transporter SGLT1	18
Figure 1-5 Basic structure of flavonoids and its subclasses.....	20
Figure 1-6 Chemical structures of gallic acid, resveratrol and secoisolariciresionol.	22
Figure 1-7 <i>Xenopus laevis</i> oocyte developmental stages and representation of undigested ovary and digested oocytes.	33
Figure 2-1 Representation of general principle of droplet making and quantification	50
Figure 2-2 Cell surface biotinylation procedure summary	53
Figure 2-3 Ligation of insert (GLUT gene) into pBF expression vector.....	61
Figure 2-4 General template for in vitro transcription reaction of plasmid constructs	64
Figure 2-5 Oocyte microinjection setup.....	67
Figure 3-1 Representation of enterocyte and culture of Caco-2/TC7 cells on transwell filters	76
Figure 3-2 Negative control for immunofluorescence detection for GLUTs in differentiated Caco-2/TC7 monolayers.	77
Figure 3-3 Immunofluorescence detection of GLUT5 in differentiated Caco-2/TC7 monolayers	78
Figure 3-4 Immunofluorescence detection of GLUT2 in differentiated Caco-2/TC7 monolayers	80
Figure 3-5 Immunofluorescence detection of GLUT7 in differentiated Caco-2/TC7 monolayers	81
Figure 3-6 GLUT7 mRNA expression in differentiated Caco-2/TC7 and Caco-2 intestinal cell lines	83
Figure 3-7 GLUT7 mRNA expression in differentiated Caco-2/TC7 intestinal cells following growth in media supplemented with different sugars.....	84

Figure 3-8 GLUT7 mRNA expression in differentiated Caco-2/TC7 intestinal cells following growth through the differentiation phase in media supplemented with fructose	85
Figure 3-9 Standard curve for GLUT7 and NaKATPase antibodies and example of protein detection by multiplexed antibodies.	87
Figure 3-10 GLUT7 protein expression in differentiated Caco-2/TC7 intestinal cells following growth through the differentiation phase in media supplemented with fructose	88
Figure 3-11 GLUT7 surface protein expression in differentiated Caco-2/TC7 intestinal cells.....	90
Figure 3-12 GLUT5 surface protein expression in differentiated Caco-2/TC7 intestinal cells.....	91
Figure 4-1 Illustration of the GLUT5pBF and pBF plasmids and primer location for PCR validation of positive colonies for GLUT5 presence	104
Figure 4-2 Gel electrophoresis image of PCR of GLUT5pBF colonies after ligation of GLUT gene to expression vector	106
Figure 4-3 Gel electrophoresis of linearized GLUT5pBF construct and denaturing gel of GLUT5 mRNA product	108
Figure 4-4 Fructose (6 mM) uptake time course experiment.....	110
Figure 4-5 Effect of solvents on oocytes	111
Figure 4-6 Inhibition of GLUT5 fructose uptake by known inhibitors.	113
Figure 4-7 Western blot image of the expression of GLUT5 on oocyte membrane extracts.	114
Figure 4-8 Confirmation of expression of GLUT5 on oocyte membrane extracts by wes	115
Figure 4-9 Determination of level of GLUT5 expression on oocyte membrane extracts by wes.	117
Figure 4-10 Effect of cocoa extracts on fructose uptake by GLUT5... ..	121
Figure 4-11 Analysis of flavanol profile of chocolate extracts using HPLC-FDL	122
Figure 4-12 Effect of extracts on fructose uptake by GLUT5	123
Figure 4-13 Effect of extracts on fructose uptake by GLUT5	125
Figure 4-14 Effect of extracts on fructose uptake by GLUT5.	126
Figure 4-15 Effect of pure compounds on fructose uptake by GLUT5.....	129
Figure 4-16 Effect of pure compounds on fructose uptake by GLUT5.....	131
Figure 4-17 Effect of pure compounds on fructose uptake by GLUT5.....	132
Figure 4-18 Effect of acarbose on fructose uptake by GLUT5.	133

Figure 4-19 Structure of GLUT5 substrate, D-fructose, and specific inhibitors	135
Figure 5-1 Illustration of the GLUT2pBF plasmid and theoretical gel electrophoresis products upon digestion of plasmid with HindIII restriction enzyme	148
Figure 5-2 Gel electrophoresis image showing digestion of GLUT2pBF colonies with HindIII after ligation of GLUT gene to expression vector	150
Figure 5-3 Gel electrophoresis of circular and linear GLUT2pBF.....	152
Figure 5-4 Gel electrophoresis of the GLUT2 mRNA product from IVT on RNA denaturing gel	154
Figure 5-5 Uptake of 0.1 mM fructose/glucose over different incubations times.	155
Figure 5-6 Inhibition of GLUT2 glucose uptake by known inhibitors..	156
Figure 5-7 Confirmation of expression of GLUT2 on oocyte membrane extracts by Wes.	158
Figure 5-8 Effect of green tea and German chamomile extracts on glucose uptake by GLUT2.....	162
Figure 5-9 Effect of Bonolive and sugar-free pomegranate extracts on glucose uptake by GLUT2.....	163
Figure 5-10 Effect of pure compounds hesperetin and hesperidin on glucose uptake by GLUT2.....	165
Figure 5-11 Effect of acarbose on glucose uptake by GLUT2.....	166
Figure 5-12 Effects of quercetin on glucose and fructose uptake by <i>X. laevis</i> oocytes expressing GLUT2.....	168
Figure 5-13 Effects of apigenin on glucose and fructose uptake by <i>X. laevis</i> oocytes expressing GLUT2.....	169
Figure 5-14 Effects of EGCG on glucose and fructose uptake by <i>X. laevis</i> oocytes expressing GLUT2.....	170
Figure 6-1 Gel electrophoresis image showing digestion of GLUT7pBF colonies with HindIII after ligation of GLUT7 gene to expression vector	182
Figure 6-2 Illustration of the GLUT7pBF plasmid and theoretical gel electrophoresis products upon digestion of plasmid with HindIII restriction enzyme	184
Figure 6-3 Illustration of the GLUT7pGEM-HE plasmid and theoretical gel electrophoresis products upon digestion of plasmid with HindIII and KpnI restriction enzymes	185
Figure 6-4 Gel electrophoresis image showing digestion of GLUT7pGEM-HE and its colonies with HindIII and KpnI after ligation of GLUT gene to expression vector.....	187

Figure 6-5 Gel electrophoresis of circular and linear GLUT7pBF and GLUT7pGEM-HE.....	189
Figure 6-6 Gel electrophoresis of the GLUT7 mRNA product, derived from GLUT7pBF, on RNA denaturing gel.....	191
Figure 6-7 Gel electrophoresis of GLUT7 mRNA product, derived from GLUT7pGEM-HE, on an RNA denaturing gel.....	193
Figure 6-8 Gel electrophoresis of GLUT7 mRNA products, derived from GLUT7pGEM-HE and GLUT7pBF linearized with PmlI or MluI, on an RNA denaturing gel.....	194
Figure 6-9 Uptake of sugars by GLUT7-expressing oocytes.....	196
Figure 6-10 Inhibition of glucose uptake by GLUT7-expressing oocytes	197
Figure 6-11 Confirmation of expression of GLUT7 on oocyte membrane extracts by Wes.....	199
Figure 6-12 Confirmation of expression of GLUT7 on oocyte membranes	201
Figure 6-13 Effect of plant extracts on glucose uptake by GLUT7-expressing oocytes.....	204
Figure 6-14 Effect of quercetin on sugar uptake by GLUT7-expressing oocytes.	208
Figure 6-15 Effect of EGCG on sugar uptake by GLUT7-expressing oocytes	209
Figure 6-16 Effect of apigenin on sugar uptake by GLUT7-expressing oocytes	210
Figure 6-17 Effect of apigenin on sugar uptake by GLUT7-expressing oocytes	211
Figure 6-18 Dot plot representing values for uptake by control oocytes in single uptake experiments with 3 and 10 oocytes.	212

List of abbreviations

ADP	Adenosine diphosphate
AMP	Adenosine monophosphate
Amp+	Ampicillin containing
ATP	Adenosine triphosphate
BP	Blood pressure
bp	Base pairs
CaCl ₂	Calcium chloride
CBG	Cytosolic β -glucosidase
CHD	Coronary heart disease
CPMA	Counts per minute
CVD	Cardiovascular disease
DAPI	4',6-diamidino-2-phenylindole
DHAP	Dihydroxyacetone-phosphate
DMSO	Dimethyl sulfoxide
DTT	Dithiothreitol
EGCG	Epigallocatechin gallate
ELE	Eucalyptus leaf extract
eNOS	Endothelial nitric acid synthase
ER	Endoplasmic reticulum
FAO	Food and Agricultural Organization
FBS	Fetal bovine serum
FOXO1	Forkhead box protein O1

GI	Glycaemic index
GLUT2	Solute carrier family 2, member 2 (SLC2A2)
GLUT5	Solute carrier family 2, member 5 (SLC2A5)
GLUT7	Solute carrier family 2, member 7 (SLC2A7)
HBSS	Hank's balanced salt solution
HEPES	N-2-hydroxyethylpiperazine-N-2-ethane sulfonic acid
HDL	High density lipoprotein
HFCS	High-fructose corn syrup
HL	Hyperladder
HPLC	High-performance liquid chromatography
IC _n	Inhibition constant
IDDM	Insulin-dependent diabetes mellitus
IGOT	Isotope-coded glycosylation-site-specific tagging
IGT	Impaired glucose tolerance
IVT	In vitro transcription
KCl	Potassium chloride
LB	Luria-Bertani broth
LC-MS	Liquid chromatography–mass spectrometry
LDL	Low density lipoprotein
LSC	Liquid scintillation counting
LPH	Lactase phloridizin hydrolase
MgCl ₂	Magnesium chloride
mRNA	Messenger ribonucleic acid
NaCl	Sodium chloride

NEFA	Non-esterified fatty acids
NIDDM	Non-insulin dependent diabetes mellitus
PBS	Phosphate buffered saline
PBS+	PBS w/ calcium chloride and magnesium chloride
PCR	Polymerase chain reaction
PKC	Protein kinase C
PMT	Photomultiplier
PTFE	Polytetrafluoroethylene
PTM	Post-translational modification
SD	Standard deviation
SDS	Sodium dodecyl sulfate
SDS-PAGE	Sodium dodecyl sulfate polyacrylamide gel electrophoresis
SEM	Standard error of mean
SGLT1	Sodium-dependent glucose transporter 1
SGLT2	Sodium-dependent glucose transporter 2
Spc+	Spectinomycin containing
SPE	Solid phase extraction
ssRNA	Single-stranded ribonucleic acid
T1DM	Type 1 diabetes mellitus
T2DM	Type 2 diabetes mellitus
TAE	Tris base, acetic acid and EDTA
TEER	Transepithelial electrical resistance
TG	Triglycerides
VLDL	Very-low-density lipoprotein

WGA

Wheat germ agglutinin

WHO

World Health Organisation

Chapter 1

Introduction and research objectives

1.1 Overview

The monosaccharide D-glucose is the most plentiful 'simple sugar' existing in nature, and is the main dietary energy producing source for most higher organisms (Nelson and Cox, 2008). Although the consumption of sugars is necessary for energy and life the development of many health conditions has been associated with the ever increasing intake of sugars in the diet. Diabetes mellitus, for instance, affects nearly 5% of the world population, with type 2 diabetes (T2DM) accounting for 90-95% of cases (Hajiaghaalipour et al., 2015). Many health organizations worldwide, including the World Health Organization (WHO) and United Nations Food and Agricultural Organization (FAO), have recommended that daily free sugar intake should not exceed 10% of the total caloric intake in adults as a measure to prevent the development of diabetes and obesity, as well as any risk factors associated with these conditions (Laville and Nazare, 2009). The increasing health burden associated with excess sugar intake has led to a lot of research currently being conducted to try and minimize the health deteriorating effects high sugar intake may have in the body. (Poly)phenols are plant derived reducing agents that, much like other compounds such as vitamin C and E, act as

antioxidants and aid the body in the prevention of oxidative stress and diseases such as inflammation and cardiovascular disease which are associated with it (Scalbert et al., 2005). Studies have also shown that (poly)phenols are able to decrease glucose absorption by the body and have a positive impact on carbohydrate metabolism, which in turn helps to control glycaemic responses, secretion of insulin and fasting hyperglycaemia (Hanhineva et al., 2010).

1.2 The health burden of diabetes mellitus and associated diseases

Diabetes mellitus is a chronic condition caused by the body's lack of insulin production or its inability to effectively recognize the availability of insulin. Type 1 diabetes mellitus (T1DM) is referred to as insulin dependent diabetes mellitus (IDDM) and usually develops in early life due to autoimmune impairment of pancreatic β cells, which leads to insufficient insulin production. Treatment of T1DM is carried out by insulin therapy where insulin dose is balanced in accordance to dietary intake (Nelson and Cox, 2008). T2DM is also known as non-insulin dependent diabetes mellitus (NIDDM) for individuals with T2DM produce insulin but become insulin resistant due to damaged insulin recognition and response system. The risk of developing T2DM is higher in individuals suffering from obesity (Nelson and Cox, 2008). The prevalence of obesity has trebled in the last 20 years in the UK alone and has contributed to elevated levels of morbidity and mortality (Jennings et al., 2009). In addition, increased dietary intake of sugars has been shown to have a corresponding link to increased prevalence of obesity in the U.S in the last two decades (Elliott et al., 2002). Diet regulation, therefore, is

strongly advised to help control this disease, which is usually managed with pharmacological treatments. Physical activity has also been shown to improve, and to a certain extent prevent or delay the onset of T2DM as individuals with a weekly energy expenditure of 1,000 kcals or above having up to 20% potential reduction in risk of T2DM development (Paffenbarger, 1996). Patients living with T2DM are also classed as at high risk of developing CVD, most likely due to lipid abnormalities, hypertension, and obesity, which are risk factors linked to both conditions (Jennings et al., 2009). Throughout the continuation of this report, specifically in chapters presenting the research results, the term diabetes is used in reference to T2DM, unless otherwise stated.

1.2.1 The role of glucose in the development of diabetes mellitus

The American Diabetes Association describes diabetes as metabolic diseases arising from hyperglycaemia caused by defective secretion and/or action of insulin. To that effect, levels of circulating glucose in the blood is a common diagnostic test for diabetes (Zeymer, 2006). By definition, diabetes mellitus comes about through the body's inability to produce or recognise insulin, secreted by the pancreatic β cells in the presence of glucose, thereby establishing a clear link between this condition and glucose (Basciano et al., 2005). Patients with a fasting plasma glucose level between 5.6 mmol/L and 6.9 mmol/L are considered to have impaired fasting glucose and patients with blood glucose levels between 7.8 mmol/L and 11.0 mmol/L 2 h following oral glucose tolerance test (OGTT) are considered to have impaired glucose tolerance (IGT). Individuals who fit into either of these groups are classified as pre-diabetic and are at a higher risk of developing diabetes (ADS, 2014). Insulin signalling following carbohydrate intake in T2DM patients is

impaired by accumulation of displaced lipids, leading to diminished uptake of glucose by skeletal muscles in response to insulin. Excess glucose travels to the liver where it contributes to lipogenesis and the increased lipid levels weakens the ability of insulin to regulate gluconeogenesis and glycogen synthesis, all contributing to the secretion of triglycerides (Samuel and Shulman, 2012). High triglycerides levels are associated with obesity and insulin resistance (Ochoa et al., 2015).

Data from epidemiological studies and surveys from 199 countries worldwide found a link between increased fasting plasma glucose and prevalence of T2DM. From 1980 to 2008 fasting plasma glucose increased by 0.07 mmol/L for men and 0.09 mmol/L for women every decade, and the number of people with T2DM more than double in this same time frame (153 million in 1980 to 347 million in 2008) (Danaei et al., 2011). To add to that, food supply data analysed from FAO concluded that for each year of exposure to high sugar (more than 300 kcal/person/day) there was an 0.053% increase in T2DM prevalence once all control variables were taken into account. These findings suggest that prevalence of T2DM can be elevated by exposure to sugar in the diets regardless of other factors such as age, exercise level and weight (Basu et al., 2013). The Iowa Women's Health Study, a prospective cohort study of over 35,000 postmenopausal women, found that the relative risk of developing TD2M was 1.30 for those women who consumed 25.8 g/day or more of glucose (Meyer et al., 2000). Some diabetic patients are, therefore, able to regulate their blood glucose through their diet as well as practicing exercise. Nevertheless, for patients with an acute β cell defect simple

diet adjustments are not sufficient and these individuals require daily injections of insulin to keep their condition under control (Jung et al., 2014).

1.2.2 The role of fructose in the development of risk factors associated with diabetes mellitus

Dietary intake of fructose, mainly from fruits, has been documented for thousands of years (Sun and Empie, 2012a). Human ancestral diet, however, was composed of high levels of fibre and protein and much lower levels of salts and carbohydrates, the latter almost exclusively derived from fruits and vegetables (Konner and Eaton, 2010). Over three-quarters of the hunter-gatherer societies around the world acquired more than 50% of their food from animals, with less than a quarter obtaining more than 50% of their sustenance from plants (Cordain et al., 2000). These hunter-gatherer groups, although having a high energy consumption from carbohydrate (around 20-40%) still consumed less than the current average American (about 50%) and very likely used no sweetener apart from honey (Welsh et al., 2011). Nevertheless, ever since the industrial revolution, when sugar prices dropped and alternative sugar sources were identified, there has been a dramatic rise in the consumption of fructose. Daily intake of fructose has increased from around 5 g in the 1700s to 180 g by 2009 (Johnson et al., 2009). In other words, the consumption of sugars increased by almost 40-fold in 300 years (Douard and Ferraris, 2013). This upturn in the amounts of fructose being incorporated into our daily diet corresponds with the increase in prevalence of obesity observed since around the 1980s in both the UK and USA (Grundy, 1998). Unlike beet and cane sugars that are composed of the disaccharide sucrose, formed by a bond between

the monosaccharide glucose and fructose molecules, corn sugars have a higher percentage of fructose; usually around 55%, but could go up to as high as 90% (Guzman-Maldonado and Paredes-Lopez, 1995). High fructose corn syrup (HFCS), produced by the enzymatic isomerization of dextrose to fructose, began to increase in popularity and be added to foodstuffs such as breakfast cereals, condiments and prepared desserts around the 1970s. In 1985 about 35% of sweeteners by dry weight was accounted for by HFCS in the food supply (Park and Yetley, 1993). Around the same time, intake of fructose accounted for 10% of total daily energy intake in adults in the U.S, with similar trends around the world (Bialostosky et al., 2002). Over two thirds of fructose consumed came from food products and beverages which had the sugar added to them and only about one third originated from fruits and other natural sources (Popkin and Nielsen, 2003). It is estimated that an individual in the U.S consumes about 600 mL of soft drinks every day (Nielsen and Popkin, 2004). Comparison of published data records from 43 countries suggests that those countries with higher consumption of HFCS have a 20% higher prevalence of T2DM than those countries with lower availability of HFCS in their foodstuffs (Goran et al., 2013). To add to that, the National Diet and Nutrition Survey reported that the daily intake of soft drinks per person per day in the UK is of approximately 240 ml and of double this amount in the younger population (Bates et al., 2012). Data analysed from four cohort studies suggest that the relative risk of developing T2DM was 1.20 per 33 ml of sugar sweetened soft drinks per day ($p < 0.001$) and 1.13 per 330 ml artificially sweetened soft drink per day ($p = 0.02$) (Greenwood et al., 2014). It is important to note that the EPIC-InterAct study reported that those individuals who regularly consumed artificially sweetened soft drinks had a higher initial BMI than regular consumers of sugar

sweetened soft drinks (28 kg/m² and 26 kg/m², respectively), meaning that the higher relative risk observed for the artificially sweetened soft drinks category might have originated from reverse causality (Forouhi and Wareham, 2014). Nonetheless, a hypothesis that the uncoupling of the sweet taste from its energy source could trigger appetite, causing a positive energy balance and thereby weight gain has been proposed to be the true reason why relative risk of T2DM is elevated in the artificially sweetened drinks group. Another hypothesis to explain the findings suggests an association between artificially sweetened drinks and an overcompensation for the discerned energy saved in other parts of the diet (Greenwood et al., 2014).

Absorption of fructose by the body is a facilitated diffusion mechanism and linear process. Fructose is metabolized in the intestine, liver and kidney by the enzymes fructokinase, aldolase B and triokinase, with most of it being metabolized by the liver following oral load (Laville and Nazare, 2009). Metabolism of fructose, unlike other carbohydrates, is mainly an insulin-independent process, meaning that following fructose ingestion fewer glycaemic excursions are caused. In vitro analysis of pancreas and isolated islet demonstrate that fructose, in the absence of glucose, is not able to stimulate insulin secretion (Coore and Randle, 1964). Le et al showed that fasting fructose concentration in venous blood was elevated from 0.005 mM to 0.3 mM following ingestion of a soft drink containing 69 g of sucrose while glucose concentration rose from 5.5 mM baseline to 6.8 mM with the same drink. Insulin release was accompanied by the rise in glucose concentration in the blood, peaking at around 30 min before returning to baseline at 90 min. Blood

fructose levels returned to baseline after 3 h of sucrose soft drink ingestion (Le et al., 2012).

A study by Vozzo et al showed that fructose leads to a higher concentration of plasma insulin in T2DM patients and was hypothesised to be a good replacement for glucose in the diet of such individuals (Vozzo et al., 2002). Nonetheless, different studies have pointed out how excess fructose intake may exacerbate risk factors associated with T2DM and cardiovascular disease, as illustrated in Figure 1.1. For instance, lysis of fructose molecule into pyruvate and dihydroxyacetone-phosphate (DHAP) by the liver provides the acyl part and the carbon to glycerol of the triglyceride (TG) molecule. It is important to note that these lipogenic effects of fructose have only been examined in the presence of glucose and insulin. Fructose on its own, however, has been shown to stimulate re-esterification of non-esterified fatty acids (NEFA), a process that is boosted in the presence of insulin (Laville and Nazare, 2009). Fructose is also a strong stimulator of *de novo* lipogenesis through excess substrate (citrate) production and conversion of TG composition into very-low-density lipoproteins (VLDL) (Lim et al., 2010). A study conducted on 32 overweight and obese subjects consuming either glucose or fructose sweetened drinks, accounting for 25% of total energy intake, for 10 weeks showed that hepatic *de novo* lipogenesis was increased significantly higher following fructose intake than glucose intake (75% and 27%, respectively) (Stanhope et al., 2009). Accumulation of TG by reduced VLDL clearance can ultimately lead to hypertriglyceridemia and insulin resistance, both of which are strong risk factors for obesity and T2DM (Laville and Nazare, 2009). Hypertriglyceridemia, in turn, causes less leptin, a satiety hormone, to be transported across the blood-brain

barrier and is another indirect way by which fructose increases chance of obesity development (Banks et al., 2004). Changes in circulating hormone levels following a high fructose or high glucose meal was examined in a study of 12 healthy women. The study concluded that ghrelin was significantly less suppressed in the women who ingested the high fructose meal and their levels of insulin and leptin were also lower. This suggests that fructose can disturb the energy balance signalling to the brain, thereby leading to potential further energy intake, to a greater extent than glucose (Teff et al., 2004). Excess lipids are taken up by the muscle form intramyocellular lipids, causing muscle insulin resistance (Laville and Nazare, 2009). In addition, synthesis of the forkhead box protein O1 (FOXO1) is increased in the presence of fructose. In a hepatic insulin resistant environment FOXO1 is not phosphorylated and upon entering the nucleus will stimulate production of enzymes that increase gluconeogenesis, leading to elevated glucose generation and hyperglycaemia (Dong et al., 2008). Usage of ATP molecules for fructose phosphorylation by fructokinase allows AMP deaminase I to take phosphate from ADP creating uric acid as a waste product. Uric acid acts as an inhibitor of endothelial nitric acid synthase (eNOS) in the smooth muscle causing a decrease in nitric oxide production and, therefore, an increase in blood pressure (Johnson et al., 2007).

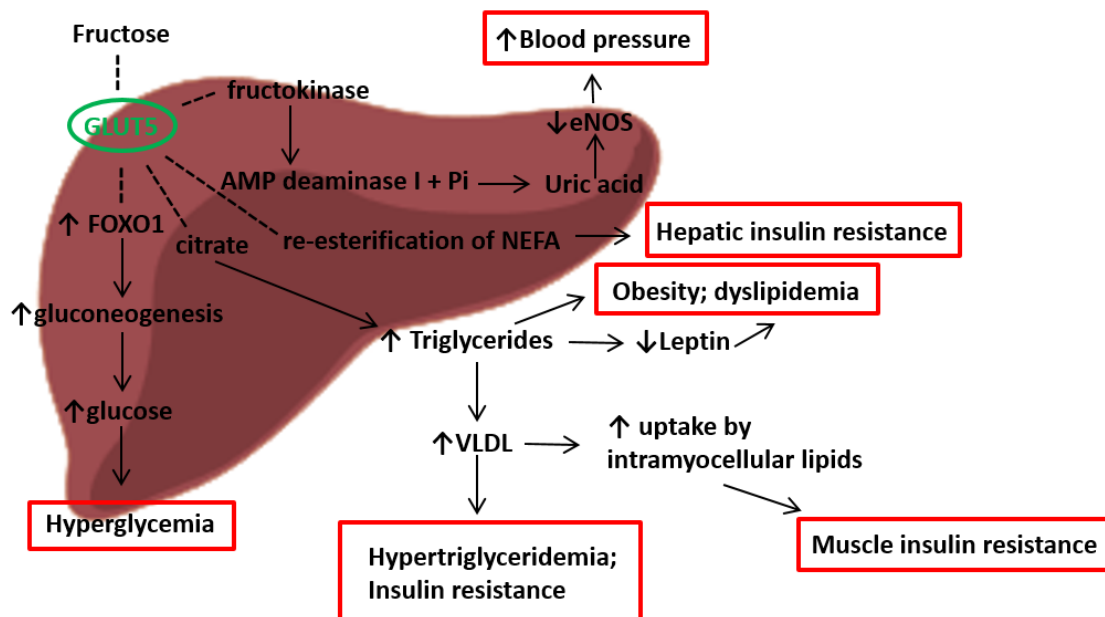


Figure 1-1 Metabolic effects of fructose on liver. Once in the liver fructose stimulates production of FOXO1 which in a hepatic insulin resistant state lead to increased gluconeogenesis, and thereby higher glucose secretion, leading to hyperglycemia. Coupling of AMP deaminase I with a phosphate from the phosphorylation of fructose by fructokinase produces uric acid, an inhibitor of eNOS, leading to decreased production of the vasodilator nitric oxide and an elevation of blood pressure. Fructose also directly causes re-esterification of NEFA leading to hepatic insulin resistance. *De novo lipogenesis* is stimulated by fructose through excess citrate production and transformation of triglycerides into VLDL. Reduction in clearance rate of VLDL leads to hyperglycaemia and insulin resistance. In addition, a higher uptake of lipids by the muscle causes muscle insulin resistance. High levels of triglycerides is in itself a risk factor for obesity and dyslipidaemia but it also leads to decreased leptin delivery to the brain, which in turn can cause further intake of fructose, increasing the risk of both conditions (Lim et al., 2010).

A study conducted by Nguyen et al showed a positive correlation between intake of sugar-sweetened drinks and hypertension in children (Nguyen et al., 2009). The same correlation has been confirmed in adults in a study by Gao et al (Gao et al., 2007). An animal model study showed that the offspring of fructose fed mice were hyperglycaemic upon birth in contrast to control group offspring suggesting a potential correlation between maternal fructose intake and development of T2DM risk factors (Jen et al., 1991). The Nurse's health study II, which followed over 91

000 women free of diabetes at the start of the study, concluded that those who consumed one sugar-sweetened drink every day had a relative risk of developing the disease of 1.83 compared to those who consumed sugar-sweetened beverages once a month. The sugar-sweetened drinks used in the study were supplemented with HFCS and fruit juice consumption was not linked to diabetes risk (Hu et al., 2001). It was hypothesised that other components of the fruits, such as minerals and fibres, could act as a counterbalance for the potential negative health effects of their naturally occurring sugars, a characteristic not present in artificially sweetened drinks (Schulze et al., 2004). Further studies need to be conducted in order to fully understand the direct effects of fructose on health, however, care should be taken when advising dietary replacement of glucose with this sugar for T2DM patients, as well as increase awareness of sugar-sweetened drinks and other products by general consumers, as it could have serious long term deleterious effects on health, as discussed above (Laville and Nazare, 2009).

1.3 Sugar uptake by GLUTs

GLUT proteins encoded by the SLC2 genes are transporters of monosaccharides and polyols across eukaryotic cell membranes (Mueckler and Thorens, 2013). All fourteen GLUT transporters are made up of around 500 amino acids and are all, apart from HMIT, facilitative transporters (Uldry and Thorens, 2004). Each GLUT protein contains 12 transmembrane segments (TM1-12) and a single site for N-linked glycosylation (Mueckler et al., 1985), (Uldry and Thorens, 2004). The GLUTs are grouped into three classes in accordance to sequence similarity; class 1 is comprised of GLUT 1-4 and 14, class 2 includes GLUT 5, 7, 9 and 11 and class 3

is made up of GLUT 6, 8, 10, 12 and HMIT (Mueckler and Thorens, 2013). A radial tree representative of the structural alignment of the members the GLUT family (1-13) is shown in Figure 1.2 (Uldry and Thorens, 2004).

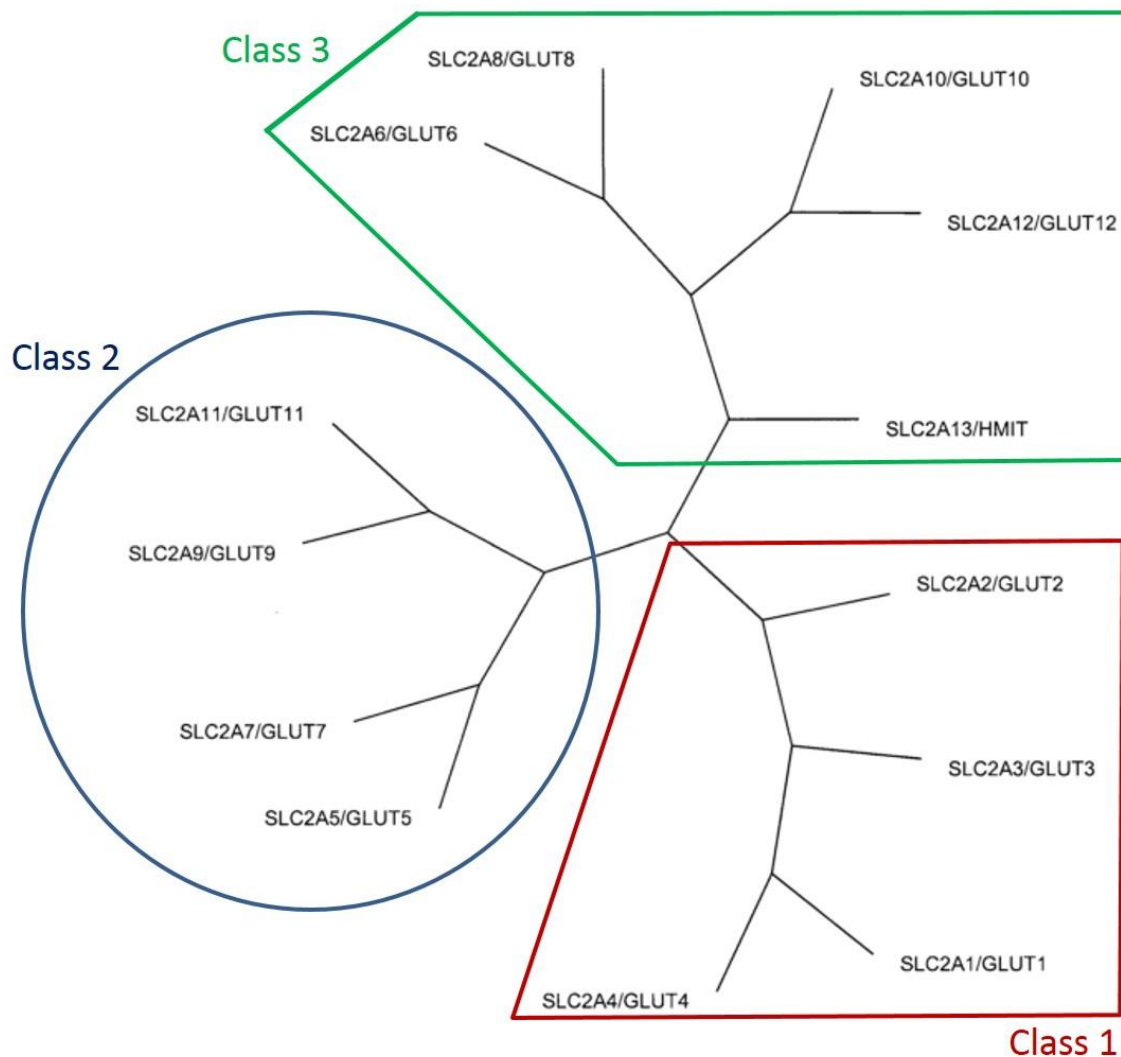


Figure 1-2 Radial tree representative of the structural alignment of the extended glucose transporter family (GLUT). This diagram was constructed, by Uldry et al, using the clustalW program from the European Bioinformatics Institute. The three different classes of this family are clearly distinguishable in this representation (Uldry and Thorens, 2004).

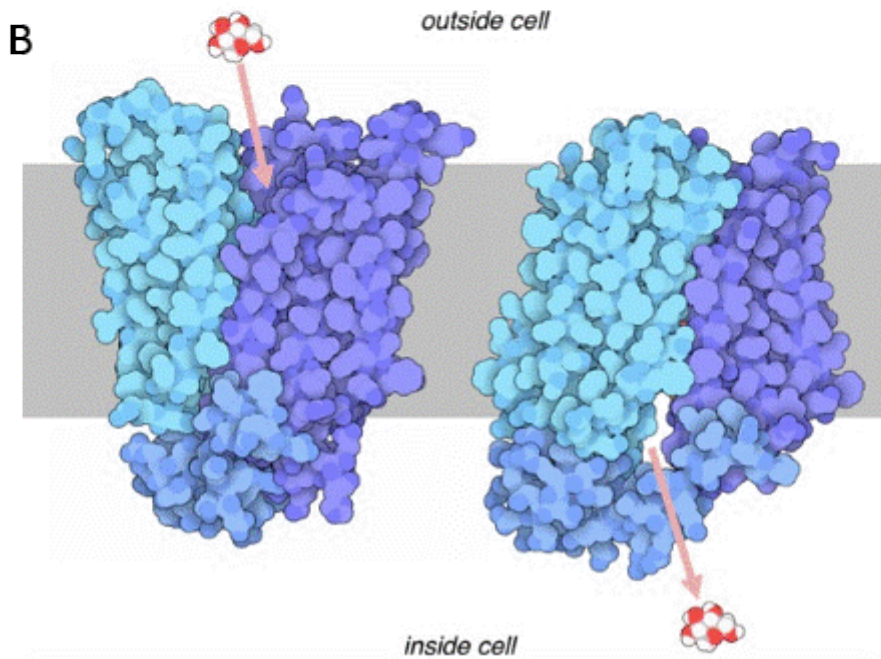
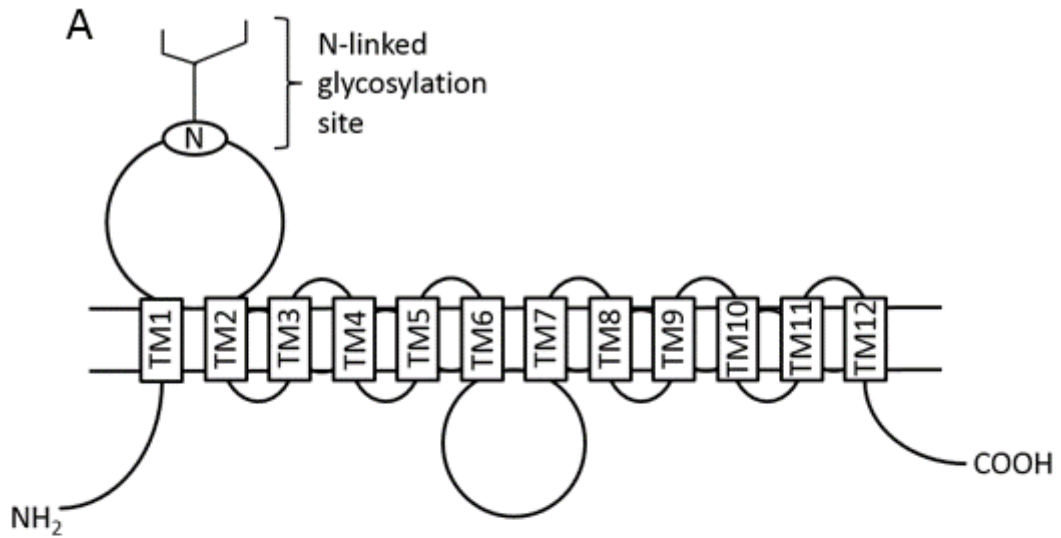


Figure 1-3 Schematic illustration of the structure of classes 1 and 2 of the GLUT family. The extracellular loop containing the N-glycosylation site(s) and the protein-containing motif between transmembrane domains 6 and 7, shown in this figure, comprise the major differences between classes 1-2 and class 3 **(A)**. Sugar molecules are transported into the cell by a structural change of the transporter's opening, which shift between outward and inward facing **(B)** (Deng et al., 2015).

Classes 1 and 2 differ structurally from class 3 by the location of the N-linked glycosylation site, found on the fifth exofacial linker domains in class 3 GLUTs as opposed to the first exofacial linker domains in class 1 and 2 GLUTs, and the protein-containing motif between transmembrane domains 6 and 7 (Mueckler and Thorens, 2013), (Uldry and Thorens, 2004). The GLUTs have an opening facing the outside of the cell that picks up sugar molecules, which are released into the cell by a shape change that causes an inward opening (Deng et al., 2015), (Henderson and Baldwin, 2012). Figure 1.3 A illustrates the overall structure of GLUTs from classes 1 and 2, and Figure 1.3 B shows the binding and release of sugar molecules by GLUTs. Out of the fourteen GLUT proteins it has been experimentally shown that eleven are able to transport glucose (Thorens and Mueckler, 2010). Effectively every cell type in the human body expresses one or multiple GLUTs and it is thought that by having a surplus of proteins able to transport glucose, with differing regulatory and kinetic properties, the body ensures it has a good circulation of this sugar as a fuel to maintain itself (Hokayem et al., 2013).

1.3.1 Sugar transport by GLUT2, GLUT5 and GLUT7

Active transport of glucose in the small intestine is achieved by the sodium-dependent transporter, sodium-glucose cotransporter 1 (SGLT1), on the apical membrane, by means of the downward sodium gradient managed by $\text{Na}^+/\text{K}^+/\text{ATPase}$ on the basolateral membrane (Hediger et al., 1987), (Thorsen et al., 2014). Complete absorption of dietary sugars involves the facilitative transporter GLUT2 which is responsible for glucose, fructose, mannose, glucosamine and galactose transport and delivery to the blood (Ferraris, 2001),

(Uldry et al., 2002). GLUT2 has low affinity for glucose ($K_M \sim 17$ mM), fructose ($K_M \sim 76$ mM), galactose ($K_M \sim 92$ mM) and mannose ($K_M \sim 125$ mM), but has high affinity for glucosamine ($K_M \sim 0.8$ mM) (Uldry et al., 2002), (Mueckler and Thorens, 2013). Although GLUT2 is expressed on the basolateral membrane of enterocytes it is now widely accepted that in the presence of high glucose levels the transport of this sugar is mediated primarily by GLUT2, through trafficking of basolateral GLUT2 to the apical surface (Kellett et al., 2008), (Helliwell et al., 2003). In other words, in response to high dietary sugar intake the rapid insertion of the low affinity and high-capacity transporter, GLUT2, into the apical membrane means that this protein accommodates for the higher concentrations of glucose, and becomes the major route of this sugar's absorption (Helliwell et al., 2000), (Affleck et al., 2003). Although trafficking of GLUT2 was not confirmed by some groups, a variety of experiments performed in cell and rat models support this proposed mechanism (Affleck et al., 2003), (Roder et al., 2014), (Helliwell and Kellett, 2002). Live imaging analysis of kidney cells also showed a rapid basal-to-apical translocation of GLUT2 in response to glucose (Cohen et al., 2014). Furthermore, localisation of GLUT2 to the apical membrane in rat intestinal models has been shown to be increased at high sugar levels (Morgan et al., 2007). Additionally, GLUT2-knockdown mice present a diabetic phenotype, experiencing characteristic symptoms of this condition, such as hyperglucagonemia and hyperinsulinemia (Thorens, 2001).

Fructose uptake in the gut is primarily mediated by GLUT5, which is specific to fructose only, with no ability to transport glucose or galactose (Kane et al., 1997). GLUT5 has evolved to be able to recognize fructose in all its forms, having a reported efficiency (K_M) of 6 mM for this sugar (Burant et al., 1992), (Girniene et

al., 2003). Secondary transport of fructose is mediated by GLUT2, which is able to recognize fructose in its furanose form (Manolescu et al., 2007b). GLUT2 is also responsible for transporting fructose across the basolateral membrane and into the blood, following absorption of this sugar on the apical membrane by GLUT5 (Kellett and Brot-Laroche, 2005). Expression of GLUT5 is reportedly regulated by developmental, hormonal and nutritional influences (Douard and Ferraris, 2008). For example, lower levels of GLUT5 expression in children is the likely cause of malabsorption following dietary fructose intake (Nobigrot et al., 1997), (Wilder-Smith et al., 2014). To add to that, studies on adipocytes and *in vivo* have shown increased expression of GLUT5 in the presence of high fructose, suggesting expression of this protein is regulated by its substrate (David et al., 1995), (Legeza et al., 2014).

Another GLUT that potentially plays a role in the uptake of glucose and fructose in the gut is GLUT7, the closest relative to GLUT5 sharing 53% sequence homology and 68% amino acid identity to the fructose specific transporter (Li et al., 2004), (Scheepers et al., 2005). GLUT7 has high affinity for both glucose and fructose ($K_M < 0.5$ mM), and due to the high levels of expression of this protein in the ileum it is thought it is potentially responsible for sugar uptake at the end or after a meal, when sugar concentrations are lower (Drozdowski and Thomson, 2006), (Cheeseman, 2008). Although there is still controversy about the ability of GLUT7 to transport sugars, expression of human GLUT7 (hGLUT7) in *X. laevis* oocytes have shown that this protein was able to transport fructose and glucose, but not galactose (Ebert et al., 2017), (Li et al., 2004). It has been hypothesised that a conserved motif, present in the sequences of GLUT2,5 and 7, is responsible for

the ability of these proteins to transport fructose (Manolescu et al., 2005), (Doege et al., 2001). Even though further characterization of this protein is required, its high levels of similarity with GLUT5 suggests it may be an active participant in fructose uptake in the gut (Uldry and Thorens, 2004). Figure 1.4 sheds light on the transport of sugars from the lumen across the enterocyte by different transporters. It can be observed from this figure that the functions of GLUT2,5 and 7 likely overlap, namely, GLUT5 is exclusively a high-affinity transporter of fructose, while GLUT7 is a high-affinity and low-capacity transporter of this sugars, and GLUT2 transports both glucose and fructose (Mueckler and Thorens, 2013), (DeBosch et al., 2012), (Cura and Carruthers, 2012).

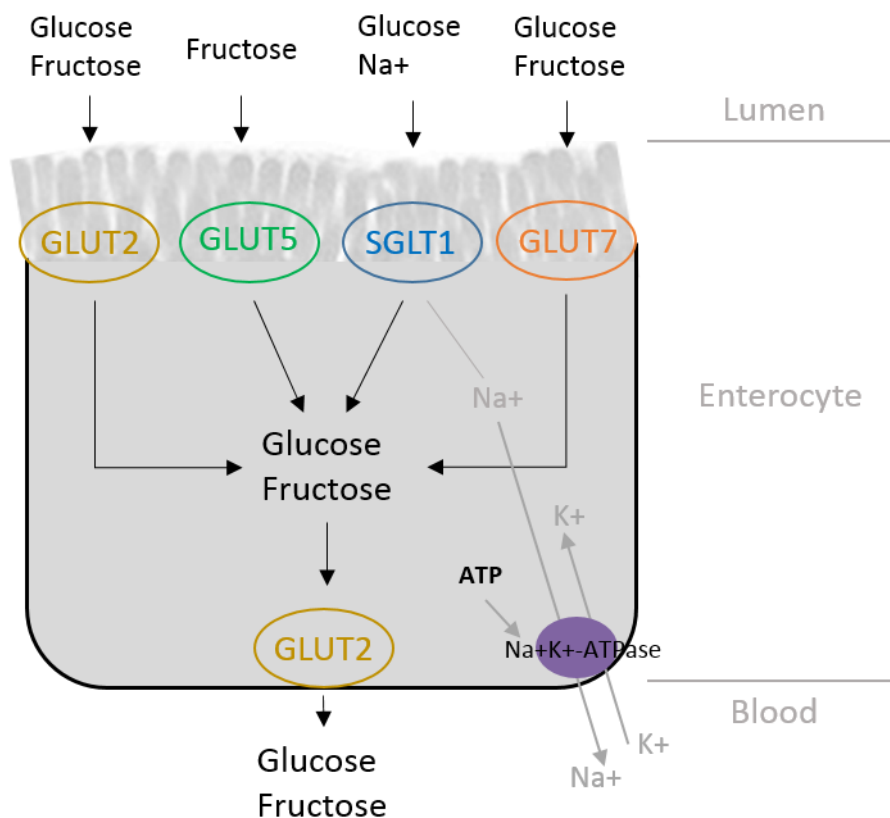


Figure 1-4 Illustration of the transport of sugars across the enterocyte by three GLUT transporters (GLUTs 2, 5 and 7) and sodium dependent transporter SGLT1. GLUT2 is responsible for the facilitative transport of glucose as well as fructose across the cell and it is present on both apical and basolateral sides. GLUT5 is only expressed on the apical side of the cell membrane and will bring fructose into the enterocyte to be transported out by GLUT2. GLUT7 is thought to contribute to the transport of fructose and glucose across the cell. Levels of expression of this protein on apical and basolateral membranes require further investigation in addition to the possible ability of this protein to transport other less common sugars. SGLT1 is responsible for the active transport of glucose through the apical membrane in a sodium dependent manner. Na⁺K⁺-ATPase on the basolateral membrane keeps the optimal gradient for this transporter. GLUT2 on the basolateral membrane will transport any glucose brought into the cell by SGLT1 active transporter out into the extracellular fluids. (Kellett et al., 2008), (Cheeseman, 2008), (Drozdowski and Thomson, 2006)

1.4 Overview of (poly)phenols

(Poly)phenols are naturally occurring plant-derived compounds, present in fruits, vegetables, cereals, and beverages composed of plant/fruit extracts (Pandey and Rizvi, 2009), (Kim et al., 2016), (Liu, 2013). In plants, (poly)phenols are involved in protection against high levels of ultraviolet radiation (Williamson and Manach, 2005). In addition, (poly)phenols may have an impact on the sensory, optical and chemical properties of foodstuffs, such as colour, flavour, and oxidative stability (Pandey and Rizvi, 2009). Significant amounts of (poly)phenols are consumed in the human diet, and these compounds are thought to have an effect on a variety of biological processes, including sugar absorption in the gut (Perez-Jimenez et al., 2010), (Nyambe-Silavwe and Williamson, 2016), (Alzaid et al., 2013). Dietary consumption of (poly)phenols is of approximately 1 g/day, achieved through consumption of unprocessed fruits and vegetables, as well as teas, jams, juices, etc (Scalbert and Williamson, 2000). Amounts of daily (poly)phenols consumption differs between different populations, for instance in the adult Polish population the average consumption of (poly)phenols was determined to be 1771.2 ± 729.5 mg/d (Grosso et al., 2014), while in elderly Japanese individuals consumption was 1492 ± 665 mg/d (Taguchi et al., 2015). The same study saw a pronounced variability in (poly)phenol consumption between individuals, namely 183–4854 mg/d, with beverages like green tea and coffee accounting for over 70% of total (poly)phenol consumption (Taguchi et al., 2015). Structurally, (poly)phenols are comprised of at least one phenolic hydroxyl group, and the different classes of (poly)phenols are determined by the number of phenol rings and how they are bound to one another (Spencer et al., 2008). The main classes of (poly)phenols of importance to human diet are phenolic acids, flavonoids, stilbenes and lignans (Del Rio et al., 2013), (de

Bock et al., 2012). The most abundant and well-studied class of (poly)phenols, flavonoids, is divided into different subgroups, all comprised of a basic C₆-C₃-C₆ structure. The main subgroups of flavonoids are flavonols, flavones, isoflavones, flavan-3-ols, flavanones and anthocyanidins (Rodriguez-Mateos et al., 2014). The basic three-ring chemical structure of flavonoids, and of its different subgroups, are illustrated in Figure 1.5.

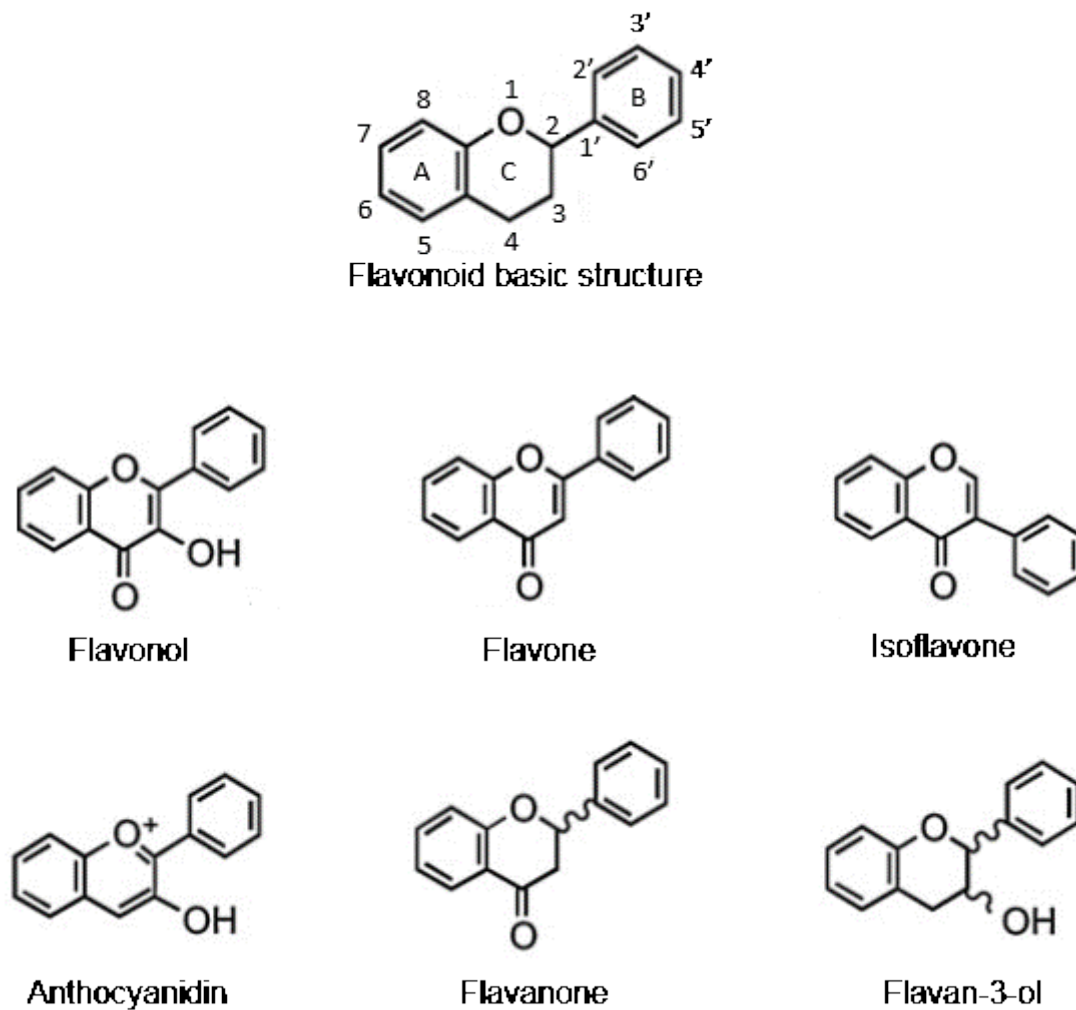
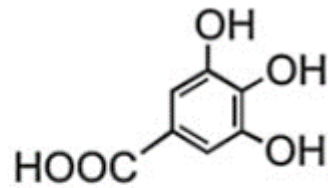


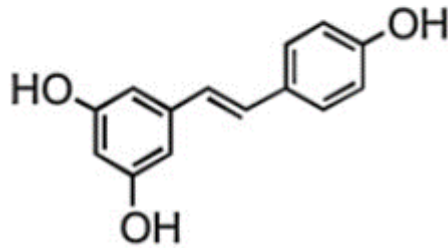
Figure 1-5 Basic structure of flavonoids and its subclasses. Flavonoids have a common C₆-C₃-C₆ structure and are divided into subclasses of dietary importance; namely, flavonols, flavones, isoflavones, anthocyanidins, flavanones and flavan-3-ols (Del Rio et al., 2013), (Rodriguez-Mateos et al., 2014), (Tsao, 2010).

The structural arrangement of hydroxyl groups and glycosylation and/or alkylation patterns of each subgroup has an impact on their biological activity (Tsao, 2010), (Del Rio et al., 2013). Figure 1.6 illustrates examples of chemical structures of compounds from the other main classes of (poly)phenols. For instance, phenolic acids and their usual C₆-C₁ structure is represented by gallic acid, the most common phenolic acid. The main dietary stilbene is resveratrol, which displays the common C₆-C₂-C₆ structure of this class. High concentrations of lignans can be found in cereals grains such as flaxseed, for which one of the main components is secoisolariciresinol (Del Rio et al., 2013), (Pandey and Rizvi, 2009).

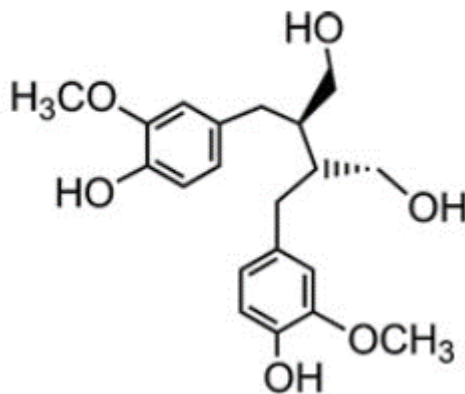
Solubility and stability of (poly)phenols can be increased significantly by glycosylation as oxidation of phenolic group is prevented by glycosyl moieties (Desmet et al., 2012), (Torres et al., 2011). In addition, biological and pharmacological properties of (poly)phenols may also be enhanced by glycosylation (Gantt et al., 2011). This is achieved through improved pharmacokinetics and potency of compounds, facilitated transport by membrane transporters, as well as cell-specific delivery by interaction with carbohydrate specific receptors (Murota et al., 2010). Enzymatic glycosylation of (poly)phenols is catalysed by glycosyltransferases, which are able to transfer sugar moieties from donor molecules to specific aglycons with stereoselectivity (Lairson et al., 2008). Glycosidases are another class of enzymes that are able to transfer single glycosyl moieties or multiple glycosyl groups to (poly)phenolic acceptors (Bojarova and Kren, 2011). Several (poly)phenols are naturally found in glycoside form and some flavonoid glycosides, such as quercetin rutinoside, have been used in the clinical setting (Fang et al., 2013), (Desmet et al., 2012), (Murota et al., 2010).



Gallic acid
(phenolic acid)



Resveratrol
(stilbene)



Secoisolariciresinol
(lignan)

Figure 1-6 Chemical structures of gallic acid, resveratrol and secoisolariciresinol. Gallic acid is the most common phenolic acid, while resveratrol is the main dietary stilbene. Lignans are found in high concentrations in cereal grains such as flaxseed. One of the main components of flaxseed is secoisolariciresinol (Del Rio et al., 2013), (Rodriguez-Mateos et al., 2014).

1.4.1 Bioavailability in humans

The effectiveness of (poly)phenols absorption by the gut, as well as the total amount absorbed, can be measured in blood plasma and urine samples (Arts and Hollman, 2005). The bioavailability of different (poly)phenols is dependent on the food source and nature of attached sugar moieties (Del Rio et al., 2013), (Manach

et al., 2004). The amount of absorption varies between individuals, dependent on microbial populations and the presence of other dietary components (Scalbert and Williamson, 2000). In addition, processing of food material can increase bioavailability of (poly)phenols, as was the case for flavonoids in cocoa powder, determined by analysis of blood and urine samples (Andújar et al., 2012). To add to that, enantiomeric forms of flavan-3-ol in cocoa and green tea have also shown to influence bioavailability of these compounds (Rodríguez-Mateos et al., 2014). Due to different absorption and metabolism rates, intrinsic activity and excretion from the body, the most common (poly)phenol compounds in our diet are not necessarily the most active (Manach et al., 2004).

There are two proposed mechanisms for (poly)phenol absorption. One mechanism involves the lactase phloridizin hydrolase (LPH) enzyme, present in the apical membrane of the small intestine, which deglycosylates and hydrolyses lactose. The very high specificity of this enzyme results in a passive diffusion of aglycone compounds into the cell (Day et al., 2000). Alternatively, absorption is achieved via a mechanism involving cytosolic β -glucosidase (CBG) (Gee et al., 2000). Glucosides are transported into the cell via SGLT1, where it can be hydrolysed and catalysed by CBG (Crozier et al., 2010). Before being released into the bloodstream, (poly)phenol aglycones are conjugated in the intestine, then carried in the bloodstream to the liver for subsequent phase II metabolism and further processing (Scalbert et al., 2002). (Poly)phenols that are not absorbed and metabolised by the gut pass to the colon, where microflora cleaves (poly)phenol glucosides into aglycones for absorption, and consequential transport to the liver (Crozier et al., 2010). In summary, absorption of dietary (poly)phenols is achieved

through hydrolysis by intestinal enzymes or colonic microflora, conjugation in the intestine, and subsequent processing in the liver (Scalbert et al., 2002). Once absorbed, (poly)phenols will accumulate in the target tissue and prompt biological processes (Bahadoran et al., 2013). Plasma concentrations of (poly)phenols after dietary intake are usually nM, with concentrations of 1 μ M generally being reached after consumption of 10-100 mg of a single compound (Scalbert and Williamson, 2000), (Manach et al., 2004). More recently, however, more sensitive analytical methods have shown that plasma concentrations of (poly)phenols might be higher than previously identified. For instance, a study on rats showed a plasma luteolin concentration ranging from 6.88-29 μ M (Li et al., 2015). Furthermore, a study investigating the effect of flavonoids on platelet aggregation identified the concentration of flavonoids in circulation to be of 0.6-122 μ M (Bojic et al., 2012).

1.4.2 Attenuation of disease risk factors by (poly)phenol rich extracts and pure compounds

Evidence from several studies show that various (poly)phenols and (poly)phenol-rich foods have a protective effect against chronic diseases, including CVD, diabetes and cancer (Del Rio et al., 2013). Table 1.1 lists examples of the positive impacts on disease risk factors, in humans, achieved through the consumption of (poly)phenol rich extracts. These same extracts, as well as pure compounds present in high amounts in the extracts, were used in sugar uptake inhibition studies presented in Chapters 4-6. For instance, although many bioactive chemicals are present in green tea catechins, such as (-)-epigallocatechin-gallate (EGCG), are particularly abundant (Higdon and Frei, 2003). In addition, two of the

major reported flavonoid constituents of German chamomile are apigenin and quercetin, the latter directly involved in the reduction of blood glucose levels in rats (Kato et al., 2008). Furthermore, epicatechin and procyanidins are present in high amounts in cocoa and oleuropein is the main constituent of Bonolive extract. Composition of all extracts is shown in Chapter 2 (refer to section 2.1).

Table 1-1 Examples of disease factor attenuation by (poly)phenolic extracts

Extracts	Impact on disease risk factors	References
Bonolive (oleuropein)	↓ inflammation ↓ LDL-cholesterol oxidation ↑ HDL-cholesterol ↓ CHD risk	(Martin-Pelaez et al., 2013) (Impellizzeri et al., 2011)
Black tea	↓ LDL-cholesterol	(Davies et al., 2003)
Cocoa	↑ HDL-cholesterol ↓ blood pressure ↓ relative risk of CVD	(Mellor et al., 2010) (Buijsse et al., 2010)
Coffee	↓ fasting glycaemia ↓ LDL-cholesterol oxidation ↑ endothelial function	(Pimentel et al., 2009) (van Dam and Feskens, 2002) (Manach et al., 2004) (Buscemi et al., 2010)
Eucalyptus Leaf Extract (ELE)	↓ sucrose activity ↓ fructose transport*	(Toda et al., 2001) (Sugimoto et al., 2005)*
German chamomile	↓ cholesterol ↓ blood glucose levels	(McKay and Blumberg, 2006) (Kato et al., 2008) (Zemestani et al., 2016)
Green tea	↓ blood pressure ↓ LDL-cholesterol ↓ all-cause mortality	(Kim and Kim, 2013) (Nantz et al., 2009) (Maron et al., 2003)
Citrus (poly)phenols: hesperidin & hesperetin	↓ hepatic TG accumulation ↓ synthetic enzyme activity ↓ cholesterol	(Jung et al., 2006) (Cha et al., 2001)
Pomegrante	↓ fasting & post-prandial glucose ↓ glycaemic response ↓ gluconeogenesis ↓ inflammation ↑ glycogen synthesis	(Jafri et al., 2000) (Viuda-Martos et al., 2010) (Banihani et al., 2013) (Parmar and Kar, 2008)

* study conducted using mice model

1.4.3 Effect of (poly)phenols on postprandial glycaemia

The glycaemic index (GI) can be defined as the indexing of a glycaemic response from a specific quantity of available carbohydrate in a test food to the same quantity in a standard foodstuff, when consumed by the same individual (Jenkins et al., 2002). In other words, the GI is the blood glucose response of 50 g of carbohydrates expressed as a percentage of the same quantity of carbohydrates from a reference food (Wolever et al., 1991). The GI is a rank of the glycaemic potential of carbohydrates present in various foods in a 'gram for gram' of carbohydrate approach (Marsh et al., 2011).

Prolonged consumption of high GI foods has been shown to play a role in the development of T2DM, obesity and CVD (Ludwig, 2002), (Bornet et al., 2007). Furthermore, serological biomarkers associated with increased relative risk of CHD were elevated after the consumption of a high-glycaemic load diet (Mathews et al., 2015). Low-GI foods, therefore, have been associated with a protection against these chronic diseases. Observational studies suggest that low-GI foods are able to reduce hyperglycaemia and hyperinsulinemia, as well as potentially increasing satiety, when compared to higher-GI foods (Aston, 2006). These observations are in agreement with the hypothesis that higher postprandial glycaemia is 'a universal mechanism for disease progression' (Barclay et al., 2008).

The hormonal control of blood glucose is a critical process in our physiology as failure to maintain energy homeostasis can lead to metabolic syndrome, a disorder associated with obesity, hyperglycaemia, impaired glucose tolerance,

hypertension, dyslipidaemia and a predisposition to T2DM development (Hanhineva et al., 2010). Therefore, slowing down the digestion or absorption of carbohydrates can have beneficial effects to overall health, by helping to reduce disease risk factors (Barclay et al., 2008). This could be achieved by reducing the consumption of high-GI foods and/or incorporating components in our diet that may reduce postprandial glucose (Hanhineva et al., 2010). Dietary (poly)phenols, for instance, may have the potential to slow down blood glucose spikes by inhibiting carbohydrate digestion and rapid sugar absorption (McDougall et al., 2005), (Williamson, 2013). For instance, (poly)phenolic compounds present in green tea, strawberry, raspberry, blueberry and blackcurrant have been shown to significantly inhibit both α -amylase and α -glucosidase, digestive enzymes that are responsible for sugar production (Nyambe-Silavwe et al., 2015), (McDougall et al., 2005). These enzymes are also the targets for a common anti-diabetic drug, acarbose, used in many countries worldwide. For this reason, it is believed that a long-term consumption of specific (poly)phenols could have a comparable effect to acarbose at reducing the risk/progression of diabetes (Williamson, 2013).

Consumption of (poly)phenols has been shown to be beneficial to glycaemic control in several studies. For instance, a meta-analysis including over 280,000 participants and more than 18,000 incidents of T2DM showed that relative risk of diabetes was 0.91 between the highest intake of flavonoids group and the lowest intake of flavonoids group (Liu et al., 2014). The same meta-analysis found that green tea consumption significantly decreased fasting blood glucose levels and lowered concentrations of glycohemoglobin (HbA1c), an early glycation product and marker of chronic glycaemia (Liu et al., 2014). Moreover, a meta-analysis of

22 trials, consisting of 1,584 participants, concluded that green tea consumption led to reductions in fasting glucose (Zheng et al., 2013). A meta-analysis of 24 trials, including 1,106 individuals, showed that cocoa consumption significantly improved insulin sensitivity (Shrime et al., 2011). In addition, short-term intake of cocoa also significantly reduced insulin resistance, as determined in a meta-analysis of 42 trials including over 1,290 individuals (Hooper et al., 2012). A systemic review of 36 trials measuring changes in HbA1c following exposure to (poly)phenol supplementation showed a significant reduction in HbA1c in T2DM patients without any other intervention at glycaemia (Palma-Duran et al., 2017). Furthermore, analysis of data from 3 longitudinal studies identified that consumption of three servings/week of fruits, in particular grapes, apples and blueberries, significantly lowered T2DM risk (Muraki et al., 2013). To add to that, a meta-analysis of 9 studies showed that oral consumption of aloe vera significantly reduced fasting blood glucose and HbA1c (Dick et al., 2016).

1.4.4 Effect of (poly)phenols on sugar uptake by GLUTs

Certain (poly)phenols have also shown to have an impact on postprandial glycaemia control by inhibiting sugar absorption, through inhibition of GLUT transporters. For instance, the flavonoids quercetin and phloretin have shown to be potent inhibitors of GLUT2, in the oocyte and cell model (Kwon et al., 2007). Furthermore, acute exposure of anthocyanin-rich berry extract significantly decreases glucose uptake by GLUT2 in Caco-2 cell model (Alzaid et al., 2013). To add to that, a (poly)phenol-rich intervention, comprised of green tea and berry extracts, had an impact on post-prandial blood glucose *in vivo* by significantly reducing the area under the curve (Nyambe-Silavwe and Williamson, 2016).

Inhibition of the fructose specific transporter GLUT5 is achieved by epigallocatechin gallate (EGCG), one of the main compounds in green tea (Slavic et al., 2009). To date, there have been no inhibitors of GLUT7 identified, which call for further studies to be carried out in order to determine further inhibitors of these three transporters. In this project, the direct inhibition of GLUT2, 5 and 7, expressed in the gut and able to transport fructose, by specific (poly)phenols was investigated. Table 1.2 below summarizes the pure compounds and extracts known to inhibit sugar uptake by GLUT2 and GLUT5. Sugar uptake experiments presented in this table were conducted on the *X. laevis* oocyte model or on both oocyte and cell model. Data from sugar inhibition studies performed for this project, presented in Chapter 4 and 5, which has been published and is included in the table below.

Table 1-2 GLUT2 and GLUT5 inhibition by (poly)phenolic compounds and (poly)phenol rich extracts

GLUT2	Reference
Phloretin, myricetin, fisetin, quercetin, isoquercitrin**	(Kwon et al., 2007)
Green tea and German chamomile tea**	(Villa-Rodriguez et al., 2017a)
Phloretin, quercetin, apigenin, myricetin, EGCG, EGC, ECG	(Johnston et al., 2005)
Quercetin*	(Song et al., 2002)
Pomegranate**	(Kerimi et al., 2017)
GLUT5	
Reference	
EGCG, ECG*	(Slavic et al., 2009)

* Sugar uptake inhibition studies performed in *X. laevis* oocyte model.

** Sugar uptake inhibition studies performed in *X. laevis* oocyte and Caco-2 cell models.

1.5 Research models

1.5.1 Caco-2/TC7 intestinal cell model

The Caco-2 cell system is a well characterized and frequently used *in vitro* model of intestinal absorption, as it allows for transport mechanisms to be investigated, as well as the ability of chemicals to cross the intestinal barrier (Angelis and Turco, 2011). As characteristics of Caco-2 cell line, such as transport properties and permeability, have been shown to be dependent on culture conditions, several clones from this cell line have been isolated (Delie and Rubas, 1997), (Briske-Anderson et al., 1997). The TC7 clone was shown to have a more homogeneous distribution of proteins functional in the gut across the different passage numbers, making it an attractive clone for mimicking the *in vivo* intestinal environment (Turco et al., 2011), (Chantret et al., 1994). In addition, Caco-2/TC7 cells express high levels of sugar transporters critical for intestinal sugar uptake, including SGLT1, GLUT2 and GLUT5 (Sambuy et al., 2005). Previous studies have looked at the effect of high glucose and fructose levels in the expression of GLUT2 and GLUT5, respectively (Mahraoui et al., 1994), (Gouyon et al., 2003). In this project, the Caco-2/TC7 cell model was used to investigate any changes in expression of GLUT7, also expressed in the intestine, in the presence of different sugars as potential substrates. Additional information on this cell model is discussed in Chapter 3.

1.5.2 *Xenopus laevis* oocytes

A 1971 study Gurdon et al showed that oocytes extracted from the South-African clawed frog *Xenopus laevis* synthesized haemoglobin following microinjection with mRNA (Gurdon et al., 1971). The oocytes have accumulated stores of enzymes,

organelles and proteins that are normally used after fertilization which are recruited for heterologous proteins, making them very good single-cell models for protein expression following microinjection with mRNA (Gurdon et al., 1973), (Bianchi, 2006). Mammalian cells express many different sugar transporters, leading to a high basal sugar transport activity. Therefore, it is challenging to determine substrate specificity and kinetics of transport of a single specific sugar transporter (Bentley et al., 2012). For this reason, *Xenopus laevis* oocytes have been extensively used in the characterization of transport kinetics and substrate specificity of an individual transporter, through over-expression of transporters (Nishimura et al., 1993), (Colville et al., 1993), (Kwon et al., 2007). Basal sugar transport activity is low in *X. laevis* oocytes, making it an ideal model for functional characterization of heterologously expressed sugar transporters using radiolabelled sugar substrates. In general, the transport properties observed by heterologously expressed GLUTs in oocytes are similar to the known characteristics of these transporters in mammalian tissues (Bentley et al., 2012). Furthermore, following translation of injected mRNA *X. laevis* oocytes are also able to modify the synthesized proteins in a manner similar to their normal post-translational modification. These modifications are thought to take place in the endoplasmic reticulum (ER) system of the oocyte stimulated by primary and secondary structural signals of the protein (Deacon and Ebringer, 1979).

Other advantages of *X. laevis* oocytes include the fact that they are readily harvested from the female ovary and are built to survive for long periods of time outside the body, needing only to be kept in a simple salt solution with antibiotics to prevent infection. In addition, because of their large size (1-1.2 mm in diameter)

these cells are straightforward to microinject, and their low expression of endogenous membrane transporters and channels means that multiple simultaneous mRNA products can be injected into one oocyte and that standard electrophysiological techniques can easily be performed (Bianchi, 2006)

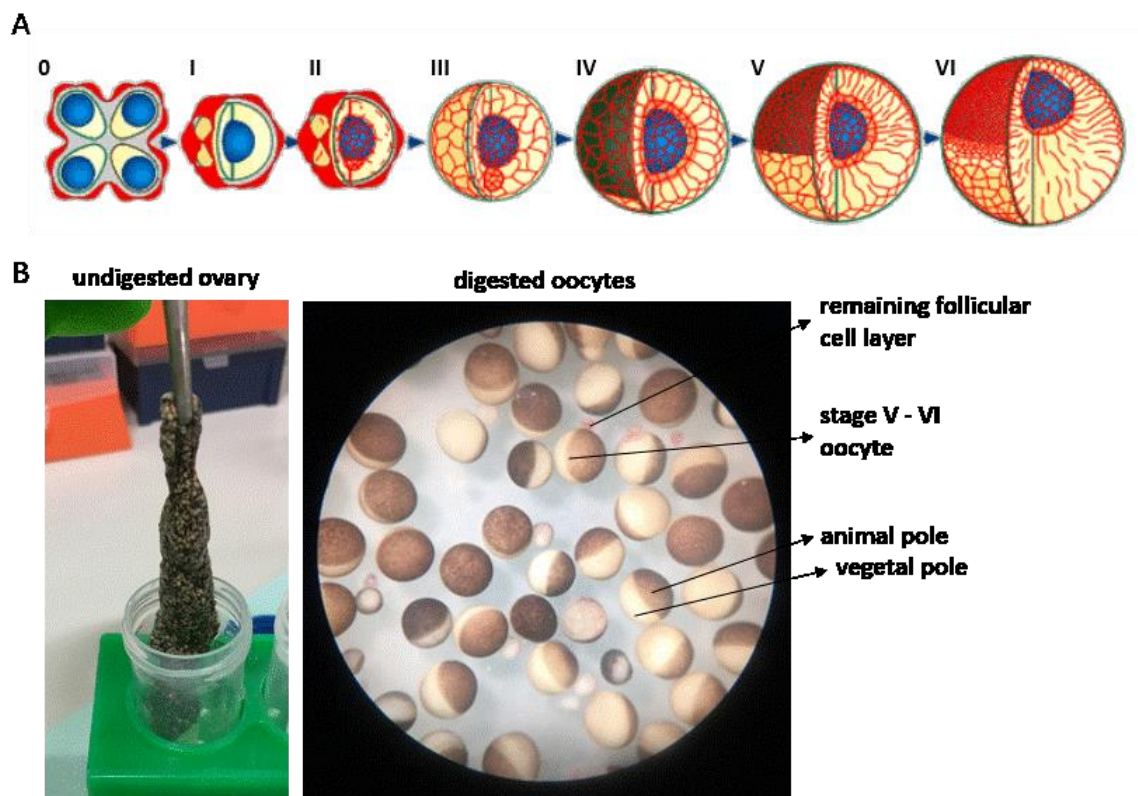


Figure 1-7 *Xenopus laevis* oocyte developmental stages and representation of undigested ovary and digested oocytes. Oocytes are large cells (1-1.2 mm in diameter) that have a characteristic black pigmented region (animal pole and a white non-pigmented region (vegetal pole) (**A**) (Ferrell, 1999). Following the enzymatic digestion of the ovary, stage V-VI oocytes are manually selected for subsequent microinjections (**B**).

Oocytes are immature eggs stored in the abdominal cavity of the adult female in clumps called ovarian lobes, which are made up of oocytes, connective tissue, blood vessels and follicle cells. Oocytes are large individual cells of 1-1.2 mm in diameter and with a surface area of 18-30 mm² (Broer, 2010). Oocytes go through six maturation stages (I-VI), as shown in Figure 1.7 A, of which stage V-VI oocytes

are generally used for heterologous expression and electrophysiological studies due to their larger size. The oocytes have a characteristic black pigmented region and a white non-pigmented region, corresponding to the animal pole and vegetal pole, respectively (Bianchi, 2006). The yolk is concentrated to the vegetal pole of the egg while the animal pole contains the germinal vesicle, or enlarged nucleus (Halley-Stott et al., 2010). A layer of follicular cells separates the oocytes from the external environment, which reportedly interferes with electrophysiological recordings and is removed prior to microinjections by treatment with collagenase (Miledi and Woodward, 1989b), (Miledi and Woodward, 1989a). Enzymatic digestion also significantly facilitates the microinjection procedure as the micropipette encounters less resistance. Figure 1.7 B shows the *X. laevis* ovary before digestion with collagenase, as well as the digested oocytes and their characteristic features. Expression of exogenous proteins in oocytes is most commonly achieved through injection of transcribed RNA into the oocyte cytoplasm (Bianchi, 2006). In this project, mRNA encoding human GLUT2, 5 and 7 was injected into oocytes for expression of these proteins. Sugar uptake experiments in the presence of different (poly)phenols and/or extracts was then carried out and quantified using radiolabelled sugars.

1.6 Research rationale, aims and objectives

1.6.1 Research rationale and purpose

As discussed above, excess dietary sugar consumption contributes to the exacerbation of disease risk factors associated with the development of diabetes and CVD. Increase in consumption of fructose, specifically, has been correlated to

an increase in prevalence of obesity in both the UK and USA (Grundy, 1998). In addition, excess fructose intake has also been directly associated with development of disease risk factors such as hyperglycaemia, hyperinsulinemia, hypertension and hyperlipidaemia (Elliott et al., 2002), (Lim et al., 2010), (Laville and Nazare, 2009), (Johnson et al., 2007). Many of these disease risk factors are also linked to the body's failure to maintain energy homeostasis, suggesting that slowing down carbohydrate digestion or absorption may help reduce disease risk factors and have a beneficial effect on overall health (Hanhineva et al., 2010), (Barclay et al., 2008). Research has shown that (poly)phenols, acquired from many different foodstuffs, have a positive effect on the reduction of many of the disease risk factors associated with CVD and diabetes, including having the potential to slow down blood glucose spikes by inhibiting carbohydrate digestion and sugar absorption (Williamson, 2013), (McDougall et al., 2005), (Hanhineva et al., 2010), (Shrestha et al., 2009). Taking these observations into account, this project focused on investigating the inhibition potential of specific (poly)phenols and extracts on sugar transporters, expressed in the gut and able to transport fructose. Ultimately, the compounds or extracts identified in this study as having the ability to inhibit one or more of the sugar transporters in the intestine could potentially be incorporated in interventions aimed at improving health markers, and control of fructose uptake and post-prandial distribution of sugars in both healthy volunteers and patients with CVD or diabetes.

1.6.2 Project aims

This research aimed to further characterize the lesser known GLUT7 by exploring the changes in expression of this protein in the presence of different sugars.

Furthermore, another main aim of this project was to set up a quantitative model to investigate molecular mechanisms of GLUT2, GLUT5 and GLUT7 inhibition by specific (poly)phenols, to validate and instigate cell culture and *in vivo* work.

1.6.3 Project objectives

Mammalian cells express many different sugar transporters, making it challenging to determine substrate specificity and kinetics of transport of a specific sugar transporter (Bentley et al., 2012). The *Xenopus laevis* oocyte model makes the isolation of each of these transporters possible, allowing for the characterization of transport kinetics and substrate specificity of each individual transporter. In addition, the Caco-2/TC7 intestinal cell model allowed for the investigation of the basal levels of GLUT7 expression, as well as any changes in expression brought about by the presence of different sugars. In summary, the main objectives of this project were:

- To determine the levels of GLUT7 expression in Caco-2/TC7 intestinal model cells.
- To identify changes in GLUT7 protein and mRNA expression caused by culture of Caco-2/TC7 intestinal model cells in the presence of different sugars.
- To design plasmid constructs for heterologous expression of human GLUT2, 5 and 7, and their subsequent expression in the *X. laevis* oocyte model.

- To investigate the potential inhibitory effects of (poly)phenols and extracts on each individual transporter by conducting uptake experiments using radiolabelled sugars.
- To identify common inhibitors for the three transporters investigated.

Chapter 2

General Methods

2.1 Extracts and pure compounds used in inhibition studies

2.1.1 Materials

All solvents used for the methods described in this section were purchased from Thermo Fisher Scientific, Paisley, UK, unless otherwise stated. Ultrapure water was supplied from the Millipore Milli-Q Integral system (resistivity of 18.2 MΩ x cm at 25 °C) and used in aqueous solvents.

Compounds utilized in sugar uptake inhibition experiments were obtained from Sigma-Aldrich, Dorset, UK and were as follows; 2,5-Anhydro-D-mannitol (41107-82-8), acarbose (56180-94-0), apigenin (520-36-5), (-)-Epigallocatechin gallate (EGCG) (989-51-5) and (-)-Epicatechin (490-46-0) derived from green tea (≥ 98%), cytochalasin B (C6762), epicatechin (490-46-0), flavone (525-82-6), galangin (548-83-4), hesperetin (69097-99-0), hesperidin (520-26-3), kaempferol (520-18-3), phloretin (60-82-2) and quercetin (117-39-5).

Extracts used in the sugar uptake inhibition studies were as follows; German chamomile and green tea plant extracts were supplied by PhytoLab & Co (Vestenbergsgreuth, Germany). Pomegranate extract was acquired from CEBAS-CSIC, Spain. Oleuropein-rich Bonolive extract was kindly supplied from BioActor, Ferrer HealthTech, Netherlands. Coffee extract was derived from Nescafe Green

Blend instant coffee and Yorkshire tea was used for experiments with black tea. GLUT5 specific inhibitor 1-O-Benzyl-2-*N*,3-*O*-carbonyl- α -L-sorbofuranosylamine (L-sorbose-Bn-OZO) was kindly supplied by Professor Arnaud Tatibouet from the Université d'Orléans, France. Procyanidins (DP2-DP8) were purified from freeze dried apples using HPLC methods (Hollands et al., 2017) by Dr Paul Needs (IFR, Norwich, UK) and provided within the BACCHUS FP7 project as study material by Dr Paul Kroon. 1 kg of eucalyptus leaves were purchased from Justingredients, Monmouthshire, UK.

All the extracts used in sugar uptake inhibition studies in Chapters 4-6, including the name of supplier and main (poly)phenolic composition, are listed in Table 2.1

Table 2-1 List of extracts used in inhibition studies, including the supplier and main (poly)phenolic composition

Extract name	Supplier	Analysis	Composition
Bonolive	BioActor	Performed by supplier	40% oleuropein
Black tea	Yorkshire tea	Not analysed	Previous documentation suggests black tea is primarily made up of thearubigins, with this phenolics accounting for almost 60% of solids found in a typical sample (Butt et al., 2014)
Baking Chocolate Standard Reference Material	National Institute of Standards and Technology	Described below in section 2.1.5 (Robbins et al., 2012)	171.6 ± 21 µM DP1; 52.1 ± 7 µM DP2; 36.4 ± 10 µM DP3; 32.7 ± 17 µM DP4; 7.5 ± 2 µM DP5; 1.3 ± 0.04 µM DP6; 1.7 ± 0.5 µM DP7; 0.6 ± 0.1 µM DP8; 1.4 ± 1 µM DP9; 1.0 ± 0.8 µM DP10
Cocoa	Lindt Excellence 85% Cocoa Dark Chocolate	Described below in section 2.1.5	120.6 ± 2.4 µM DP1; 99.8 ± 1.9 µM DP2; 39.1 ± 0.8 µM DP3; 17.3 ± 1.7 µM DP4; 9.7 ± 0.2 µM DP5; 3.3 ± 0.3 µM DP6
Coffee	Nescafe Green Blend	Performed by Dr. N. Kraut (Kraut, 2014)	In 4 g (1 cup): 160 ± 8.4 µmol 3-caffeoylquinic acid; 103 ± 6.0 µmol 4-caffeoylquinic acid; 467 ± 9.2 µmol 5-caffeoylquinic acid
Eucalyptus Leaf Extract (ELE)	leaves were purchased from Justingredients	Not analysed	Not entirely identified but isolated components include hydrolysable tannins and favonol glycosides (Sugimoto et al., 2005)

German chamomile	PhytoLab & Co	Performed by Dr. J. Villa-Rodriguez (Villa-Rodriguez et al., 2017b)	12.32% apigenin-7-O-glucoside; 0.28% apigenin 0.13% luteolin-7-O-glucoside; 0.07% 4,5-dicaffeoylquinic acid
Green tea	PhytoLab & Co	Performed by Dr. H. Nyambe (Nyambe, 2016)	199.8 ± 6.7 mg/g (-)-Epigallocatechin gallate (EGCG); 124.4 ± 9.3 mg/g (-)-Epigallocatechin; 34.4 ± 1.9 mg/g (-)-Epicatechin gallate; 23.3 ± 2.4 mg/g (-)-Epicatechin
Pomegrante	CEBAS-CSIC	Performed by Dr. H. Nyambe (Nyambe-Silavwe and Williamson, 2016)	121 mg/g punicalagin; 6 mg/g puricalin; 5.9 mg/g ellagic acid hexose; 101 mg/g ellagic acid

2.1.2 Preparation of Eucalyptus Leaf Extract (ELE) by reflux extraction of eucalyptus leaves

Eucalyptus leaves were extracted following methods previously reported (Sugimoto et al., 2005). In short, 25 g of leaves were extracted in 250 mL 1:2 ethanol-water (1:2 v/v) under reflux for 2 h. Ultrapure water, supplied from the Millipore Milli-Q Integral system (resistivity of 18.2 M Ω x cm at 25 °C), was used in the reflux system. The resulting liquid was filtered with a common paper filter and centrifuged for 20 min at 3,000 *g*. Supernatant was dried in a centrifugal evaporator (Genevac Ltd, Ipswich, UK) and reconstituted in DMSO to 5 mg/mL.

2.1.3 Defatting of dark chocolate product for extract preparation

Defatting of dark chocolate product was conducted as previously described (Robbins et al., 2009). Namely, the dark chocolate product Lindt Excellence 85% Cocoa Dark Chocolate was snap-frozen using dry ice and ethanol, and 20 g was ground to a powder. Defatting of ground chocolate powder was achieved by adding 5 g of powder to 45 mL of hexane (H/0406/PB17) and sonicating for 5 min at 50 °C. The suspension was then centrifuged at 885.4 x *g* for 5 min and hexane supernatant decanted to waste. Sonication and centrifugation steps were carried out twice more and sample was placed in the fume cupboard overnight to allow for all residual hexane to evaporate.

2.1.4 Preparation of dark chocolate extract

A flavanol-rich extract from fat-free Lindt Excellence 85% Cocoa Dark Chocolate product was prepared as previously described (Robbins et al., 2009). In short, an extraction solution of acetone (A/0606/17), water and acetic acid (A/0360/PB15) was prepared (70:29.5:0.5 v/v/v) and a volume of 10 mL was added to 3.4 g of fat-free chocolate powder. The suspension was firstly shaken by hand then vortexed for ~ 2 min, in order to facilitate dispersion of the sample, before being sonicated for 5 min at 50 °C and centrifuged at 885.4 x *g* for 5 min. The supernatant was collected and passed through a strong mixed-mode cation exchange solid phase extraction cartridge (30 µm particle size, MCX 186000252, Walters Oasis, Hertfordshire, UK) after cartridge condition and equilibration, according to manufacturer's instructions, and then filtered through a 0.45 µm pore sized polytetrafluoroethylene (PTFE) membrane syringe filter with 25 mm diameter (6874-2504, Sigma-Aldrich, Dorset, UK). Filtrate was collected, diluted and placed in a HPLC vial (03-FIVA, Thermo Fisher Scientific, Paisley, UK) for chromatographic analysis.

2.1.5 HPLC-FLD protocol for chocolate extract analysis

The flavanol profile of dark chocolate extract was analysed using an Agilent 1200 series with fluorescence detection, as previously described (Robbins et al., 2012). In summary, a Phenomenex Develosil Diol 100 Å column (particle size of 5 µm, 250 × 4.6 mm) and a Phenomenex Cyano SecurityGuard cartridge (4 × 3.0 mm), installed in accordance with the SecurityGuard cartridge kit, were held at a temperature of 35 °C. The flow rate was set to 1 mL/min, injection volume of 5 µL,

and autosampler was set to and held at 5 °C. The mobile phase was a binary gradient of solvents A, consisting of 2% acetic acid in acetonitrile (A/0626/17) (98:2 v/v) and B, consisting of acetic acid in aqueous methanol (M/4058/17) (95:3:2 v/v/v). The starting condition of mobile phase was 7% B, held isocratic for 3 min. Solvent B was then ramped to 37.6% for 57 min and subsequently to 100% for 3 min. This condition of 100% solvent B was held for 7 min before returning to the starting condition of 7% solvent B for 6 min. A post run equilibration was held for 10 min at 7% solvent B. Changes in mobile phase conditions during the total run time of 86 min are listed in Table 2.2. Fluorescence detection was conducted with excitation set at 230 nm and emission set at 321 nm. Varying dilutions of epicatechin were prepared in order to create a calibration standard curve relative to known concentrations of epicatechin. Photomultiplier (PMT) level was set to 9. Calibration curve linearity was maintained for the prepared epicatechin concentrations, ranging from 0.02 mM to 0.5 mM, and linear regression analysis was performed to obtain the R-squared and gradient values. The concentration of each flavanol (μM) present in the chocolate extract was calculated using the epicatechin calibration curve and the individual relative response factors for each fraction (DP1-10), as reported previously (Robbins et al., 2012). Chocolate extract analysis was performed with an increased gain setting (i.e., PMT 12), as well as the PMT 9, to ensure proper dynamic range and enable better measurement of all procyanidins. Flavanol concentration values were adjusted for the change in gain setting by normalization with a correction factor, namely, the average ratio difference in concentration from fractions of same sample analysed at PMT 9 and 12.

Table 2-2 Specific conditions of the mobile phase during the full length of the run.

Run time (min)	% solvent B
0	7
3	7
60	37.6
63	100
70	100
76	7
86	7

The profile obtained for the defatted chocolate extract, from monomer to decamer, was compared against Baking Chocolate Standard Reference Material (2384) kindly supplied by the National Institute of Standards and Technology (USA). Fat-free chocolate reference standard was prepared and analysed in the same manner, described above (refer also to section 2.1.2), as the chocolate extract.

2.2 General methods applied to Caco-2 and Caco-2/TC7 cell model

2.2.1 Materials

Cell culture materials were purchased from Sigma-Aldrich, Dorset, UK, unless otherwise stated. Ultrapure water, supplied from the Millipore Milli-Q Integral system (resistivity of 18.2 M Ω x cm at 25 °C), was used for rinsing cells on the immunostaining protocol. Buffers used in the methods described below were tris buffered saline (TBS) buffer (1706435, Bio-Rad, Hemel Hempstead, UK), phosphate buffered saline (PBS) (P4417), PBS with calcium chloride and

magnesium chloride (PBS+) (D1283) and Hank's balanced salt solution (HBSS) (55021C). Sugars added to growth medium in protein and gene expression analysis were as follows: D-fructose (F/1950/50, Thermo Fisher Scientific, Paisley, UK), D-galactose (BP656-500, Thermo Fisher Scientific, Paisley, UK), D-sucrose (10638403, Thermo Fisher Scientific, Paisley, UK), sorbitol (W302902) and L-glucose (G5500).

2.2.2 Caco-2 and Caco-2/TC7 basic cell culturing

Caco-2/TC7 cells kindly donated by Dr M. Rousset (U178 INSERM, Villejuif, France) were routinely cultured in 25 mM glucose Dulbeccos's modified Eagle's DMEM Medium (D5671) supplemented with 20% (v/v) fetal bovine serum (FBS) (F7524), 2% (v/v) Glutamax™ (35050, Thermo Fisher Scientific, Paisley, UK), 2% (v/v) non-essential amino acids (M7145), 100 U/mL penicillin and 0.1 mg/mL streptomycin (P0781) at 37 °C with 10% CO₂ in a humidified atmosphere. Caco-2 cell line (HTB-37) was obtained from ATCC (Manassas, USA). This cell line was cultured in the same conditions as Caco-2/TC7 with the following alterations; cultured in 5.5 mM glucose Dulbeccos's modified Eagle's Medium (D5546), supplemented with 15% (v/v) FBS, with 5% CO₂ in a humidified atmosphere. Both Caco-2 and Caco-2/TC7 cells were sub-cultured at ~ 90% confluence, through detachment with 0.25% trypsin (T4049), and seeded on flasks at a density of $1 \times 10^4 \text{ cm}^{-2}$ and medium was replaced every two days. Cells were used between passage number 28 and 45. Transepithelial electrical resistance (TEER) is a good indicative of cell layer differentiation state, as with the formation of tight junctions the TEER of a cell layer is increased. Therefore, to confirm integrity of cell layer

TEER was measured prior to cell scraping for mRNA and/or protein analysis. A TEER value of 200 Ω or above was deemed acceptable.

2.2.3 GLUT7 gene expression analysis

Caco-2/TC7 cells were seeded on 6-well Transwell plates (0.4 μm pore size, polycarbonate, Corning, UK) at a density of $6 \times 10^4 \text{ cm}^{-2}$ and kept for 21 days in the conditions listed above. During the first 7 days post-seeding cells were grown in asymmetric conditions, namely, FBS was only included in the medium added to the basolateral side of each well in the Transwell plates. Throughout the whole differentiation period cells were grown in glucose-only medium or medium supplemented with 25 mM of one of the following sugars; fructose, sorbitol, galactose, L-glucose and sucrose on apical side only, or both apical and basolateral sides. Medium was replaced every second day. At day 21, cells were washed twice with ice-cold PBS solution, scraped, and mRNA material was extracted from cells using the Aurum Total RNA Mini Kit (Bio-Rad 732-6820, Hemel Hempstead, UK), following manufacturer's instructions. Reverse transcription of RNA to cDNA was performed using the Applied Biosystems high capacity RNA to cDNA kit (4387406, Life Technologies, USA) and PCR reaction to quantitatively determine gene expression was performed using TaqMan's duplexed FAM/VIC assays in a QX100 Droplet digital PCR system (Bio-Rad), as previously described (McDermott et al., 2013). In short, triplicate reactions of 20 μL stock sample solution were prepared by adding 9 μL total transcribed nucleic acids (5 ng), 1 μL GLUT7 (SLC2A7) FAMTM-labelled TaqMan primer (Hs01013553_m1, Thermo Fisher Scientific, Paisley, UK) and 10 μL of ddPCR Supermix for Probes (Bio-Rad).

TBP (TATA box binding protein) (Hs00427620_m1, Thermo Fisher Scientific, Paisley, UK) was added to final stock sample solution to act as a reference. Droplets were generated through the PCR reactions, as per manufacturer's instructions, by the QX100 Droplet generator (Bio-Rad) and then transferred to a 96-well PCR plate, which was subsequently sealed at 180 °C using a PX1 PCR plate sealer (Bio-Rad). End point PCR was conducted in a C1000 Touch thermal cycler (Bio-Rad) under the following conditions; 95 °C (10 min), 39 cycles of 94 °C (0.5 min) followed by 57.8 °C (1 min), 98 °C (10 min) and cooling at 12 °C. The fluorescence produced by the droplets was quantified by the QX100 droplet reader (Bio-Rad). Concentrations of target and reference DNA (copies/ μ L) were presented as a ratio. All reactions were performed in duplex mode. All data were analysed with the QuantaSoft software (Kosice, Slovakia). General principle droplet making and quantification is represented in Figure 2.1.

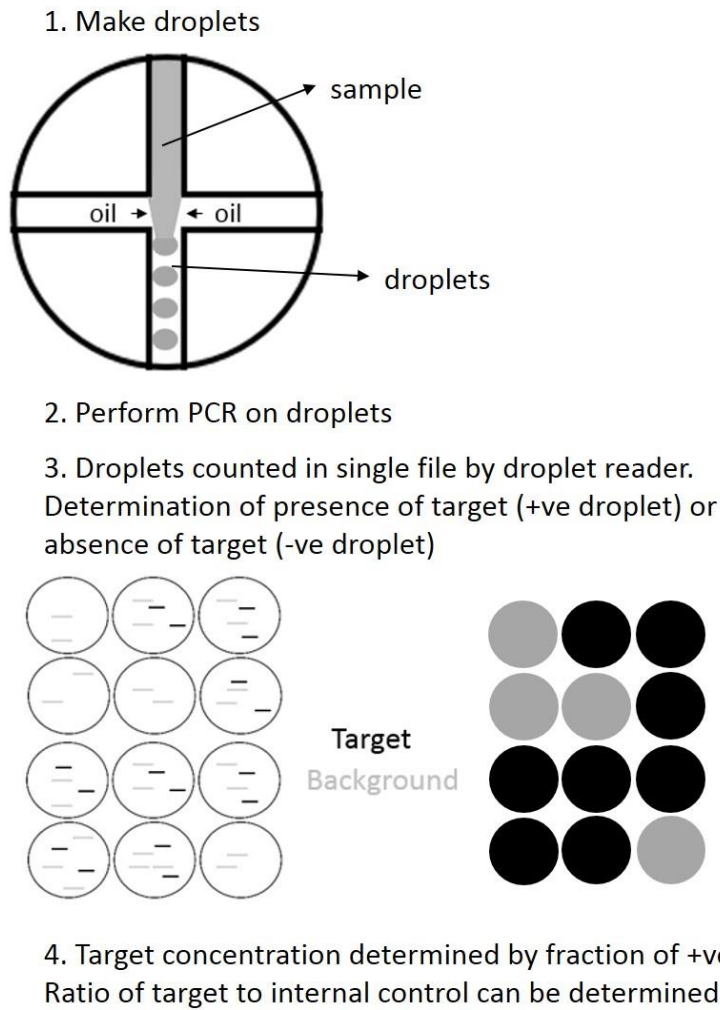


Figure 2-1 Representation of general principle of droplet making and quantification. Once droplets are formed and PCR is conducted individual droplets are passed through a two-colour detection system that determines which droplets are positive/negative for presence of target. (Adapted from Bio-Rad digital PCR workflow)

2.2.4 Immunofluorescence staining

Caco-2/TC7 cells were seeded at a density of $6 \times 10^4 \text{ cm}^{-2}$ on Millicell cell culture inserts (12-well, PET 0.4 mm pore size, Millipore) and maintained in conditions described above for 21 days, with media changed every two days. Cells were fixed with the addition of 4% *para*-formaldehyde in PBS to each well and insert. Inserts were then placed on a small volume of 5 $\mu\text{g}/\text{mL}$ Fluorescein labelled Wheat Germ

Agglutinin (WGA) (FI-1021, Vector Laboratories, Peterborough, UK) in HBSS and incubated at 37 °C for 10 min. Cells were washed three times with PBS+ and permeabilized with 0.1% Triton-X100 for 20 min at room temperature before being incubated with GLUT2 (ab95256, Abcam, Cambridge, UK), GLUT5 (sc271055, Santa Cruz Biotechnology, Dallas, TX, USA) or GLUT7 (NBP1-81821, Novus Biologicals, Littleton, CO, USA) primary antibody at a 1:50 dilution for 1 h, also at room temperature. Three washes with PBS were performed on the cells which were then incubated with either Cy3-conjugated AffiniPure donkey anti-mouse IgG (415-165-150, Jackson ImmunoResearch, USA) or anti-rabbit IgG (711-165-152, Jackson ImmunoResearch, USA) secondary antibodies at a dilution of 1:300. Cells were washed three times with PBS, stained with 2 µg/mL 4',6-diamidino-2-phenylindole (DAPI) for 5 min, rinsed with water, and mounted onto microscopy slides using ProLong Gold antifade reagent mounting medium (P36930, Thermo Fisher Scientific, Paisley, UK). Images were obtained from a Zeiss LSM 700 Inverted Confocal Microscope. Cells imaged without the WGA cell membrane marker were permeabilized once fixed and processed for imaging in the same way as described above, with the exception that Alexa Fluor 488-conjugated AffiniPure donkey anti-rabbit IgG (711-545-152, Jackson ImmunoResearch, USA), at a dilution of 1:300, was used in the secondary antibody incubation step.

2.2.5 Cell surface protein biotinylation

Cells were seeded onto 6-well Transwell plates and maintained for 21 days, as described previously. During the first 7 days post-seeding, cells were grown in asymmetric conditions with no FBS added to the apical medium. Throughout the

whole differentiation period, cells were grown in glucose-only medium or medium supplemented with 25 mM fructose on the apical side only, or on both apical and basolateral sides. A change of media was done every second day. Cell surface biotinylation was performed using Pierce Cell Surface Protein Isolation Kit (89881, Thermo Fisher Scientific, Paisley, UK) according to manufacturer's instructions. The general principle for this method is illustrated in Figure 2.2. In brief, cells were washed twice with ice cold PBS+ before being incubated with Sulfo-NHS-SS-Biotin for 30 min, on ice, on a low speed shaker. Quenching solution was added to each well and cells were then washed twice with TBS. Cells were scraped and lysed in 60 mM octylglucoside/150 mM NaCl/ 20 mM Tris solution (pH 7.4), containing protease inhibitors (P8340), for 30 min on ice, then cell debris was pelleted by centrifugation at 14,000 x g for 5 min. Clarified supernatant was transferred into a new tube and protein concentration for each cell lysate was determined using LabTech-Nanodrop ND100 spectrophotometer. Meanwhile, NeutrAvidin Agarose beads were added to Pierce Spin Columns (69725, Thermo Fisher Scientific, Paisley, UK) and columns were then washed twice with TBS and lysis buffer. Lysates were added to their corresponding filter columns, at comparable protein concentrations, and incubated at room temperature on a rotator at low speed for 1 h. Filter columns were washed twice with TBS and then treated with Rapid PNGase F (P0710S, New England Biolabs, Ipswich, USA) for 15 min at 37 °C. Biotinylated membrane fractions were eluted with SDS-PAGE sample buffer containing 0.5 M dithiothreitol (DTT) following a 20 min incubation at 37 °C with this elution solution. Samples were stored at -80 °C.

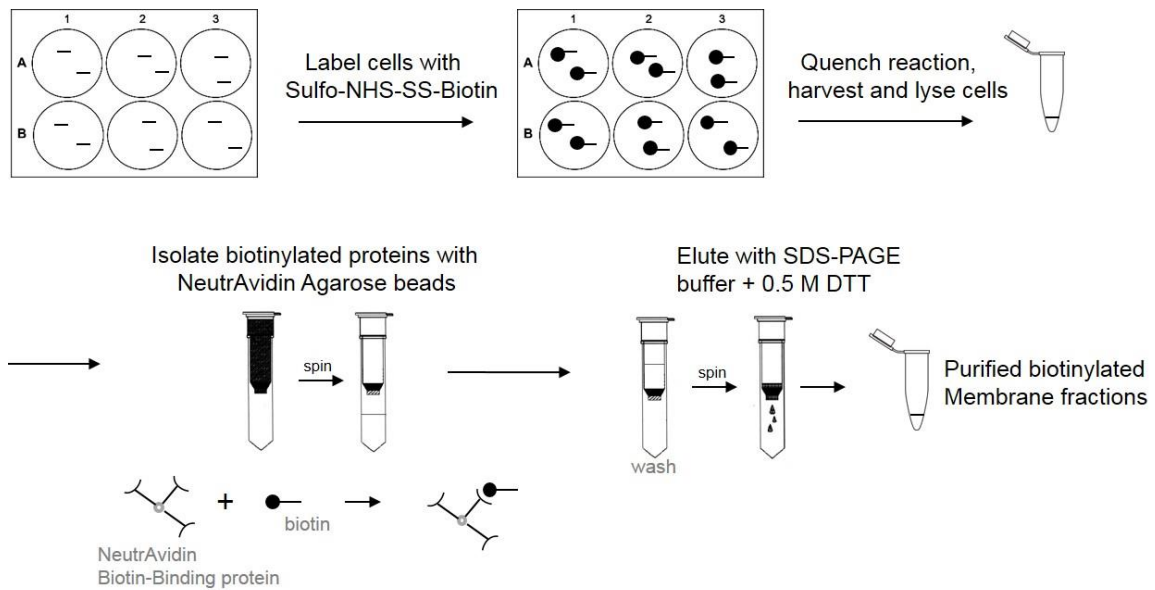


Figure 2-2 Cell surface biotinylation procedure summary. Cultured Caco-2/TC7 cells were labelled with Sulfo-NHS-SS-Biotin for 30 min on ice. Quenching solution is added to the cells which were washed, harvested and lysed. Cell proteins bound to biotin were isolated with NeutrAvidin Biotin-binding protein with the use of a filter spin column. Purified biotinylated membrane protein extract was eluted with SDS-PAGE elution buffer containing 0.5 M DTT.

2.2.6 Protein analysis

Expression of GLUT7 on biotinylated membrane cell samples was determined with ProteinSimple's automated Western blot system 'Wes' according to manufacturer's instructions with the exception of denaturing of samples, which was done at 37 °C for 15 min as GLUTs have shown a tendency to degrade at higher temperatures. Cell lysate samples were treated with Rapid PNGase F (P0710S, New England Biolabs, Ipswich, USA) for 15 min prior to the denaturing step. GLUT7 antibody (NBP1-81821, Novus Biologicals, Littleton, CO, USA) dilution was 1:10 and NaKATPase antibody dilution was 1:100. Optimal loading concentration for cell lysate samples was 0.4 mg/mL and membrane fraction biotinylated samples were loaded without dilution.

2.2.7 Statistical analysis

Protein and gene expression experiment results were interpreted as a ratio of loading controls. Each data point represents the mean of three biological replicates, and three technical replicates in gene expression assays, \pm SEM. Cells cultured in standard medium containing only glucose were used as controls for all experiments, for which results were normalized to. Data from biological replicates were combined by normalizing each individual experiment by the control and ANOVA was performed to determine any statistical difference. Two tailed homoscedastic Student's t-test was used to award significance to specific conditions normalized to the glucose control.

2.3 Molecular biology

2.3.1 Materials

Bacterial competent cells used for transformations were Stellar™ Competent Cells (*E. coli* HST08 strain) (636763, Clontech, Saint-Germain-en-Laye, France). Agar powder (L2897, Sigma-Aldrich, Dorset, UK) was solubilized with Ultrapure water, supplied from the Millipore Milli-Q Integral system (resistivity of 18.2 M Ω x cm at 25 °C), and autoclaved. Under a flame, antibiotics were added to melted agar and poured onto D x H 120 mm x 20 mm petri dishes (CLS430591, Sigma-Aldrich, Dorset, UK) which were left to set at room temperature then stored at 4 °C for up to 14 days. Before use all agar plates were warmed, upside down, at 37 °C. Ampicillin (BP1760-5, Thermo Fisher Scientific, Paisley, UK) was used to make Amp+ plates, and Spectinomycin (22189-32-8, Sigma-Aldrich, Dorset, UK) was

utilised to make Spc+ plates. Luria-Bertani (LB) broth (71751, Lennox-Novagen, Hertfordshire, UK) was solubilized in Ultrapure water and autoclaved before use.

Gels used for electrophoresis were made up using agarose (EP-0010-05, Eutogentec, Hampshire, UK) in 1% Tris base, acetic acid and EDTA (TAE) buffer (diluted with Ultrapure water from 50x TAE buffer, 161-0743, Bio-Rad, Hertfordshire, UK) with SYBR Safe DNA Gel Stain (S33102, Thermo Fisher Scientific, Paisley, UK). Size of DNA products was compared against a 1 kb DNA HyperLadder (BIO-33025, Bionline, London, UK).

RNA denaturing gels were made by dissolving 0.75 g agarose in 36 mL Ultrapure water and adding 5 mL 10x MOPS buffer (BP2900500, Thermo Fisher Scientific, Paisley, UK) and 9 mL 37% formaldehyde (C5300-1, Bio Basic, Ontario, Canada). The size of mRNA products was determined against a ssRNA Ladder. All gel images were obtained from exposing the gel on a Dark Reader Transilluminator (DR-46B, Clare Chemical Research, Dolores, CO, USA) and imaging on a DigiDoc-It Imaging System darkroom (76-0311-01, UVP, Cambridge, UK).

Universal and customized primers used for sequencing reactions of each vector are listed in Tables 2.3 and 2.4, respectively.

Glycerol stocks were made by adding 500 μ L 50% glycerol to 500 μ L cells in LB broth into a Cryotube Vial (368632, Thermo Fisher Scientific, Paisley, UK). All glycerol stocks were stored at -80 °C. Glycerol (G/P450/05, Thermo Fisher Scientific, Paisley, UK) was diluted with Ultrapure water to 50% and autoclaved before use.

Complete sequence of expression vector and plasmid constructs can be found in the appendix.

Table 2-3 List of universal primers, and their sequence, used for sequencing reactions of each vector.

Universal primer name	Sequence	Plasmid
T7	5' - TAA TAC GAC TCA CTA TAG GG - 3'	SLC2A5 in pANT7_cGST, GLUT7pGEM-HE
SP6	5' - GAT TTA GGT GAC ACT ATA G - 3'	pBF GLUT5pBF GLUT2pBF GLUT7pBF
CMV-Forward	5' - CGC AAAT GGG CGG TAG GCG TG - 3'	pcDNA3.2/v5-DEST hGlut2
M13-Forward	5' - GTA AAA CGA CGG CCA G - 3'	SLC2A7 in pENTR223.1
M13-Reverse	5' - CAG GAA ACA GCT ATG AC - 3'	pcDNA3.2/v5-DEST hGlut2 SLC2A7 in pENTR223.1

Table 2-4 List of customized primers, and their sequence, used for sequencing reactions of each vector.

Primer name	Sequence	Plasmid
pBF-Forward	5' - CGC TCA ACT TTG GCA GGG ATC CG - 3'	GLUT5pBF GLUT2pBF GLUT7pBF
pBF-Reverse	5' - GTG TTC TTG AGG CTG GTT TAG TGG - 3'	GLUT5pBF GLUT2pBF GLUT7pBF
GLUT5_1703-F	5' - CAG CAT CGT CTG TGT CAT CTC CTA CG - 3'	SLC2A5 in pANT7_cGST GLUT5pBF
GLUT5_1068-F	5' - GTG GTG CCC CAG CTC TTC ATC ACT G - 3'	GLUT5pBF
GLUT2_509-F	5' - TTG GAG TTG GCG CTG TAA AC - 3'	pcDNA3.2/v5-DEST hGlut2, GLUT2pBF
GLUT7_1390-F	5' - GGC TAC AAC CTC TCT GTG GT - 3'	GLUT7pGEM-HE SLC2A7 in pENTR223.1 GLUT7pBF
GLUT7_2124-F	5' - CTC CTC TCC ATC ATC GTG CT - 3'	GLUT7pBF
GLUT7_2254-F	5' - CTG GCG TCG TCA ACA TAG TG - 3'	GLUT7pGEM-HE GLUT7pBF
GLUT7_841-F	5' - CTC CTC TCC ATC ATC GTG CTC ATG G - 3'	GLUT7pBF

2.3.2 Propagation of pBF expression vector and human GLUT2, 5 and 7 gene containing vectors

Plasmid vector pBF (SP6 promoter), an amphibian expression vector widely used in heterologous expression of proteins in *X. laevis* oocytes that contains specific

characteristics contributing to mRNA stability, was kindly provided by Dr. Jonathan Lippiat (Faculty of Biological Sciences, University of Leeds, UK) Human GLUT5 gene was obtained from SLC2A5 in pANT7_cGST plasmid (DNASU, Tempe, USA), human GLUT2 gene was derived from pcDNA3.2/v5-DEST hGlut2 plasmid (Addgene, Cambridge, MA, USA) and human GLUT7 gene was acquired from SLC2A7 in pENTR223.1 plasmid (DNASU, Tempe, USA). GLUT7 mRNA was also prepared from GLUT7pGEM-HE plasmid (T7 promoter), kindly supplied by Debbie O'Neill of Prof. Chris Cheeseman's group (Department of Physiology, Alberta University, Canada). All vectors were sequenced with universal primers for their promoter or specific regions, as well as specific primers designed against the different areas of the gene of interest, to confirm sequence provided. A list of primers used for sequencing of each vector is listed above in Table 2.4. The vectors, excluding SLC2A7 in pENTR223.1 plasmid, were transformed into competent cells (*E. coli* HST08 strain), according to supplier's instructions. Cells were spread over an Ampicillin containing agar plate (Amp⁺ agar plate) and incubated overnight at 37 °C before being added to 250 mL LB broth, containing 250 µL Ampicillin, and incubated overnight on a shaker at 37 °C and 190 rpm. A portion of purchased glycerol stock from SLC2A7 in pENTR223.1 plasmid was spread over a Spectinomycin containing agar plate, incubated overnight at 37 °C, then added to LB broth with Spectinomycin and incubated overnight in the same conditions described above. Contents of each LB broth flask were put through a EndoFree Plasmid Maxikit (12362, Qiagen, Les Ulis, France) for plasmid DNA extraction. Nucleic acid concentration was measured using a LabTech-Nanodrop ND100 spectrophotometer.

2.3.3 Design of plasmid constructs by insertion of human GLUT genes into pBF expression vector

2.3.3.1 Recombinant hGLUT5 plasmid construct (GLUT5pBF)

Expression vector, pBF, was linearized with XbaI (RG181 Promega, Madison, WI, USA). Primers were designed to contain a short end region homologous to each end of the GLUT5 gene sequence, as available in SLC2A5 in pANT7_cGST plasmid, as well as a region homologous to linear pBF. Specific primers containing homologous 'sticky-ends' were as follows; forward primer 5'-GGT TAA CTA GTC CGA ACC ACG GGG ACG TG- 3' and reverse primer 5' -CGA TGA ATT CTA TCA CAA CTG TTC CGA AG- 3'. Primers were added to SLC2A5 in pANT7_cGST plasmid and CloneAmp HiFi PCR premix (639298, Clontech, Saint-Germain-en-Laye, France) and PCR was conducted in a C1000 Touch thermal cycler (Bio-Rad) under the following conditions; 98 °C (1 min), 35 cycles of 95 °C (0.5 min), 60 °C (0.5 min) and 72 °C (2 min), followed by 72 °C (4 min) and cooling/hold at 4 °C. Figure 2.3 below illustrates, in general terms, the process of ligation of GLUT gene insert into pBF expression vector. Electrophoresis was performed on linear pBF and PCR product on a 1% agarose gel for 45 min at 70 V in 1% TAE buffer. DNA was extracted from gel band products using Zymoclean Gel DNA recovery kit (D4002, Zymo Research, Cambridge, UK). The DNA products were ligated together to produce GLUT5pBF using In-Fusion HD Cloning kit (638909, Clontech, Saint-Germain-en-Laye, France). The insert was transformed into bacterial competent cells and incubated overnight, as described above (refer to 1.3.1). Individual colonies were extracted and added to 5 µL of water. A streak

plate of colonies was created by gently running the end of each pipette tip used to extract colonies onto an Amp⁺ plate. Colonies were boiled at 95 °C for 5 min and PCR was performed with the addition of GoTaq Green Master Mix (M7123, Promega, Southampton, UK), pBF-Reverse primer and GLUT5_1703-Forward primer in a C1000 Touch thermal cycler (Bio-Rad). Electrophoresis was performed on PCR products, as above, and colonies that produced individual bands (product size equal to number of base pairs between two primers; 466 base pairs, and number of base pairs from start of GLUT5_1703-Forward primer until the end of sequence; 3244 base pairs) were propagated from the streak plate in 5 mL LB broth, containing 5 µL ampicillin, and incubated overnight on a shaker at 37 °C and 190 rpm. Plasmid DNA extraction was performed using Qiaprep Spin Miniprep Kit (27106, Qiagen, Les Ulis, France) and nucleic acid concentration was measured using a LabTech-Nanodrop ND100 spectrophotometer. Sequencing confirmed which colonies were positive for the presence of the GLUT5 gene. A chosen positive GLUT5pBF colony was propagated from streaked plate in 250 mL LB broth plus Ampicillin and DNA was then extracted, as described above (see 2.3.1). A glycerol stock of this GLUT5pBF clone was prepared and stored at - 80 °C.

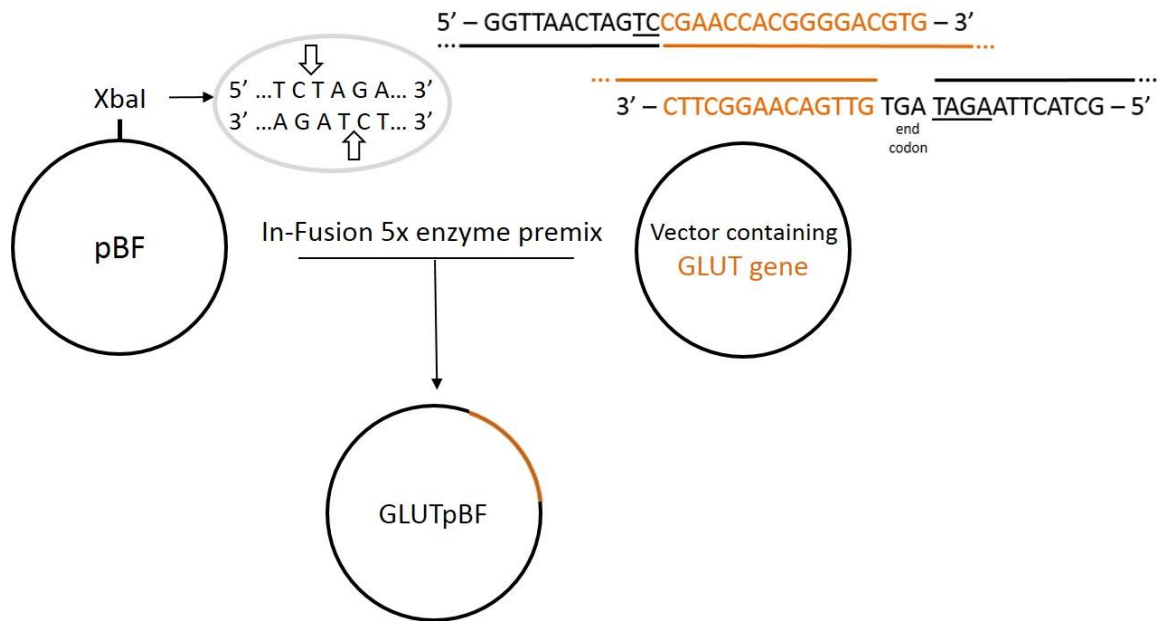


Figure 2-3 Ligation of insert (GLUT gene) into pBF expression vector. pBF is digested with XbaI restriction enzyme at a specific site, creating 'sticky-ends'. Primers are designed to have homology to linear pBF as well as GLUT sequence; in this example, GLUT5pBF primers are shown. PCR of GLUT containing plasmid is performed, followed by ligation of products with linear pBF vector.

2.3.3.2 Recombinant hGLUT2 plasmid construct (GLUT2pBF)

Primers were designed, as described previously, to contain homologous ends to linear pBF expression vector as well as GLUT2 sequence. Specific primers with homologous 'sticky-ends' were as follows; forward and reverse primers were 5' - CCG GGT TAA CTA GTC CCA CTG CTT ACT GGC TTA TC- 3' and 5' -TAT CGA TGA ATT CTA TCA GGG TTC CTT CCG GTA TTG TC- 3', respectively. Expression vector was linearized and PCR was performed on SLC2A5 in pANT7_cGST plasmid with the homologous end primers, as described above (refer to 2.3.2.1), under the following conditions; 95 °C (1 min), 30 cycles of 98 °C (10 sec), 65 °C (15 sec) and 72 °C (10 sec), followed by 72 °C (2 min) and cooling/hold at 4 °C. Much the same as the methods described above (see 2.3.2.1)

electrophoresis of linear product and PCR product was performed, followed by DNA extraction from agarose gel and ligation of DNA products, with subsequent transformation into competent bacterial cells. Colonies extracted from Amp⁺ plates were added to 5 mL LB broth with 5 µL Ampicillin and incubated overnight on shaker at 37 °C and 190 rpm. Plasmid DNA extraction was performed using Qiaprep Spin Miniprep Kit and nucleic acid concentration was measured using a LabTech-Nanodrop ND100 spectrophotometer. Glycerol stocks were prepared for each colony by adding 500 µL 50% glycerol to 500 µL propagated DNA in LB broth. DNA from all extracted colonies was digested with HindIII restriction enzyme (R60471, Promega, Madison, WI, USA). Electrophoresis was performed on digested plasmid DNA and positive colonies for GLUT2pBF (those that produced a two band product, one for restriction site on the pBF sequence and one for restriction site on the GLUT2 sequence) were sequenced to confirm the presence of the GLUT2 gene. DNA from one chosen positive GLUT2pBF colony was propagated from its glycerol stock in 250 mL LB broth plus Ampicillin, followed by DNA extraction, as described above (see 2.3.1). A glycerol stock of this GLUT2pBF clone was prepared and stored at - 80 °C.

2.3.3.3 Recombinant hGLUT7 plasmid construct (GLUT7pBF)

This construct was made using the same methods described in the previous section (refer to 2.3.2.2), with the following exceptions; primers containing homologous ends to linear pBF and GLUT7 sequence were designed and are as follows; forward primer 5' - CCG GGT TAA CTA GTC GTT GTA AAA CGA CGG CCA GT - 3' and reverse primer 5' - TAT CGA TGA ATT CTA TCA CCA GGA AAC

AGC TAT GAC CAT - 3'. PCR was conducted on SLC2A7 in pENTR223.1 plasmid using homologous end primers under the following conditions; 30 cycles of 98 °C (10 sec), 55 °C (15 sec) and 72 °C (0.5 min), followed by cooling/hold at 4 °C.

2.3.4 Confirmation of G7pGEM-HE plasmid sequence

In order to confirm the presence of hGLUT7 gene in the GLUT7pGEM-HE plasmid, the DNA extracted following the propagation of the plasmid was digested with KpnI (R6341, Promega, Madison, WI, USA) and HindIII restriction enzymes. Electrophoresis of the digest on a 1% agarose gel was performed. A two band product (one for each restriction enzyme) was sequenced to confirm presence of the GLUT7 gene. The primers used for sequencing of this vector are listed in Table 2.3.

2.3.5 Isolation of mRNA encoding hGLUT2, hGLUT5 and hGLUT7 genes

Restriction enzymes were utilized to digest each individual recombinant plasmid; PmlI (R05325, New England Biolabs, Ipswich, USA) was used to linearize GLUT2pBF plasmid, MluI (RG381, Promega, Madison, WI, USA) was used to linearize GLUT5pBF plasmid, either PmlI and MluI were used to linearize GLUT7pBF, and GLUT7pGEM-HE was digested with NheI (R6501, Promega, Madison, WI, USA). Linear DNA products, with the exception of GLUT7pGEM-HE, were added to SP6 polymerase mMESSAGE mMACHINE® (AM1340, Ambion, Applied Biosystems, Warrington, UK) in vitro transcription kit and capped RNA

products were obtained, according to manufacturer instructions. A T7 polymerase mMESSAGE mMACHINE® (AM1344, Ambion, Applied Biosystems, Warrington, UK) *in vitro* transcription kit was used to produce mRNA derived from linear GLUT7pGEM-HE product. A general template for the *in vitro* transcription method described here is presented in Figure 2.4. Concentration of the mRNA products was measured using LabTech-Nanodrop ND100 spectrophotometer. The size of each product was determined by electrophoresis of a small quantity of mRNA on a 1.5% agarose 2.2 M formaldehyde RNA denaturing gel for 70 min at 75 V in 1x MOPS buffer. Gel was stained with SYBR Gold Nucleic Acid Stain (S11494, Thermo Fisher Scientific, Paisley, UK) for 30 min before being imaged.

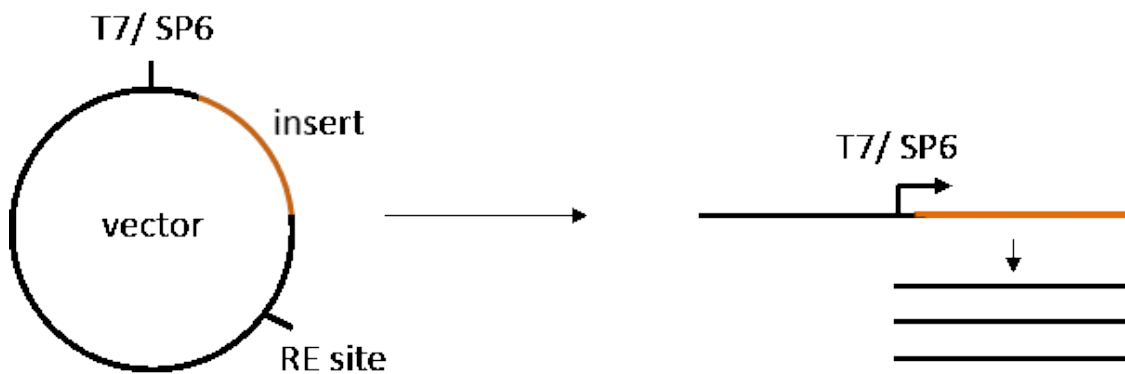


Figure 2-4 General template for *in vitro* transcription reaction of plasmid constructs. GLUT gene inserts were all inserted between a specific single restriction enzyme (RE) site and the promoter (T7 or SP6). Vector is linearized at the RE site and the transcription begins on the first base of promoter region, ending when template terminates and enzyme falls off it. This set up allows for generation of multiple specific RNA transcripts. (Beckert and Masquida, 2011)

2.4 Microinjection of mRNA into oocytes and sugar uptake experiments

2.4.1 Materials

Xenopus laevis ovary from adult females were received from the European Xenopus Resource Centre, University of Portsmouth, UK. Materials utilized for this method were purchased from Sigma-Aldrich, Dorset, UK, unless otherwise stated. Before and following digestion, oocytes were washed in a filter sterilised salt solution entitled OR2, containing 82.5 mM NaCl (433209), 2.5 mM KCl (7447-40-7, Thermo Fisher Scientific, Paisley, UK), 1 mM MgCl₂ (M8266), 5 mM HEPES (7365-45-9) at pH 7.4. Once digested and/or microinjected, oocytes were kept in calcium containing ND96-ACT filter sterilized salt solution containing 96 mM NaCl, 2 mM KCl, 1.8 mM CaCl₂ (10043-52-4, Thermo Fisher Scientific, Paisley, UK) 1 mM MgCl₂, 5 mM HEPES at pH 7.4 with the addition of 50 µg/mL tetracycline (BP912-100, Thermo Fisher Scientific, Paisley, UK), 100 µg/mL amikacin (BP2643-1, Thermo Fisher Scientific, Paisley, UK) and 100 µg/mL ciprofloxacin (33434-100MG-R, Sigma-Aldrich, Dorset, UK). Solutions were made up using ultrapure water, supplied from the Millipore Milli-Q Integral system (resistivity of 18.2 MΩ x cm at 25 °C), which was also used in the control water microinjections.

Radiolabelled sugars used in uptake experiments were as follows: 2-[¹⁴C(U)]-Deoxy-D-Glucose ([¹⁴C] deoxy-D-glucose) [Specific Activity: 250-350 mCi (9.25-13.0 GBq)/mmol, 50 µCi (1.85 MBq)] (NEC720A050UC) and D-[¹⁴C(U)]-Glucose ([¹⁴C] glucose) [Specific Activity: 250-360 mCi (9.25-13.3 GBq)/mmol, 250 µCi (9.25 MBq)] (NEC042X250UC) were purchased from PerkinElmer, Waltham, MA,

USA. D-[¹⁴C(U)]-Fructose ([¹⁴C] fructose) [in ethanol:water (9:1) solution, 100 μCi/mL, 50 μCi (1.85 MBq)] was purchased from Moravek Inc., Brea, CA, USA.

Incubation solutions were made up with the following sugars, D-fructose (F/1950/50), D-glucose (50-99-7) and 2-deoxy-D-glucose (154-17-6) purchased from Thermo Fisher Scientific (Paisley, UK).

2.4.2 Preparation of *Xenopus laevis* oocytes for microinjection and expression of recombinant hGLUT2, hGLUT5 and hGLUT7

Xenopus laevis oocytes were isolated and microinjected as described previously (Kwon et al., 2007). Briefly, approximately one quarter of the ovary was manually cut, placed into a 50 mL tube and washed three times with calcium free OR2 solution. The ovary was incubated in 1 mg/mL collagenase A (10103578001) in OR solution at room temperature for 90 min or until fully digested. The digest was washed with OR2 solution and subsequently kept at 18°C in ND96-ACT medium, containing antibiotics, until microinjection. One day post digestion stage V-VI oocytes were visually selected from digest using a pasteur pipette and microinjected with 50 nl of protein mRNA or water, to be used as controls, using an air pressure injector (PV 820, Pneumatic PicoPump, WPI) (Figure 2.5). Microinjection tips were made using a programmable micropipette puller (PMP 100, MicroData instrument Inc.) from custom made narrow glass cylinders (20.3 cm in length, 10 μL maximum volume). Following microinjections oocytes were kept at 18°C in ND96-ACT medium with antibiotics for 24 h (GLUT5 injected oocytes), 48 h (GLUT2 injected oocytes) or 120 h (GLUT7 injected oocytes) before

experiments were carried out. Media with antibiotics was changed every day to every second day for GLUT7 microinjected oocytes.

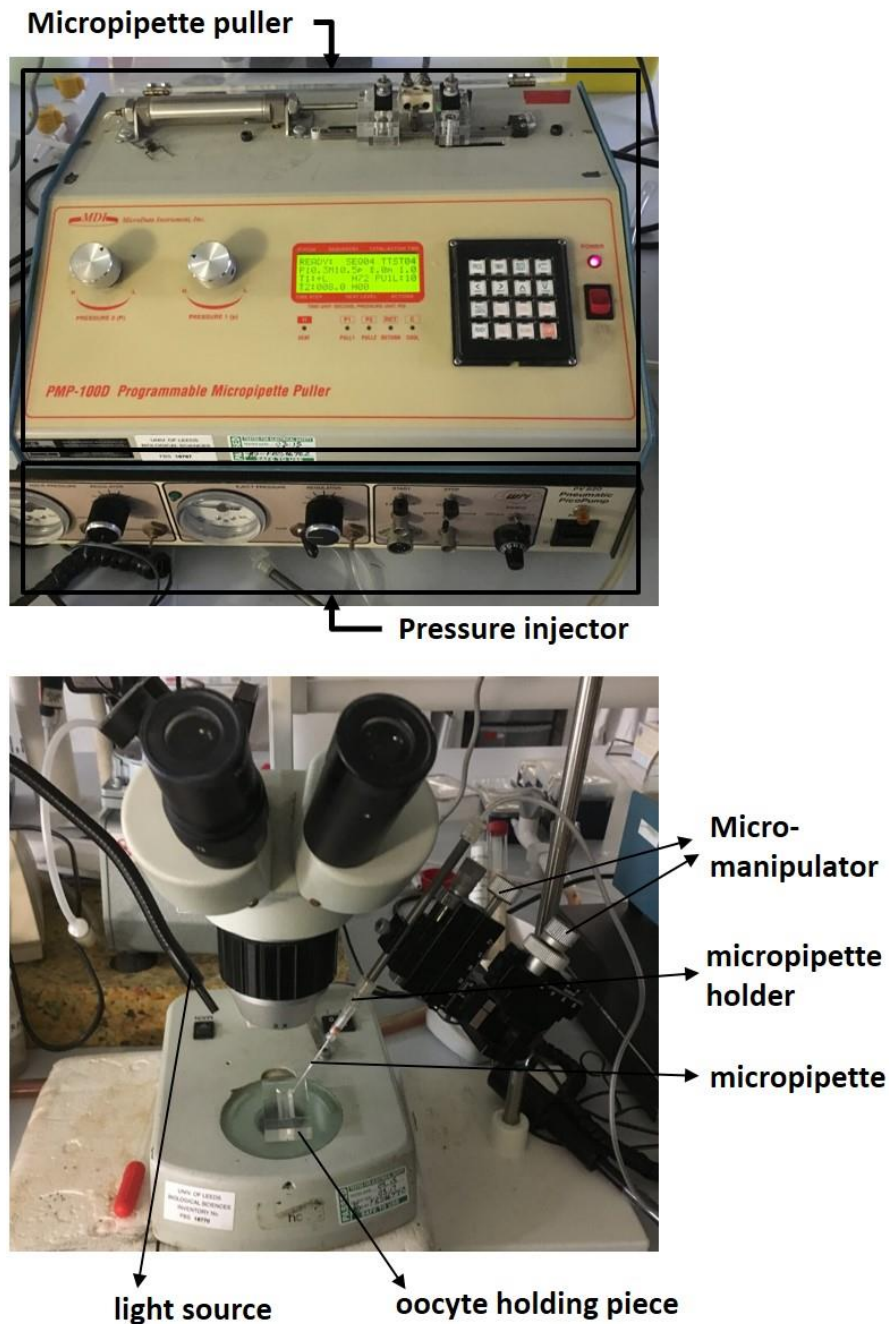


Figure 2-5 Oocyte microinjection setup. Micropipettes were made from narrow glass cylinders using a micropipette puller and then secured onto the micropipette holder. Oocytes were placed onto a holding piece under a microscope for magnified visualisation [10x magnification eyepiece, 2x (dual) built-in objective lens]. Oocytes were microinjected, using the manipulation controls on the micropipette holder, by an air pressure injector.

2.4.3 [¹⁴C] Fructose uptake by GLUT5

Following microinjection with protein mRNA or water *Xenopus* oocytes were incubated in 6 mM or 100 μ M fructose solution with ¹⁴C-fructose at a concentration of 0.5 μ Ci/mL. Incubation solutions were made up in the presence and absence of increasing concentrations of the compounds/extracts being tested. In cases where the stock solution of compound being tested was made using solvents (DMSO or ethanol), the equivalent amount of solvent was added to all control sugar incubation solutions. Incubations were carried out at 25 °C for 5 min (100 μ M fructose incubation solution) or 15 min at 37 °C (6 mM fructose incubation solution). All uptake experiments were carried out with three to six replicates of three oocytes. After the termination of the incubation period, oocytes were washed with ice cold fructose solution, at the same molarity as the incubation solution, and homogenised in 0.3 M sucrose (10638403, Thermo Fisher Scientific, Paisley, UK), plus 10 mM sodium phosphate (7601-54-9) and protease inhibitor mixture (P8340) solution. In order to separate the yolk and pellet cell debris the homogenized samples were spun at 3,000 g for 15 min at 4 °C. The supernatant was then centrifuged at 48,000 g for 1 h at 4 °C to pellet the membranes, which were re-suspended in the same solution used for the homogenisation step and stored at – 20 °C until protein expression analysis. The supernatant of the second centrifugation step was added to a vial containing 5 mL of scintillation fluid and sample radioactivity counts were measured using Packard Tri-Carb 1900 TR Liquid Scintillation Counter. Samples not used for protein analysis were homogenized and added directly to the vials for counting as neither the yolk or cell debris interfere with this process. Protein concentration for membrane extract sample was determined using LabTech-Nanodrop ND100 spectrophotometer.

2.4.4 [¹⁴C] Fructose and [¹⁴C] Glucose uptake by GLUT2

Uptake experiments in *Xenopus* oocytes expressing GLUT2 were carried out in the same manner as described above (see 2.4.3), with the following changes; concentration of glucose and fructose incubation solutions was 100 μM and incubations were carried out at 25 °C for 5 min. Homogenization of each three oocyte replicate was performed with 1% sodium dodecyl sulfate (SDS) (A1112, AppliChem, Darmstadt, Germany).

2.4.5 [¹⁴C] Deoxy-D-glucose, [¹⁴C] Fructose and [¹⁴C] Glucose uptake by GLUT7

Uptake experiments in *Xenopus* oocytes expressing GLUT7 were carried out in the same manner as described above (see 2.4.3), with the following changes; concentration of sugar incubation solutions was 100 μM and incubations were carried out at 25 °C for 30 min. Homogenization of each three oocyte replicate was performed with 1% SDS. Uptake experiments were carried out with six replicates of three oocytes or three replicates of 10 oocytes.

2.4.6 Protein analysis of *X. laevis* membrane extracts by Western blot

Western blot analysis of oocyte membrane extracts was performed as described previously (Manolescu et al., 2007a). In short, oocyte membrane samples of GLUT5 injected oocytes, as well as positive control TC7 cell lysate samples, were denatured following addition of 4X Laemmli reducing buffer (1610747, Bio-Rad, Hemel Hempstead, UK) for 15 min at 37 °C. All samples were resolved using SDS-

PAGE Mini-PROTEAN TGX Stain-Free precast 10% gels (4568033, Bio-Rad, Hemel Hempstead, UK) for 30 min at 200 V and subsequently transferred to Immun-Blot PVDF membranes (1620175, Bio-Rad, Hemel Hempstead, UK) by electrophoresis. Immunoblotting was performed with primary anti-GLUT5 antibody (ab36057, Abcam, Cambridge, UK) at a 1:250 dilution, followed by secondary anti-mouse antibody (ab125323, Abcam, Cambridge, UK) at a 1:10.000 dilution. Membrane was washed three times with Tris buffered saline (TBS) buffer (1706435, Bio-Rad, Hemel Hempstead, UK) with Tween 20 (1706531, Bio-Rad, Hemel Hempstead, UK). Membranes are then incubated with 50:50 peroxide and luminol from Clarity Western ECL substrates kit (1705060, Bio-Rad, Hemel Hempstead, UK) for 5 min away from light. In a dark room membrane was exposed onto a photographic film revealing the bands produced by GLUT5 protein expression. Alternatively, membranes were imaged with ChemiDoc XRS+ (Bio-Rad, Hemel Hempstead, UK) western blot digital imaging system, according to manufacturer instructions.

2.4.7 Protein analysis of *X. laevis* membrane extracts by Wes

Expression of hGLUT2, hGLUT5 and hGLUT7 in *Xenopus* oocyte membranes was determined with ProteinSimple's automated western blot system 'Wes' according to manufacturer's instructions, as formerly reported (Ziegler et al., 2016), with the exception of sample denaturing condition, which was done at 37 °C for 15 min. Membrane extracts of hGLUT2 and hGLUT7 injected oocytes were treated with Rapid PNGase F (P0710S, New England Biolabs, Ipswich, USA) for 15 min prior to denaturing step. GLUT2 antibody (ab95256, Abcam, Cambridge, UK) dilution

was 1:50, as was the dilution of GLUT5 antibody (sc271055, Santa Cruz Biotechnology, Dallas, TX, USA) used for protein detection on oocyte membrane samples. Optimal loading concentration for GLUT2 oocyte membrane samples was 0.4 mg/mL and 0.2 mg/mL was used for GLUT5 oocyte membrane samples. GLUT7 antibody (NBP1-81821, Novus Biologicals, Littleton, CO, USA) dilution was 1:10. Membrane extracts of hGLUT7 expressing oocytes were used undiluted.

2.4.8 Statistical analysis

Sugar uptake experimental results are all representative of three to six replicates of three oocytes, or three replicates of 10 oocytes, per individual condition. Water injected control oocytes were used in every experiment and individual condition. Each data point represents the mean of all replicates \pm SEM normalized to the mean of its respective control replicates, unless controls are included in the figures. Two tailed homoscedastic Student's t-test was used to award significance, as previously reported (Manolescu et al., 2005). Uptake of sugar per oocyte (pmol/oocyte/incubation time) was determined by using a standard curve, produced for each experiment and every condition, and taking into consideration the concentration of sugar incubation solution. Firstly, radioactive counts (CPMA) were converted into ng/ μ L by dividing it by the slope of its respective standard curve. The result was adjusted for the amount of sugar available for uptake (in pmol) and by the maximum volume of the average oocyte (\sim 0.52 mm³ or 0.52 μ L), and divided by the number of oocytes in each replicate. IC₅₀ were determined by identifying the concentration of the added compound at which the uptake of sugar was decreased by half.

Chapter 3

Characterization of hGLUT2, hGLUT5 and hGLUT7 using the Caco-2/TC7 cell culture model

3.1 Abstract

A common cell culture model of the small intestine, namely the Caco-2/TC7 cell model, was used to investigate changes in GLUT7 expression in response to the presence of different sugars, with the aim to further characterize the substrates of this transporter. Cells were seeded onto Transwell filters and cultured throughout the differentiation period in media supplemented with 25 mM of different sugars on the apical side only, or on both apical and basolateral sides. There was a significant increase in GLUT7 mRNA expression (13%, $p \leq 0.001$) in cells grown in the presence of fructose, on both apical and basolateral sides, when compared to glucose control. In addition, a significant rise in total protein expression (2.7-fold, $p \leq 0.05$) was observed in cells grown under the same conditions. Localization of GLUT7 on the apical and basolateral membranes was determined using cell surface biotinylation and confocal imaging. Nonetheless, protein expression at the cell surface was unchanged in the presence of fructose. As levels of expression of GLUTs are reportedly increased in the presence of their substrates, it can be extrapolated from these findings that fructose is a substrate of the GLUT7 transporter. Further investigations are required in order to fully understand the role of GLUT7 on the regulation of sugar uptake in the gut.

3.2 Introduction

The Caco-2 cell system is a well characterized and frequently used *in vitro* model of intestinal absorption, commonly used to examine transport mechanisms and the ability of specific chemicals or compounds to cross the intestinal barrier (Angelis and Turco, 2011). Seeding of these cells on semi-permeable membranes (eg. transwell filters) enables them to differentiate and polarize in long-term culture, forming a monolayer with tight junctions, and properties which mimic the intestinal barrier (Turco et al., 2011). Caco-2 cell line characteristics have been shown to be highly dependent on culture conditions leading to reports on variability of transport properties and permeability (Delie and Rubas, 1997), (Briske-Anderson et al., 1997). Therefore, several clones from this cell line have been isolated, including the TC7 clone, which was acquired from a late passage of the parental cell line (Chantret et al., 1994). This clone was shown to have more homogenous distribution of proteins functional in the small intestine across different passage numbers, as well as more developed intercellular junctions and characteristic transporter and some brush border enzymes expression profile (Turco et al., 2011), (Chantret et al., 1994).

It is known that Caco-2/TC7 cells express different sugar transporters, critical for sugar transport, including SGLT1, GLUT2 and GLUT5 (Sambuy et al., 2005), (Alzaid et al., 2013), and studies have looked at the effect of high glucose and fructose levels in the expression of GLUT2 and GLUT5, respectively (Mahraoui et al., 1994), (Gouyon et al., 2003). In addition, data has shown that GLUT5 expression is higher in adipocytes cultured in the presence of fructose, proposing

a stimulation, albeit not conclusive, of transport by the protein substrate itself (Legeza et al., 2014). Furthermore, the GLUT2 basolateral to apical membrane trafficking proposed by Kellett et al was confirmed in a live cell imaging study with liver cells, where translocation of GLUT2 from basal to apical membrane was prompted by high glucose levels (Cohen et al., 2014). As localization of transporters is critical for function, confocal microscopy was used in this chapter to look at GLUT transporter cellular distribution in Caco-2/TC7 cells (Grefner et al., 2014), (Kipp et al., 2003). Images of Caco-2/TC7 cells incubated with anti-GLUT2, 5 and 7 antibodies were taken with the aim to determine precise localization of each protein in the cells and further characterize the lesser known GLUT7 protein. GLUT7 is reportedly expressed on the apical membrane of intestinal cells (Cheeseman, 2008), (Douard and Ferraris, 2008) and has been shown to transport both glucose and fructose when expressed in oocytes (Li et al., 2004), (Chapter 6). Nevertheless, the effects of any substrates on the expression levels of GLUT7 remains to be investigated. Therefore, this chapter examines changes in GLUT7 mRNA expression levels in the presence of fructose, sucrose, L-glucose, sorbitol and galactose, when compared to glucose. In addition, the effect of fructose on total and surface protein expression is determined.

Caco-2/TC7 cells used for experiments presented in this chapter were cultured on transwell filters (Figure 3.1 B), with the aim of mimicking the environment encountered by enterocytes *in vivo*. Briefly, cells are seeded onto transwell filters and placed into a well allowing separation of apical and basolateral medium. This imitates the situation *in vivo*, where sugars are absorbed into the cell from the

lumen by transporters on the apical membrane and released into the blood on the basal membrane (Lodish et al., 2008). Basolateral membranes refer to the basal/lateral domains of the enterocyte (Figure 3.1 A).

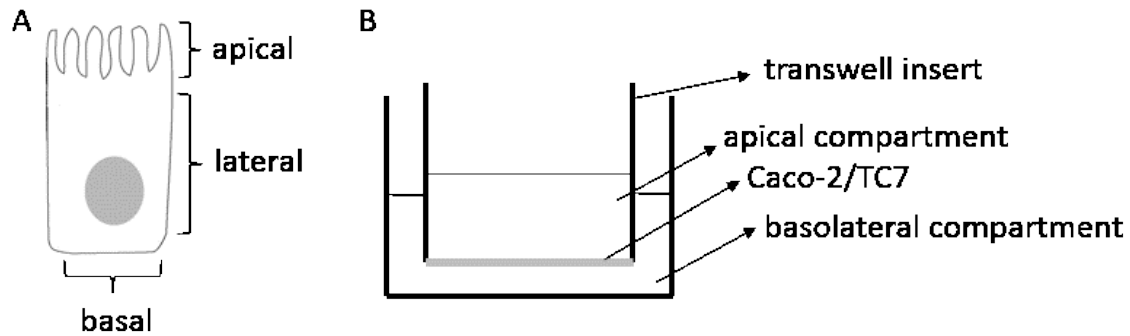


Figure 3-1 Representation of enterocyte and culture of Caco-2/TC7 cells on transwell filters. Membranes of enterocyte (apical, lateral and basal) are marked with their locations (**A**). Characteristics of culture of Caco-2/TC7 enterocytes, seeded onto a transwell filter, and exposed to media on apical and basolateral compartments (**B**).

3.3 Determination of location of GLUTs on cellular membranes by immunostaining

Mammalian intestinal cells, Caco-2/TC7, were cultured following methods described in Chapter 2 (section 2.2.2). In order to establish the precise localisation of each GLUT transporter on cellular membranes, fixed cells were imaged using inverted confocal microscopy following immunofluorescence staining (refer to section 2.2.4, Chapter 2). Cells were stained with membrane marker wheat germ agglutinin (WGA) (emitting green fluorescence), nuclear stain DAPI (emitting blue fluorescence) and Cy3-conjugated donkey anti-rabbit/mouse secondary antibody (emitting red fluorescence). Detection of proteins was performed by incubating the

cells with primary anti-GLUT2, 5 or 7 antibody, followed by incubation with secondary antibody, which is conjugated to Cy3, allowing detection (red fluorescence). Images are presented as a range from apical membrane (far left) to basal membrane (far right). As a negative control, primary antibody was omitted, resulting in absence of Cy3 fluorescence (Figure 3.2).

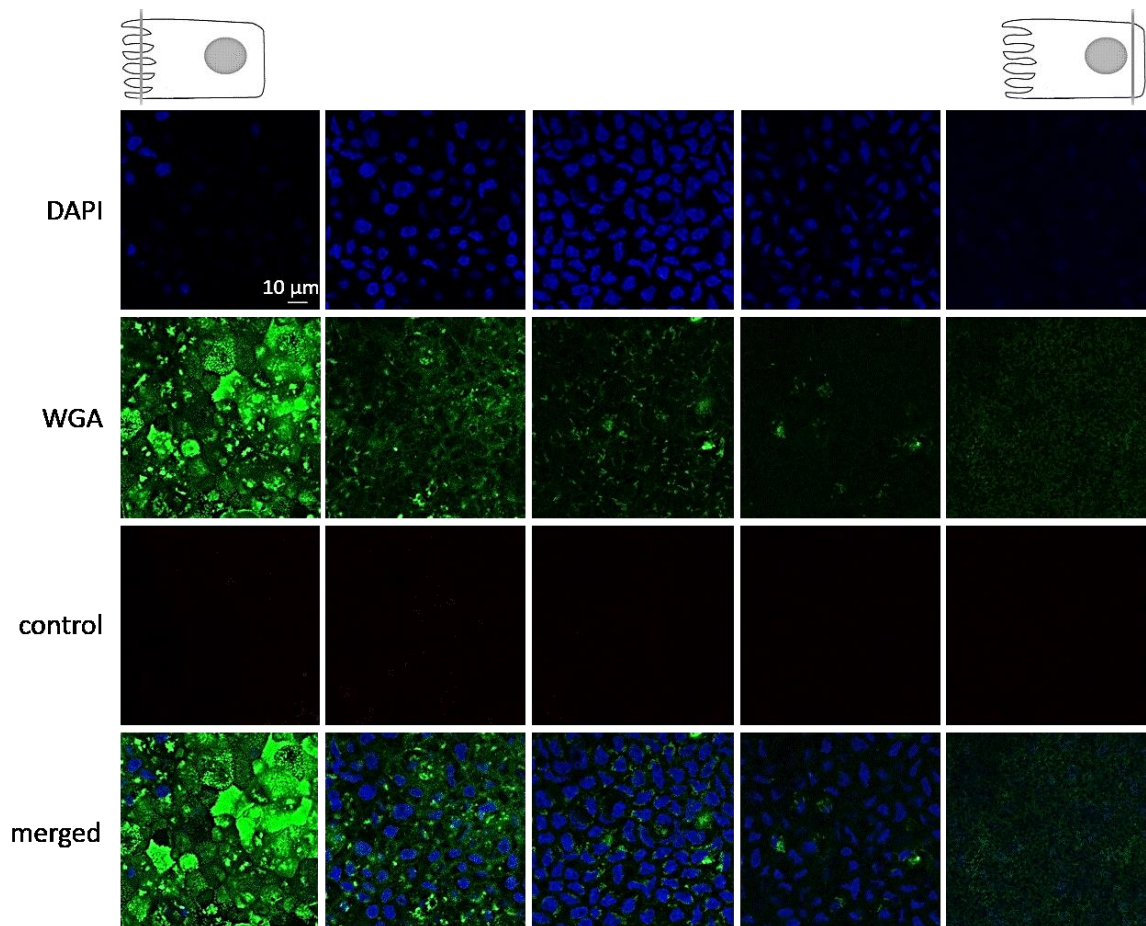


Figure 3-2 Negative control for immunofluorescence detection for GLUTs in differentiated Caco-2/TC7 monolayers. Cells were incubated with nuclear stain DAPI (blue), membrane marker wheat germ agglutinin (WGA) (green), no primary antibody and Cy3-conjugated donkey anti-rabbit secondary antibody (red). Scale bar (10 μm) is shown in the lower left corner of first DAPI image and applies to all images. Images from left to right represent sections through the cell from the apical to basal side of enterocyte. Images represent one of 3 biological replicates.

Immunostaining with anti-GLUT5 primary antibody detected GLUT5 (red fluorescence), predominantly on the apical membrane of the enterocyte, and with less intensity on lateral domain. Virtually no GLUT5 was detected on the basal membrane (Figure 3.3). This is in agreement with data suggesting that fructose is transported into the cell by GLUT5, present at high levels on the apical membrane (Burant et al., 1992), (Drozdowski and Thomson, 2006), (Reinicke et al., 2012).

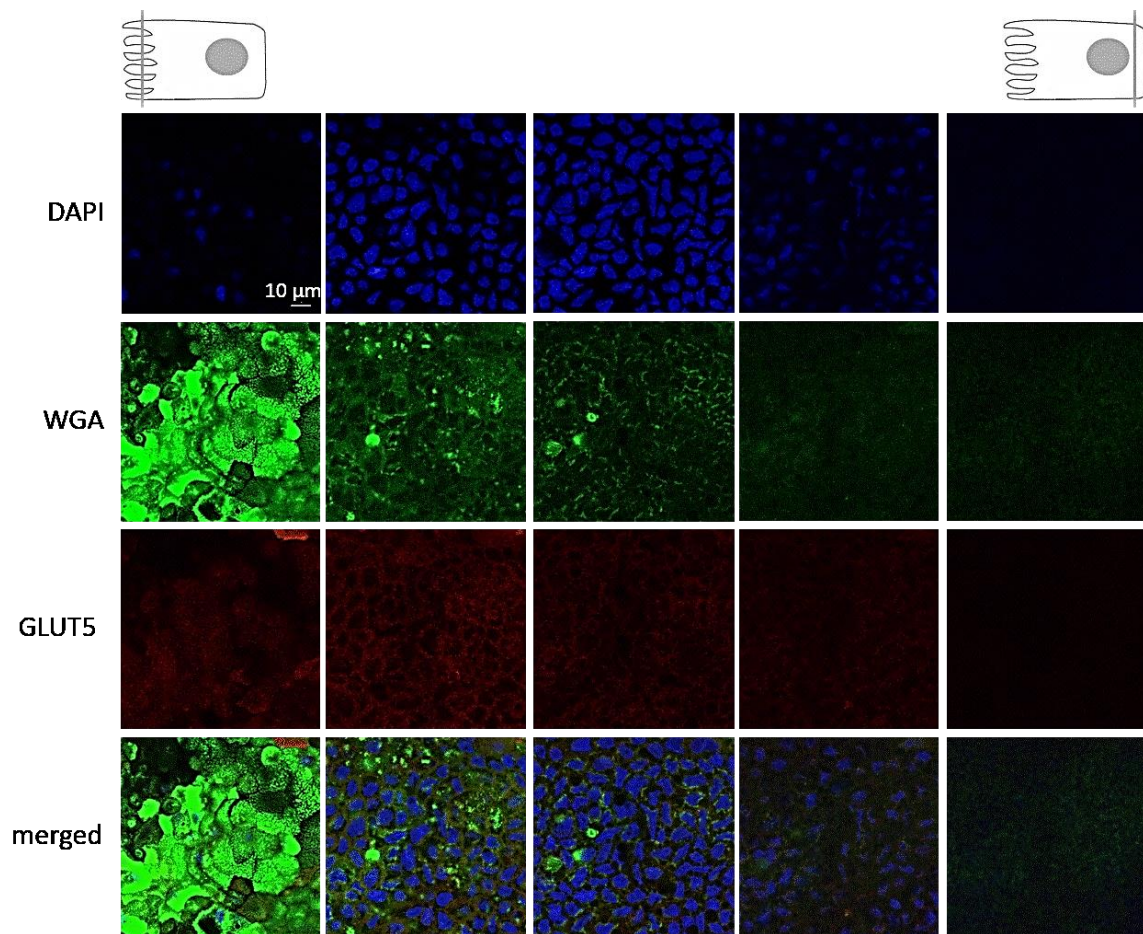


Figure 3-3 Immunofluorescence detection of GLUT5 in differentiated Caco-2/TC7 monolayers. Cells were incubated with nuclear stain DAPI (blue), membrane marker wheat germ agglutinin (WGA) (green), mouse anti-GLUT5 primary antibody and Cy3-conjugated donkey anti-mouse secondary antibody. GLUT5 is shown in red, predominantly on the apical membrane. Scale bar (10 µm) is shown in the lower left corner of first DAPI image and applies to all images. Images from left to right represent sections through the cell from the apical to basal side of enterocyte. Images represent one of 3 biological replicates.

Immunostaining with anti-GLUT2 primary antibody detected GLUT2 (green fluorescence) across both apical and basal/lateral membranes of the enterocyte (Figure 3.4). This corroborates the findings by Kellett et al, who conclude that the main route for glucose absorption into cells is by translocation of GLUT2 transporter to the cell apical surface in response to high glucose levels (Kellett and Helliwell, 2000). Presence of GLUT2 on basolateral membrane was shown in studies using liver cells and rat intestinal models (Cohen et al., 2014), (Helliwell and Kellett, 2002), (Cheeseman, 1993). Immunostaining images of GLUT2 incubated with WGA produced a granular staining, making visualization of the protein less clear, and this is why immunostaining was carried out without the membrane marker. Immunostaining images of GLUT2 with WGA can be found in the appendix.

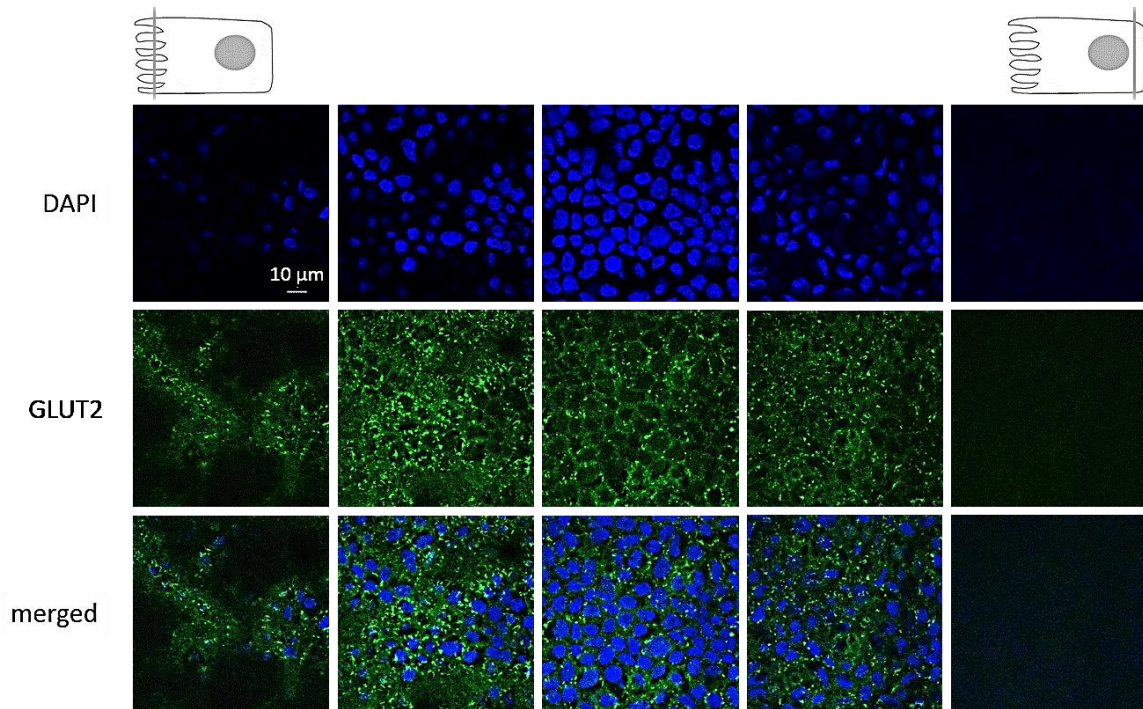


Figure 3-4 Immunofluorescence detection of GLUT2 in differentiated Caco-2/TC7 monolayers. Cells were incubated with nuclear stain DAPI (blue) and rabbit anti-GLUT2 primary antibody and Cy3-conjugated donkey anti-rabbit secondary antibody. GLUT2 is shown in green, ranging from both the apical to the basal membranes. Scale bar (10 μm) is shown in the lower left corner of first DAPI image and applies to all images. Images from left to right represent sections through the cell from the apical to basal side of enterocyte. Images represent one of 3 biological replicates.

Lastly, immunostaining with anti-GLUT7 primary antibody showed GLUT7 localization (green fluorescence) mainly on the apical membrane of the enterocyte (Figure 3.5). A fainter detection of this protein was localized on the lateral membrane, with little localisation of this protein on basal membrane. The possibility of GLUT7 being expressed on the apical brush border membrane, due to the high sequence similarity with GLUT5, has been previously proposed (Cheeseman, 2008), (Li et al., 2004). In addition, immunohistochemistry assays using rat tissue localized GLUT7 to the apical membrane of the small intestinal epithelial cells (Cheeseman, 2008). Nevertheless, the presence and/or localisation of GLUT7 in

Caco2-TC7 cells has not previously been reported. As for GLUT2, immunostaining images of GLUT7 incubated with WGA did not produce images with good visualization, and so, immunostaining was carried out without the membrane marker. Immunostaining images of GLUT7 with WGA can be found in the appendix.

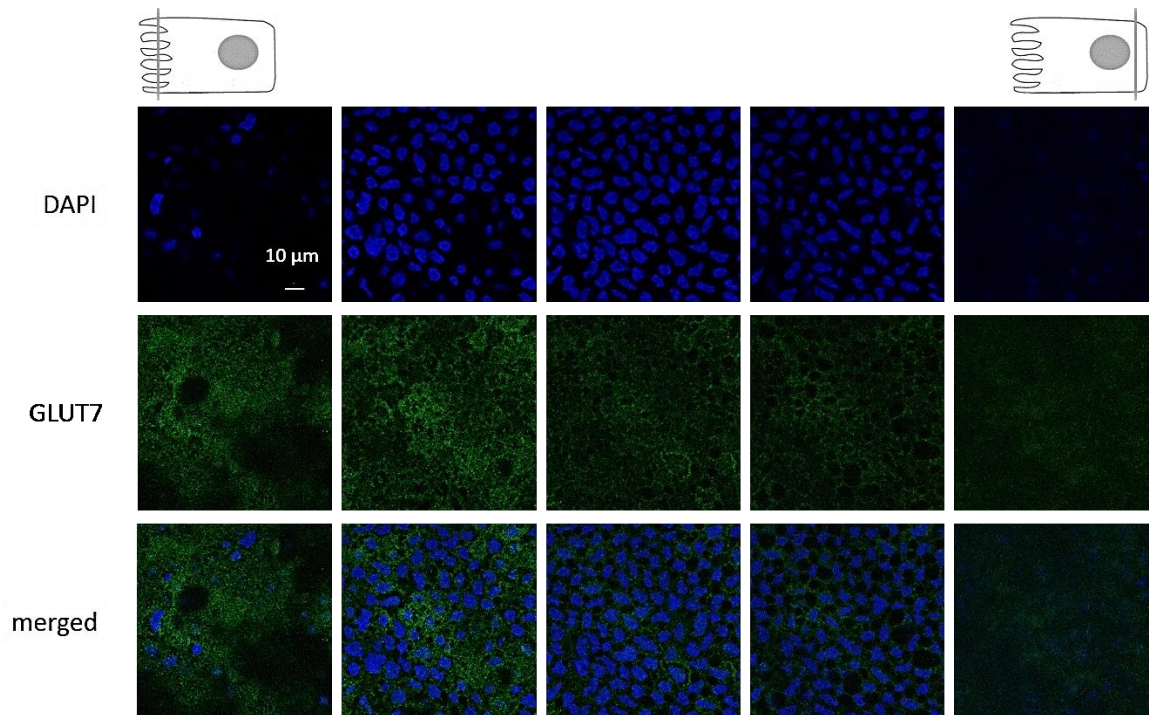


Figure 3-5 Immunofluorescence detection of GLUT7 in differentiated Caco-2/TC7 monolayers. Cells were incubated with nuclear stain DAPI (blue) and rabbit anti-GLUT7 primary antibody and Cy3-conjugated donkey anti-rabbit secondary antibody. GLUT7 is shown in green, predominantly on the apical side. Scale bar (10 μm) is shown in the lower left corner of first DAPI image and applies to all images. Images from left to right represent sections through the cell from the apical to basal side of enterocyte. Images represent one of 3 biological replicates.

3.4 Characterization of hGLUT7 through quantitative protein and mRNA analysis

GLUT7 has been previously reported to transport both glucose and fructose and it has also been determined that glucose uptake by this transporter was significantly inhibited in the presence of fructose (Li et al., 2004), (Chapter 6). In order to further characterize GLUT7 and investigate the role of fructose on mRNA levels and protein expression, cells on Transwell filter plates were cultured during the differentiation stage in medium supplemented with 25 mM fructose or other sugars either on the apical side only or on both apical and basolateral sides (refer to Chapter 2 section 2.2 for full protocols).

3.4.1 Quantification of hGLUT7 mRNA following cell differentiation in the presence of different sugars

Methods used in the quantification of mRNA were described in Chapter 2 (refer to section 2.2.3). Differences in mRNA levels when cells were grown in media supplemented with different sugars, were quantified using TATA-box binding protein (TBP), a general transcription initiator in mammalian cells (Lodish et al., 2008) as a housekeeping gene control. A preliminary analysis of GLUT7 mRNA levels present in Caco-2/TC7 and Caco-2 showed that the former expressed 3.7-fold more GLUT7 than Caco-2 cells ($p \leq 0.01$) (Figure 3.6). This highlighted the differences in protein expression between the parental cell line Caco-2 and its clone TC7, as previously reported for other intestinal transporters (Chantret et al.,

1994), (Turco et al., 2011). For this reason all further investigations were carried out with Caco-2/TC7 cells only.

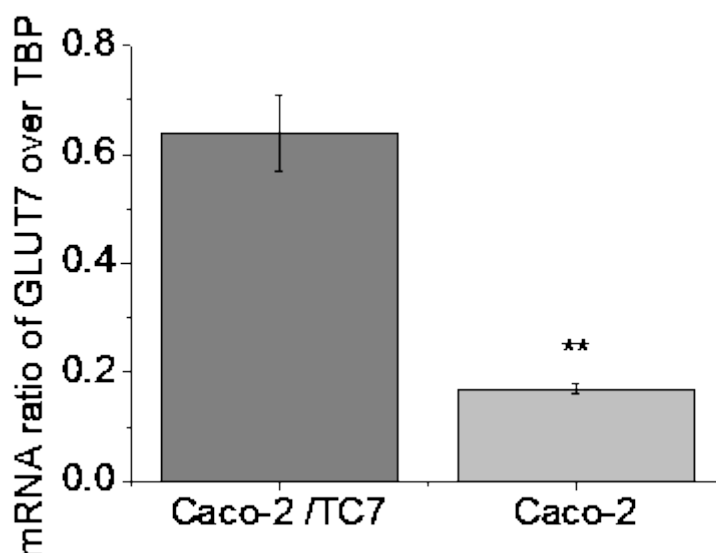


Figure 3-6 GLUT7 mRNA expression in differentiated Caco-2/TC7 and Caco-2 intestinal cell lines. TBP was multiplexed with GLUT7 as a housekeeping gene and results are shown as a ratio of the individual copy numbers for each gene. Ratio of GLUT7 to TBP showed that differentiated Caco-2/TC7 cells had 3.7-fold more mRNA of this protein than Caco-2 cells. Each data point represents the mean of 3 technical replicates from 1 biological sample, analysed in triplicates, \pm SD. ** $p \leq 0.01$

Expression of GLUT7 in Caco-2/TC7 cells grown in media supplemented with 25 mM of either fructose, sorbitol, galactose, L-glucose or sucrose on apical side only during cell differentiation period (21 days) remained unchanged when compared to glucose control (Figure 3.7 A). On the other hand, cells grown in media supplemented with fructose on both apical and basolateral sides showed a significant increase (13%, $p \leq 0.001$) in GLUT7 expression when compared to glucose control (Figure 3.7 B). No other sugar had a significant impact on GLUT7 expression when added to growth media on both apical and basolateral sides.

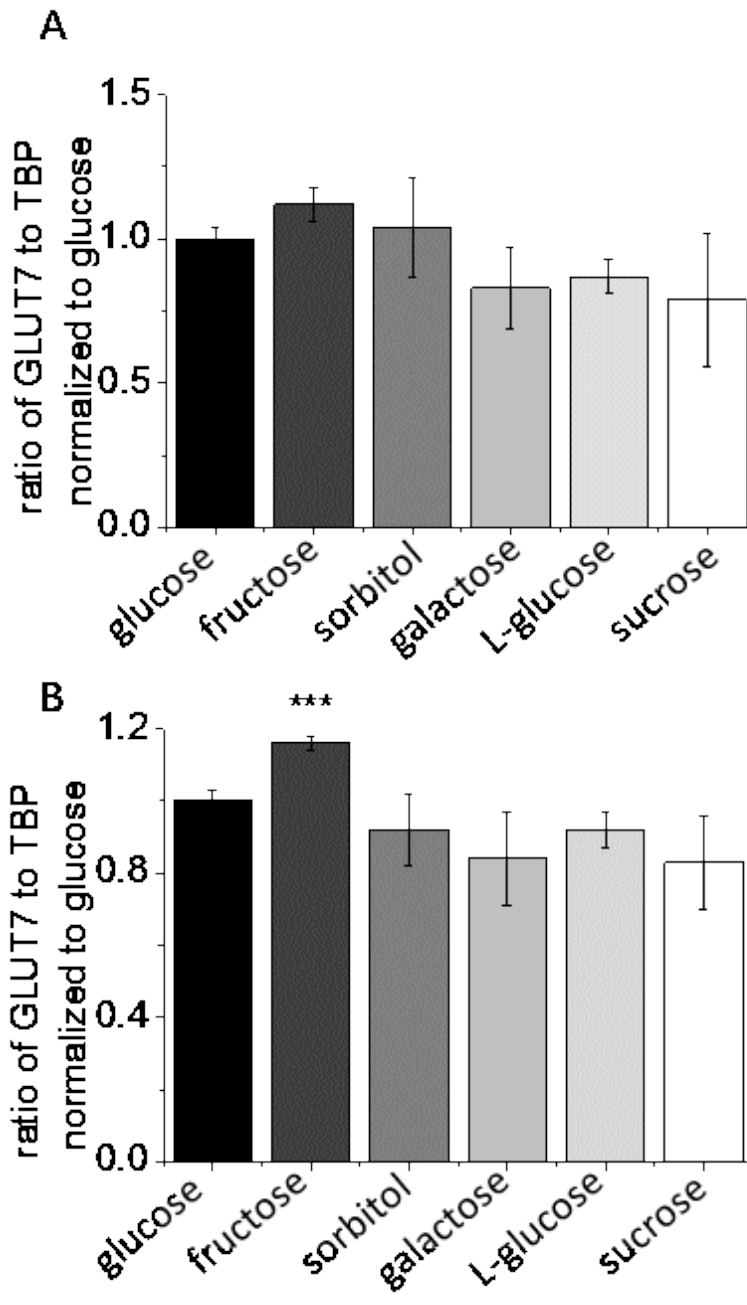


Figure 3-7 GLUT7 mRNA expression in differentiated Caco-2/TC7 intestinal cells following growth in media supplemented with different sugars. TBP was multiplexed with GLUT7 as a housekeeping gene and results are shown normalized to the glucose control, and as a ratio of the individual copy numbers for each gene. Fructose, sorbitol, galactose, L-glucose and sucrose added to apical media did not lead to any change in GLUT7 expression (**A**). A significant increase in GLUT7 expression (13%) was observed when media for both apical and basolateral sides was supplemented with fructose. No other sugar had the same effect (**B**). Each data point represents the mean of 3 biological replicates and 3 technical replicates, analysed in triplicates, \pm SEM. *** $p \leq 0.001$

Because of some variation in expression between the biological replicates, results in each experiment were normalized to the respective glucose control. Selected results from the effect of fructose, as well as one additional biological replicate, are presented in Figure 3.8 below to allow for a better comparison. From this figure it looks like the GLUT7 mRNA levels also increased when cells were cultured in apical medium supplemented with fructose. However, potentially due to variation in expression between replicates a significance could not be attributed to these results.

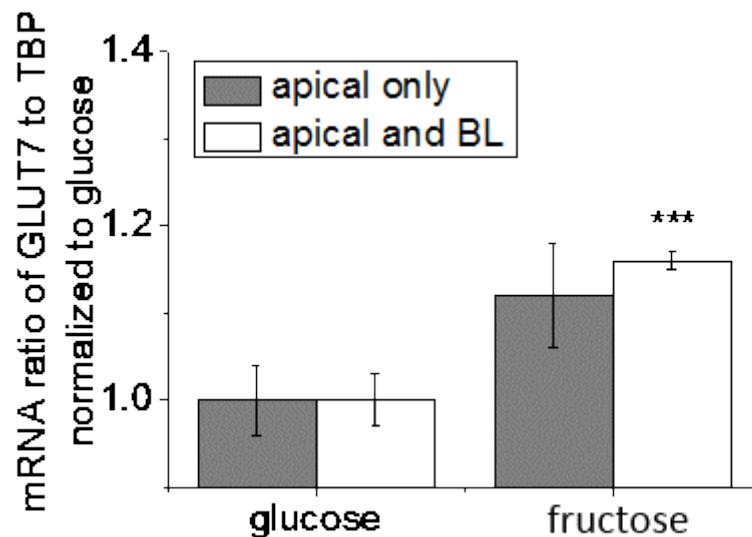


Figure 3-8 GLUT7 mRNA expression in differentiated Caco-2/TC7 intestinal cells following growth through the differentiation phase in media supplemented with fructose. TBP was multiplexed with GLUT7, as a housekeeping gene, and results are shown as a ratio of the individual copy numbers for each gene. Fructose added to apical media only did not lead to a change in GLUT7 expression. However, a significant increase in GLUT7 expression (13%) was attributed to fructose supplementation in media for both apical and basolateral sides (apical and BL). Each data point represents the mean of 4 biological replicates and 3 technical replicates, analysed in triplicates, \pm SEM. *** $p \leq 0.001$

3.4.2 Quantification of total and cell surface hGLUT7 protein expression following cell differentiation in the presence of different sugars

Protein expression was measured using ProteinSimple capillary automated western blotting (Wes). Differences in protein expression levels were measured by normalizing to Na⁺/K⁺ ATPase (NaKATPase), an ion pump present in the plasma membranes of all animal cells (Lodish et al., 2008). Amount of protein localised to the surface was quantified following cell surface biotinylation (refer to Chapter 2, section 2.2.5). Initially, a standard curve was constructed with different amounts of Caco-2/TC7 cell lysate to test linearity of both the GLUT7 and NaKATPase antibodies and a loading sample concentration of 0.4 mg/ml was found optimal for signals of both antibodies (Figure 3.9 A). Antibody dilutions were 1:100 for NaKATPase and 1:10 for GLUT7. Cell surface biotinylation samples were used undiluted. All results are shown as a ratio of the area of the peak obtained for GLUT7 protein to the area of the peak representative of the NaKATPase protein (Figure 3.9 B).

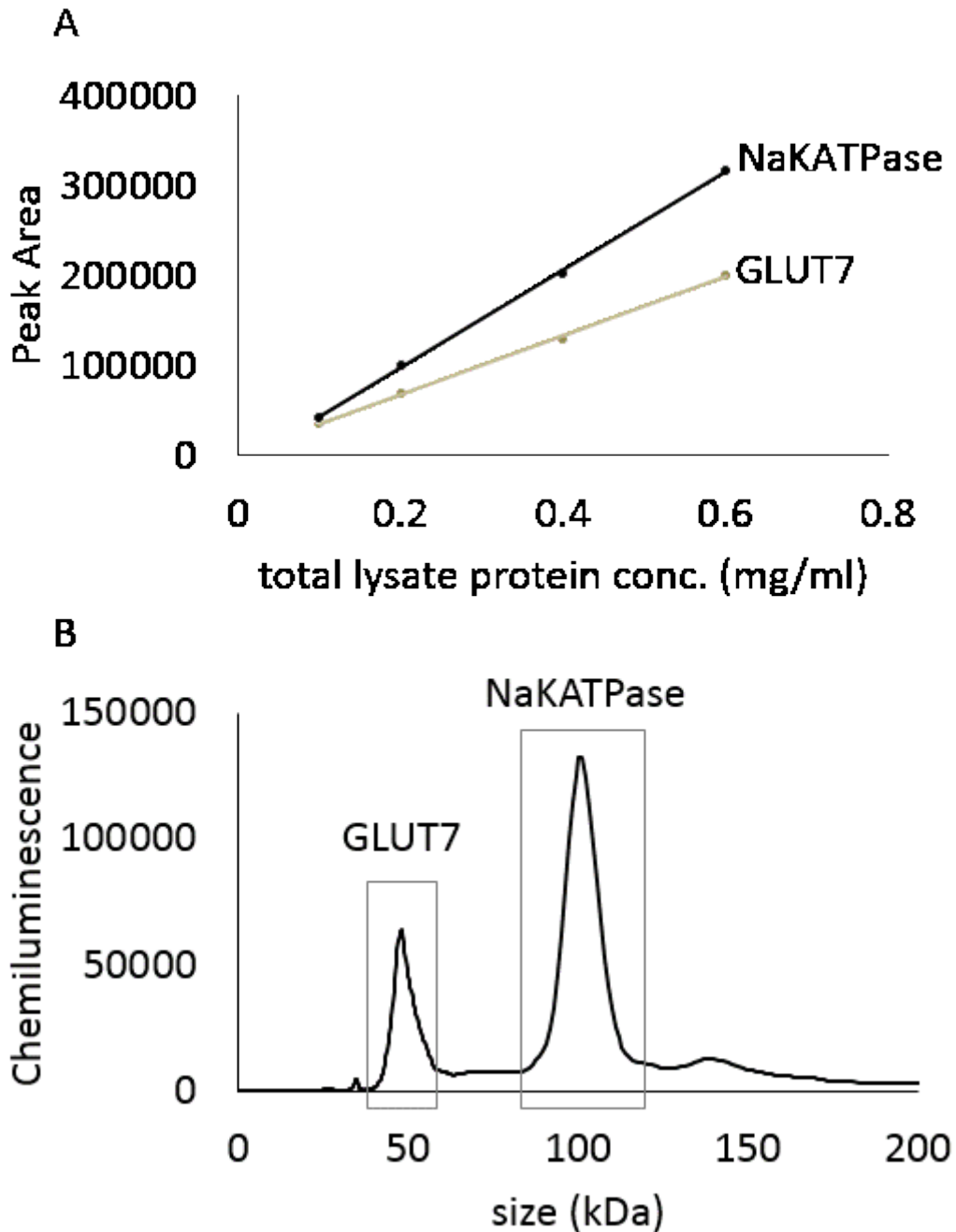


Figure 3-9 Standard curve for GLUT7 and NaKATPase antibodies and example of protein detection by multiplexed antibodies. Standard curved showed that both antibodies have linearity at protein concentrations of Caco-2/TC7 lysate between 0.1 – 0.6 mg/mL **(A)**. Example of protein detection in Caco-2/TC7 lysate analysed with multiplexed GLUT7 and NaKATPase antibodies, at a lysate loaded concentration of 0.5 mg/ml **(B)**. GLUT7 antibody dilution was 1:10, and NaKATPase antibody dilution was 1:100. Detected protein size for GLUT7 was 49 kDa, and 101 kDa for NaKATPase.

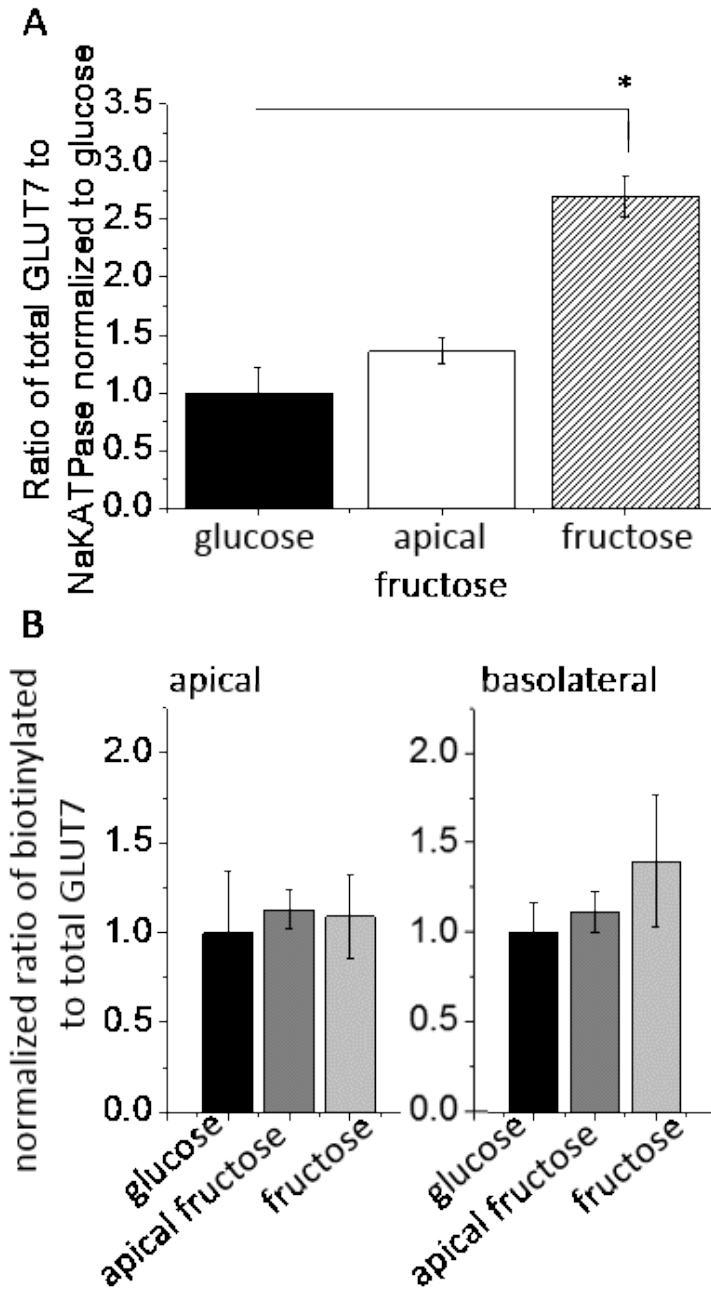


Figure 3-10 GLUT7 protein expression in differentiated Caco-2/TC7 intestinal cells following growth through the differentiation phase in media supplemented with fructose. NaKATPase was multiplexed with GLUT7, as a housekeeping gene, and results are shown as a ratio of the individual peak area for each protein. Fructose added to apical medium only (apically only) did not lead to a change in total GLUT7 protein expression. A significant increase in total GLUT7 expression (2.7-fold) was found after apical and basolateral media fructose supplementation (**A**). Surface protein expression was not changed significantly with either treatment (**B**). Each data point represents the mean of 3 biological replicates and 2 technical replicates, \pm SEM. * $p \leq 0.05$

GLUT7 protein expression, measured in crude cell lysate, was significantly increased (by 2.7-fold, $p \leq 0.05$) following addition of with 25 mM fructose to apical and basolateral growth media compared to glucose control (Figure 3.10 A). Analysis of lysates from cells grown with apical fructose supplementation showed no change in protein expression. Furthermore, there was no significant change detected in surface GLUT7 protein expression on apical or basolateral sides following supplementation either with fructose apically or on both sides, when compared to glucose control (Figure 3.10 B). These results suggest that fructose increased GLUT7 expression in the total lysate, however, this did not translate into an increase in protein levels on the cell surface.

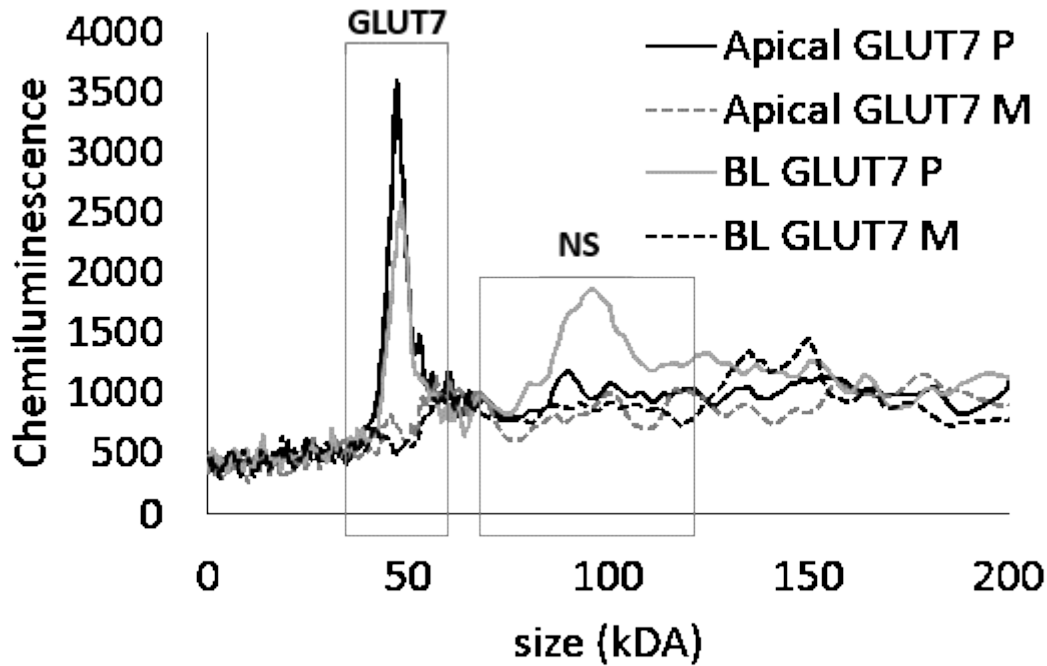


Figure 3-11 GLUT7 surface protein expression in differentiated Caco-2/TC7 intestinal cells. Analysis of surface biotinylation samples (apical and basolateral (BL) fractions), after treatment with PNGase (P) and mock treatment (M), by capillary automated western blotting. Results show that protein detection, on both apical and basolateral membranes, is greatly improved following treatment with PNGase. Detected protein size for GLUT7 was 47-49 kDa. Antibody dilution was 1:10. Biotinylation samples were undiluted.

Imaging results presented above show poor expression of both GLUT7 and GLUT5 on cellular basal membranes, with a good detection of both on apical domain. Interestingly, cell surface biotinylation was able to detect a strong expression of GLUT7 on basolateral membrane, as well as on the apical membrane. This could be attributed to treatment of samples with the glycosidase PNGase prior to protein analysis, which significantly increased the detection of GLUT7 (Figure 3.11). On the other hand, analysis of samples from cell surface biotinylation of differentiated Caco-2/TC7 cells detected presence of GLUT5 on apical cellular membrane only

(Figure 3.12). These differences in the localization highlights a potential difference in the function of both transporters.

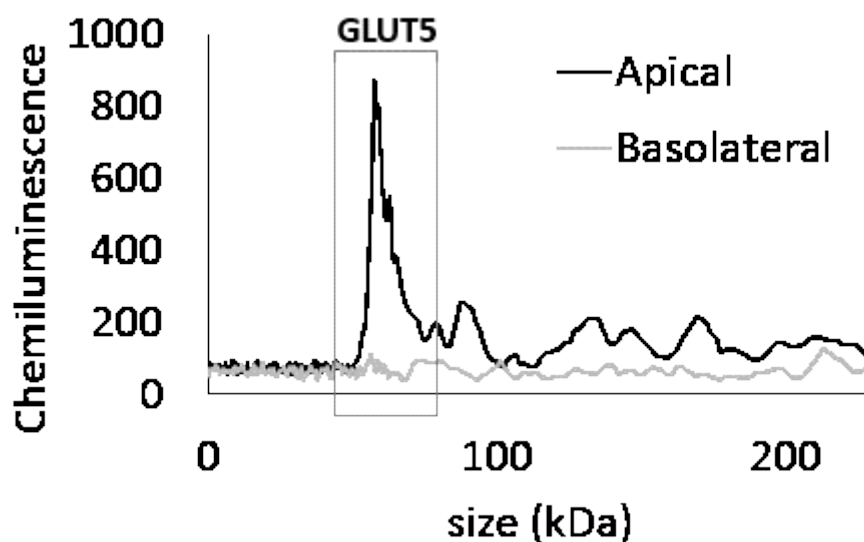


Figure 3-12 GLUT5 surface protein expression in differentiated Caco-2/TC7 intestinal cells. Analysis of surface biotinylation samples by capillary automated western blotting show GLUT5 protein expression on the apical membrane only. Detected protein size for GLUT5 was 59 kDa, with antibody dilution of 1:50. Biotinylation samples were un-diluted.

3.5 Summary and discussion of results

Immunostaining was used to detect expression of GLUT2, GLUT5 and GLUT7 in Caco-2/TC7 cells. GLUT2 transporter was expressed across the enterocyte, being present on the apical as well as the basal membranes. This agrees with the concept that in conjunction with SGLT1, GLUT2 is responsible for the absorption of glucose after translocation to the apical membrane from the basal domain (Kellett and Helliwell, 2000). Nevertheless, a recent sugar uptake study in GLUT2-knockout mice showed no decrease in glucose uptake in the absence of this transporter (Roder et al., 2014). Although in this study GLUT2 was detected on the

apical membrane of brush border membrane fractions, it was attributed to a contamination with basolateral membrane (Roder et al., 2014). There is currently an ongoing debate about the contribution to glucose uptake attributed to GLUT2 directly, with some studies showing glucose uptake predominantly by SGLT1 (Gorboulev et al., 2012), whereas others show GLUT2 as the primary transporter of this sugar (Helliwell et al., 2003), (Kellett and Helliwell, 2000). Nonetheless, at least at high glucose concentrations, it has become generally accepted that GLUT2 is in fact present on apical membranes and does contribute to the uptake of glucose (Morgan et al., 2007), (Wright et al., 2007), (Thorens and Mueckler, 2010), (Cohen et al., 2014). Further evidence of the ability of GLUT2 to transport glucose, as well as fructose, into cells can be concluded from uptake experiments by oocytes expressing this transporter (Kwon et al., 2007), (Uldry and Thorens, 2004), presented in Chapter 5.

Two different methods were used to determine cellular localization of GLUT2, GLUT5 and GLUT7. Immunostaining showed, primarily, that both GLUT5 and GLUT7 transporters are localized to the apical membrane of the enterocytes, with only faint detection on basal membrane. In agreement, cell surface biotinylation confirmed the presence of GLUT5 on the apical membrane only, whereas biotinylated GLUT7 was detected both on apical and basolateral membranes (Reinicke et al., 2012), (Drozdowski and Thomson, 2006), (Burant et al., 1992). Differences in localization of GLUT7 between the two methods could be explained by the need for de-glycosylation in order to increase GLUT7 antibody binding, as the presence of glycosylation could mask the epitope from recognition.

Biotinylation samples are treated with the glycosidase PNGase prior to protein analysis, whereas immunostaining is performed on untreated cells, which could be leading to less GLUT7 than is available being recognized. Treatment of fixed cells with PNGase prior to confocal imaging could potentially increase the detectability of GLUT7 on the basolateral side when using this method. Nonetheless, the difference in distribution of GLUT5 and GLUT7 highlights the different functions of these proteins, regardless of their structural similarities. For instance, GLUT5 transports fructose only, while GLUT7 is able to transport both glucose and fructose, as determined by uptake experiments in oocytes discussed in Chapters 4 and 6.

To date, GLUT7 has been shown to transport glucose and fructose only, with no uptake of galactose, xylose or deoxy-D-glucose observed by GLUT7-expressing oocytes (Li et al., 2004). It has been reported that expression of GLUT2 is increased in the brush border membrane at high glucose concentrations in rat models (Kellett and Helliwell, 2000). Live cell imaging, in liver cell lines, showed a rapid translocation of GLUT2 from basal to apical membrane in response to glucose stimulation, a process regulated by PKC (Cohen et al., 2014). Similarly, GLUT5 expression has been shown to be higher in adipocytes cultured in the presence of fructose compared to glucose, suggesting the substrate for this protein stimulates its own uptake (Legeza et al., 2014). Based on these observations, it could be hypothesised that high levels of substrate elevate the expression of GLUT transporters. Therefore, with the aim to further characterize the lesser known GLUT7 transporter, mRNA and protein levels were measured following culture of

Caco-2/TC7 intestinal cells in the presence of different sugars. There was a significant increase in mRNA levels (13%, $p \leq 0.001$) when cells were cultured in 25 mM fructose on both apical and basolateral sides, compared to glucose. No other sugars had a significant effect on GLUT7 mRNA levels. In agreement, protein expression was also increased by the same treatment (2.7-fold, $p \leq 0.05$). Nonetheless, surface protein levels were unchanged in cells grown in media supplemented with fructose. It can be concluded from these novel findings, therefore, that the presence of fructose increases expression levels of GLUT7 at the mRNA and total protein levels, but not surface proteins. This could be attributed to an inefficient mechanism of translocation of the protein to the cell surface, or re-internalisation of protein once cells were no longer exposed to this sugar, namely, during the biotinylation procedure. Furthermore, as sugars are transported from the apical to the basolateral side the total amount of fructose gets diluted in the system when cells are cultured in only apical medium supplemented with fructose, which could be masking any potential differences in GLUT7 expression by the presence of this sugar. Addition of higher concentrations of fructose to the apical medium, equalizing to a final total concentration of 25 mM following transport across the apical membrane, would give a more direct comparison between GLUT7 expression levels in cells cultured in apical versus apical and basolateral fructose supplemented media. To add to that, a fructose-only experimental condition, such as when cells are periodically depleted of glucose, as well as alternating low/high fructose during different or short exposure periods, could help determine the direct role of fructose on GLUT7 expression level.

Studies on Caco-2/TC7 cell models, as well as liver cell lines, showed that in the presence of insulin the expression of GLUT2 at the apical cell surface is reduced, whereas GLUT5 expression remains unchanged (Cohen et al., 2014), (Tobin et al., 2008). Future investigations on the effects of insulin on GLUT7 localisation would help characterize this protein further and highlight the potential similarities between GLUT7 and GLUT2, as localization results from biotinylated samples suggest a similar pattern for this two GLUTs. Although phloretin does not inhibit glucose uptake by GLUT7-expressing oocytes (Chapter 6), this compound has been shown to inhibit GLUT2 translocation by inhibiting PKC activity (Cohen et al., 2014). Further investigations on the effect of apigenin, the only compound shown to decrease the uptake of fructose by GLUT7-expressing oocytes (Chapter 6), on GLUT7 expression in the Caco-2/TC7 cell model should be carried out under different conditions (eg., sodium free and in the presence of insulin) to shed light on the potential GLUT7 protein mechanisms of inhibition. Differentiated Caco-2 and Caco-2/TC7 cell monolayers have been previously used in sugar transport inhibition studies in the presence of (poly)phenols (Villa-Rodriguez et al., 2017b), (Johnston et al., 2005), but these cells, as for the intestine *in vivo*, express a variety of GLUTs and other sugar transporters, which makes them unsuitable for determination of the role of individual transporters. Therefore the *Xenopus laevis* expression system was used to elucidate effects of (poly)phenols as inhibitors on individual functional GLUTs, as described in the following chapters (Chapter 4, 5 and 6).

Chapter 4

Fructose uptake inhibition of heterologously expressed hGLUT5 by (poly)phenols

4.1 Abstract

The prevalence of type 2 diabetes (T2DM) has been linked to increasingly high intakes of sugars through the diet. Excess fructose, in particular, increases serum triglyceride and LDL-cholesterol in humans, and promotes hepatic insulin resistance, hyperinsulinemia and hyperglycemia. The impact of specific plant derived (poly)phenols and food extracts on fructose transport by GLUT5, a membrane bound protein with specificity for fructose only, was investigated through expression of human GLUT5 (hGLUT5) in *X. laevis* oocytes. Analysis of oocyte membrane extracts microinjected with hGLUT5 mRNA show expression of this protein at the cell surface (size: 60 kDa). In addition, the uptake of ¹⁴C-fructose by GLUT5 was significantly inhibited by its known specific inhibitors L-sorbose-Bn-OZO (L-sorbose) and 2,5-anhydro-D-mannitol (a-mannitol), as expected. A reduction in fructose uptake by GLUT5 of more than 50% ($p \leq 0.01$) was attributed to a-mannitol when added to incubation solutions containing high and low concentrations of fructose. At low fructose concentration, German chamomile (*Matricaria recucita*) tea extract and sugar-free pomegranate extract inhibited the uptake of fructose by GLUT5 (IC_{50} of 0.73 ± 0.18 mg/ml and 0.48 ± 0.22 mg/ml for German chamomile and pomegranate extract, respectively). Furthermore, fructose

transport by GLUT5 was decreased in the presence of pure compounds apigenin ($IC_{50} = 40 \pm 4 \mu M$), EGCG ($IC_{50} = 72 \pm 13 \mu M$) and hesperidin ($IC_{50} = 264 \pm 72 \mu M$), at incubation conditions of low fructose concentration. These results suggest that specific extracts and pure compounds may have potential to be used in interventions aimed at the control of post-prandial blood sugar levels in both healthy volunteers and diabetic patients.

4.2 Introduction

Excessive ingestion of fructose has been associated with increased prevalence of obesity, which in turn is one of the most well documented risk factors of type 2 diabetes (T2DM), metabolic syndrome and cardiovascular disease (CVD) (Bantle, 2009). Fructose has been shown to directly contribute to the amplification of disease risk factors by elevating total LDL-cholesterol and decreasing VLDL clearance in the body (Elliott et al., 2002). Other examples of disease risk factor development pathways activated by the presence of fructose include pathways leading to hepatic insulin resistance, hyperinsulinemia, hyperglycemia and leptin resistance, as previously discussed in Chapter 1 (Lim et al., 2010).

In the body, fructose is transported across membranes by the membrane bound facilitative transporter GLUT5, which has specificity for fructose only, with no ability to transport glucose or galactose (Kane et al., 1997), (Manolescu et al., 2007b). Expression of GLUT5 is mainly observed in the small intestine, but this protein is also found in the brain, musculoskeletal tissue, kidney, liver, testis and adipocyte

(Lim et al., 2010), (Thompson et al., 2016), (Wilder-Smith et al., 2014). A K_m of 6 mM has been reported for GLUT5-mediated fructose uptake in a study investigating the specificity of GLUT5 for fructose through expression of this protein on *Xenopus laevis* oocytes (Burant et al., 1992). Six other GLUT transporters have the ability to transport fructose, with GLUT2 being the second major transporter of this sugar after GLUT5 (Manolescu et al., 2007b). Nevertheless, unlike GLUT5, GLUT2 has shown to recognize glucose, glucosamine as well as galactose, and to be inhibited by phloretin and cytochalasin B (Manolescu et al., 2007b), (Krupka, 1985), (Uldry et al., 2002). Healthy individuals have been reported to be able to absorb up to 25 g of fructose, with higher doses leading to malabsorption and intolerance (Rao et al., 2007). Dietary fructose absorption is mostly regulated in the small intestine, where GLUT5 is found in great abundance (Blakemore et al., 1995), (Dyer et al., 2002). Expression of GLUT5 has been reported to be regulated by developmental, hormonal as well as nutritional influences (Douard and Ferraris, 2008). For instance, in the prenatal stage, levels of intestinal GLUT5 mRNA, as well as fructose transport rates, are low (Buddington and Diamond, 1989). Fructose malabsorption in young children, following the consumption of honey and fruit juice containing fructose, is likely associated with the low expression levels of GLUT5 (Nobigrot et al., 1997), (Wilder-Smith et al., 2014). Cui et al have investigated the role of specific genes on fructose modulation *in vivo*, hypothesising that corticosteroids play a major role in regulating intestinal GLUT5 (Cui et al., 2004). To add to that, studies have confirmed that GLUT5 is regulated by its substrate, fructose, with increased levels of GLUT5 mRNA available following consumption of a diet high in this sugar *in vivo* (David et al., 1995). Adipocytes cultured in the

presence of fructose also showed a higher expression of GLUT5 (Legeza et al., 2014).

Due to its expression in insulin-sensitive tissues in humans, such as skeletal muscle and adipocytes, the interest in GLUT5 expression levels in association with diseases has increased over the recent years. Although the link between excess dietary fructose consumption and development of disease risk factors is widely accepted, as is the importance of GLUT5 for fructose transport, the direct link between GLUT5 and the development of diseases such as diabetes in these tissues remains to be determined (Douard and Ferraris, 2008). Nevertheless, diabetic patients have exhibited increases in GLUT5 mRNA and protein expression in skeletal muscle as well as in the intestine (Stuart et al., 2007), (Dyer et al., 2002). Furthermore, studies have shown a correlation between GLUT5 expression and diabetes, or diabetic complications, in fat tissue of rodent models (Hajduch et al., 1998). Chronic exposure of fructose has been indirectly linked with obesity and hyperinsulinemia, even though fructose does not lead to an acute increase in insulin levels. This has been proposed to be caused by the significantly higher levels of expression of GLUT5 in diabetic human and animal models when compared to non-diabetic controls (Basciano et al., 2005), (Litherland et al., 2004). To add to that, a study by Litherland et al on obese rats concluded that GLUT5 expression, as well as rate of fructose transport, are dependent on insulin sensitivity, supporting the hypothesis of a potential role for GLUT5 in increased circulating fructose detected during diabetes (Litherland et al., 2004). Other disease risk factors, namely fructose-induced hypertension, have also been

directly associated with GLUT5 as seen in a study conducted on GLUT5-deficient mice, which demonstrated a malabsorptive phenotype and resistance to hypertension induced by fructose, when compared to wild-type mice (Barone et al., 2009).

GLUT5-mediated fructose uptake inhibition is not achieved in the presence of quercetin, phloretin or cytochalasin B, examples of competitive inhibitors of facilitative glucose transport by GLUT2 transporter (Burant et al., 1992), (Song et al., 2002). A study by Slavic et al showed that epigallocatechin gallate (EGCG) was an effective GLUT5-mediated fructose transport inhibitor, when protein was expressed in *Xenopus laevis* oocytes (Slavic et al., 2009). Other reports have demonstrated that plant products rubusoside and astragalin-6-glucoside also inhibited GLUT5 protein in proteoliposomes (Thompson et al., 2015). The same group showed GLUT5-mediated fructose transport inhibition by the chemical N-[4(methylsulfonyl)-2-nitrophenyl]-1,3-benzodioxol-5-amine (MSNBA) in proteoliposomes (Thompson et al., 2016). To date, the only other known specific inhibitors of GLUT5 are the sugar analogues L-sorbose-Bn-OZO and 2,5-anhydro-D-mannitol, both of which were engineered to specifically inhibit GLUT5 (Girniene et al., 2003), (Tatibouet et al., 2000). A study on adipocyte differentiation showed less lipid accumulation in L-sorbose-Bn-OZO treated cells compared to control in medium with no added fructose (Du and Heaney, 2012). Furthermore, the compound 2,5-anhydro-D-mannitol demonstrated high affinity for GLUT5 and significantly inhibited fructose uptake in human breast adenocarcinoma cell line, MCF-7 (Tanasova et al., 2013).

The membrane bound GLUT5 transporter evolved to recognize different configurations of fructose (furanose and pyranose), while excluding glucose completely, thereby becoming exclusively specific to fructose (Tatibouet et al., 2000), (Cura and Carruthers, 2012). The role of GLUT5 in fructose transport and its overexpression pattern in diseases such as diabetes highlights the importance of this protein for potential therapeutic interventions (Thompson et al., 2015). Plant-derived compounds, (poly)phenols, present in our daily diet, have been reported to have a positive impact on carbohydrate metabolism by a number of different mechanisms, including controlling post-prandial sugar distribution and regulating sugar digestion (Hanhineva et al., 2010). As described above, some (poly)phenols, such as EGCG, have shown to have an impact on fructose uptake by GLUT5. In this chapter, the effects of specific (poly)phenols and plant extracts on GLUT5-mediated fructose transport, and their potential as bioactives in disease prevention interventions, were investigated through uptake experiments performed on *X. laevis* oocytes expressing GLUT5. Extracts and compounds used in the uptake experiments presented in this chapter were selected based on their reported impacts on disease risk factors associated with excess fructose intake.

4.3 Validation of GLUT5pBF plasmid construct functionality

4.3.1 Confirmation of adequate placement of hGLUT5 gene in expression vector

Human GLUT5 gene was inserted into pBF expression vector, commonly used in heterologous expression of proteins in *X. laevis* oocytes, following the methods

described in Chapter 2 (see section 2.3). The successful ligation of gene of interest and the expression vector was determined through PCR of plasmid construct colonies with two primers; one designed against a region of the pBF sequence (pBF-reverse) and one homologous to the sequence of GLUT5 gene (GLUT5_1703-Forward). A positive product for presence of GLUT5 gene produced clear individual DNA bands of size corresponding to the number of base pairs (bp) between the two primers, as well as the number of bp from start of GLUT5_1703-Forward until the end of the sequence when analysed on gel electrophoresis, as can be seen in Figure 4.2. Serving as a control, PCR was also performed on pBF plasmid, which produced no DNA products. Fifteen individual colonies were extracted, and those considered positive for the presence of GLUT5 gene and were sequenced to confirm exact sequence (refer to Chapter 2 section 2.3.1 for list of primers used). Exact position of each primer, as well as basic structure of plasmids, are shown in Figure 4.1.

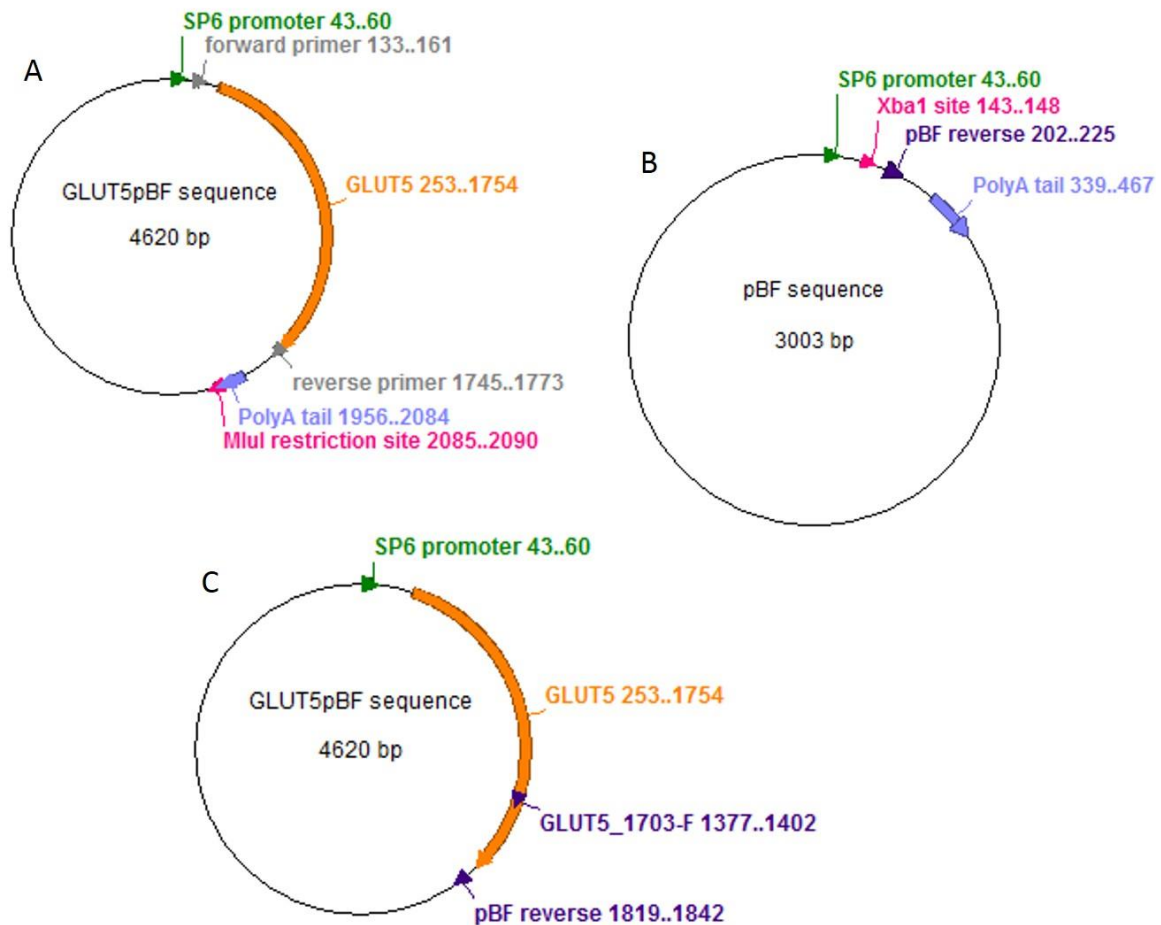


Figure 4-1 Illustration of the GLUT5pBF and pBF plasmids and primer location for PCR validation of positive colonies for GLUT5 presence. Representation of the full GLUT5pBF plasmid and all its different attributes, including SP6 promoter (green) region and PolyA tail (light purple), as well as location of the inserted GLUT5 gene (orange) **(A)**. Representation of the pBF plasmid and its characteristics, prior to the insertion of the GLUT5 gene, including the location of pBF reverse primer (dark purple) **(B)**. Representation of primer location (dark purple) on GLUT5pBF plasmid sequence **(C)**.

The two primers used to perform PCR for positive colony validation are shown in dark purple in Figure 4.1 B and C, above. The size of DNA products expected to be observed in gel electrophoresis was calculated by determining the number of base pairs between either end of the two primers (466 bp), in dark purple on Figure 4.1 C, as well as the number of base pairs from the beginning of GLUT5_1703 forward primer up until the end of the sequence (3244 bp). The exact location of

the GLUT5 sequence (orange) in reference to the other characteristics of the pBF plasmid are shown in Figure 4.1 A. The gene was inserted in between the SP6 promoter region (green), where in vitro transcription of mRNA starts, and MluI restriction site (pink), where transcription ends (Beckert and Masquida, 2011). To add to that, GLUT5 is also located before the PolyA region (light purple), a stretch of sequence that contains only adenosine. The PolyA tail is crucial for the stability of mRNA and is important for the translation process. It also acts as an identifying element for mRNA nuclear export (Fuke and Ohno, 2008). The same figure shows the site of the specific primers with homology to pBF and GLUT5 sequences (light grey) used in the ligation of the two vectors (refer to Chapter 2, section 2.3.3.1). These characteristics are derived from amphibian expression vector pBF (Figure 4.1 B). The different attributes of this plasmid aids the expression of heterologous proteins from microinjected mRNA in the host, *X. laevis*. For this reason, the molecular biology methods were set up to incorporate the GLUT genes into the sequence of this specific expression vector. Full sequences of the pBF expression vector and of the GLUT5pBF construct can be found in the appendices.

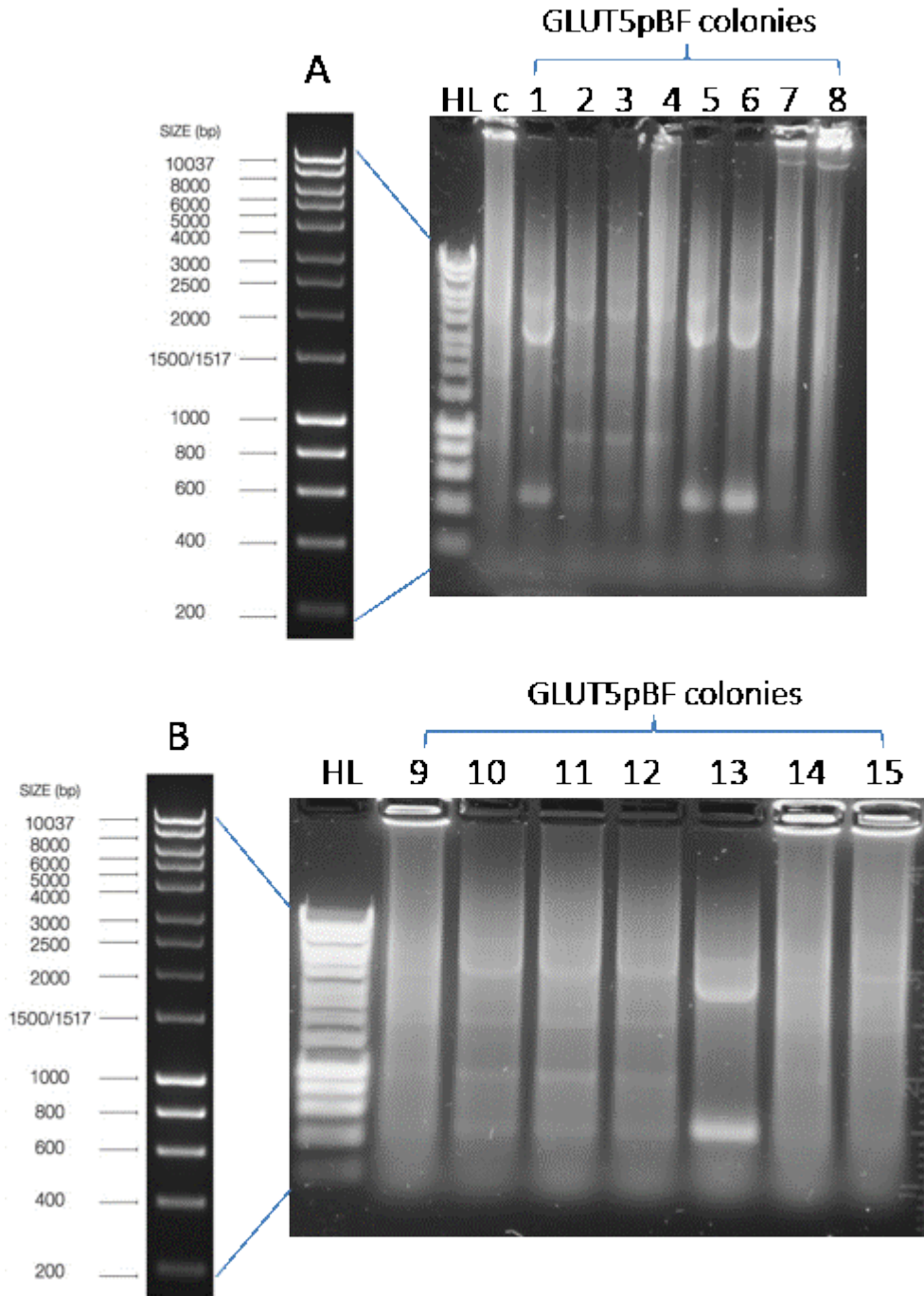


Figure 4-2 Gel electrophoresis image of PCR of GLUT5pBF colonies after ligation of GLUT gene to expression vector. Primers used were pBF-reverse and GLUT5_1703- Forward. A colony positive for the presence of GLUT5 gene produced a clear individual band [colony 1, 5, 6 (**A**) and 13 (**B**)], whereas negative colonies and control (c, pBF plasmid) (**A**) produced no products. Product sizes are equal to number of base pairs between two primers (466 bp) and number of base pairs from start of GLUT5_1703-Forward primer until the end of sequence (3244 bp). Size of products was determined against a DNA hyperladder (HL).

Figure 4.2 shows the DNA products from PCR reaction of colonies with pBF-reverse and GLUT5_1703- Forward primers. Colonies 1, 5, 6 and 13 (Figure 4.2 A and B) were considered positive for the presence of GLUT5 as they produced products around 400 bp and 3000 bp in size, which are comparable to the expected product sizes of 466 bp and 3244 bp. Control PCR of pBF plasmid without GLUT5 insert produced no products, as expected. Sequencing results from positive colonies for the presence of GLUT5 gene showed that the sequence of all four colonies matched the expected sequence for GLUT5pBF. One single colony was randomly chosen for propagation (colony 5) and used for all subsequent experiments.

4.3.2 Confirmation of specificity and quality of mRNA product

The in vitro transcription (IVT) reaction was carried out with linearized GLUT5pBF plasmid obtained from digestion with MluI restriction enzyme, as its restriction site is located after the gene of interest (refer to Chapter 2, section 2.3.5 for details). The mobility of circular plasmid DNA in agarose gels is dependent on various factors, including the type and concentration of agarose gel, current strength, and density of superhelical twists. Supercoiled DNA is tightly compact and occupies less space in the gel, therefore migrating at a faster rate than relaxed linear DNA (Sambrook and Russell, 2001). Figure 4.3 A illustrates the migration pattern of circular GLUT5pBF (circ.) and of linear digest (lin.). Circular plasmid produces two distinct band products; the higher molecular weight band corresponding to nicked DNA and the lowered molecular weight band indicating supercoiled DNA. Linear GLUT5pBF digest migrates through the gel at a slower rate than circular DNA and

produces a band at a size comparable to that of the full plasmid sequence (4620 bp). The mRNA product of IVT reaction is analysed in a denaturing RNA gel (see Chapter 2 section 2.3.5) confirming that its size matched the expected size obtained from the sequence (2031 bp) (Figure 4.5 B). The presence of formaldehyde in agarose gel maintains RNA in the denatured state by preventing intra-strand base pairing, making the visualisation of mRNA product possible (Sambrook and Russell, 2001).

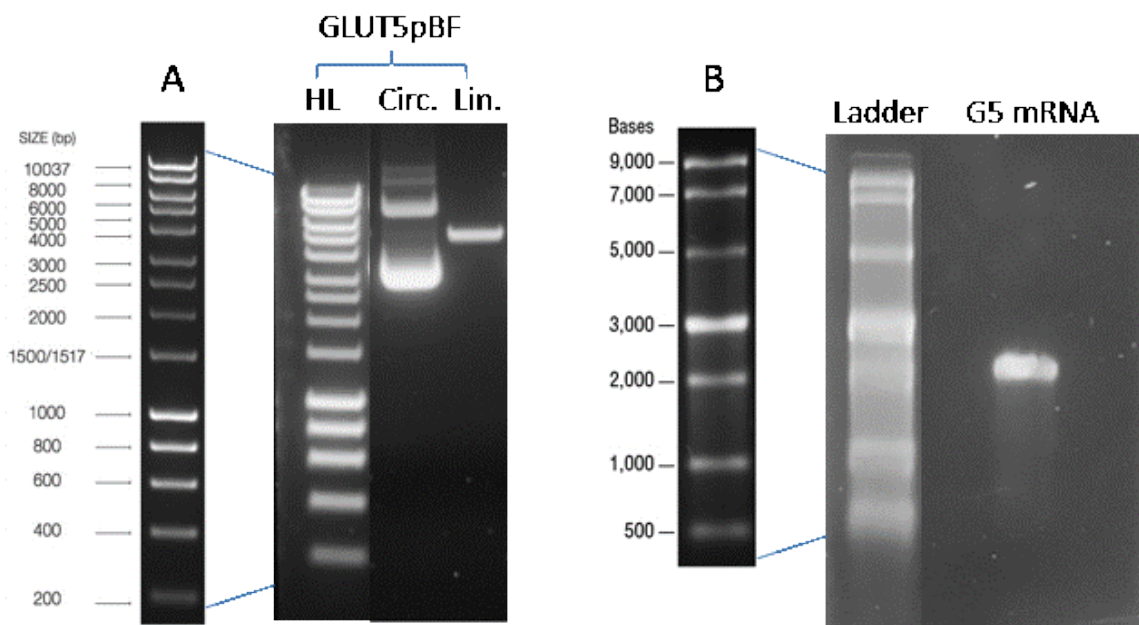


Figure 4-3 Gel electrophoresis of linearized GLUT5pBF construct and denaturing gel of GLUT5 mRNA product. GLUT5pBF plasmid was linearized by digestion with MluI restriction enzyme before IVT reaction. Circular GLUT5pBF plasmid (circ.) produces bands on gel characteristic of its structure, whereas linear plasmid (lin.) produces a single band corresponding in size to the full sequence of the plasmid (4620 bp) (A). After IVT reaction the mRNA product was run on a formaldehyde denaturing gel to confirm that its size matched that expected from sequence of the plasmid (2031 bp) (B). The size of the products was determined against a DNA hyperladder (HL) (A) and ssRNA ladder (B). Gel electrophoresis confirming linearization of plasmid and RNA denaturing gel of mRNA products were performed for every new mRNA sample prepared.

4.4 Validation of *X. laevis* model functionality

4.4.1 Fructose uptake by GLUT5-expressing oocytes and inhibition by known specific inhibitors

The uptake of fructose by GLUT5-expressing oocytes was measured using different concentrations of fructose and ¹⁴C-fructose in an incubation solution. The optimal specific radioactivity was determined to be 0.5 μCi, which remained unchanged for all uptake experiments. Two fructose concentrations were used to carry out GLUT5 uptake experiments, namely 6 mM and 100 μM. A time course experiment measuring uptake of fructose over time was used to determine the optimal incubation time for the initial uptake experiments, all conducted with 6 mM fructose incubation solution. Although there was no significant difference between uptake at the different time points tested the highest uptake, with the least variability, was attributed to a 15 min incubation period. Results of this time course experiment are presented in Figure 4.4. GLUT5 k_m for fructose has been reported to be around 6 mM (Manolescu et al., 2007a), hence why this particular concentration was used for initial experiments. Incubations were carried out at 37 °C to try and mimic the temperature conditions of the body, where this protein is active. Oocyte incubation conditions for the initial fructose uptake experiments were, therefore, 6mM fructose for 15 min at 37 °C. Water injected oocytes were used as controls in all uptake experiments. Results of uptake by GLUT5-expressing oocytes are shown normalized to the uptake observed by their respective water injected controls, unless otherwise stated.

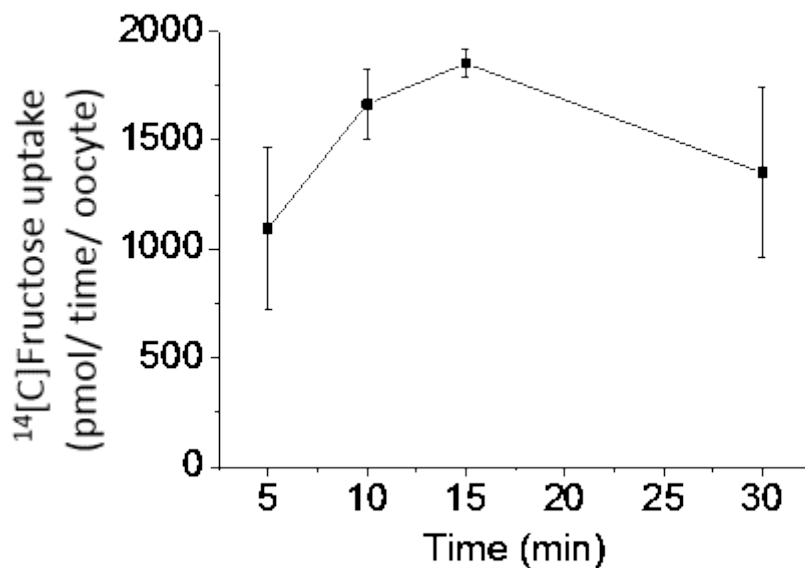


Figure 4-4 Fructose (6 mM) uptake time course experiment. One day post GLUT5 mRNA microinjection oocytes were incubated in 6 mM fructose solution containing [¹⁴C] fructose over 5-30 min at 37 °C. Each data point represents the mean of 3 replicates (of 3 oocytes), normalized to control for each condition, ± SEM. There was no statistical difference between the incubation times tested, however, the highest uptake and less variability was attributed to 15 min incubation. All 6 mM fructose uptake experiments were carried out for 15 min at 37 °C.

The possible effects of solvents on oocytes, in particular ethanol and DMSO, were investigated by addition of increasing concentrations of each solvent in a fructose incubation solution. Radiolabelled ¹⁴C-fructose used in uptake experiments is available in ethanol:water (9:1) solution, meaning standard incubation solution contains 1.25% of ethanol. There were no significant changes in fructose with the addition of up to 11.25% ethanol (Figure 4.5 A) or up to 10% DMSO (Figure 4.5 B). In addition, the oocytes seemed to be visually unaffected. All uptake experiments for which added compounds were stored in either DMSO or ethanol, the equivalent amount of the solvent was added to the standard fructose only incubation solution.

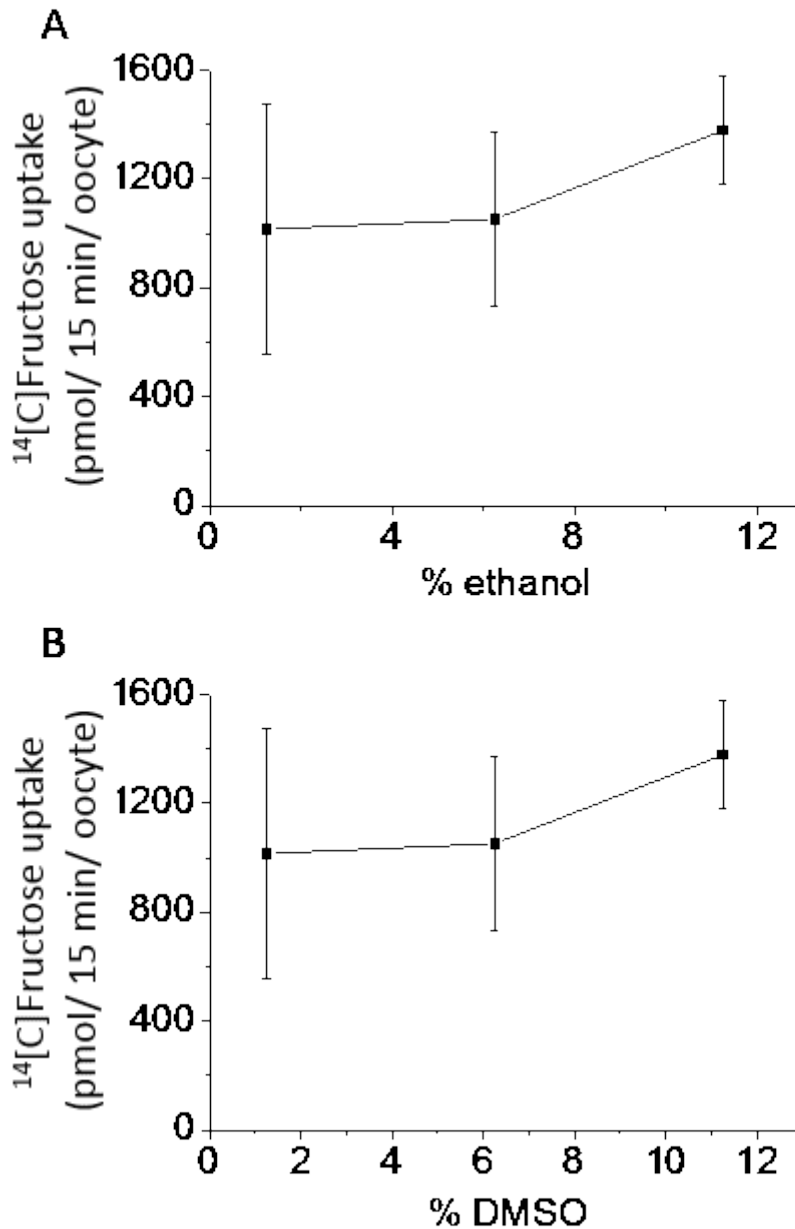


Figure 4-5 Effect of solvents on oocytes. One day post GLUT5 mRNA microinjection oocytes were incubated in 6 mM fructose solution containing [¹⁴C] fructose with and without ethanol (1.25-11.25%) **(A)** and DMSO (0-10%) **(B)** for 15 min at 37 °C. There was no significant change in uptake of fructose by the oocytes in the presence of either solvent **(A)** **(B)**. Oocytes were visually unaffected. Each data point represents the mean of 3 replicates (of 3 oocytes), normalized to control for each condition, ± SEM.

The addition of 6 mM of the GLUT5 specific inhibitor of L-sorbose-Bn-OZO (L-sorbose) to fructose incubation solution significantly decreased the uptake of this

sugar in oocytes microinjected with GLUT5 mRNA by 53%, $p \leq 0.01$ (Figure 4.6 A). Similarly, 7.6 mM 2,5-anhydro-D-mannitol (a-mannitol), another compound synthesised to specifically inhibit GLUT5, significantly decreased the uptake of fructose in hGLUT5-expressing oocytes by 54%, $p \leq 0.001$ (Figure 4.6 B).

Alternative GLUT5 fructose uptake experiments were carried out at a fructose incubation solution concentration of 0.1 mM, as previously reported in similar oocyte uptake experiments (Li et al., 2004). Incubation time was decreased to 5 min and experiments were carried out at 25 °C. There was a significant difference between fructose uptake by GLUT5 mRNA injected oocytes and water injected control oocytes, as for previous uptake experiments at higher fructose concentration. Moreover, addition of 7.6 μ M 2,5-anhydro-D-mannitol (a-mannitol) significantly reduced GLUT5-mediated fructose uptake by 61% ($p \leq 0.01$) (Figure 4.6 C). Inhibition of fructose uptake observed by this inhibitor was comparable at both fructose incubation solution concentrations, therefore, determining that the oocyte model is functional and that oocytes were able to translate the protein from hGLUT5 mRNA and transported it to the membrane, where it is active as a transporter.

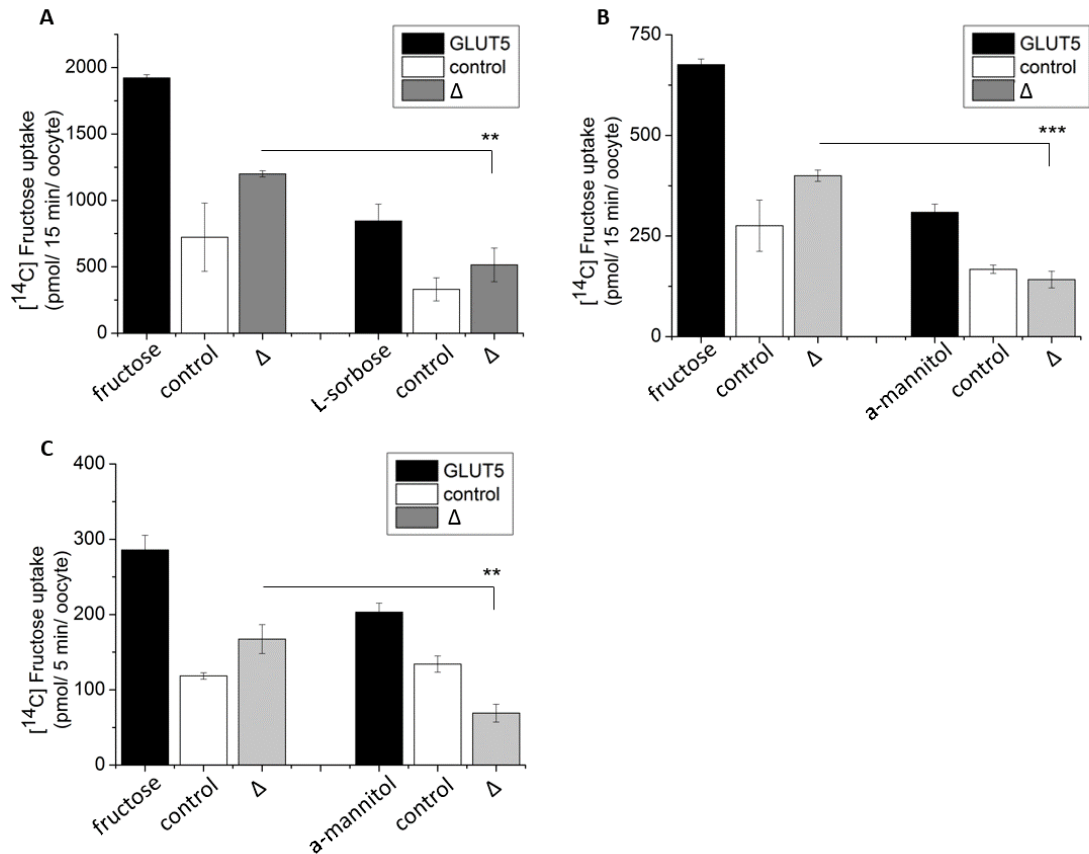


Figure 4-6 Inhibition of GLUT5 fructose uptake by known inhibitors. One day post GLUT5 mRNA microinjection oocytes were incubated in 6 mM fructose solution containing [^{14}C] fructose with and without 6 mM L-sorbose-Bn-OZO (L-sorbose) **(A)** and 7.6 mM 2,5-anhydro-D-mannitol (a-mannitol) for 15 min **(B)** or incubated in a 0.1 mM fructose solution containing [^{14}C] fructose with and without 7.6 μM 2,5-anhydro-D-mannitol (a-mannitol) for 5 min **(C)**. Internalized sugar uptake was determined by scintillation spectrometry for protein expressing oocytes (black bars) and water injected controls (open bars). Net change in uptake, Δ , (grey bars) was determined by normalizing the uptake observed by GLUT5 to control uptake. The mean \pm SEM of three **(A and B)** or six **(C)** replicates (of 3 oocytes) is shown per individual condition. L-sorbose-Bn-OZO reduced GLUT5 uptake of fructose by 53% **(A)** and 2,5-anhydro-D-mannitol decreased fructose uptake by GLUT5 by 54% **(B)** when incubated in 6 mM fructose. 2,5-anhydro-D-mannitol reduced GLUT5-mediated fructose uptake by 61% when incubated in 0.1 mM fructose **(C)**. ** $p \leq 0.01$ and *** $p \leq 0.001$.

4.4.2 Determination of expression of recombinant hGLUT5 on oocyte membrane extracts

Expression of GLUT5 on oocyte membranes post microinjection with protein mRNA was observed by traditional western blot techniques (refer to Chapter 2 sections 2.4.3 and 2.4.6). Membranes extracts from 10 oocytes (Figure 4.7 A) and 3 oocytes (Figure 4.7 B) injected with GLUT5 mRNA or water were compared to positive control TC7 cell lysate. Images confirm that GLUT5 was expressed on GLUT5 mRNA injected oocyte membranes (G5) and positive control (TC7) but not in water injected control membrane extracts (C).

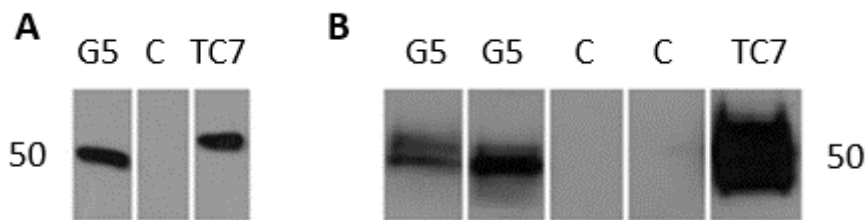


Figure 4-7 Western blot image of the expression of GLUT5 on oocyte membrane extracts. Membrane extract derived from oocytes injected with GLUT5 mRNA (G5) or water (C), two days following microinjections, were compared to positive lysate TC7 lysate (TC7) for expression of GLUT5. Membrane extracts from 10 oocytes, imaged at exposure time of 5 s, show expression of GLUT5 on mRNA injected membrane extracts and positive control, but not in control injected extracts (**A**). Similarly, membrane extracts of three oocytes, imaged at exposure time of 1 min, confirms expression of protein in mRNA injected membrane extracts (G5, 2 replicates) and positive control (TC7) only (**B**). TC7 lysate concentration was 0.2 mg/ml; oocyte membrane concentrations were 0.5 mg/ml. This image is one of 7 replicates.

GLUT5 expression on oocyte membranes was also investigated through capillary automated Western blot system, Wes (see Chapter 2 section 2.4.7). Two days post microinjection with GLUT5 mRNA oocyte membranes were extracted and analysed on Wes under varying protein concentrations (0.4-0.02 mg/ml). A gel

image of the decreasing concentrations of protein shows a correlation between concentration and signal produced (Figure 4.8 A), also noticeable in electropherogram (Figure 4.8 C). Lower loading concentrations of protein produced a cleaner signal and less non-specific binding. An alternative sample of oocyte membranes extracted one day post microinjection with GLUT5 mRNA was compared to a membrane extract of water injected control oocytes and showed protein detection in mRNA injected samples only (Figure 4.8 B). This data is also presented as an electropherogram (Figure 4.8 D), showing no protein detection in water injected control membrane samples.

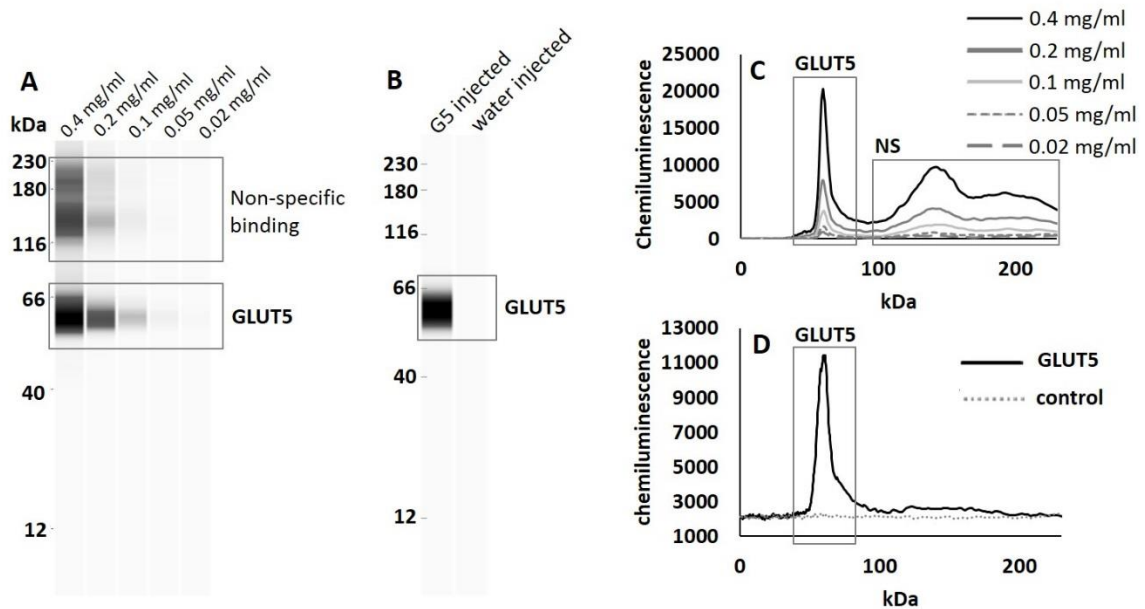


Figure 4-8 Confirmation of expression of GLUT5 on oocyte membrane extracts by wes. Membranes extracted from three oocytes two days post injection with GLUT5 mRNA, as well as water injected control membranes, were analysed using automated capillary Western blot (Wes). Analysis of a membrane extract sample is shown as a gel-like image at varying protein concentrations (0.4-0.02 mg/ml) (**A**) and as an electropherogram of the same samples (**C**). An alternative oocyte membrane sample of mRNA injected oocytes was compared to that of water injected controls, both at 0.2 mg/ml, and showed GLUT5 expression on mRNA injected membranes extract only (**B**, **D**). This data is shown as a gel image (**B**) as well as electropherogram (**D**). The detected protein size for GLUT5 was 60 kDa. Antibody dilution was 1:50. This image represents one of 4 replicates.

Previous reports of uptake experiments in GLUT5 expression oocytes were conducted after two days post microinjection with mRNA (Kwon et al., 2007) (Slavic et al., 2009). Membranes were extracted from three oocytes one to four days post microinjection with GLUT5 mRNA, in order to assess at what point the protein expression was at its highest. GLUT5 protein expression was comparably high after 24 hrs and four days post microinjection, as can be observed in a gel like image and electropherogram (Figure 4.9 A and B). Although GLUT5 was still detectable after two and three days post microinjection, its expression was not as pronounced as in the other days. For this reason, all further uptake experiments with GLUT5 were performed only 24 hrs after microinjection, as opposed to 48 hrs.

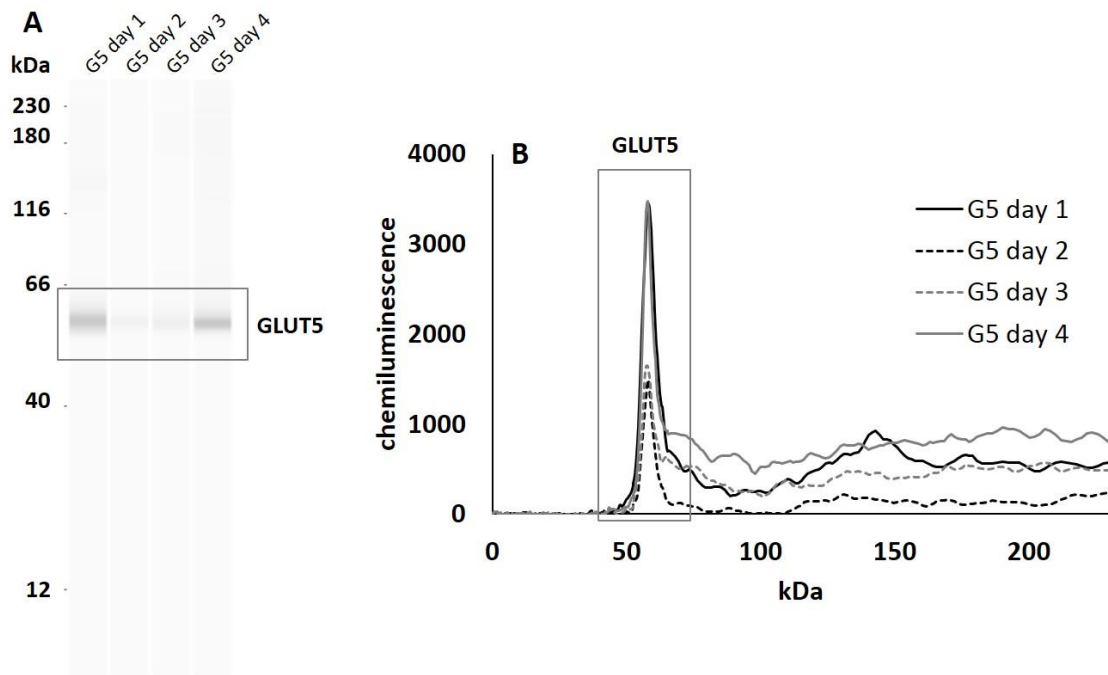


Figure 4-9 Determination of level of GLUT5 expression on oocyte membrane extracts by wes. Membranes were extracted from three oocytes one to four days post injection with GLUT5 mRNA and analysed using automated capillary Western blot (Wes). Analysis of membrane extract samples is shown as a gel-like image **(A)** and as an electropherogram of the same samples **(B)**. GLUT5 protein expression was at its highest after 1 day (G5 day1) and four days (G5 day4) post microinjection. Protein was still detected but at a lower expression after 2 days (G5 day2) and three days (G5 day3) post microinjection. All samples were loaded at a concentration of 0.1 mg/ml. Detected protein size for GLUT5 was 58-59 kDa. Antibody dilution was 1:50.

GLUT5 antibody used for both protein detection techniques was raised against an internal region of the human protein and recognizes a product of 49-60 kDa in size. Optimal GLUT5 antibody dilution of 1:50 for Wes experiments was determined by Dr. S. Tumova.

4.5 Uptake experiment results and discussion

In order to attribute inhibition of GLUT5-mediated fructose transport by a specific compound or extract oocytes expressing this transporter were incubated in a fructose solution, containing ^{14}C -fructose, in the presence and absence of each compound/extract. Uptake inhibition experiments were conducted using plant extracts that from the literature have shown to have an impact on disease risk factors associated with excess fructose consumption (refer to Chapter 1). In addition, extracts which were being used, or would in the future be used, in human studies conducted by other individuals in the research group were also tested (e.g. German chamomile, green tea and pomegranate) (Villa-Rodriguez et al., 2017a), (Nyambe-Silavwe and Williamson, 2016). This was done with the aim to validate results and to attribute inhibition to specific transporters. Initial incubation conditions were as follows; 6 mM ^{14}C -fructose for 15 mins at 37 °C. Table 4.1 shows all the compounds/extracts tested for inhibition using these experimental conditions. Nevertheless, following inhibition experiments with GLUT2-expressing oocytes (Chapter 5) it became apparent that another experimental condition might be more suited, namely, 0.1 mM fructose for 5 mins at 25 °C. Specific radioactivity of radiolabelled fructose (0.5 μCi) remained unchanged for both conditions. Because of the amount of time necessary to microinject the oocytes and to conduct the experiments only a few of the extracts and compounds could be re-tested using the revised experimental condition (these are marked in Table 4.1 with an asterisk). Once extracts that significantly decreased the uptake of GLUT5 were identified pure compounds were then tested, using the revised 0.1 mM fructose for 5 mins at 25 °C experimental condition only.

Table 4-1 Compounds/extracts used in GLUT5-mediated fructose uptake inhibition studies described in this chapter

Compound/ extract	Experimental condition
2,5-anhydro-D-mannitol *	6 mM fructose for 15 mins at 37 °C 0.1 mM fructose for 5 mins at 25 °C
Acarbose *	6 mM fructose for 15 mins at 37 °C 0.1 mM fructose for 5 mins at 25 °C
Apigenin	0.1 mM fructose for 5 mins at 25 °C
Bonolive *	6 mM fructose for 15 mins at 37 °C 0.1 mM fructose for 5 mins at 25 °C
Black tea	6 mM fructose for 15 mins at 37 °C
Baking Chocolate Standard Reference Material	6 mM fructose for 15 mins at 37 °C
Cocoa	6 mM fructose for 15 mins at 37 °C
Coffee	6 mM fructose for 15 mins at 37 °C
EGCG	0.1 mM fructose for 5 mins at 25 °C
Eucalyptus Leaf Extract (ELE)	6 mM fructose for 15 mins at 37 °C
Epicatechin	6 mM fructose for 15 mins at 37 °C
German chamomile *	6 mM fructose for 15 mins at 37 °C 0.1 mM fructose for 5 mins at 25 °C
Green tea *	6 mM fructose for 15 mins at 37 °C 0.1 mM fructose for 5 mins at 25 °C
Hesperidin	0.1 mM fructose for 5 mins at 25 °C
Hesperetin	0.1 mM fructose for 5 mins at 25 °C
L-sorbose-Bn-OZO	6 mM fructose for 15 mins at 37 °C
(Poly)phenol mixture: apigenin, flavone, galangin and kaempferol	6 mM fructose for 15 mins at 37 °C
Pomegrante	6 mM fructose for 15 mins at 37 °C 0.1 mM fructose for 5 mins at 25 °C
Procyanidins	6 mM fructose for 15 mins at 37 °C
Quercetin	0.1 mM fructose for 5 mins at 25 °C

* uptake inhibition studies conducted with both experimental conditions

4.5.1 Effect of extracts on fructose uptake by GLUT5

The effect of dark chocolate extract (see section 2.1.3 of Chapter 2 for details) and Baking Chocolate Standard Reference Material (kindly supplied by the National Institute of Standards and Technology, USA) on GLUT5-mediated fructose transport was determined by the incubation of oocytes in 6 mM fructose solution with increasing concentrations of the chocolate extract (Figure 4.10 A) and in the presence of cocoa reference standard (Figure 4.10 B). There was no significant change in uptake in the presence of either extract.

The flavanol profile of dark chocolate extract, as well as that of chocolate reference standard material, were analysed following HPLC-FLD protocol (Chapter 2 section 2.1.4). Concentrations (μM) of each flavanol for both samples were calculated using an epicatechin calibration curve (Figure 4.11 A) and individual relative response factors for each fraction. The flavanol profile of dark chocolate extract consisted of monomer to hexamer (DP1-DP6) only (Figure 4.11 B, C), whereas the chocolate reference standard material's flavanol profile ranged from monomer to decamer (Figure 4.11 B, D), matching previously reported analysis (Robbins et al., 2012). The monomer (DP1, epicatechin) was the most abundant in both samples, with lower concentrations of other oligomeric fractions.

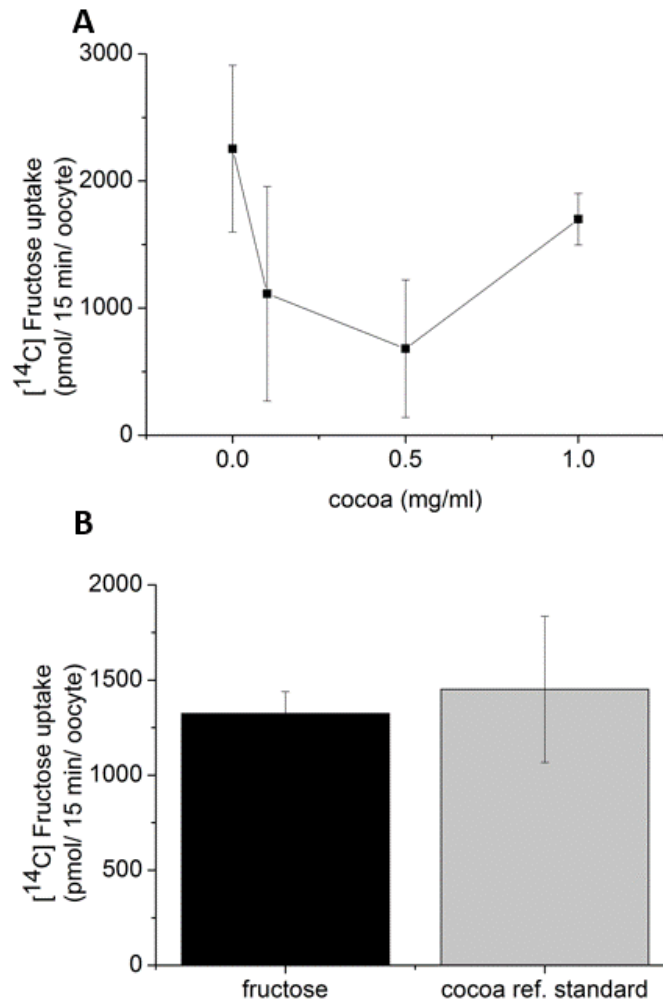


Figure 4-10 Effect of cocoa extracts on fructose uptake by GLUT5. One day post GLUT5 mRNA microinjection oocytes were incubated in 6 mM fructose solution containing [¹⁴C] fructose with increasing concentrations of dark chocolate extract (cocoa) (0-1 mg/ml) **(A)** and in the presence of chocolate reference standard material (cocoa ref. standard) **(B)** for 15 min at 37 °C. There was no significant change in uptake of fructose by the oocytes in the presence of either extract under these conditions **(A)** **(B)**. Each data point represents the mean of 3 replicates (of 3 oocytes), normalized to control for each condition, ± SEM.

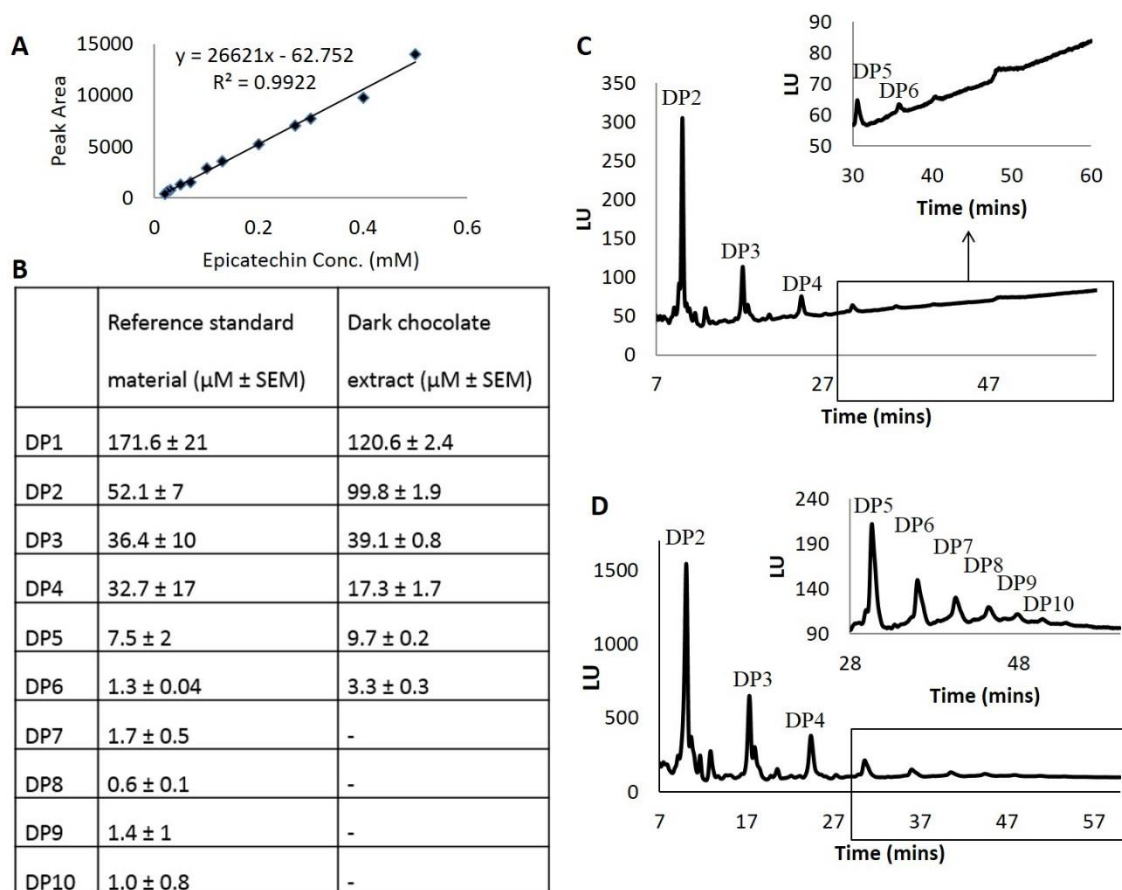


Figure 4-11 Analysis of flavanol profile of chocolate extracts using HPLC-FDL. Epicatechin calibration curve (**A**) and relative response factor values were used to calculate the concentration of each fraction in both sample (mean \pm SEM of three replicates) (**B**). Dark chocolate extract produced a profile consisting of monomer to hexamer (**C**), while chocolate reference material produced a full monomer to decamer profile (**D**). Flavanol profiles were obtained at PMT level 12. Expanded inserts in (**C**) and (**D**) were obtained for pentamer to decamer by magnification and isolation of these fractions in the original image. Monomer (DP1) is not shown due to difference in signal intensity.

Uptake of fructose by GLUT5 expressed in oocytes was further investigated with coffee, black tea and eucalyptus leaf extract (ELE) (see Chapter 2, section 2.1.2) by addition of increasing concentrations of each extract to 6 mM fructose incubation solution (Figure 4.12). Coffee extract composition was rich in caffeoylquinic acids, composed majorly of 3-, 4- and 5-caffeoylquinic acids. The

amount of each caffeoylquinic acid in 4 g of instant coffee (equivalent to 1 cup) were 160 ± 8.4 , 103 ± 6.0 and 467 ± 9.2 μmol for 3-, 4- and 5-caffeoylquinic acids, respectively (Kraut, 2014). Based on previous documentation the composition of black tea is thought to be primarily made up of thearubigins, with this phenolics accounting for almost 60% of solids found in a typical black tea sample (Butt et al., 2014). Composition of ELE has not been entirely identified, however, isolated components include hydrolysable tannins and favonol glycosides (Sugimoto et al., 2010). There was no significant change in fructose uptake in the presence of any of these three extracts.

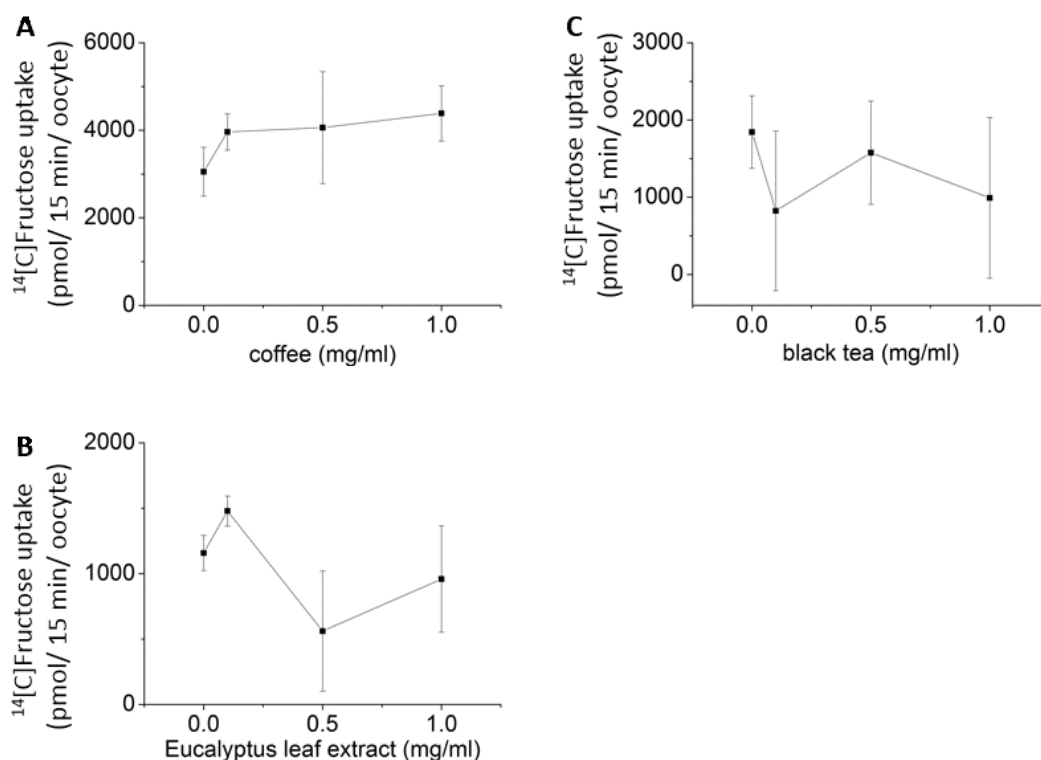


Figure 4-12 Effect of extracts on fructose uptake by GLUT5. One day post GLUT5 mRNA microinjection oocytes were incubated in 6 mM fructose solution containing ^{14}C fructose with increasing concentrations of coffee (0-1 mg/ml) **(A)**, black tea (0-1 mg/ml) **(B)** and ELE (0-1 mg/ml) **(C)** for 15 min at 37 °C. There was no significant change in uptake of fructose by the oocytes in the presence of any of the three extracts under these conditions **(A)** **(B)** **(C)**. Each data point represents the mean of 3 replicates (of 3 oocytes), normalized to control for each condition, \pm SEM.

Additional extracts used to investigate their potential effects on GLUT5-mediated fructose uptake were green tea, German chamomile, pomegranate and Bonolive (Figure 4.13). As previously, increasing concentrations of these extracts were added to 6 mM fructose incubation solution. There was no significant change in fructose uptake in the presence of any of the four extracts under the incubation conditions tested.

The main active components of green tea are (-)-Epigallocatechin gallate (EGCG) (199.8 ± 6.7 mg/g), (-)-Epigallocatechin (124.4 ± 9.3 mg/g), (-)-Epicatechin gallate (34.4 ± 1.9 mg/g) and (-)-Epicatechin (23.3 ± 2.4 mg/g), as analysed by HPLC (Nyambe-Silavwe and Williamson, 2016). The most abundant phenolic compounds present, percentage wise, in dry weight of the German chamomile extract are apigenin-7-O-glucoside (12.32%), apigenin (0.28%), luteolin-7-O-glucoside (0.13%) and 4,5-dicaffeoylquinic acid (0.07%) (Villa-Rodriguez et al., 2017a). Bonolive extract, kindly supplied by BioActor, is composed in its vast majority by oleuropein, this compound accounting for 40% of the extract composition. Pomegranate extract is composed mainly of punicalagin (121 mg/g), puricalin (6 mg/g), ellagic acid hexose (5.9 mg/g) and ellagic acid (101 mg/g) (Nyambe, 2016). All sugars were removed from pomegranate extract through solid phase extraction (SPE) by Dr. Hilda Nyambe, to make a sugar-free extract.

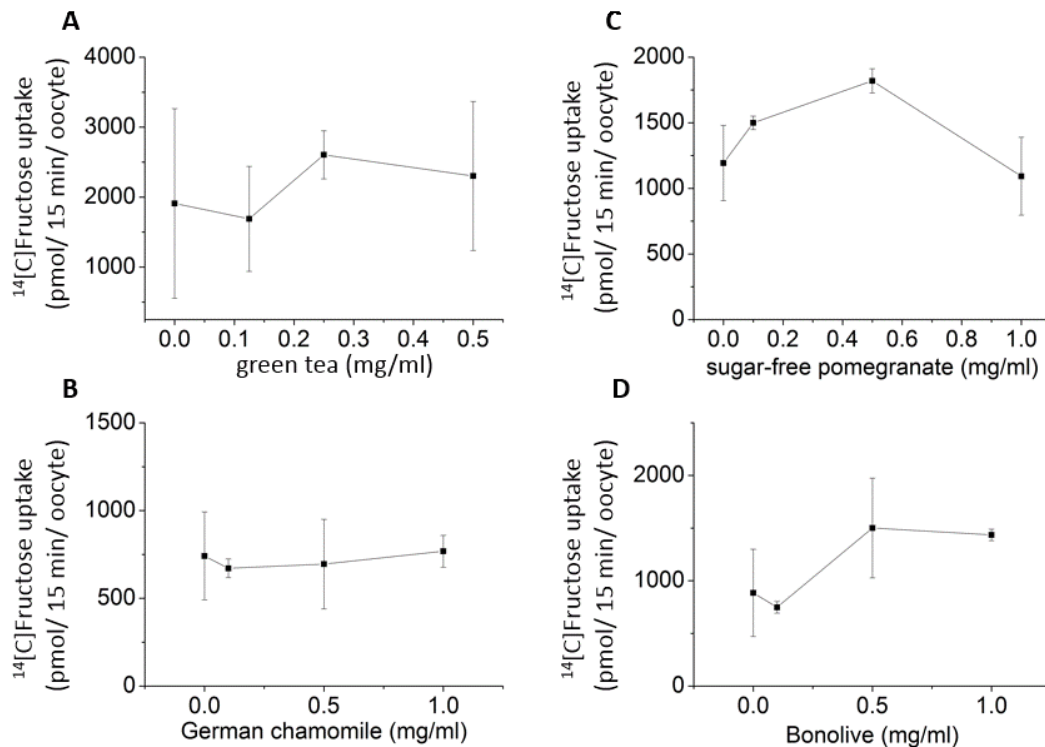


Figure 4-13 Effect of extracts on fructose uptake by GLUT5. One day post GLUT5 mRNA microinjection oocytes were incubated in 6 mM fructose solution containing [^{14}C] fructose with increasing concentrations of green tea (0-0.5 mg/ml) **(A)**, German chamomile (0-1 mg/ml) **(B)**, sugar-free pomegranate (0-1 mg/ml) **(C)** and Bonolive (0-1 mg/ml) **(D)** for 15 min at 37 °C. There was no significant change in uptake of fructose by the oocytes in the presence of any of the extracts under these conditions **(A)** **(B)** **(C)** **(D)**. Each data point represents the mean of 3 replicates (of 3 oocytes), normalized to control for each condition, \pm SEM.

The same four extracts mentioned above were used to investigate fructose uptake by oocytes expressing GLUT5 under different incubation conditions, namely, incubation at 25 °C for 5 min in a 0.1 mM fructose solution containing [^{14}C] fructose. Oleuropein-rich extract Bonolive (Figure 4.14 D) and green tea extract (Figure 4.14 A) still had no effect on fructose transport under these varying conditions. German chamomile (Figure 4.14 B) and sugar-free pomegranate extract (Figure 4.14 C), however, significantly decreased the uptake of fructose by GLUT5. IC_{50} values

were 0.73 ± 0.18 mg/ml and 0.48 ± 0.22 mg/ml for German chamomile and sugar-free pomegranate extracts, respectively.

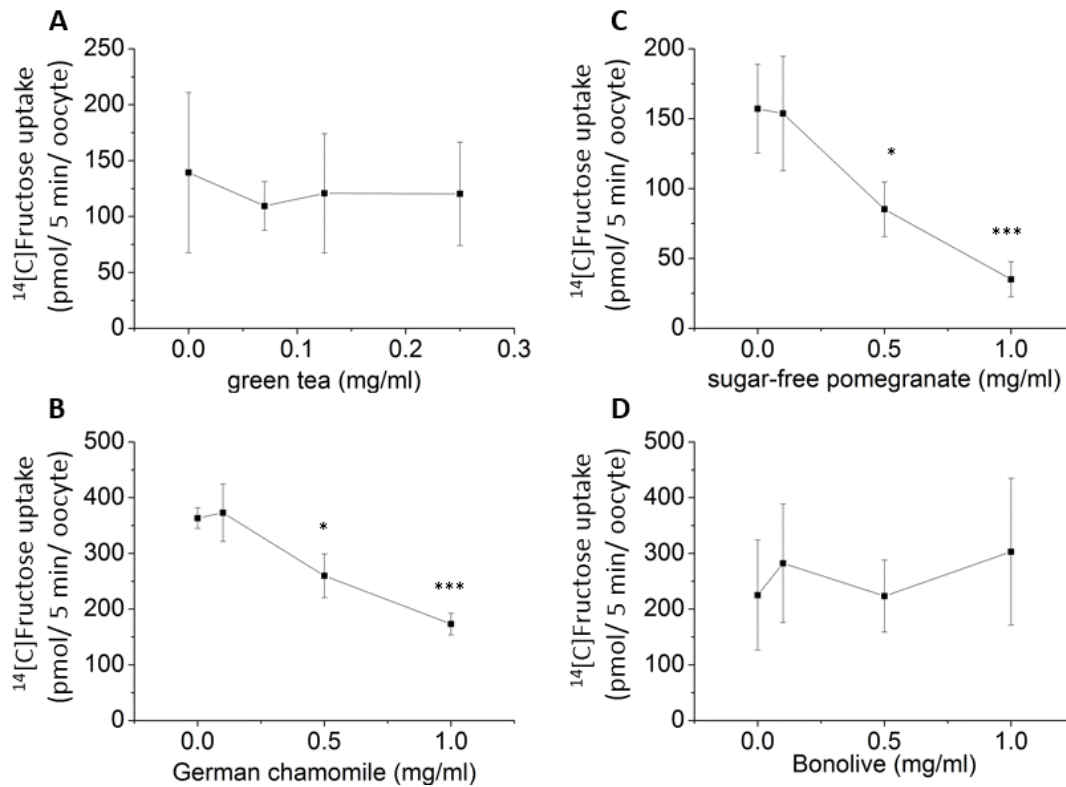


Figure 4-14 Effect of extracts on fructose uptake by GLUT5. One day post GLUT5 mRNA microinjection oocytes were incubated in 0.1 mM fructose solution containing [^{14}C] fructose with increasing concentrations of green tea (0-0.5 mg/ml) **(A)**, German chamomile (0-1 mg/ml) **(B)**, sugar-free pomegranate (0-1 mg/ml) **(C)** and Bonolive (0-1 mg/ml) **(D)** for 5 min at 25 °C. There was no significant change in uptake of fructose by the oocytes in the presence of green tea or Bonolive extracts under these conditions **(A)** **(D)**. GLUT5-mediated fructose uptake was significantly decreased in the presence of German chamomile ($\text{IC}_{50} = 0.73 \pm 0.18$ mg/ml) **(B)** and sugar-free pomegranate ($\text{IC}_{50} = 0.48 \pm 0.22$ mg/ml) **(C)**. Each data point represents the mean of 6 replicates (of 3 oocytes), normalized to control for each condition, \pm SEM. * $p \leq 0.05$, *** $p \leq 0.001$ and **** $p \leq 0.0001$.

Results obtained from uptake experiments with extracts show that variability between replicates is substantial. This variability could be attributed to the individual oocytes in each replicate, as biological variability is expected. This also

includes the ability of each oocyte to express the protein from the injected mRNA. Differing batches of oocytes, derived from different female ovaries, also play a considerable role in variability. It has been reported that husbandry and housing of the animals affect the quality of oocytes for membrane transport experiments. To add to that, a significant change was observed in the deterioration of oocytes derived from specific husbandry conditions over the summer months, adding a seasonal variation component (Delpire et al., 2011) (Conn, 1991). Oocytes at stage V-VI of development were visually selected for uptake experiments, as endogenous transporter activity is not only variable between batches of oocytes but also in oocytes of different developmental stages (Miller and Zhou, 2000). Nonetheless, as the method of selection is purely visual, it is possible that oocytes in transition to or from stage V-VI were selected for uptake experiments, adding another factor that could contribute to variability between experiments. There were no significant changes in fructose uptake when experiments were carried out with incubation conditions that included a longer incubation time, at higher temperature and fructose concentration. Nevertheless, a significant decrease in GLUT5 mediated fructose transport was achieved in the presence of two extracts, previously used in uptake experiments, when incubation time and fructose concentrations were decreased and temperature lowered. Possible explanations for this includes the possibility that at a higher sugar concentration the radiolabelled sugar is less likely to be picked up by the transporter. In addition, human GLUT transporters are active in the body where the average temperature is around 37 °C. However, the host, responsible for the expression in this case, is kept at lower temperatures. Even though there were no visual damages to the oocytes at 37 °C this could have affected the uptake and/or provoked variation. Lastly, a longer

incubation time poses the risk of a plateau in uptake being reached, meaning an inhibition could go undetected. Although the radiolabelled counts were lower under these alternative conditions (0.1 mM fructose for 5 min at 25 °C) there was still a clear and significant difference between mRNA and water injected samples.

4.5.2 Effect of pure compounds on fructose uptake by GLUT5

Extracts, even though rich in a combination of (poly)phenols, can contain a lot of impurities, which may or may not affect how sugar is transported by the transporters on the membrane of the oocyte. For this reason, uptake experiments were carried out in the presence of several pure compounds. There was no inhibition of GLUT5-mediated fructose uptake observed in the presence of dark chocolate extract or chocolate reference standard. Nevertheless, the actual amounts of individual procyanidins were considerably low in both extracts (refer to section 3.5.1). In order to investigate the effect of individual components of the chocolate extracts on fructose uptake, experiments were carried out in the presence of each individual procyanidins from monomer to octamer, as well as pure epicatechin (Figure 4.15 A and B). Uptake experiments were also performed with a mixture of individual (poly)phenols, containing apigenin, flavone, galangin and kaempferol at 50 µM each. In addition, specific GLUT5 inhibitor L-sorbose-Bn-OZO (at 6 mM) was added to the incubation solution as well as this (poly)phenol mixture to explore the possibility that presence of compounds could be standing in the way of the binding site of inhibitors. These uptake experiments were carried out under the following conditions; 6 mM fructose incubation solution, at 37 °C for

15 min. There was no significant change in fructose uptake in the presence of any of the pure compounds mentioned above, under the incubation conditions tested.

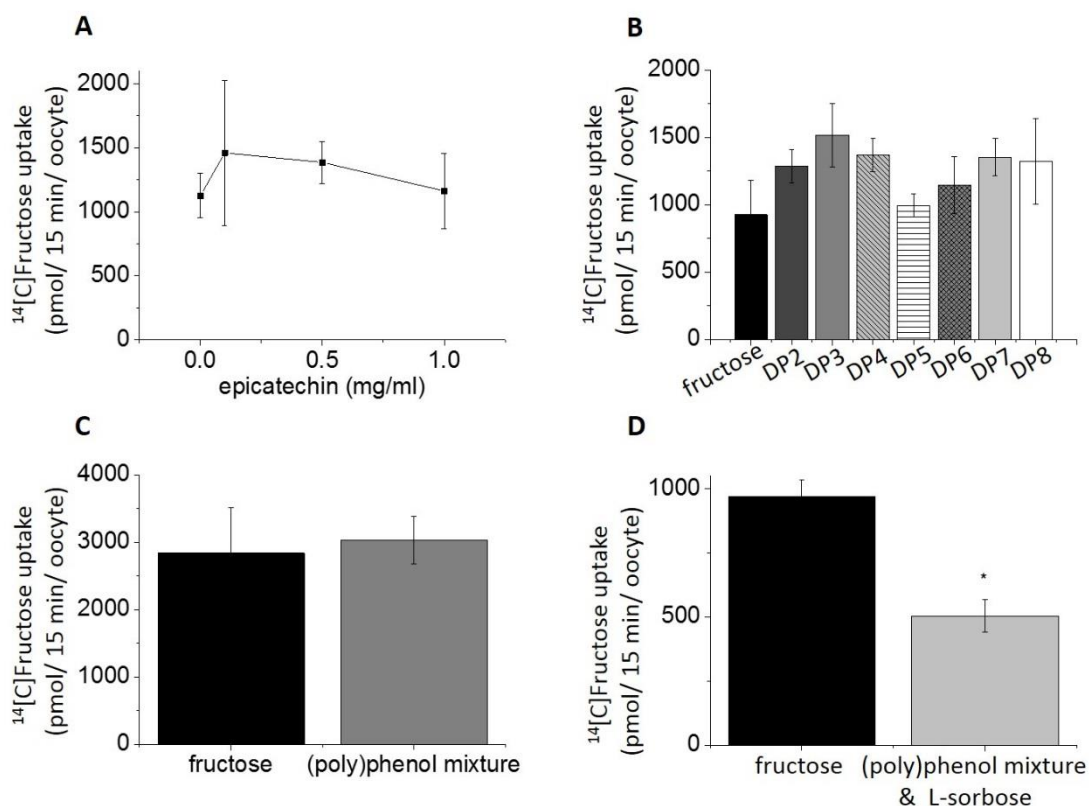


Figure 4-15 Effect of pure compounds on fructose uptake by GLUT5. One day post GLUT5 mRNA microinjection oocytes were incubated in 6 mM fructose solution containing [¹⁴C] fructose with increasing concentrations of epicatechin (0-1 mg/ml) **(A)**, in the presence of procyanidins, monomer to octamer **(B)**, in the presence (poly)phenol mixture of apigenin, flavone, galangin and kaempferol, at 50 μM **(C)** and in the presence of (poly)phenol mixture with 6 mM specific inhibitor, L-sorbose-Bn-OZO (Lsorbose) **(D)** for 15 min at 37 °C. There was no significant change in uptake of fructose by the oocytes in the presence of epicatechin **(A)**, procyanidins **(B)** or (poly)phenol mixture **(C)**. GLUT5 inhibitor decreased the uptake of fructose by 38% in the presence of (poly)phenol mixture **(D)**. Each data point represents the mean of 3 replicates (of 3 oocytes), normalized to control for each condition, ± SEM. * $p \leq 0.05$

Fructose uptake by GLUT5 was significantly decreased by 38% in the presence of L-sorbose-Bn-OZO and the (poly)phenol mixture (Figure 4.15 D). As there was no inhibition attributed to the (poly)phenol mixture alone, one can conclude this

decrease is attributed to the specific inhibitor L-sorbose-Bn-OZO (Figure 4.15 C). Although the presence of a mixture of different compounds did not seem to be blocking the binding site of specific inhibitors, these GLUT5 inhibitors have high affinity for the transporter and were engineered with the sole purpose of inhibiting fructose uptake by structural similarities with this sugar, allowing them to compete for the binding site. Therefore, it was considered that the incubation conditions could be masking some potential subtler inhibition by individual compounds or extracts, structurally more dissimilar to the substrate, for reasons discussed previously (see section 3.5.1). Henceforth, all additional uptake experiments with individual pure compounds were conducted at the following incubation conditions; 0.1 mM fructose incubation solution, for 5 min at 25 °C. Compounds tested under these specific incubation conditions were apigenin, EGCG, quercetin, hesperetin and hesperidin.

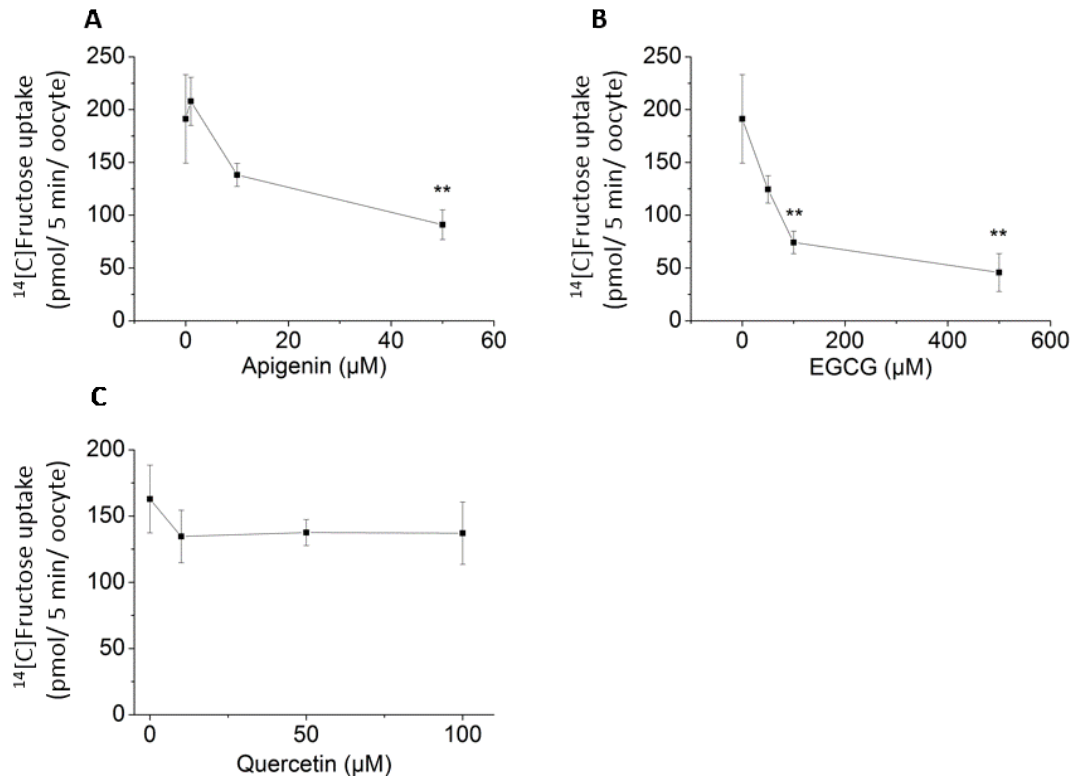


Figure 4-16 Effect of pure compounds on fructose uptake by GLUT5. One day post GLUT5 mRNA microinjection oocytes were incubated in 0.1 mM fructose solution containing [¹⁴C] fructose with increasing concentrations of apigenin (0-50 μM) (**A**), EGCG (0-500 μM) (**B**) and quercetin (0-100 μM) (**C**) for 5 min at 25 °C. There was no significant change in uptake of fructose by the oocytes in the presence of quercetin under these conditions (**C**). GLUT5-mediated fructose uptake was significantly decreased in the presence of Apigenin ($IC_{50}= 40 \pm 4 \mu\text{M}$) (**A**) and EGCG ($IC_{50}= 72 \pm 13 \mu\text{M}$) (**B**). Each data point represents the mean of 6 replicates (of 3 oocytes), normalized to control for each condition, \pm SEM. ** $p \leq 0.01$

GLUT5-mediated fructose uptake was significantly inhibited in the presence of apigenin ($IC_{50}= 40 \pm 4 \mu\text{M}$) (Figure 4.16 A), EGCG ($IC_{50} = 72 \pm 13 \mu\text{M}$) (Figure 4.16 B) and hesperidin ($IC_{50} = 264 \pm 72 \mu\text{M}$) (Figure 4.17 A). Neither quercetin nor hesperetin had any effect on fructose uptake by this protein, under the conditions tested (Figure 4.16 C and 4.17 B, respectively).

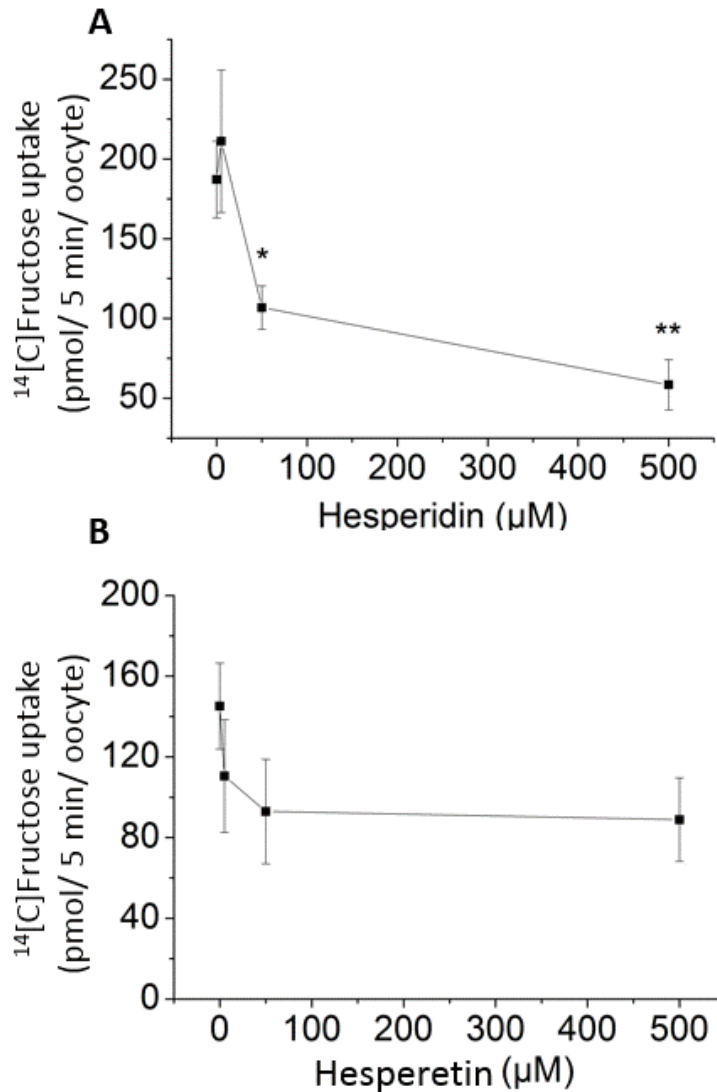


Figure 4-17 Effect of pure compounds on fructose uptake by GLUT5. One day post GLUT5 mRNA microinjection oocytes were incubated in 0.1 mM fructose solution containing [^{14}C] fructose with increasing concentrations of hesperidin (0-500 μM) (**A**) and hesperetin (0-500 μM) (**B**) for 5 min at 25 °C. GLUT5-mediated fructose uptake was significantly decreased in the presence of hesperidin ($\text{IC}_{50} = 264 \pm 72 \mu\text{M}$) (**A**) but not of hesperetin (**B**). Each data point represents the mean of 12 replicates (of 3 oocytes), normalized to control for each condition, \pm SEM. * $p \leq 0.05$, ** $p \leq 0.01$

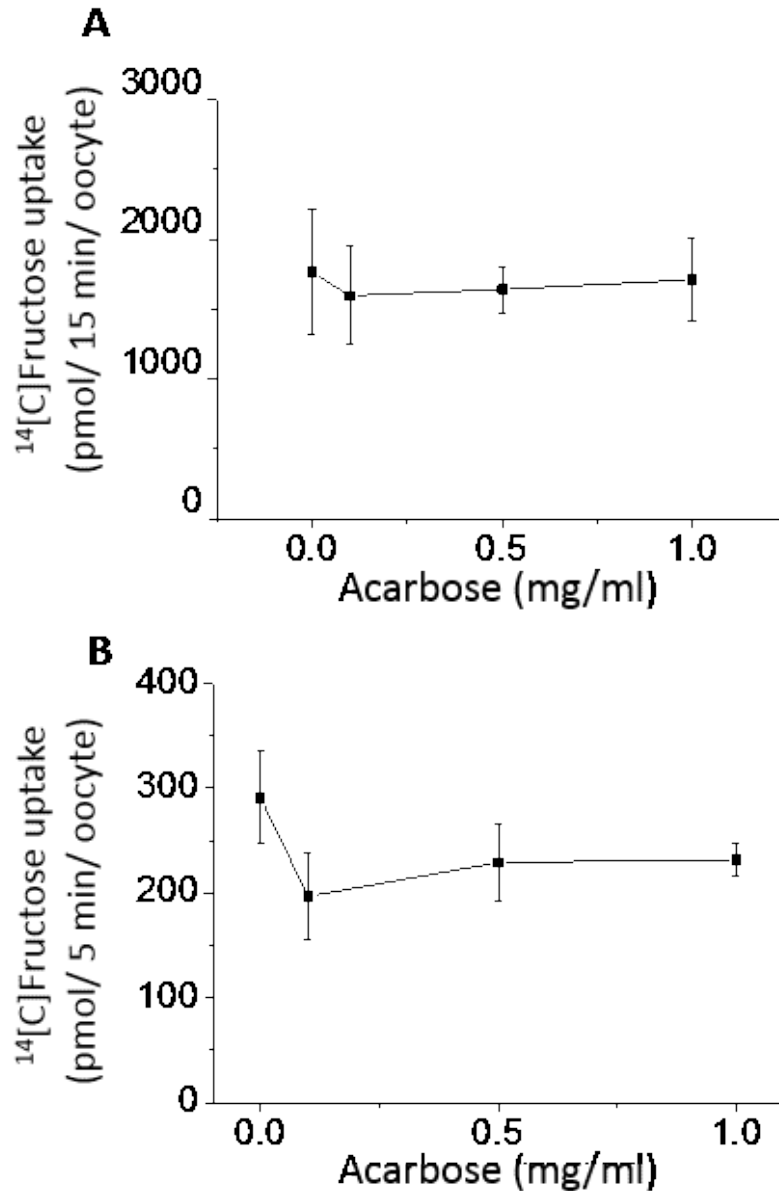


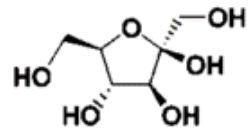
Figure 4-18 Effect of acarbose on fructose uptake by GLUT5. One day post GLUT5 mRNA microinjection oocytes were incubated in 6 mM fructose incubation solution containing [¹⁴C] fructose for 15 min at 37 °C **(A)** or 0.1 mM fructose solution containing [¹⁴C] fructose for 5 min at 25 °C. **(B)** with increasing concentrations of acarbose (0-1 mg/ml). There was no change in GLUT5-mediated uptake of fructose in the presence of acarbose **(A)** **(B)**. Each data point represents the mean of 3-6 replicates (of 3 oocytes), normalized to control for each condition, ± SEM.

Acarbose, a synthetic drug used in the management of diabetes by slowing digestion of carbohydrates down, is a potent inhibitor of α -amylase and α -

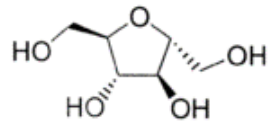
glucosidase enzymes (Zeymer, 2006). The effect of this drug on intestinal membrane transporters has not been previously established. For this reason, varying concentrations of acarbose were used in the uptake experiments to determine its effect on GLUT5-mediated fructose transport. As this is a potent drug its effect on both incubation conditions of high and low fructose concentration, at different temperatures and different incubation times, was investigated (Figure 4.18 A and B). Acarbose did not inhibit GLUT5 uptake of fructose.

4.5.3 Summary of results from fructose uptake experiments

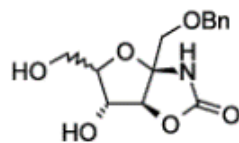
GLUT5-mediated fructose transport was inhibited under both incubation conditions (high and low fructose concentration) by their specific inhibitors L-sorbose-Bn-OZO and 2,5-anhydro-D-mannitol. The structure of these inhibitors is similar to that of the substrate fructose (Figure 4.19 and Table 4.1). The affinity of 2,5-anhydro-D-mannitol is almost identical to that of D-fructose and the modifications in the compound's 1 hydroxyl group (OH) bind to the site normally occupied by 6-OH position of fructose molecule (Yang et al., 2002). The binding to this compound is well tolerated by GLUT5, which has evolved to recognize furanose and pyranose ring forms of D-fructose while completely excluding D-glucose (Tatibouet et al., 2000). As for L-sorbose-Bn-OZO, it is hypothesised that the bulky benzyl group of this compound binds to a position out of the binding site, potentially in the binding-site cleft where steric restrictions do not pose a critical problem. In addition, the oxygen molecule in the OZO derivation increases hydrogen interactions with the protein, allowing for a better binding (Girniene et al., 2003).



D-fructose



2,5-anhydro-D-mannitol



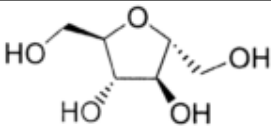
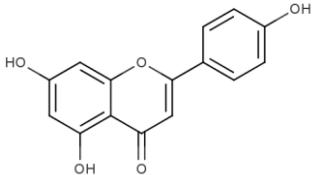
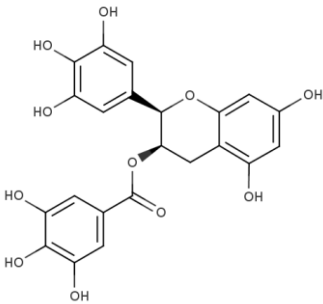
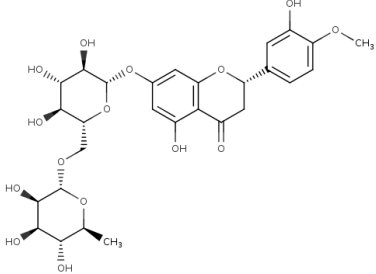
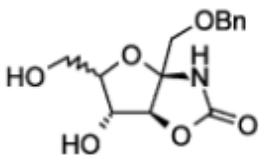
L-sorbose-Bn-OZO

Figure 4-19 Structure of GLUT5 substrate, D-fructose, and specific inhibitors. Hydroxyl group of 2,5-anhydro-D-mannitol binds to the active site of GLUT5, replacing fructose. Bulkier groups of L-sorbose-Bn-OZO compound bind to an alternative site off the active site (Girniene et al., 2003), (Tatibouet et al., 2000).

Fructose uptake by GLUT5 was also inhibited by the pure compounds apigenin, EGCG and hesperidin. An inhibition was also achieved in the presence of German chamomile extract, which has apigenin as one of its main components after apigenin-7-O-glucoside. Interestingly, although EGCG proved to be a potent inhibitor of GLUT5, confirming previous reports (Slavic et al., 2009), and is one of the main components of green tea, this extract did not have an effect on fructose uptake, suggesting that impurities in the extract could be masking some inhibition detection by the oocyte model. A previous investigation of the effects of the main components on green tea on GLUT5 concluded that fructose inhibition was achieved by the gallated catechins (-)-Epicatechin-gallate (ECG) and EGCG, but not the ungallated catechins (-)-epicatechin (EC) and (-)-epigallocatechin (EGC)

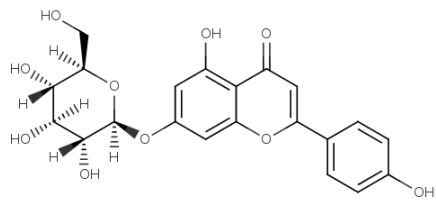
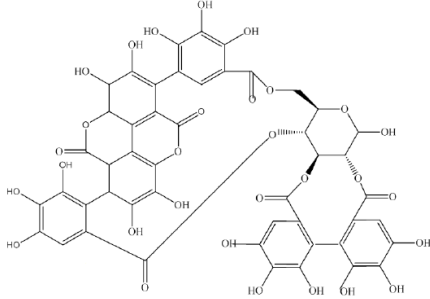
(Slavic et al., 2009). Similarly, an inhibition of fructose uptake was attributed to hesperidin, but not to its aglycone hesperetin. This suggests that the gallate group and glycoside potentially aid interactions with the GLUT5 protein, perhaps by binding to the binding-site cleft as the bulkier groups of the L-sorbose-Bn-OZO inhibitor. This hypothesis, however, does not necessarily fit with the concentration dependent inhibition of GLUT5 in the presence of German chamomile extract ($IC_{50} = 0.73 \pm 0.18$ mg/ml; equivalent to 75 μ M apigenin) which has as its main component apigenin-7-O glucoside, as apigenin alone was a more powerful inhibitor (predicted 50% inhibition at 40 μ M). Lastly, presence of sugar-free pomegranate extract, composed in majority by the hydrolysable tannin punicalagin and phenolic acid elagic acid, resulted in a concentration dependent inhibition of GLUT5. The effective inhibition by this extract suggest that the structure of its main components interact strongly with the protein. All compounds which significantly inhibited uptake of fructose by GLUT5, including their structure, are shown in Table 4.2. Extracts which significantly inhibited GLUT5-mediated fructose uptake when incubated in a low fructose concentration, namely 0.1 mM fructose (for 5 mins at 25 °C), are shown in Table 4.3. The structure of the main component of each extract is also shown in this table.

Table 4-2 Compounds and their respective inhibition on fructose uptake by GLUT5

Compound	Experimental condition	Inhibition ¹	Structure
2,5-anhydro-D-mannitol	6 mM fructose for 15 mins at 37 °C 0.1 mM fructose for 5 mins at 25 °C	54% and 61% inhibition of uptake with high and low fructose, respectively, at 7.6 mM	
Apigenin	0.1 mM ¹⁴ C-fructose for 5 mins at 25 °C	IC ₅₀ = 40 ± 4 μM	
EGCG	0.1 mM fructose for 5 mins at 25 °C	IC ₅₀ = 72 ± 13 μM	
Hesperidin	0.1 mM fructose for 5 mins at 25 °C	IC ₅₀ = 264 ± 72 μM	
L-sorbose-Bn-OZO	6 mM fructose for 15 mins at 37 °C	53% inhibition of uptake at 6 mM	

¹ compounds for which a single concentration was tested were attributed a percentage inhibition at that concentration.

Table 4-3 Extracts and their respective inhibition on fructose uptake by GLUT5. Experimental condition was 0.1 mM fructose for 5 mins at 25 °C

Extract	Composition ¹	Inhibition	Structure ²
German chamomile	12.32% apigenin-7-O-glucoside; 0.28% apigenin 0.13% luteolin-7-O-glucoside; 0.07% 4,5-dicaffeoylquinic acid	IC ₅₀ = 0.73 ± 0.18 mg/ml	
Pomegranate	121 mg/g punicalagin; 6 mg/g puricalin; 5.9 mg/g ellagic acid hexose; 101 mg/g ellagic acid	IC ₅₀ = 0.48 ± 0.22 mg/ml	

¹ analysis of extracts were performed previously; please refer to Chapter 2, section 2.1

² structure of the component present at the highest concentration in the extract is shown.

From the results presented in this chapter it can be concluded that uptake inhibition experiments were successfully conducted on the oocyte model of GLUT5 expression. Data shown here supports previous reports of no GLUT5-mediated fructose uptake inhibition by phloretin and quercetin (Burant et al., 1992), (Song et al., 2002), while confirming that the presence of specific inhibitors L-sorbose-Bn-OZO and 2,5-anhydro-D-mannitol, as well as of the pure compound EGCG, do lead to an inhibition of fructose uptake by this protein (Slavic et al., 2009), (Girniene et al., 2003), (Yang et al., 2002).

Moreover, additional novel GLUT5 inhibitors were revealed from fructose uptake inhibition experiments discussed in this chapter, namely; German chamomile extract and sugar-free pomegranate extracts, as well as pure compounds apigenin and hesperidin. These findings highlight the potential of these specific compounds and plant extracts to have a positive effect on the attenuation of disease risk factors and propose a benefit of their inclusion in interventions aimed at disease prevention.

Chapter 5

Glucose and fructose uptake inhibition of heterologously expressed hGLUT2 by (poly)phenols

5.1 Abstract

Fructose uptake into the liver and small intestine is mediated by GLUT2, alongside the fructose specific transporter GLUT5. To add to that, once absorbed fructose is released into the blood by GLUT2 present on the basolateral membrane of the enterocyte (Kellett and Brot-Laroche, 2005). In order to investigate the effect of pure compounds and (poly)phenol rich extracts on sugar uptake by this transporter, human GLUT2 (hGLUT2) gene was expressed in *X. laevis* oocytes. Expression of GLUT2 on *X. laevis* membranes was confirmed using automated western blotting (Wes), which identified a product of 53-60 kDa in size, and internalized sugar uptake was determined by scintillation spectrometry. Uptake of ^{14}C -glucose by GLUT2 was significantly inhibited by known inhibitors of this protein, phloretin (81% inhibition at 100 μM , $p \leq 0.0001$) and cytochalasin B (70% inhibition at 100 μM , $p \leq 0.0001$). Glucose uptake by GLUT2 was also significantly reduced in the presence of four plant extracts, namely, green tea ($\text{IC}_{50} = 0.13 \pm 0.02$ mg/ml), German chamomile ($\text{IC}_{50} = 0.49 \pm 0.24$ mg/ml), oleuropein-rich Bonolive extract ($\text{IC}_{50} = 0.03 \pm 0.002$ mg/ml) and sugar-free pomegranate extract ($\text{IC}_{50} = 0.05 \pm 0.01$ mg/ml). In addition, the pure compound hesperetin significantly decreased GLUT2-mediated glucose uptake ($\text{IC}_{50} = 30 \pm 9$ μM), its glucoside

hesperidin also having an inhibitory effect ($IC_{50} = 219 \pm 40 \mu\text{M}$). Furthermore, the rate of uptake inhibition of glucose and fructose transported by GLUT2 was determined through oocyte uptake experiments with each individual sugar in the presence of increasing concentrations of the pure compounds EGCG, apigenin and quercetin. The known GLUT2 inhibitor quercetin decreased the uptake of glucose ($IC_{50} = 7 \pm 1 \mu\text{M}$) and of fructose ($IC_{50} = 8 \pm 2 \mu\text{M}$) by a comparable rate. Apigenin and EGCG also significantly reduced the uptake of both sugars in a similar fashion; IC_{50} values for glucose uptake were of $27 \pm 4 \mu\text{M}$ and $72 \pm 16 \mu\text{M}$, and of $28 \pm 10 \mu\text{M}$ and $93 \pm 16 \mu\text{M}$ for fructose uptake, as seen by presence of apigenin and EGCG, respectively. These results show that some plant extracts and pure compounds may be useful in dietary interventions focused on disease prevention in healthy individuals, as well as disease management in diabetic patients.

5.2 Introduction

The membrane-bound facilitative sugar transporter, GLUT2, is expressed most abundantly in the small intestine, but also in the kidney, pancreatic islets, liver and brain (Lacombe, 2014). Active transport of glucose through the apical membrane of enterocytes is conducted by the sodium-dependent transporter, sodium-glucose cotransporter 1 (SGLT1), by means of the downward sodium gradient managed by $\text{Na}^+/\text{K}^+/\text{ATPase}$ on the basolateral membrane (Hediger et al., 1987), (Thorsen et al., 2014). GLUT2, on the basolateral membrane, is responsible for facilitative transport of both fructose and glucose, as well as galactose and glucosamine from

the cytosol to the blood (Ferraris, 2001). Therefore, complete absorption of dietary glucose in the small intestine is attributed to the sodium dependent active transporter SGLT1 and the facilitative transporter GLUT2 (Wright et al., 2007).

Nevertheless, in addition to the active transport of glucose across the enterocyte, it is now widely accepted that a facilitative transport, mediated by trafficking of basolateral GLUT2 to apical surface in response to high glucose levels, also takes place and contributes to higher levels of transport than sugars transported by SGLT1 alone (Kellett et al., 2008). Studies conducted in diabetic rats demonstrated that GLUT2 was able to traffic to and from the basolateral membrane in those rats fed a normal diet (Helliwell and Kellett, 2002). Insertion of GLUT2 into the apical membrane happens quickly ($T_{1/2}$ approximately 3.5 minutes) and has been associated with protein kinase C (PKC) β II activation (Helliwell et al., 2003). This rapid movement of GLUT2 from one membrane to another allows this protein to contribute to the absorption of fructose alongside its specific transporter, GLUT5 (Helliwell et al., 2000). Secondary transport of fructose is attributed to GLUT2, which is able to recognize fructose in its furanose form (Manolescu et al., 2007b). To add to that, in the small intestine, following apical transport of fructose by GLUT5, this sugar is then transported across the basolateral membrane by GLUT2 (Kellett and Brot-Laroche, 2005). Absorption of fructose from the dietary components is regulated in the small intestine, which also controls the availability of fructose to other tissues (Douard and Ferraris, 2008), (Blakemore et al., 1995). Higher levels of glucose and fructose have been associated with a higher localisation of GLUT2 by PKC to the apical membrane, while SGLT1 is integral and

remains on the apical membrane regardless of sugar level (Morgan et al., 2007). Interestingly, human intestinal cells cultured under sodium free conditions show that apical sugar transport is mediated by GLUT2 only, with its basolateral function remaining unchanged (Manzano and Williamson, 2010). In addition, knock down of β cell GLUT2 in mice by homologous recombination created a diabetic phenotype with mice experiencing hyperglycaemia, high levels of circulating fatty acids, hyperglucagonemia, hyperinsulinemia as well as a loss in pancreatic first phase insulin secretion in response to glucose (Thorens, 2001).

T2DM is considered to be a progression of postprandial hyperglycaemia, or increased blood glucose levels (Zeymer, 2006). In pancreatic β -cells a rise in blood sugar level triggers insulin secretion. In the absence of GLUT2, however, insulin secretion by pancreatic β -cells in response to glucose is not detected (Marty et al., 2007). Furthermore, functional studies reveal that GLUT2 is essential for glucose-sensing in the brain, where it suppresses glucagon secretion during the fed state (Burcelin and Thorens, 2001). These findings highlight the importance of GLUT2 as a glucose transporter and the potential benefits of reduction of glucose and fructose uptake into enterocytes. GLUT2 is a high capacity and low affinity transporter for both glucose and fructose ($K_M = \sim 17$ mM and ~ 76 mM for glucose and fructose, respectively) (Cura and Carruthers, 2012), (Mueckler and Thorens, 2013). The high K_M values attributed to GLUT2 allows it to transport glucose and fructose in amounts proportional to the levels available in the circulation, meaning that sugar transport varies as a result of sugar concentration in physiological and diabetic conditions (Morgan et al., 2007), (Mueckler and Thorens, 2013).

Antidiabetic drugs, such as acarbose, inhibit the sugar digestive enzymes α -amylases and α -glucosidases, leading to less sugar production and, thereby, aiding in the regulation of post-prandial sugar excursions associated with impaired glucose tolerance (IGT) and the development of diabetes (Williamson, 2013). Another class of drugs used in the treatment of diabetes, shown to be effective at reducing CVD mortality in diabetic patients, targets sodium-glucose cotransporter 2 (SGLT2), responsible for the reabsorption of glucose by the kidneys following intestinal absorption by SGLT1 and GLUT2 (Baud et al., 2016). Plant-derived (poly)phenols, which are present in our daily diet, have the potential to limit post-prandial sugar excursions by inhibiting sugar digestive enzymes, leading to a decrease in sugar production, and inhibiting sugar transporters, thus reducing sugar absorption (Williamson, 2013). For instance, human α -amylase is inhibited by flavonols and (poly)phenols present in tea (Forester et al., 2012), (Goto et al., 2012). Transporters GLUT2 and SGLT1 were both inhibited by tiliroside in experiments conducted in Caco-2 human intestinal cell model (Goto et al., 2012). Furthermore, it has been previously reported that quercetin is a particular strong inhibitor of GLUT2 glucose and fructose uptake and it was determined that this flavonoid achieved its effects through non-competitive inhibition. In other words, quercetin binds to an alternative site to the binding site of substrate on this transporter, implying that binding sites for this flavonoid are a characteristic of the GLUT2 transporter itself rather than the membrane it is expressed in (Kwon et al., 2007), (Song et al., 2002). Inhibition of GLUT2-mediated fructose and glucose uptake has also been achieved with the apple (poly)phenol, phloretin, and quercetin's glucoside precursors isoquercetin and spiraeoside. Other flavonoids are likely to exert inhibition on GLUT2 in a non-competitive manner as well (Kwon

et al., 2007), (Lin et al., 2016). The inhibition studies mentioned here conducted using a range of (poly)phenols suggest that a lifetime of dietary (poly)phenol intake could have an effect on disease risk reduction comparable to that of synthetic drugs such as acarbose (Williamson, 2013).

This Chapter aims to determine the direct effect of additional (poly)phenols and/or plant extracts on the GLUT2-mediated transport of not only glucose, but also of fructose. In addition, as GLUT2 is responsible for secondary uptake of fructose the characterization of an inhibitor for this transporter, which is also able to inhibit the main fructose transporter GLUT5 (see Chapter 4), would shed light onto what compounds would be most beneficial in an intervention aimed at the control of fructose uptake and post-prandial distribution of sugars. Uptake experiments were performed using the *X. laevis* oocyte expression model with oocytes expressing human GLUT2 (hGLUT2). Following the incubation of cells in a fructose or glucose incubation solution containing radiolabelled sugars and varying concentrations of different compounds and/or plant extracts, internalized radioactivity was measured using liquid scintillation counting (LSC).

5.3 Validation of GLUT2pBF plasmid construct functionality

5.3.1 Confirmation of adequate placement of hGLUT2 gene in expression vector

Human GLUT2 gene was inserted into pBF expression vector using the methods described in Chapter 2 (see section 2.3). Successful ligation of the sequences of

the gene of interest and the expression vector was confirmed through digestion of individually selected colonies from ligation reaction with HindIII restriction enzyme. This enzyme has a single restriction site in the pBF sequence as well as a single restriction site embedded in the sequence of the GLUT2 gene. Therefore, upon gel electrophoresis a positive product for the presence of GLUT2 produced two distinct bands, one at a size equivalent to 3909 bp (digestion at the pBF restriction site) and another at a size comparable to 970 bp (digestion at the GLUT2 gene restriction site). Only one single band was produced for the control digestion containing pBF plasmid without the gene insert, as can be seen in Figure 5.2. Of the fifteen individual colonies extracted, eight were considered positive for the presence of the GLUT2 gene and were sequenced in full (refer to Chapter 2 section 2.3.1 for list of primers used).

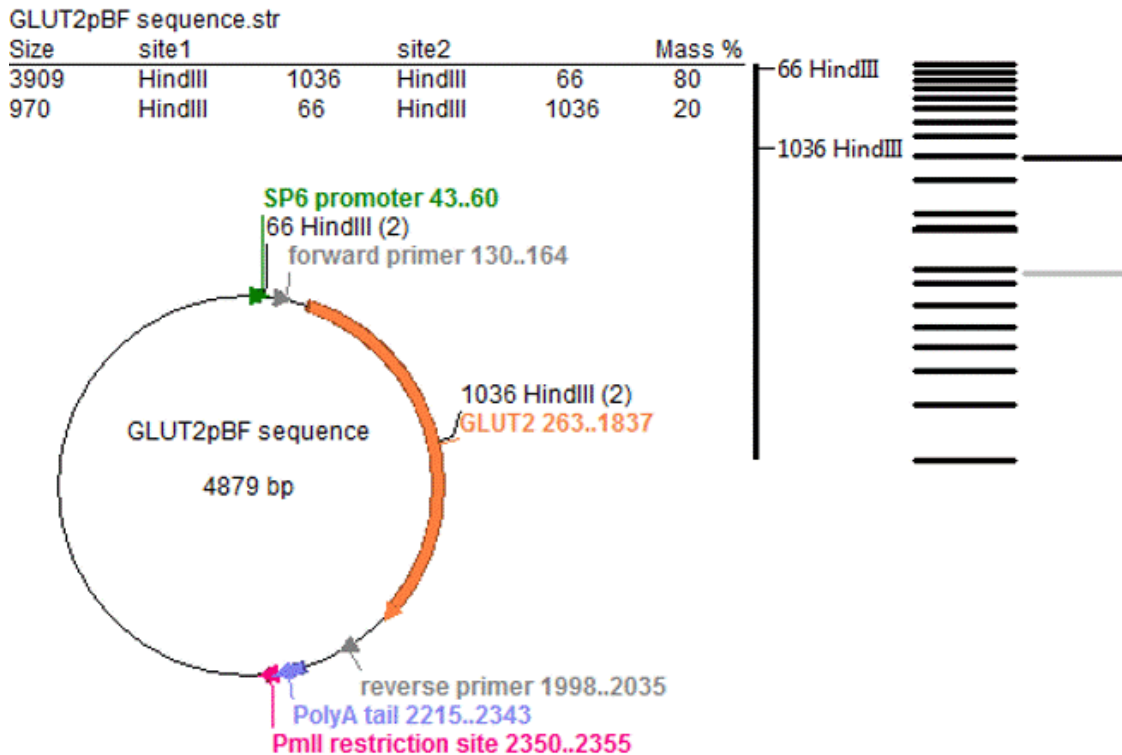


Figure 5-1 Illustration of the GLUT2pBF plasmid and theoretical gel electrophoresis products upon digestion of plasmid with HindIII restriction enzyme. Varying key attributes of the full GLUT2pBF sequence are shown including SP6 promoter (green) region, PmlI restriction site (pink) and PolyA tail (light purple), as well as the location of the inserted GLUT2 gene (orange) and specific homologous primers used in ligation reaction (light grey). Location of HindIII restriction sites in the GLUT2pBF sequence (dark grey) and the theoretical digestion of the sequence, including electrophoresis products, are shown around the circular plasmid structure.

Figure 5.1 illustrates the complete GLUT2pBF sequence with its key attributes, including the SP6 promoter site where in vitro transcription begins (green) and PmlI restriction site (pink) where transcription ends (Beckert and Masquida, 2011). The GLUT2 gene (orange) was positioned in between the promoter site and the PolyA tail site (light purple), a stretch of sequence containing only adenosine bases that aids with stability of mRNA and nuclear export (Fuke and Ohno, 2008). The site of specific primers with homology to pBF and GLUT2 sequences used in the ligation

of the gene to the expression vector are shown in light grey (for full sequences refer to Chapter 2, section 2.3.3.2). Specific position of restriction sites of HindIII (dark grey) are shown in relation to the rest of the plasmid sequence and to each other. To add to that, the same figure shows a theoretical digestion of GLUT2pBF with this enzyme and the derived gel electrophoresis products based on the DNA sequence. A table, also shown in this figure, lists the precise location in the sequence for each of the HindIII restriction sites (third column), which in turn determine the sizes (in bp) of each digest (first column), as well as the percentage of the total mass for which the digest products account for (sixth column).

Restriction enzyme digest products produced from each individual colony extracted after ligation reaction, obtained by gel electrophoresis, are shown in Figure 5.2. Colonies 4, 5, 7, 8, 12, 13, 14 and 15 (Figure 5.2 A and B) were considered positive for the presence of GLUT2 gene as they generated products around 4000 bp and 1000 bp in size, which are comparable to the expected product sizes of 3909 bp and 970 bp. Control digestion of pBF plasmid without GLUT2 insert produced a single band product only, as expected. Sequencing results from these colonies showed that the sequence from all positive colonies matched with the expected sequence of GLUT2pBF. One single colony was randomly chosen for propagation (colony 5) and used for all subsequent experiments.

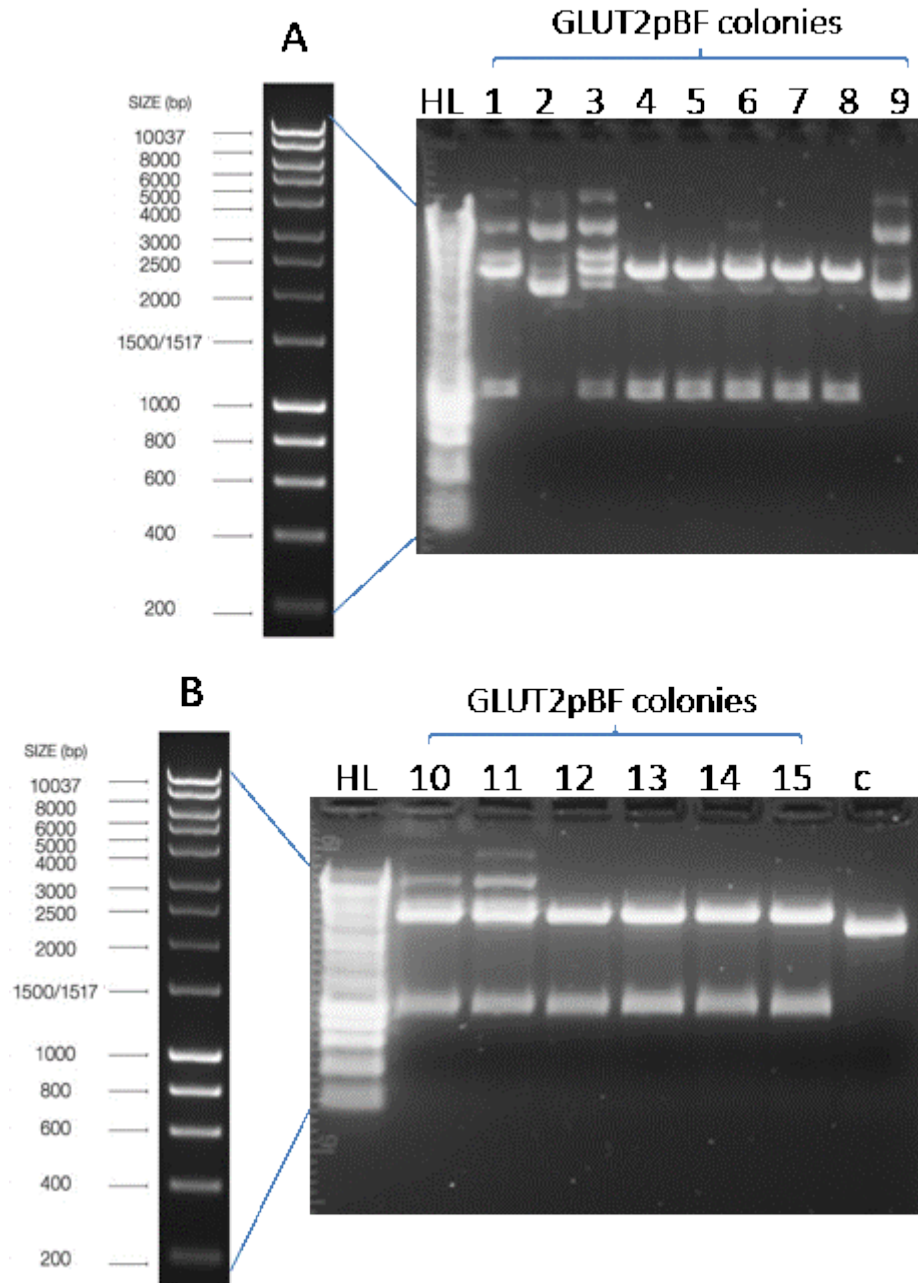


Figure 5-2 Gel electrophoresis image showing digestion of GLUT2pBF colonies with HindIII after ligation of GLUT gene to expression vector. A colony positive for the presence of GLUT2 gene produced two individual bands [colony 4, 5, 7, 8 **(A)**, 12, 13, 14 and 15 **(B)**]. Control (c) **(B)**, consisting of pBF plasmid without gene insert, produced a single band product. Product sizes are comparable to the theoretical sizes of digestion of this sequence with HindIII, namely around 3909 bp (digestion at the pBF restriction site) and 970 bp (digestion at the GLUT2 gene restriction site). Size of products was determined against a DNA hyperladder (HL).

5.3.2 Confirmation of specificity and quality of mRNA product

The IVT reaction was carried out with linearized GLUT2pBF plasmid obtained from digestion with PmlI restriction enzyme, for its restriction site is located after the gene of interest and PolyA tail. As previously discussed in Chapter 4 (section 4.3.2), circular plasmid DNA migrates through agarose gels in a distinct manner, producing two band products corresponding to the nicked DNA (higher molecular weight product) and the supercoiled DNA (lower molecular weight product) (Sambrook and Russell, 2001). Linear DNA migrates through the gel at a slower rate than circular DNA, producing a band at a size comparable to the full plasmid sequence, which in the case of GLUT2pBF is 4879 bp. The migration pattern of the circular GLUT2pBF and the linearized digest are shown in Figure 5.3.

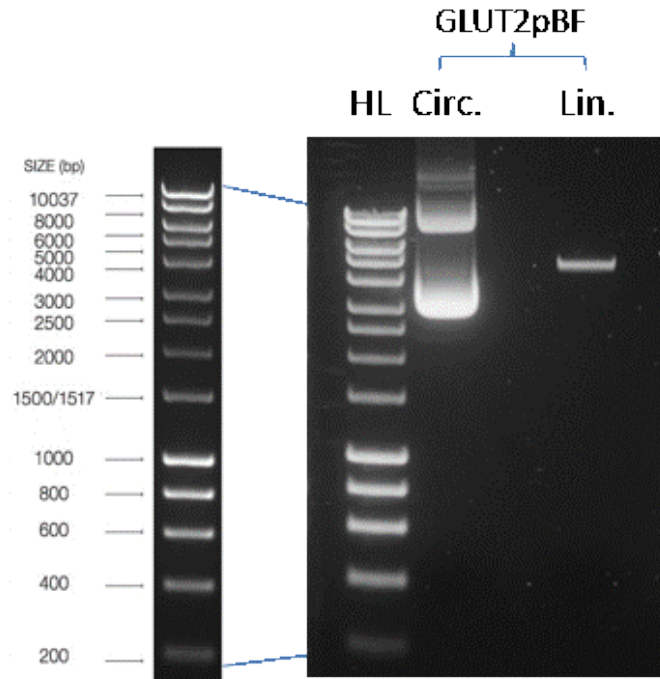


Figure 5-3 Gel electrophoresis of circular and linear GLUT2pBF. GLUT2pBF plasmid was linearized by digestion with PmlI restriction enzyme before IVT reaction. Circular GLUT2pBF plasmid (circ.) produced bands on the gel characteristic of its structure, whereas linear plasmid (lin.) produced a single band corresponding in size to the sequence of the full plasmid (4879 bp). Gel electrophoresis confirming linearization of plasmid was performed for every new mRNA sample prepared.

After the IVT reaction is performed the mRNA product was analysed in a denaturing RNA gel (see Chapter 2 section 2.3.5) in order to confirm that the product size was consistent with the expected size derived from the plasmid sequence (2296 bp). The mRNA product obtained from IVT of GLUT2pBF produced two band products following gel electrophoresis on RNA denaturing gel, one at a lower molecular weight in agreement with that expected of the mRNA from the plasmid sequence (around 3000 bp), and one at a higher molecular weight (Figure 5.4 A). According to the IVT kit user guide, provided with the product, a migration pattern such as this may occur due to persistent secondary structure

(mMessage mMachine ® Kit User Guide, Ambion). In order to confirm this possibility both bands were cut from the gel, RNA was extracted, and gel electrophoresis of extracts was performed on another denaturing gel. The RNA extracted from the higher molecular weight band migrated through the gel producing a faint band consistent in size to that expected of the GLUT2 mRNA. In addition, the RNA extracted from the lower molecular weight band (expected size for GLUT2 mRNA) migrated through the gel as a doublet, as with the original sample (Figure 5.4.B). Migration patterns from both extracted RNA samples confirm that the higher molecular weight band produced by the mRNA following IVT is indeed leftover secondary structure brought about as a consequence of the electrophoresis reaction. Secondary structure can also contribute to the improper denaturing of samples in the gel causing it to migrate abnormally or at an improper size to that expected. The size of the band produced by GLUT2 mRNA (3000 bp), when compared to the ssRNA ladder, was similar to that expected from the plasmid sequence (2296 bp). However, the presence of left over secondary structure could explain the more pronounced gap between expected and actual sizes.

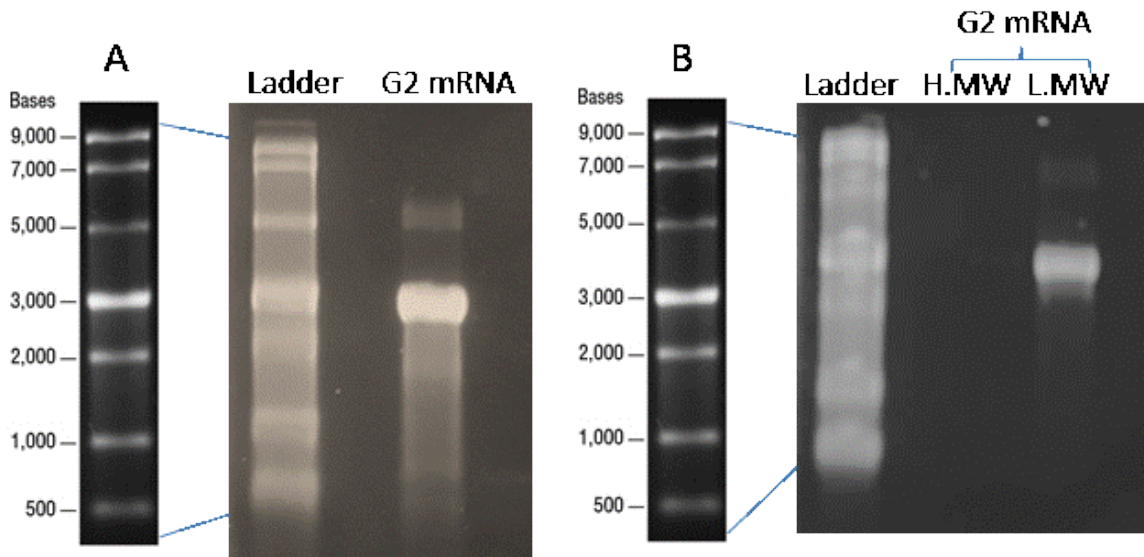


Figure 5-4 Gel electrophoresis of the GLUT2 mRNA product from IVT on RNA denaturing gel. After IVT reaction the mRNA product was run on a formaldehyde denaturing gel to confirm that its size matched that expected from the plasmid sequence (2296 bp). mRNA produced two bands, one at a size corresponding to that expected and one at a higher molecular weight (**A**). Individual bands were cut from the gel, RNA was extracted, and gel electrophoresis of extracts on denaturing gel was performed. Migration pattern of each extract on the gel confirms that the higher molecular weight band (H.MW) consists of left over secondary structure while the lower molecular weight band (L.MW) corresponds to the mRNA product size (**B**). Size of products was determined against an ssRNA ladder. Gel electrophoresis of mRNA on RNA denaturing gel was performed for every new mRNA sample prepared.

5.4 Validation of *X. laevis* model functionality

5.4.1 Glucose uptake by GLUT2-expressing oocytes and inhibition by known specific inhibitors

Uptake experiments with both fructose and glucose on oocytes expressing GLUT2 were carried out under the same conditions discussed previously in Chapter 4, namely, oocytes were incubated at 25 °C in a 0.1 mM fructose/glucose solution. Incubation time remained at 5 min, as preliminary uptake experiments

demonstrated no significant increase in uptake at longer incubation periods (Figure 5.5). Water injected oocytes were used as controls in all uptake experiments. Results of uptake by GLUT2-expressing oocytes are shown normalized to the uptake observed by their respective water injected controls, unless otherwise stated.

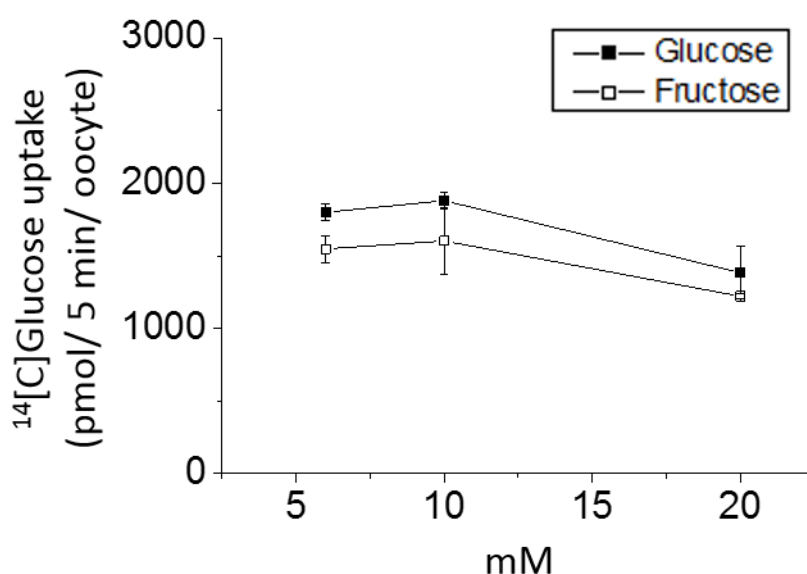


Figure 5-5 Uptake of 0.1 mM fructose/glucose over different incubations times. Two days post GLUT2 mRNA microinjection oocytes were incubated in 0.1 mM fructose/glucose solution containing [¹⁴C] fructose/glucose over 5-20 min at 25 °C. Each data point represents the mean of 6 replicates (of 3 oocytes), normalized to control for each condition, ± SEM. There was no statistical difference between the incubation times tested, however, less variability was attributed to 5 min incubation.

Oocytes were exposed to two known inhibitors of GLUT2, added to the incubation solution to serve as positive controls and to confirm that inhibition was achievable with this expression model. Uptake of glucose by GLUT2 was significantly decreased in the presence of 100 μM of phloretin (Figure 5.6 A) and 100 μM cytochalasin B (Figure 5.6 B). Phloretin inhibited GLUT2 uptake of glucose by 81% ($p \leq 0.0001$), while cytochalasin B reduced glucose uptake by 70% ($p \leq 0.0001$).

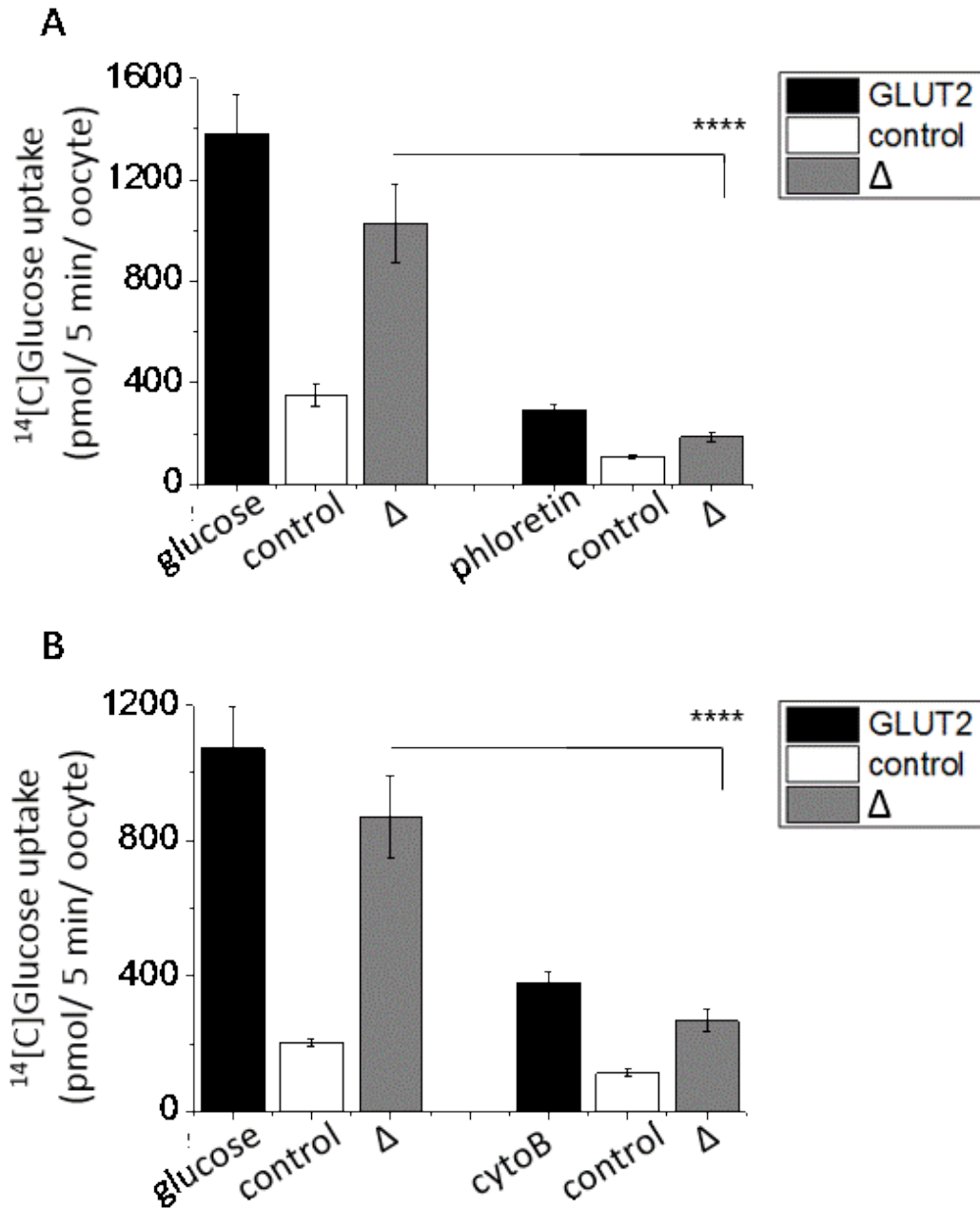


Figure 5-6 Inhibition of GLUT2 glucose uptake by known inhibitors. Two days post GLUT2 mRNA microinjection oocytes were incubated in 0.1 mM glucose solution containing [¹⁴C] glucose with and without 100 μM phloretin (**A**) and 100 μM cytochalasin B (cytoB) (**B**) for 5 min. Internalized sugar uptake was determined by scintillation spectrometry for protein expressing oocytes (black bars) and water injected controls (open bars). Net change in uptake, Δ, (grey bars) was determined by normalizing the uptake observed by GLUT2 to control uptake. The mean ± SEM of 12 replicates (of 3 oocytes) is shown per individual condition. Phloretin reduced GLUT2 uptake of glucose by 81% (**A**) and cytochalasin B decreased glucose uptake by GLUT2 by 70% (**B**) when added to the 0.1 mM glucose incubation solution. **** $p \leq 0.0001$.

5.4.2 Determination of expression of recombinant hGLUT2 on oocyte membrane extracts

The expression of hGLUT2 on oocyte membranes was determined through automated capillary Western blot, Wes (see Chapter 2 section 2.4.7). Membranes were extracted from three oocytes for analysis with Wes following one to three days post microinjection with GLUT2 mRNA or water (Figure 5.7 A). Images show the presence of GLUT2 protein on membranes extracted from oocytes microinjected with GLUT2, and on positive control HepG2 cell lysate, but not in water injected controls. This is also made clear by the electropherogram of extracts from day 2 (Figure 5.7 B). All oocyte membrane extracts were treated with PNGase, a glycosidase, before imaging. This could explain the shift in size of GLUT2 observed between oocyte membranes (between 54-60 kDa in size) and the HepG2 cell lysate (around 63 kDa in size) (Figure 5.7 C). Differences in protein glycosylation across species could also contribute to sizes marginally diverging from the oocyte membrane extract and mammalian cell lysates. Due to the abundance of protein present two days post microinjection with GLUT2 mRNA, all further uptake experiments were carried out after oocytes had an expression period of 48 hrs. GLUT2 antibody used for protein detection was raised against an internal region of the human protein, reported to recognize a GLUT2 protein product of 53-61 kDa in size. Optimal GLUT2 antibody dilution of 1:50 for Wes experiments was determined by Dr. S. Tumova.

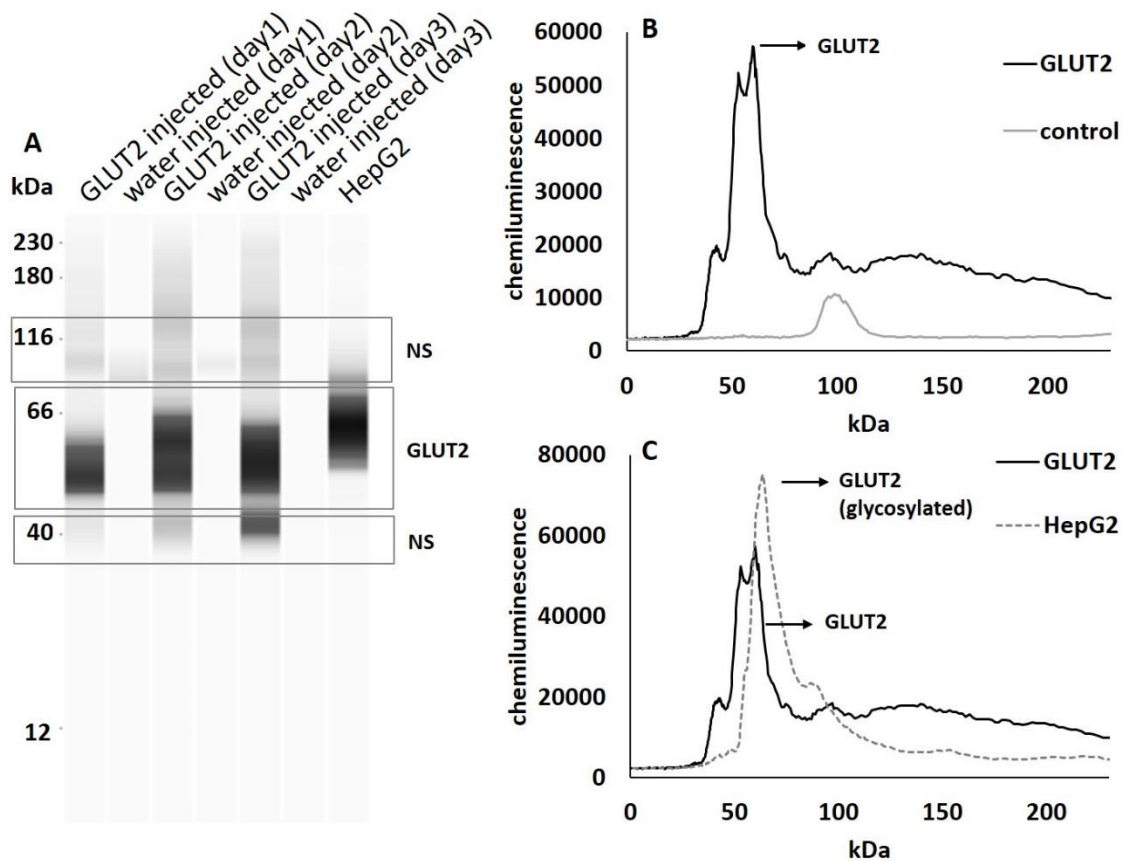


Figure 5-7 Confirmation of expression of GLUT2 on oocyte membrane extracts by Wes. Membranes extracted from three oocytes one to three days post injection with GLUT2 mRNA (day1-day3), as well as water injected control membranes, were analysed using automated capillary Western blot (Wes). Analysis of a membrane extract sample shown as a gel-like image, together with a HepG2 cell lysate positive control (**A**). A comparison of GLUT2 mRNA injected and control water injection membrane extracts two days post microinjection (day2) is shown as an electropherogram (**B**). The shift in GLUT2 size between oocyte membrane extracts and HepG2 cell lysate is highlighted as an electropherogram (**C**). Detected protein size for GLUT2 was 53-60 kDa for oocyte membrane extract and 63 kDa for HepG2 cell lysate. Concentration of oocyte membrane extracts and HepG2 cell lysate loaded was 0.5 mg/ml. Antibody dilution was 1:50. This image represents one of 3 replicates.

5.5 Uptake experiment results and discussion

In order to attribute inhibition of GLUT2-mediated glucose/fructose transport by a specific compound or extract oocytes expressing this transporter were incubated in a sugar solution, containing ^{14}C -glucose/fructose, in the presence and absence of each compound/extract. Uptake inhibition experiments were conducted using plant extracts and compounds also used in GLUT5 uptake inhibition studies, in the previous chapter (Chapter 4), with the aim to identify common inhibitors of both transporters. Due to the amount of time required for oocyte microinjections and to perform inhibition studies, not all the extracts tested for GLUT5 inhibition potential could be used in the experiments presented in this chapter. For this reason, extracts which were being used, or would in the future be used, in human studies conducted by other individuals in the research group were prioritized (e.g. German chamomile, green tea and pomegranate) (Villa-Rodriguez et al., 2017a), (Nyambe-Silavwe and Williamson, 2016). Similarly, compounds incorporated by other individuals in the group for *in vitro* cell culture work, as well as compounds shown to inhibit GLUT2 from the literature, were also investigated using the oocyte model. In other words, extract and compounds were chosen with the aim to validate results within the research group and to attribute inhibition to specific transporters. All extracts and compounds used in the uptake inhibition studies by GLUT2 described in this chapter are listed in Table 5.1. Inhibition of GLUT2 uptake by two of its substrates, namely fructose and glucose, was conducted with three pure compounds, marked in Table 5.1 with an asterisk.

Table 5-1 Compounds/extracts used in GLUT2-mediated glucose/fructose uptake inhibition studies described in this chapter

Compound/ extract	Inhibition of GLUT2 mediated sugar uptake
Acarbose	Glucose
Apigenin *	Glucose and fructose
Bonolive	Glucose
Cytochalasin B	Glucose
EGCG *	Glucose and fructose
German chamomile	Glucose
Green tea	Glucose
Hesperidin	Glucose
Hesperetin	Glucose
Phloretin	Glucose
Pomegranate	Glucose
Quercetin *	Glucose and fructose

* compounds for which investigation of uptake inhibition was carried out with two GLUT2 substrates.

The pure compounds apigenin, EGCG and quercetin were chosen to conduct GLUT2-mediated fructose uptake inhibition, as well as glucose uptake inhibition, for two of these compounds were shown to inhibit fructose uptake by GLUT5 (apigenin and EGCG, Chapter 4). Although quercetin did not inhibit GLUT5 it is a known potent inhibitor of GLUT2 (Kwon et al., 2007), (Song et al., 2002). Considering the research objective of investigating the inhibition profiles of GLUTs and identifying novel inhibitors of these two transporters and GLUT7, which like GLUT2 also transports glucose and fructose, these compounds were thought to be good candidates. Once again, due to the time consuming nature of experiments

other pure compounds could not be investigated for inhibition of GLUT2 using fructose as a substrate.

5.5.1 Effect of extracts on glucose uptake by GLUT2

The effect of plant extracts on glucose uptake by GLUT2 was investigated by incubation of the oocytes in a 0.1 mM glucose solution, containing radiolabelled glucose, with increasing concentrations of a particular extract for 5 min at 25 °C. Green tea and German chamomile extracts both significantly reduced the uptake of glucose by GLUT2 in a concentration dependent manner (figure 5.8). IC₅₀ values were determined to be 0.13 ± 0.02 mg/ml and 0.49 ± 0.24 mg/ml for green tea and German chamomile extracts, respectively.

Oleuropein-rich Bonolive extract and sugar-free pomegranate extract were tested for their potential effects on GLUT2-mediated glucose uptake using the same conditions. There was a significant decrease in glucose uptake by this transporter in the presence of both extracts (Figure 5.9). Glucose uptake reduction followed a concentration dependent pattern with the addition of Bonolive extract, IC₅₀ reached at 0.03 ± 0.002 mg/ml (Figure 5.9 A). Sugar-free pomegranate extract proved to be a very potent inhibitor, leading to a 93% ($p \leq 0.001$) reduction in uptake at 0.1 mg/ml (Figure 5.9 B).

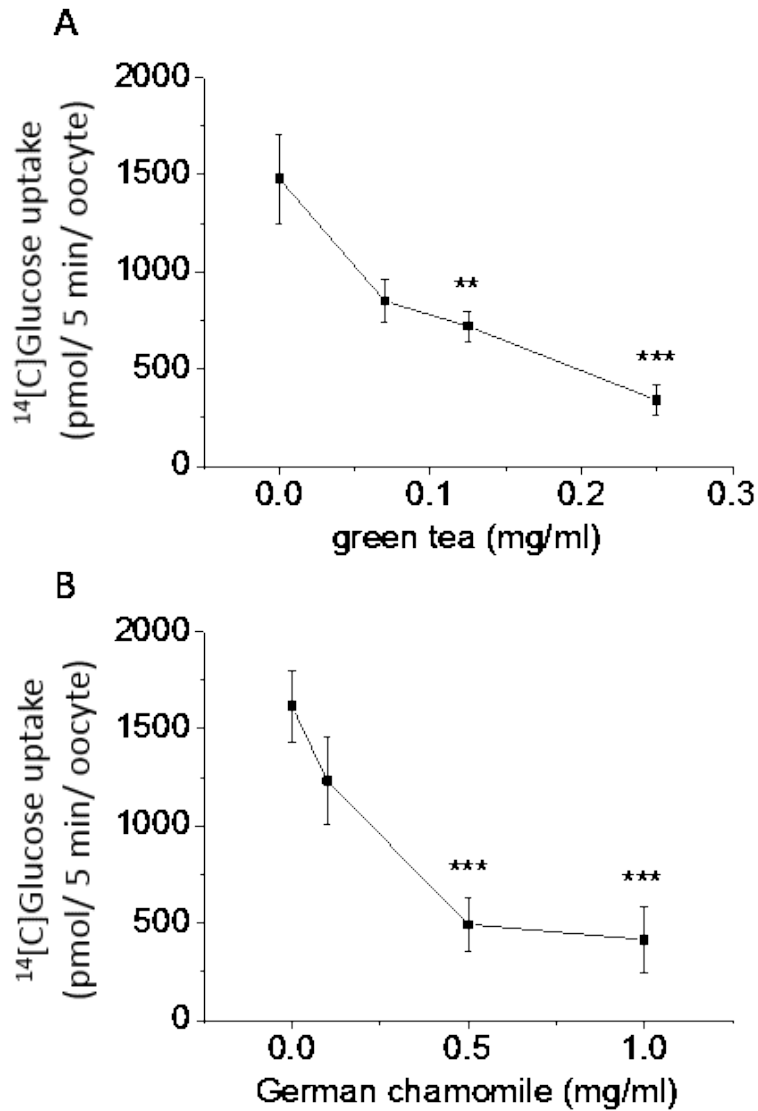


Figure 5-8 Effect of green tea and German chamomile extracts on glucose uptake by GLUT2. Two days post GLUT2 mRNA microinjection oocytes were incubated in 0.1 mM glucose solution containing [¹⁴C] glucose with increasing concentrations of green tea extract (0-0.25 mg/ml) **(A)** and German chamomile extract (0-1 mg/ml) **(B)** for 5 min at 25 °C. There was a significant concentration dependent change in uptake of glucose by the oocytes in the presence of both extracts under these conditions. IC₅₀ = 0.13 ± 0.02 mg/ml for green tea extract **(A)** and IC₅₀ = 0.49 ± 0.24 mg/ml for German chamomile extract **(B)**. Each data point represents the mean of 12 replicates (of 3 oocytes), normalized to control for each condition, ± SEM. ** *p* ≤ 0.01 and *** *p* ≤ 0.001.

Composition of extracts used here for uptake experiments in GLUT2-expressing oocytes are the same as previously stated in Chapter 4 (section 4.5.1).

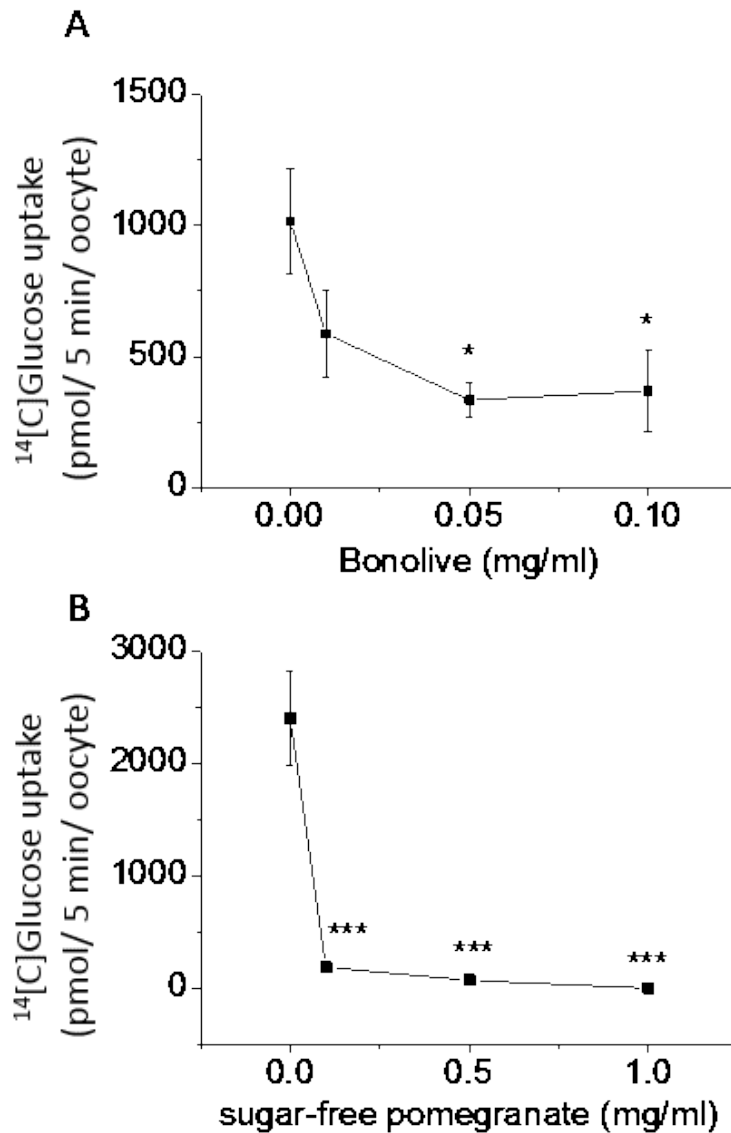


Figure 5-9 Effect of Bonolive and sugar-free pomegranate extracts on glucose uptake by GLUT2. Two days post GLUT2 mRNA microinjection oocytes were incubated in 0.1 mM glucose solution containing [¹⁴C] glucose with increasing concentrations of Bonolive extract (0-0.1 mg/ml) **(A)** and sugar-free pomegranate extract (0-1 mg/ml) **(B)** for 5 min at 25 °C. There was a significant change in uptake of glucose by the oocytes in the presence of both extracts under these conditions. $IC_{50} = 0.03 \pm 0.002$ mg/ml for Bonolive extract **(A)** and $IC_{50} = 0.05 \pm 0.01$ mg/ml for sugar-free pomegranate extract **(B)**. Each data point represents the mean of 12 **(A)** and 6 **(B)** replicates (of 3 oocytes), normalized to control for each condition, \pm SEM. * $p \leq 0.05$ and *** $p \leq 0.001$.

5.5.2 Effect of pure compounds on glucose uptake by GLUT2

The direct impact of pure compounds on glucose uptake by GLUT2 was measured using the same experimental conditions as for the extracts. The two pure compounds tested were hesperetin and its glucoside hesperidin. There was a significant decrease in GLUT2-mediated glucose uptake in the presence of both compounds. However, the aglycone hesperetin provided a much stronger inhibition. In the presence of hesperetin glucose uptake was decreased by 82.9% ($p \leq 0.0001$) at 50 μM of compound (Figure 5.10 B), and IC_{50} was reached in the presence of hesperidin at $219 \pm 40 \mu\text{M}$ (Figure 5.10 A).

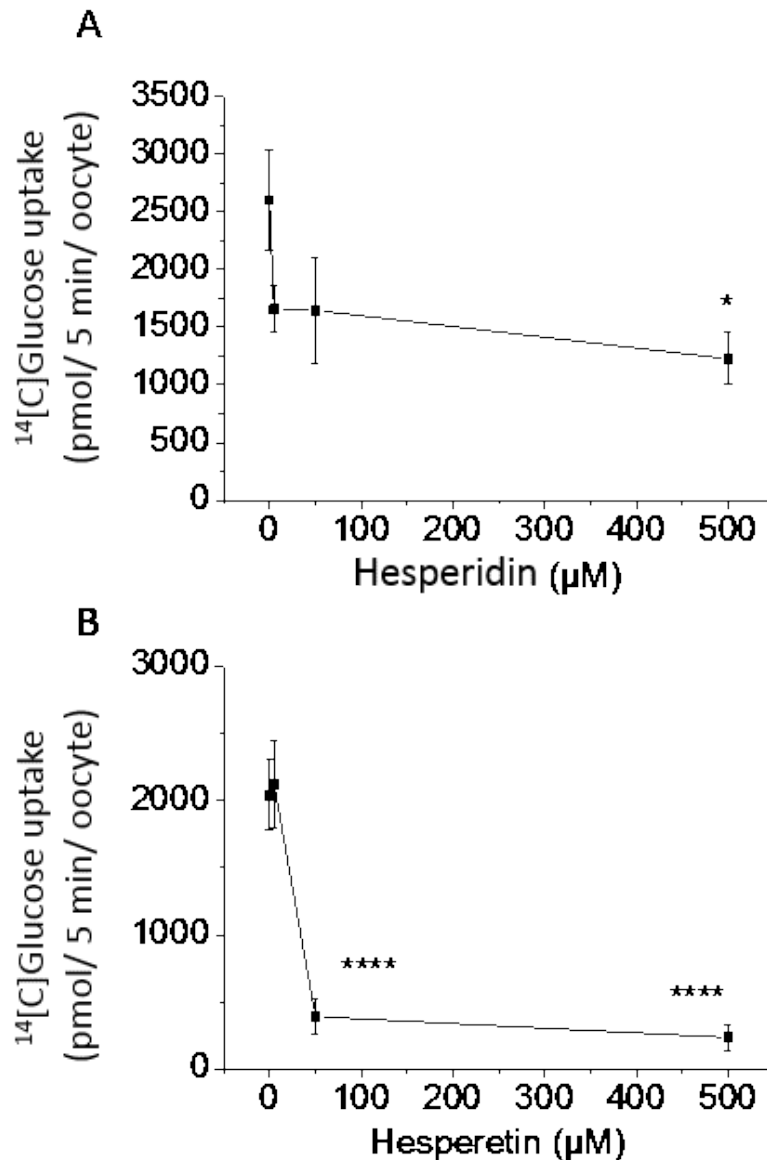


Figure 5-10 Effect of pure compounds hesperetin and hesperidin on glucose uptake by GLUT2. Two days post GLUT2 mRNA microinjection oocytes were incubated in 0.1 mM glucose solution containing [¹⁴C] glucose with increasing concentrations of hesperidin (0-500 μM) **(A)** and hesperetin (0-500 μM) **(B)** for 5 min at 25 °C. There was a significant change in uptake of glucose by the oocytes in the presence of both compounds under these conditions. IC₅₀ = 219 ± 40 μM for hesperidin **(A)** and IC₅₀ = 30 ± 9 μM for hesperetin **(B)**. Each data point represents the mean of 6 **(A)** and 12 **(B)** replicates (of 3 oocytes), normalized to control for each condition, ± SEM. * $p \leq 0.05$ and **** $p \leq 0.0001$.

The synthetic drug acarbose, used in the management of diabetes, has shown potent inhibitory effects on enzymes such as of α-amylase and α-glucosidase

(Zeymer, 2006). In the previous Chapter, the effect of this drug on GLUT5-mediated fructose transport was investigated (Chapter 4, section 4.5.2), concluding that acarbose did not inhibit GLUT5 uptake of fructose. In order to investigate the effect of this drug on another intestinal membrane transporter, increasing concentrations of acarbose were added to the glucose incubation solution of GLUT2-expressing oocytes (Figure 5.11). Acarbose did not have any significant effect on glucose transport by GLUT2 under the conditions tested.

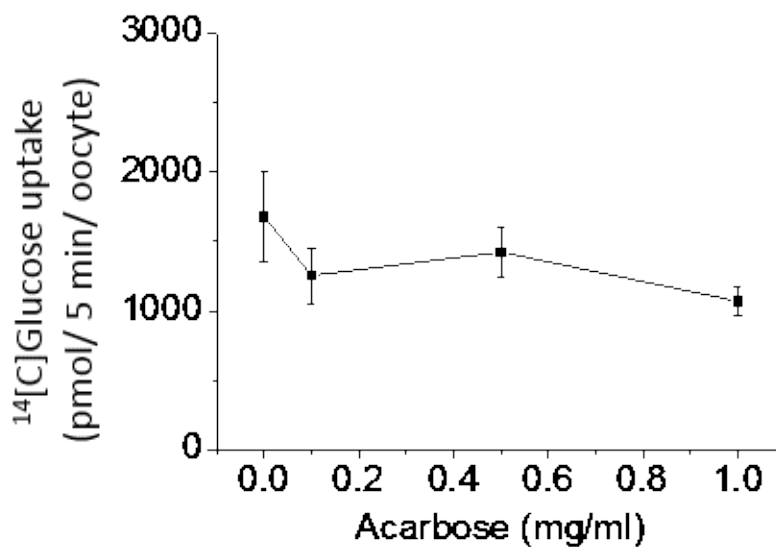


Figure 5-11 Effect of acarbose on glucose uptake by GLUT2. Two days post GLUT2 mRNA microinjection oocytes were incubated in 0.1 mM glucose solution containing [¹⁴C] glucose with increasing concentrations acarbose (0-1 mg/ml) for 5 min at 25 °C. There was no significant change in uptake of glucose by the oocytes in the presence of acarbose under these conditions. Each data point represents the mean of 6 replicates (of 3 oocytes), normalized to control for each condition, ± SEM.

5.5.3 Comparison of effect of pure compounds on glucose and fructose uptake by GLUT2

Reports have concluded that GLUT2 has high affinity for fructose as well as glucose (K_M of 66 mM and 17 mM for fructose and glucose, respectively) (Cura and Carruthers, 2012). Translocation of GLUT2 from the basolateral to the apical membrane allows it to transport fructose alongside GLUT5, also located on the apical membrane (Helliwell et al., 2003). In order to characterize any differences in the inhibition pattern of uptake of either sugar by GLUT2, oocytes expressing this protein were incubated in a fructose or glucose incubation solution in the presence of increasing concentrations of pure compounds. Quercetin is a known inhibitor of GLUT2 and a concentration dependent inhibition was observed when this compound was added to both the fructose and the glucose incubation solution (Figure 5.12). IC_{50} values in the presence of quercetin were of $7 \pm 1 \mu\text{M}$ and $8 \pm 2 \mu\text{M}$ for GLUT2-mediated glucose and fructose uptake, respectively.

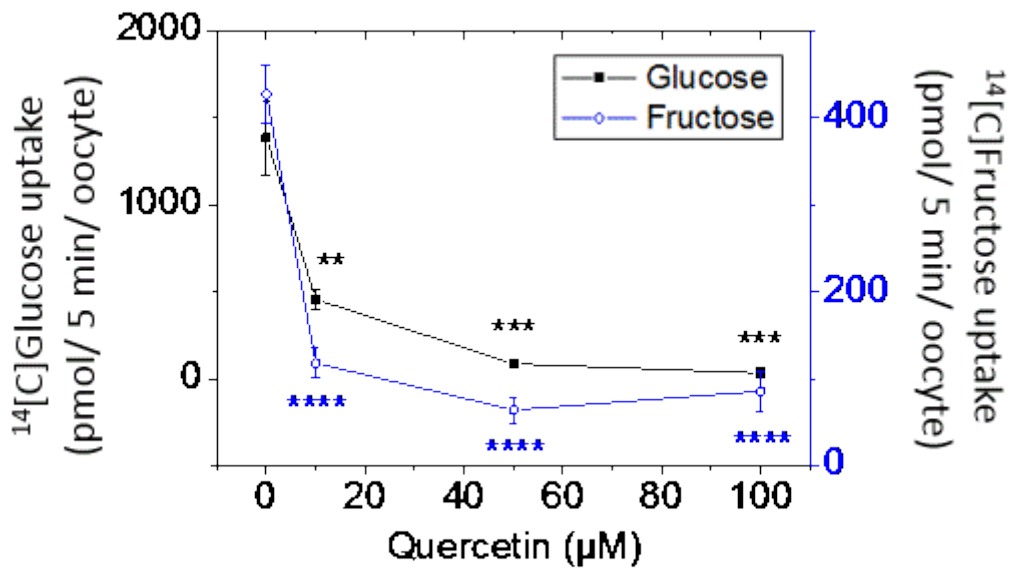


Figure 5-12 Effects of quercetin on glucose and fructose uptake by *X. laevis* oocytes expressing GLUT2. Two days post mRNA microinjection oocytes were incubated in either 0.1 mM glucose solution containing [¹⁴C] glucose (left axis, ●) or 0.1 mM fructose solution containing [¹⁴C] fructose (right axis, ○) with increasing concentrations of quercetin (0-100 μM) for 5 min at 25 °C. Each data point represents the mean of 6 replicates (of 3 oocytes), normalized to control for each condition, ± SEM. IC₅₀ = 7 ± 1 μM and 8 ± 2 μM for glucose and fructose, respectively, in the presence of quercetin. ** $p \leq 0.01$, *** $p \leq 0.001$ and **** $p \leq 0.0001$.

Two other pure compounds were used in the investigation of GLUT2-mediated sugar transport inhibition pattern, namely apigenin and EGCG. Apigenin considerably inhibited GLUT2-mediated uptake of glucose (IC₅₀ = 27 ± 4 μM) and of fructose (IC₅₀ = 28 ± 10 μM) in a concentration dependent manner (Figure 5.13). EGCG also showed to be a powerful inhibitor of GLUT2, concentration dependently decreasing uptake of both glucose (IC₅₀ = 72 ± 13 μM) and fructose (IC₅₀ = 93 ± 16 μM) by this transporter (Figure 5.14).

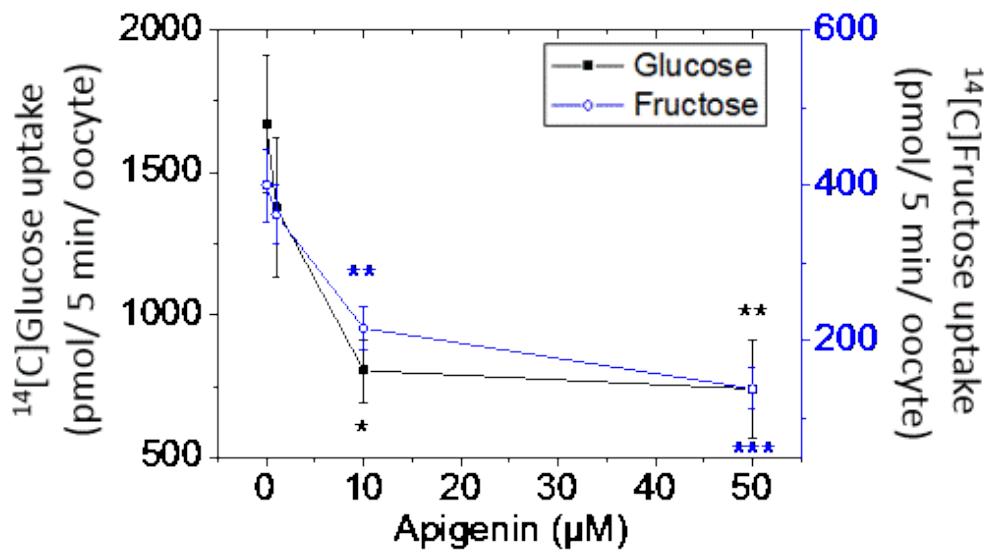


Figure 5-13 Effects of apigenin on glucose and fructose uptake by *X. laevis* oocytes expressing GLUT2. Two days post mRNA microinjection oocytes were incubated in either 0.1 mM glucose solution containing [¹⁴C] glucose (left axis, ●) or 0.1 mM fructose solution containing [¹⁴C] fructose (right axis, ○) with increasing concentrations of apigenin (0-50 μM) for 5 min at 25 °C. Each data point represents the mean of 6 replicates (of 3 oocytes), normalized to control for each condition, ± SEM. IC₅₀ = 27 ± 4 μM and 28 ± 10 μM for glucose and fructose, respectively, in the presence of apigenin. * $p \leq 0.05$, ** $p \leq 0.01$ and *** $p \leq 0.001$.

Apigenin had a greater effect on fructose transport at the highest concentration tested, inhibiting transport of this sugar by 85% ($p \leq 0.001$) at 50 μM, compared to 56% ($p \leq 0.01$) reduction of glucose uptake at the same concentration (Figure 5.13). Similarly, fructose transport was inhibited to a greater extent than glucose transport in the presence of the highest concentration of EGCG; inhibition was of 84% ($p \leq 0.0001$) and 74% ($p \leq 0.01$) for fructose and glucose, respectively, at 500 μM (Figure 5.14). Of the three compounds tested the most potent inhibitor of glucose uptake by GLUT2 was shown to be quercetin, decreasing the transport of this sugar by 67% ($p \leq 0.01$) at the lowest concentration tested and by 95% ($p \leq 0.001$) at 100 μM. Although a GLUT2-mediated fructose uptake inhibition by

quercetin was also observed, this compound was marginally less effective at the highest concentration tested than apigenin and EGCG, decreasing fructose transport by 80% ($p \leq 0.0001$) at 100 μM . Nevertheless, uptake of fructose was reduced by 70% ($p \leq 0.0001$) at the lowest concentration of quercetin tested and by 85% ($p \leq 0.0001$) at 50 μM , suggesting a potential plateau in inhibition was reached at a lower compound concentration for this sugar (Figure 5.12).

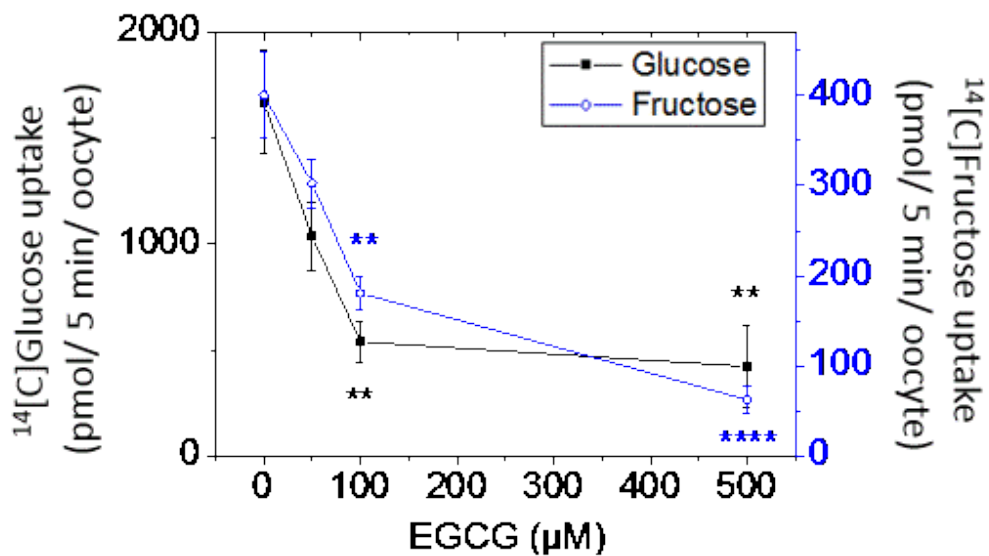


Figure 5-14 Effects of EGCG on glucose and fructose uptake by *X. laevis* oocytes expressing GLUT2. Two days post mRNA microinjection oocytes were incubated in either 0.1 mM glucose solution containing [^{14}C] glucose (left axis, ●) or 0.1 mM fructose solution containing [^{14}C] fructose (right axis, ○) with increasing concentrations of EGCG (0-500 μM) for 5 min at 25 °C. Each data point represents the mean of 6 replicates (of 3 oocytes), normalized to control for each condition, \pm SEM. $\text{IC}_{50} = 72 \pm 13 \mu\text{M}$ and $93 \pm 16 \mu\text{M}$ for glucose and fructose, respectively, in the presence of EGCG. ** $p \leq 0.01$ and **** $p \leq 0.0001$.

Oocytes expressing GLUT2 were able to transport more glucose than fructose, at an average ratio of approximately 1 to 3. Although all three compounds tested were more effective at inhibiting glucose uptake by this transporter, as observed by the lower IC_{50} values, inhibition patterns over the varying concentrations were

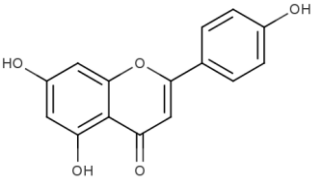
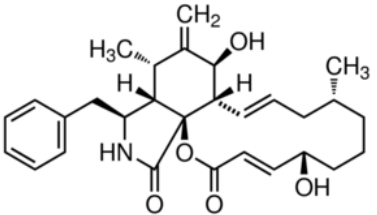
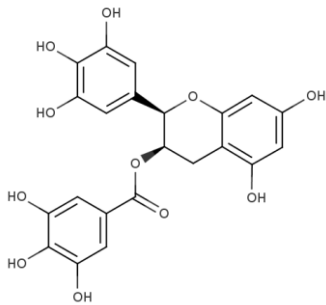
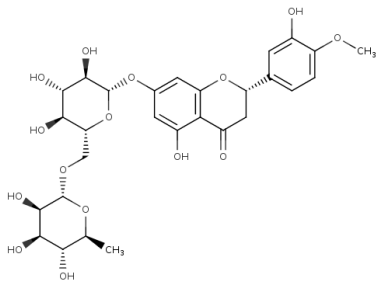
comparable between both sugars. This suggests that these compounds acted in a similar fashion when inhibiting glucose transport or fructose transport by GLUT2.

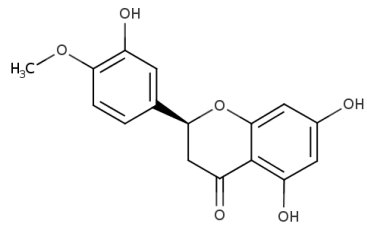
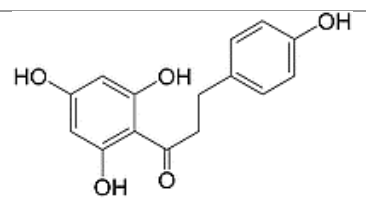
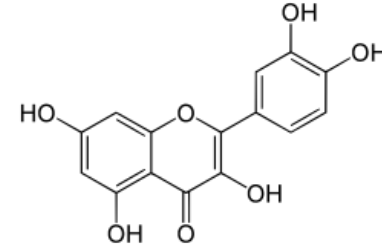
5.5.4 Summary of results from glucose and fructose uptake experiments

GLUT2-mediated glucose transport in oocytes was significantly inhibited in the presence of the known GLUT2 inhibitors phloretin and cytochalasin B, as expected (Krupka, 1985). Glucose uptake was also reduced in the presence of the four plant extracts tested, namely green tea extract, German chamomile extract, Bonolive extract and sugar-free pomegranate extract. Furthermore, a decrease in glucose uptake by GLUT2 was also observed when oocytes expressing this protein were exposed to hesperetin and its glucoside hesperidin. Cytochalasin B, when tested on human erythrocyte membrane samples, was shown to exert a competitive inhibition on GLUT2 through interaction with three sites on the protein. Glucose, phloretin and other sugars competitively displaced cytochalasin B from one of the interaction sites, site 1. This site is suspected not to be the substrate binding site as these two sites display varying structure-activity interactions. (Jung and Rampal, 1977). While the inward-facing form of the protein was determined to support the cytochalasin B binding site, phloretin is reported to bind to the external surface of GLUT2 (Krupka, 1985). Smaller than cytochalasin B, phloretin is likely to bind to the active site of GLUT2 and in this manner compete for the substrate. The structures of both inhibitors are shown in Table 5.2. A great addition to what is currently known about competitive inhibition of GLUT2 would be the investigation of the exact interactions of the main components of each extract with this protein

to determine the manner in which they exert their inhibition. The same is true for their interactions with hesperetin and hesperidin. All compounds which significantly inhibited uptake of glucose and/or fructose by GLUT2, including their structure, are shown in Table 5.2. Extracts which significantly inhibited GLUT2-mediated glucose uptake and their compositions, as well as the structure of the main component of each extract, are shown in Table 5.3.

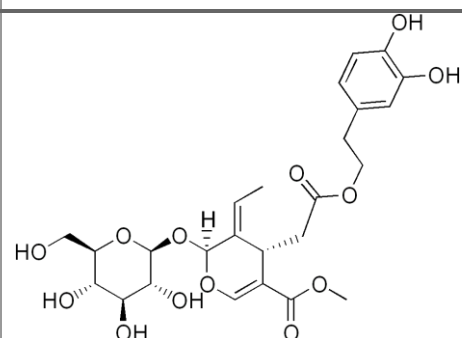
Table 5-2 Compounds and their respective inhibition on sugar uptake by GLUT2

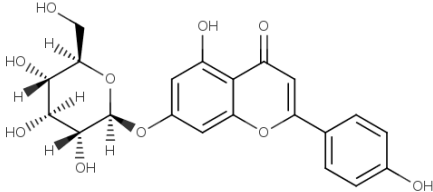
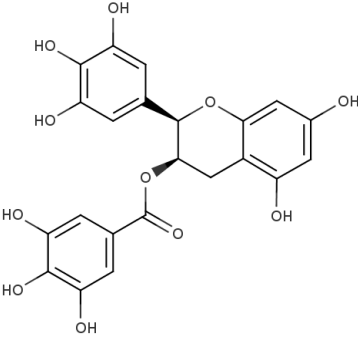
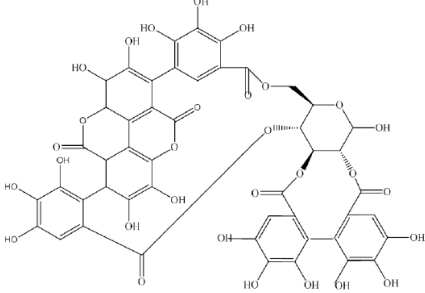
Compound	Substrate	Inhibition ¹	Structure
Apigenin	Glucose and fructose	IC _{50G} = 27 ± 4 μM IC _{50F} = 28 ± 10 μM	
Cytochalasin B	Glucose	70% inhibition at 100 μM	
EGCG	Glucose and fructose	IC _{50G} = 72 ± 13 μM IC _{50F} = 93 ± 16 μM	
Hesperidin	Glucose	IC ₅₀ = 219 ± 40 μM	

Hesperetin	Glucose	$IC_{50} = 30 \pm 9 \mu M$	
Phloretin	Glucose	81% inhibition at 100 μM	
Quercetin	Glucose and fructose	$IC_{50G} = 7 \pm 1 \mu M$ $IC_{50F} = 8 \pm 2 \mu M$	

¹ compounds for which a single concentration was tested were attributed a percentage inhibition at that concentration.

Table 5-3 Extracts and their respective inhibition on glucose uptake by GLUT2.

Compound	Composition¹	Inhibition	Structure²
Bonolive	40% oleuropein	$IC_{50} = 0.03 \pm 0.002 \text{ mg/ml}$	

German chamomile	12.32% apigenin-7-O-glucoside; 0.28% apigenin 0.13% luteolin-7-O-glucoside; 0.07% 4,5-dicaffeoylquinic acid	$IC_{50} = 0.49 \pm 0.24$ mg/ml	
Green tea	199.8 ± 6.7 mg/g (-)-Epigallocatechin gallate (EGCG); 124.4 ± 9.3 mg/g (-)-Epigallocatechin; 34.4 ± 1.9 mg/g (-)-Epicatechin gallate; 23.3 ± 2.4 mg/g (-)-Epicatechin	$IC_{50} = 0.13 \pm 0.02$ mg/ml	
Pomegranate	121 mg/g punicalagin; 6 mg/g puricalin; 5.9 mg/g ellagic acid hexose; 101 mg/g ellagic acid	$IC_{50} = 0.05 \pm 0.01$ mg/ml	

¹ analysis of extracts were performed previously; please refer to Chapter 2, section 2.1

² structure of the component present at the highest concentration in the extract is shown.

Inhibition pattern of GLUT2- mediated fructose and glucose transport was similar in the presence of pure compounds apigenin, EGCG and quercetin. Oocytes

expressing GLUT2 protein were able to transport three times more glucose than fructose and all three compounds had greater inhibitory effects on glucose transport, as concluded from IC_{50} values. Nevertheless, the rate of decrease in uptake by GLUT2 with increasing concentrations of each compound was comparable for both substrates. Inhibition of glucose by German chamomile extract and apigenin, one of the most abundant compounds in this extract (Villa-Rodriguez et al., 2017a), are both concentration dependent. Taking the composition of the extracts into account apigenin ($IC_{50} = 27 \pm 4 \mu\text{M}$) was better at inhibiting glucose transport by GLUT2 than the German chamomile extract ($IC_{50} = 0.49 \pm 0.24 \text{ mg/ml}$; equivalent to $51 \mu\text{M}$ apigenin). On the other hand, green tea extract ($IC_{50} = 0.13 \pm 0.02 \text{ mg/ml}$; equivalent to $43 \mu\text{M}$ EGCG) was a more potent inhibitor of glucose uptake by GLUT2 than EGCG alone ($IC_{50} = 72 \pm 13 \mu\text{M}$), possibly due to the presence of other gallated catechins in the extract, also shown to have an inhibitory effect on GLUT2 (Johnston et al., 2005).

Variability observed between uptake experiments is likely due to biological differences of the varying female ovaries digested to obtain oocytes for experiments, husbandry and housing of the animals, developmental stage variation, as well as a seasonal component affecting the quality of oocytes and their ability to express heterologous proteins (Delpire et al., 2011), (Conn, 1991), (Miller and Zhou, 2000). These factors were previously discussed in more detail in Chapter 4 (section 4.5.1). To add to that, multiple products were produced following IVT reaction with linear GLUT2pBF plasmid. Although this was determined to be leftover secondary structure, it still represented a fraction of the overall mRNA

concentration, meaning that less translational mRNA was injected into the oocytes, potentially leading to less protein expression on membrane of varying oocytes.

Inhibitors of GLUT2-mediated glucose transport German chamomile extract, sugar-free pomegranate extract, and hesperidin also inhibited GLUT5-mediated fructose transport. Moreover, EGCG and apigenin were able to inhibit GLUT2-mediated fructose and glucose transport, as well as inhibit GLUT5. Further research with these compounds, including *in vivo* studies with novel fructose uptake inhibitors able to decrease the uptake of fructose by its two major transporters, would help determine their potential as active compounds in preventive interventions aimed at reducing risk factors associated with CVD, diabetes and other health conditions.

Chapter 6

Glucose and fructose inhibition of heterologously expressed hGLUT7 by (poly)phenols

6.1 Abstract

Sugar uptake by the lesser known intestinal transporter GLUT7 has been under debate in recent years. As the closest related protein to GLUT5, it has been speculated that GLUT7 is also a fructose transporter. Nevertheless, contradicting data on fructose and glucose transport capability by this protein have been reported. Studies which concluded that GLUT7 can transport sugars have not been able to identify any inhibitors of this protein. In order to investigate if GLUT7 does in fact transport glucose and/or fructose, and the potential inhibitory effects of (poly)phenols, the protein was heterologously expressed in *X. laevis* oocytes, which were then incubated in a ¹⁴C-glucose/fructose solution containing individual (poly)phenols and extracts. Automated capillary ProteinSimple Western blotting confirmed protein expression on oocyte membranes and uptake of internalised ¹⁴C-glucose/fructose was observed by liquid scintillation counting. Results showed that GLUT7 expressed in oocytes transports fructose and glucose, uptake of which is competitively inhibited in the presence of fructose, but not deoxy-glucose. In addition, of the plant extracts and pure compounds tested, only apigenin had an impact on sugar transport by this protein, significantly inhibiting glucose uptake ($IC_{50} = 38 \pm 2 \mu M$) and fructose uptake ($IC_{50} = 16 \pm 12 \mu M$) by GLUT7. These

results show that, although perhaps not the primary physiological substrates, GLUT7 is a transporter for glucose and fructose and that uptake inhibition is achieved by the (poly)phenolic compound apigenin. This novel finding may help in the further characterization of this transporter in terms of substrate-protein interactions and binding.

6.2 Introduction

The human GLUT7 (hGLUT7) protein is most abundantly expressed in the small intestine, colon, testis and prostate (Li et al., 2004). This GLUT transporter is the closest relative to GLUT5, also expressed in the gut, sharing 53% sequence homology and 68% amino acid identity to the fructose specific transporter (Li et al., 2004), (Scheepers et al., 2005). Although GLUT7 has yet to be completely characterized, due to its similarity to the GLUT5, this protein has been proposed to be a fructose transporter (Uldry and Thorens, 2004). It has been determined that GLUT7 has high affinity for fructose and glucose (< 0.5 mM), however, the physiological substrate for this transporter has not yet been conclusively established (Cheeseman, 2008). Affinity of GLUT7 has been reported to be marginally higher for fructose (~ 0.1 mM) than glucose (~ 0.3 mM) (Li et al., 2004), (Manolescu et al., 2005). Sequencing alignment analysis indicated that GLUTs 2, 5 and 7 have a conserved isoleucine containing-motif thought to be essential for transport of fructose, as it was not observed in other non-fructose transporting GLUTs (Doblado and Moley, 2009). To add to that, a study by Manolescu et al showed that a single point mutation substituting isoleucine for valine or serine in

the sequences of GLUTs 2, 5 and 7 abolished their ability to transport fructose, while glucose transport remained unaffected (Manolescu et al., 2005), (Manolescu et al., 2007a). GLUT11, a fructose transporter in the heart and skeletal muscle that shares 41.7% amino acid identity with GLUT5, has an aspartic acid and serine motif in the same position, and is thought to have the same function as the isoleucine motif observed in the sequences of GLUTs 2, 5, and 7 (Doege et al., 2001). Mechanisms of substrate recognition by GLUTs that transport both glucose and fructose, e.g. GLUTs 2 and 7, are not yet fully understood. It has been suggested that the different binding sites and/or modes are the key to transport of multiple substrates (Thompson et al., 2015). Due to GLUT7 protein distribution in the gut, and based on its affinity for fructose, it has been speculated that the principal role of GLUT7 may be of fructose absorption at the end or after a meal, when fructose is present at low concentrations in the intestinal lumen (Drozdowski and Thomson, 2006). The expression of this transporter is highest in the ileum, suggesting it potentially works as a scavenger for luminal glucose and fructose in the ileum when abundance of sugars are low (Cura and Carruthers, 2012). Nevertheless, although some GLUT7 uptake studies have determined that this protein transports both glucose and fructose when expressed in *X. laevis* oocytes (Li et al., 2004), (Cheeseman, 2008), others were unable to detect any sugar uptake by this transporter (Ebert et al., 2017). In this chapter, uptake experiments by heterologously expressed hGLUT7 were executed with the aim to determine if GLUT7 can in fact transport glucose and/or fructose. There currently are no data on the ability of (poly)phenols to inhibit sugar uptake by GLUT7, and common GLUT inhibitors such as phloretin or cytochalasin B did not exert any effect on sugar uptake by this transporter (Li et al., 2004). A study by Thompson et al

identified the N-[4-(methylsulfonyl)-2-nitrophenyl]-1,3-benzodioxol-5-amine (MSNBA) compound as a specific GLUT5-mediated fructose inhibitor in proteoliposomes, which was speculated to perhaps inhibit GLUT7 as well based on the sequence similarity between the two transporters (Thompson et al., 2016). Nevertheless, further investigations on GLUT7-mediated sugar uptake inhibition needs to be conducted in order to conclusively establish an inhibitor of this transporter. For this reason, the potential inhibitory effect of plant extracts and pure compounds on sugar uptake by GLUT7 will be assessed in this chapter using the same model, previously described in earlier chapters, of expression of human GLUT7 (hGLUT7) in *X. laevis* oocytes.

6.3 Validation of GLUT7pBF and GLUT7pGEM-HE plasmid construct functionality

6.3.1 Confirmation of adequate placement of hGLUT7 gene in expression vector

Two plasmid constructs containing the human GLUT7 gene were used for sugar uptake experiments, namely GLUT7pBF and GLUT7pGEM-HE. The former was designed by myself and the latter was kindly supplied by Debbie O'Neill of Prof. Chris Cheeseman's group (Department of Physiology, Alberta University, Canada). Described below are the processes applied to ensure correct positioning of the gene in either plasmid.

6.3.1.1 GLUT7pBF plasmid construct

The human GLUT7 gene was inserted into the expression vector pBF through methods described previously in chapter 2 (see section 2.3). Confirmation of successful ligation of the sequences of expression vector and gene of interest was determined by digestion of colonies selected after ligation with the restriction enzyme HindIII. This particular restriction enzyme recognizes a single restriction site embedded in the sequence of the GLUT7 gene as well as one restriction site located in the the pBF plasmid sequence. This means that upon gel electrophoresis of digest products, a positive colony for the presence of GLUT7 produced two distinct bands, one at a size comparable to 3173 bp (digestion at the pBF restriction site) and another at a size equivalent to 1692 bp (digestion at the GLUT7 gene restriction site), as determined by a theoretical digestion of the plasmid sequence with the restriction enzyme (refer to Figure 6.2). All fifteen individual colonies extracted were considered positive for the presence of GLUT7 (Figure 6.1) and were sequenced for confirmation (refer to Chapter 2 section 2.3.1 for list of primers used). Digestion of colonies 1-10 (Figure 6.1 A) and 11-15 (Figure 6.1 B) with HindIII produced bands of around 3000 bp and 2000 bp following gel electrophoresis, both of which are comparable to expected product sizes of 3173 bp and 1692 bp. Sequencing results showed that DNA from all colonies sequenced matched that expected for GLUT7pBF plasmid. One single colony was randomly chosen for propagation (colony 5) and used for all subsequent experiments.

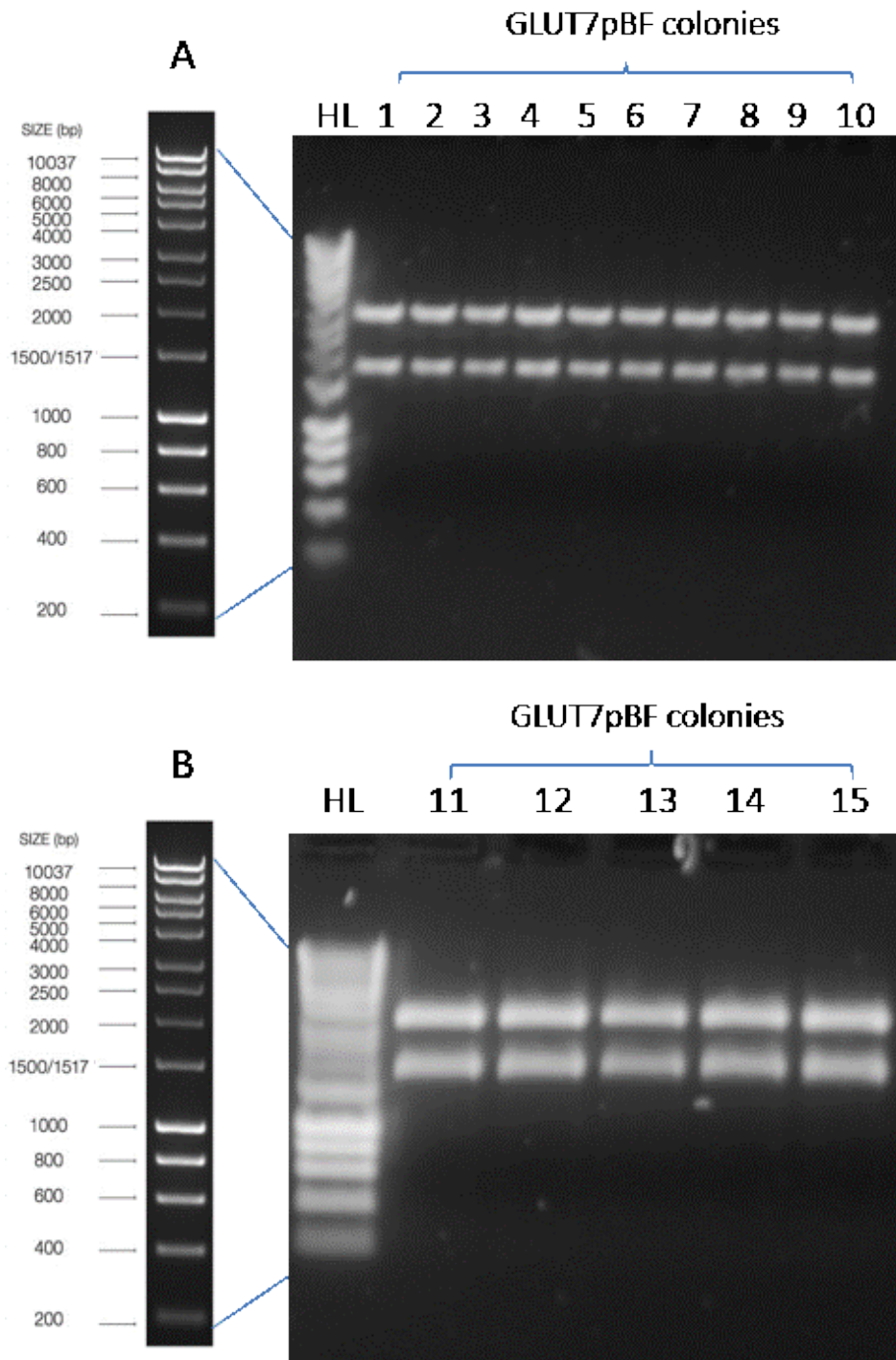


Figure 6-1 Gel electrophoresis image showing digestion of GLUT7pBF colonies with HindIII after ligation of GLUT7 gene to expression vector. A colony positive for the presence of GLUT7 gene produced two individual bands [colony 1-10 (**A**), 11-15 (**B**)]. Product sizes are comparable to the theoretical sizes of digestion of this sequence with HindIII, namely around 3173 bp (digestion at the pBF restriction site) and 1692 bp (digestion at the GLUT7 gene restriction site). Size of products was determined against a DNA hyperladder (HL).

The complete GLUT7pBF sequence with its key attributes, such as the SP6 promoter site where in vitro transcription begins (green), is shown in Figure 6.2. This plasmid could be linearized using two restriction enzymes prior to the IVT reaction, namely MluI and PmlI (pink), as the restriction site for both enzymes is found after the PolyA tail (light purple), a stretch of sequence consisting of adenosine bases that aids with stability of mRNA and nuclear export (Fuke and Ohno, 2008). The site of linearization is where sequence template for the RNA polymerase ends, as does the transcription reaction (Beckert and Masquida, 2011), and hence why it is important to opt for a restriction enzyme site after the PolyA tail. The GLUT7 gene (orange) was positioned after the transcription start site (SP6 promoter, green) and before the PolyA tail and transcription end site (MluI and PmlI, pink). The site of specific primers with homology to pBF and GLUT7 sequences used in the ligation of the gene to the expression vector are shown in light grey (for full sequences refer to Chapter 2, section 2.3.3.2). Specific position of restriction sites of HindIII (dark grey) are shown in relation to the rest of the plasmid sequence and to each other. The same figure also illustrates a theoretical digestion of GLUT7pBF with the HindIII restriction enzyme, giving the theoretical products to be expected from gel electrophoresis reaction based on the DNA sequence. A table is shown in the same figure listing the precise location in the sequence for each of the HindIII restriction sites (third column), which in turn determine the sizes (in bp) of each digest (first column), as well as the percentage of the total mass for which the digest products account for (sixth column).

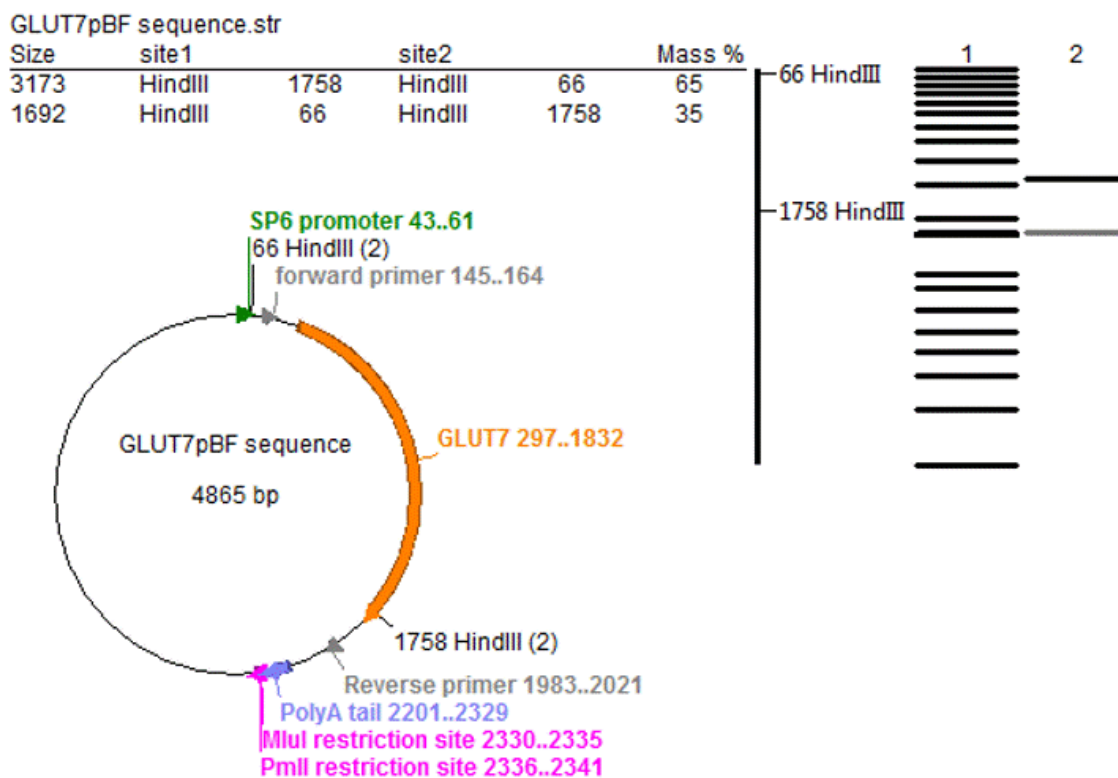


Figure 6-2 Illustration of the GLUT7pBF plasmid and theoretical gel electrophoresis products upon digestion of plasmid with HindIII restriction enzyme. Varying key attributes of the full GLUT7pBF sequence are shown including SP6 promoter (green) region, PmlI and MluI restriction sites (pink) and PolyA tail (light purple), as well as location of the inserted GLUT7 gene (orange) and specific homologous primers used in ligation reaction (light grey). Location of HindIII restriction sites in the GLUT7pBF sequence (dark grey) and the theoretical digestion of the sequence, including expected gel electrophoresis products, are shown around the circular plasmid structure.

6.3.1.2 GLUT7pGEM-HE plasmid construct

This plasmid was transformed into competent cells, propagated, and colonies were extracted to be digested with restriction enzymes in order to confirm presence of GLUT7 gene. Exact location of GLUT7 gene in expression vector pGEM-HE was determined using restriction enzyme and specific primer information previously published (Li et al., 2004) and confirmed through sequencing reactions (refer to Chapter 2 section 2.3.1 for list of primers used).

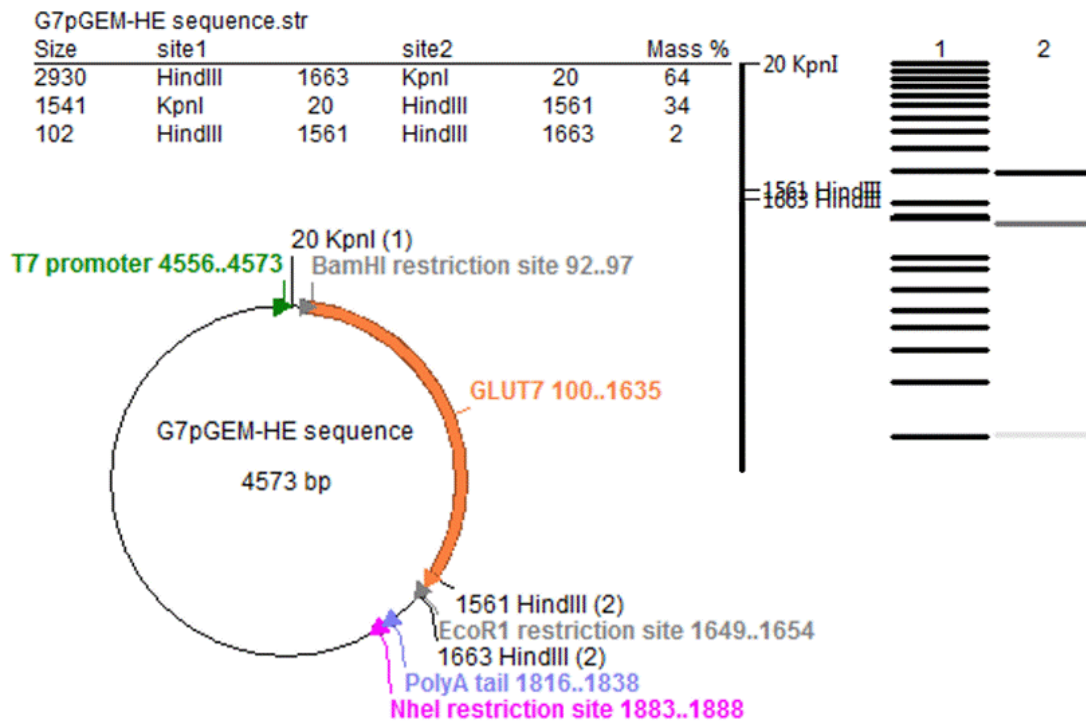


Figure 6-3 Illustration of the GLUT7pGEM-HE plasmid and theoretical gel electrophoresis products upon digestion of plasmid with HindIII and KpnI restriction enzymes. Varying key attributes of the full GLUT7pGEM-HE sequence are shown including T7 promoter (green) region, NheI restriction site (pink) and PolyA tail (light purple), as well as location of the inserted GLUT7 gene (orange) and the specific enzyme restriction sites used in the original ligation reaction (light grey). Location of HindIII and KpnI restriction sites in the GLUT7pGEM-HE sequence (dark grey) and the theoretical digestion of the sequence, including expected gel electrophoresis products, are shown around the circular plasmid structure.

Figure 6.3 illustrates the complete GLUT7pGEM-HE sequence and its key features. The GLUT7 gene (orange) was positioned between the T7 promoter site (green) and PolyA tail (light purple) and NheI restriction enzyme site (pink). Specific primers used for PCR ligation reaction were designed to include the sequence corresponding to the sites of two restriction enzymes, BamHI and EcoRI (dark grey). This ensured correct positioning of the gene of interest in relation to other features of the expression vector, as previously mentioned in 5.3.1.1. A table is shown in the same figure listing the precise location in the sequence for each of

the restriction sites of the two restriction enzymes (third column), which in turn determine the sizes (in bp) of each digest (first column), as well as the percentage of the total mass for which the digest products account for (sixth column).

Much like GLUT7pBF, this plasmid also contains two HindIII restriction sites, one in the pGEM-HE sequence and one within the sequence of the GLUT7 gene. However, proximity of the two restriction sites meant that the digestion product at the expression vector restriction site was 102 bp, which was not very clear on the gel following electrophoresis (Figure 6.4). For this reason, the plasmid was digested with the addition of another restriction enzyme, namely KpnI, which is only present in the pGEM-HE sequence and not in the GLUT7 gene sequence. Theoretical digestion of GLUT7pGEM-HE with both enzymes and the theoretical products to be expected from gel electrophoresis reaction based on the DNA sequence are shown in Figure 5.3. Of the six colonies extracted, only one was considered positive for the presence of the GLUT7 gene as it produced two clear products upon gel electrophoresis, namely one around 1500 bp, consistent with digestion of the sequence at the GLUT7 gene HindIII restriction site, and another about 3000 bp in size, corresponding to the digestion at the pGEM-HE KpnI restriction site. Control digestion of pGEM-HE plasmid without inserted GLUT7 produced a single clear band product at around 3000 bp (Figure 6.4 A). DNA from the colony deemed positive for the presence of GLUT7 gene was sequenced, confirming agreement with the theoretical GLUT7pGEM-HE sequence. This colony (colony 5) was propagated and used for all subsequent experiments. Once propagated, GLUT7pGEM-HE, as well as pGEM-HE, were digested with HindIII

and KpnI and gel electrophoresis confirmed the presence, albeit faint, of the smaller product of about 200 bp in size consistent with the 102 bp product of digestion at the pGEM-HE HindIII restriction site (Figure 6.4 B).

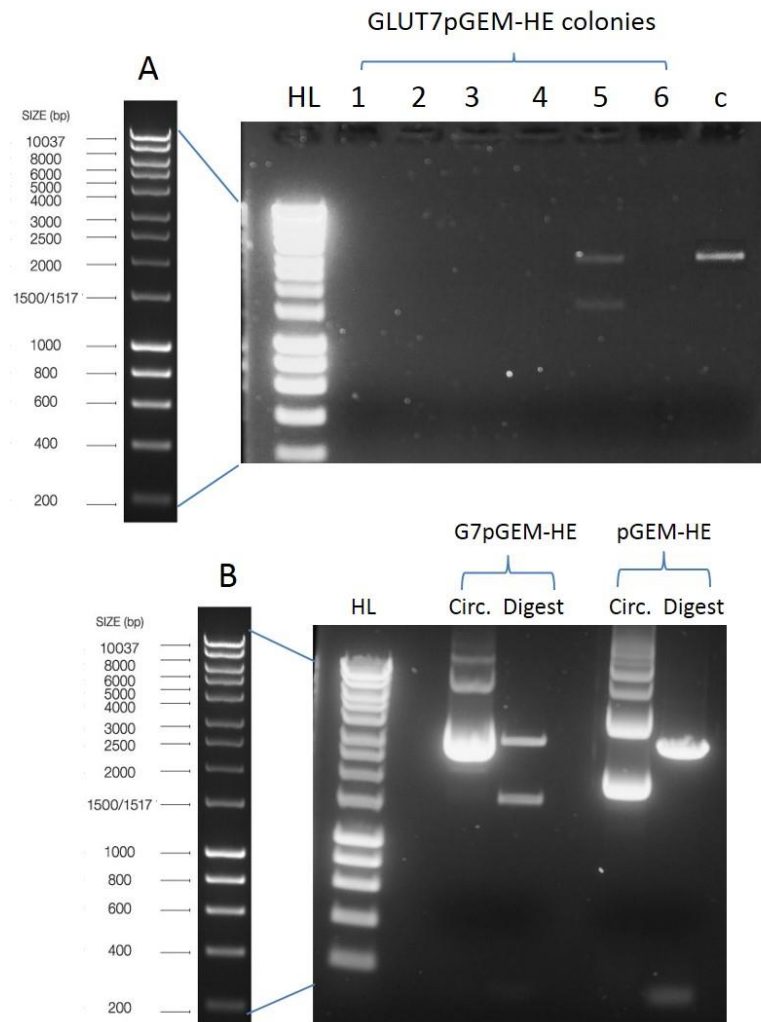


Figure 6-4 Gel electrophoresis image showing digestion of GLUT7pGEM-HE and its colonies with HindIII and KpnI after ligation of GLUT gene to expression vector. A colony positive for the presence of GLUT7 gene produced three individual bands [colony 5 (A)], while control digestions produced two bands (c). Comparison of circular GLUT7pGEM-HE (circ.) and digested product (digest) to pGEM-HE following plasmid propagation (B). Product sizes are comparable to the theoretical sizes of digestion of this sequence with HindIII and KpnI, namely around 102 bp (digestion at the pGEM-HE HindIII restriction site), 1541 bp (digestion at the GLUT7 gene HindIII restriction site) and 2930 bp (digestion at the pGEM-HE KpnI restriction site). Size of products was determined against a DNA hyperladder (HL).

6.3.2 Confirmation of specificity and quality of mRNA product

The IVT reactions were carried out with linearized GLUT7pBF and GLUT7pGEM-HE plasmids following digestion with restriction enzymes for which restriction sites were located after the gene of interest and PolyA tail. GLUT7pBF was linearized with either MluI or PmlI, and GLUT7pGEM-HE was digested with NheI. Gel electrophoresis of both circular plasmids showed the characteristic migration pattern for the combination of nicked and supercoiled DNA, as previously mentioned in Chapters 4 and 5 (section 4.3.2 and 5.3.2, respectively). Linear DNA of GLUT7pBF produced by digestion with both MluI and NheI migrated through the gel producing a band corresponding in size to that of the full plasmid sequence (4865 bp), as did the linear DNA of GLUT7pGEM-HE from digestion with PmlI (4573 bp). The migration pattern of circular and linear DNA of both plasmids are shown in Figure 6.5.

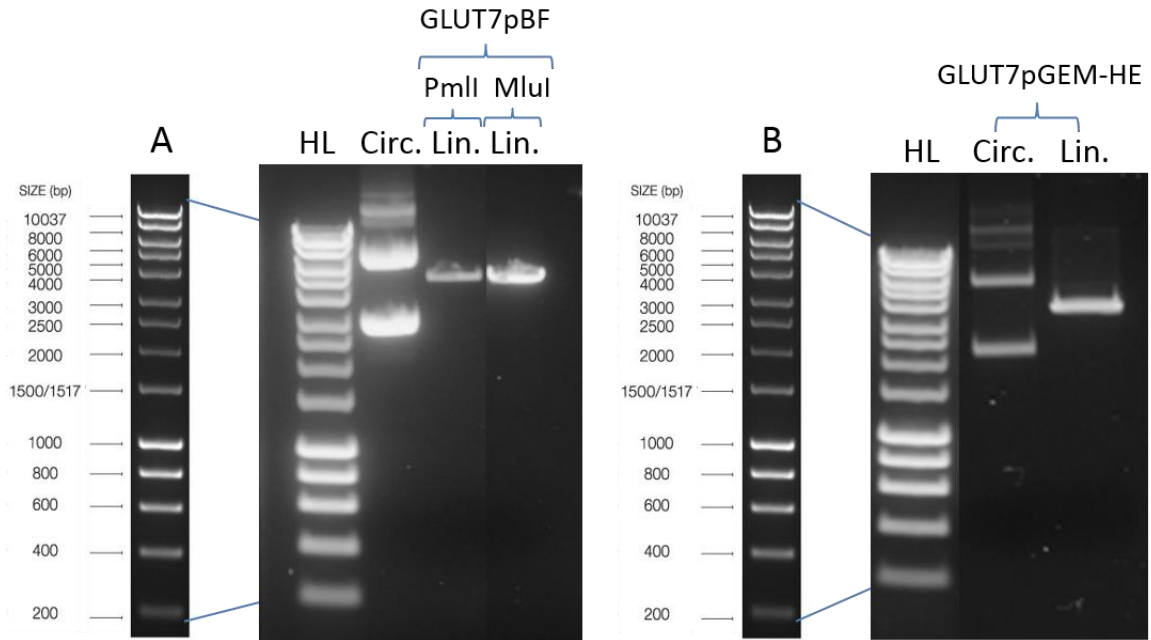


Figure 6-5 Gel electrophoresis of circular and linear GLUT7pBF and GLUT7pGEM-HE. GLUT7pBF plasmid (circ.) was linearized by digestion with PmlI and MluI restriction enzymes (lin.) before IVT reaction **(A)**. Circular GLUT7pGEM-HE plasmid (circ.) was linearized by digestion with NheI restriction enzyme (lin.) before IVT reaction **(B)**. Both circular plasmids produced bands on the gel characteristic of their structure, whereas linear digests produced a single band corresponding in size to the sequence of the full plasmid (4865 bp and 4573 bp for GLUT7pBF and GLUT7pGEM-HE, respectively). Gel electrophoresis confirming linearization of plasmid and was performed for every new mRNA sample prepared.

Once the IVT reaction was performed the mRNA product is analysed in a denaturing gel (see Chapter 2 section 2.3.5) in order to confirm that the product size was consistent with the expected size determined from the sequence of each plasmid.

6.3.2.1 GLUT7pBF derived mRNA

The mRNA product obtained from IVT of GLUT7pBF produced two band products following gel electrophoresis on RNA denaturing gel. Much the same as the GLUT2

mRNA which also produced two bands on denaturing gel (Chapter 5, section 5.3.2), the GLUT7 mRNA produced two distinct bands, one at higher molecular weight (around 2000 bp) and one at lower molecular weight (around 1000 bp). However, unlike previously the size of the higher molecular weight band was in agreement with that expected of the GLUT7 mRNA derived from this plasmid (2276 bp or 2341 bp by digestion with MluI or PmlI, respectively) (Figure 6.6 A). Bands were cut from the gel, RNA was extracted and gel electrophoresis of extracts was performed on another denaturing gel. RNA extracted from both the higher and lower molecular weight band migrated through the gel in the same manner as when present together in the original GLUT7 mRNA sample (Figure 6.6 B), meaning the IVT reaction produced two distinct products. The IVT kit user guide states that premature termination by the polymerase is the most likely cause for multiple products. Potential reasons for early termination by polymerase include sequences with resemblance to the polymerase termination signals, GC-rich templates, and stretches of a single nucleotide (mMessage mMachine® Kit User Guide, Ambion). Analysis of plasmid sequence determined that GC was 57%, which is within the optimal range of 40-60% (Lorenz, 2012) and there were no identified long stretches of a single nucleotide. This led to the conclusion that the polymerase must have recognized a particular stretch of the sequence as a termination signal. Based on the size of the product upon gel electrophoresis this stretch of sequence with similarity to the termination site of the enzyme would be located within the GLUT7 gene sequence, therefore, there was no possibility of adjusting the sequence to try and rectify the problem. The IVT reaction temperature was lowered to try and alleviate premature termination, however, no changes were observed (RNA denaturing gel of IVT reaction at different temperatures can be found in Figure 6.8).

Although the GLUT7 mRNA obtained from GLUT7pBF produced two products, only one product, where polymerase did not terminate prematurely, would contain all the features necessary for translation of product once microinjected. Therefore, uptake experiments were still carried out with oocytes microinjected with this mRNA.

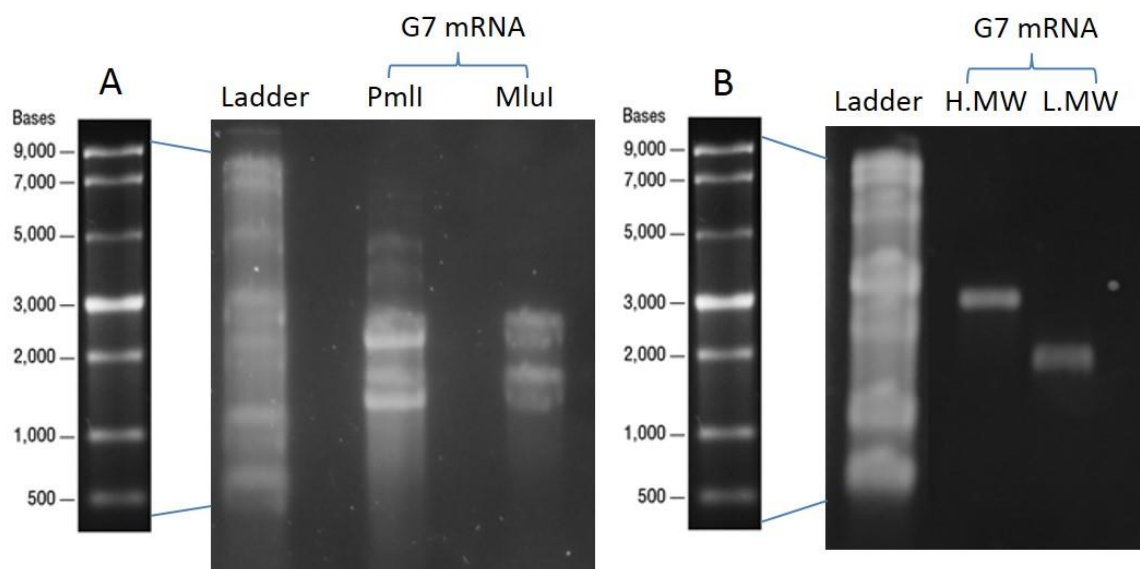


Figure 6-6 Gel electrophoresis of the GLUT7 mRNA product, derived from GLUT7pBF, on RNA denaturing gel. After IVT reaction the mRNA product was run on a formaldehyde denaturing gel to confirm that its size matched to that expected from the plasmid sequence (2276 bp or 2341 bp by digestion with MluI or PmlI, respectively). GLUT7 mRNA produced two bands, one at a size corresponding to that expected and one at a lower molecular weight (**A**). Individual bands were cut from the gel, RNA was extracted, and gel electrophoresis of extracts on denaturing gel was performed. Migration pattern of each extract on the gel showed that RNA from higher (H.MW) and lower (L.MW) molecular weight bands migrated through the gel in the same way as in original mRNA sample, meaning the IVT reaction produced two products (**B**). Size of products was determined against an ssRNA ladder. Gel electrophoresis of mRNA product on RNA denaturing gel was performed for every new mRNA sample prepared.

As the GLUT7 gene sequence contained a particular stretch of sequence with resemblance to the termination signal of the SP6 RNA polymerase, it is possible

that a different polymerase would not recognize any sites in the gene sequence as a termination signal, thereby, producing one single mRNA product. This possibility was pursued by obtaining the GLUT7pGEM-HE plasmid, which contains the T7 promoter.

6.3.2.2 GLUT7pGEM-HE derived mRNA

The mRNA product obtained from IVT of GLUT7pGEM-HE also produced two distinct band products following gel electrophoresis on RNA denaturing gel. The GLUT7 mRNA produced one higher molecular weight (around 5000 bp) product and one lower molecular weight product (around 2000 bp). As seen previously with the GLUT2 mRNA, the lower molecular weight band was in agreement with that expected of the GLUT7 mRNA derived from this plasmid (1888 bp) (Figure 6.7 A). Bands were cut from the gel, RNA was extracted and gel electrophoresis of extracts was performed on another denaturing gel. Extracted RNA from both the higher molecular weight band and lower molecular weight band migrated through the gel in the same manner as in the original GLUT7 mRNA sample (Figure 6.6 B). Although this did not confirm that the higher molecular weight product was leftover secondary structure, as discussed previously (Chapter 5 section 5.3.2), this is extremely likely based on the size of the product (around 4000 bp). Uptake experiments were carried out with oocytes microinjected with this mRNA.

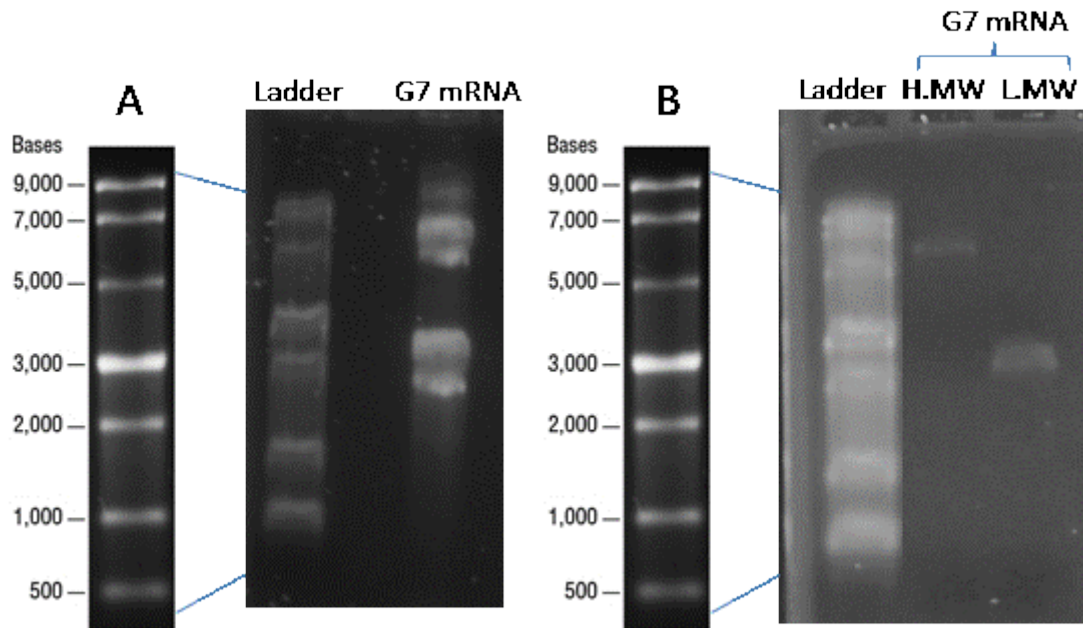


Figure 6-7 Gel electrophoresis of GLUT7 mRNA product, derived from GLUT7pGEM-HE, on an RNA denaturing gel. After IVT reaction, the mRNA product was run on a formaldehyde denaturing gel to confirm that its size matched that expected from the plasmid sequence (1888 bp). GLUT7 mRNA produced two bands, one at a size corresponding to that expected and one at a higher molecular weight (**A**). Individual bands were cut from the gel, RNA was extracted, and gel electrophoresis of extracts on denaturing gel was performed. Migration pattern of each extract on the gel confirms that the higher molecular band (H.MW) consists of left over secondary structure while the lower molecular weight band (L.MW) corresponds to the mRNA product size (**B**). Size of products was determined against an ssRNA ladder. Gel electrophoresis of mRNA product on RNA denaturing gel was performed for every new mRNA sample prepared.

The GC content of this sequence was within range (57%) and lowering of the IVT reaction temperature (usually performed at 37 °C), although seemingly increasing specificity, significantly reduced the yield of mRNA product. Lower temperatures for IVT reaction also decreased the concentration of mRNA products derived from GLUT7pBF plasmid (linearized with either PmlI or MluI restriction enzymes), with no conclusive improvements in mRNA quality or specificity (Figure 6.8).

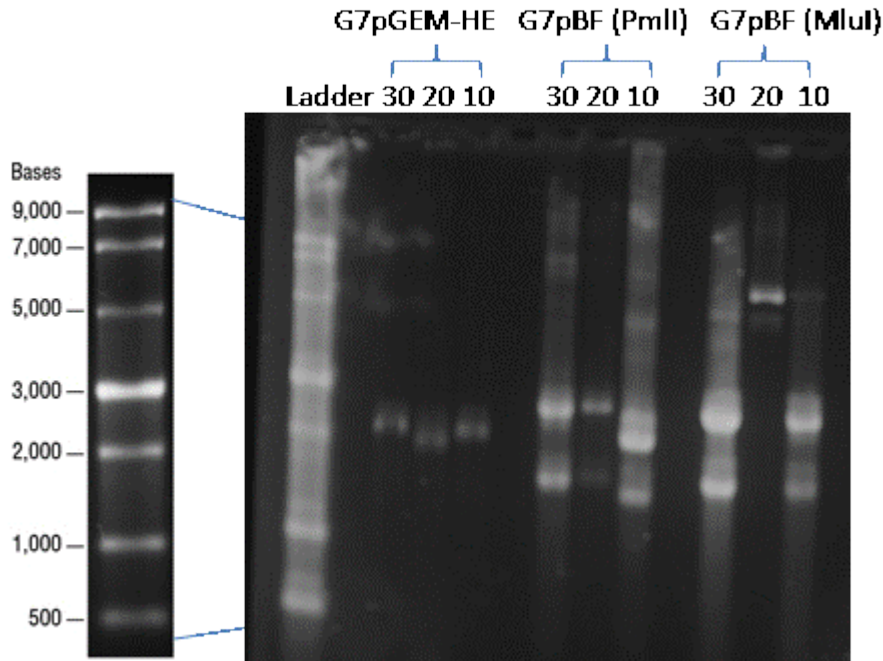


Figure 6-8 Gel electrophoresis of GLUT7 mRNA products, derived from GLUT7pGEM-HE and GLUT7pBF linearized with PmlI or Mlul, on an RNA denaturing gel. mRNA products from IVT reactions performed at 10 °C (10), 20 °C (20) or 30 °C (30) were run on a formaldehyde denaturing gel to determine any improvements in specificity and quality of mRNA. Specificity of mRNA products derived from GLUT7pGEM-HE plasmid improved, however, yield was significantly reduced. There were no changes in specificity of mRNA products derived from GLUT7pBF plasmid (linearized with either Mlul or PmlI), with two distinct products still being produced. Concentrations of mRNA products were also reduced for samples derived from this plasmid at the lower IVT reaction temperatures.

6.4 Validation of *X. laevis* model functionality

6.4.1 Sugar uptake by GLUT7-expressing oocytes and inhibition by known specific inhibitors

There are contradicting reports of what the substrate(s) of GLUT7 may be. While some have detected uptake of both glucose and fructose, but not galactose or deoxy-glucose, by this transporter (Li et al., 2004) others have not observed uptake

of any sugars by oocytes microinjected with GLUT7 mRNA (Ebert et al., 2017). Presence of GLUT7 on the membranes of GLUT7-injected oocytes was shown in both instances (Li et al., 2004), (Ebert et al., 2017). In order to assess the possible transport of sugars by GLUT7 uptake experiments by oocytes expressing GLUT7 were carried out under conditions previously optimised (Li et al., 2004), namely oocytes were incubated at 25 °C in a 0.1 mM sugar solution for 5 min following a 5 day expression period post-microinjection. For all uptake experiments in this chapter one replicate is equivalent to 3 oocytes homogenized together, unless otherwise stated. Oocytes microinjected with GLUT7 mRNA derived from GLUT7pBF showed a significant uptake of glucose as well as fructose (Figure 6.8 A). Similarly, significant glucose and fructose uptake, but not of deoxy-glucose (70% less uptake than glucose, $p \leq 0.01$), was observed by oocytes microinjected with GLUT7 mRNA derived from GLUT7pGEM-HE (Figure 6.9 B). In addition, glucose uptake by GLUT7 seems to be inhibited in the presence of fructose (42% less uptake of glucose in the presence of fructose, $p \leq 0.01$) (Figure 6.9 A), which is in accordance with previously reported uptake experiments (Li et al., 2004).

To date there have been no accounts of GLUT7 inhibitors, with compounds such as phloretin and cytochalasin B having no impact on glucose uptake by this transporter, as previously demonstrated (Li et al., 2004) and assessed here by oocytes microinjected with GLUT7 mRNA derived from both the GLUT7pBF (Figure 6.10 A) and GLUT7pGEM-HE plasmids (Figure 6.10 B). Water injected oocytes were used as controls in all uptake experiments. Results of uptake by

GLUT7-expressing oocytes are shown normalized to the uptake observed by their respective water injected controls, unless otherwise stated.

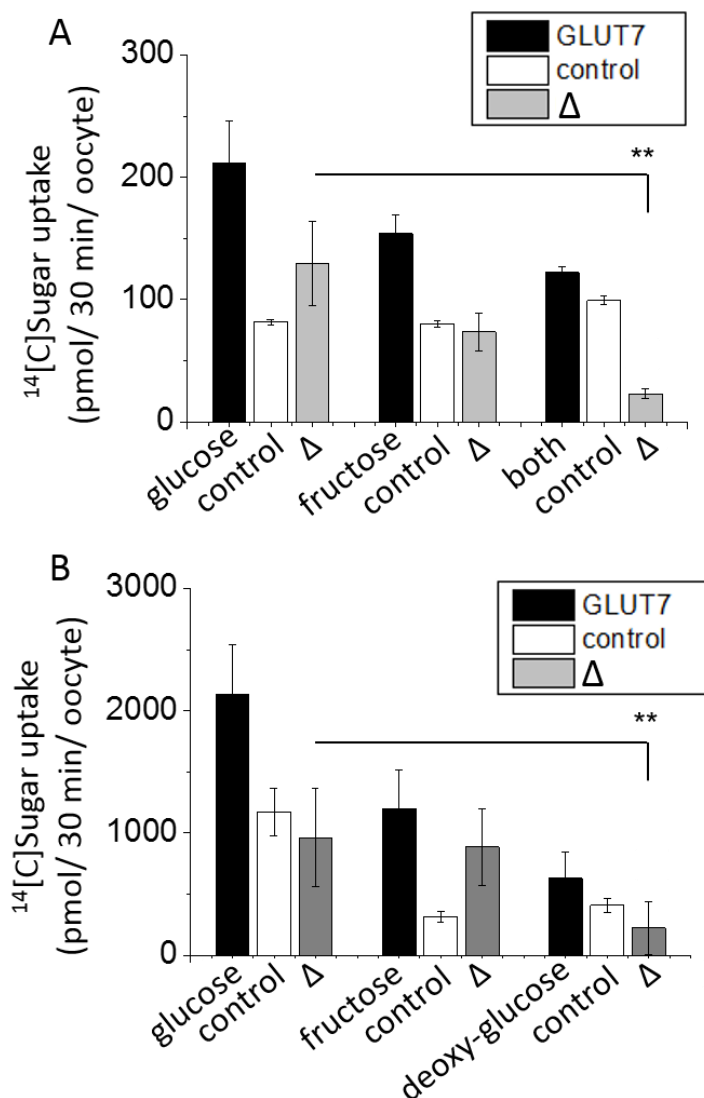


Figure 6-9 Uptake of sugars by GLUT7-expressing oocytes. Five days post GLUT7 mRNA microinjection oocytes were incubated in 0.1 mM glucose/ fructose/ deoxy-glucose solution containing the corresponding [¹⁴C] sugar for 30 min. Internalized sugar uptake was determined by scintillation spectrometry for GLUT7-expressing oocytes (black bars) and water injected controls (open bars). Net change in uptake, Δ, (grey bars) was determined by normalizing the uptake observed by GLUT7 to control uptake. The mean ± SEM of 6 replicates (of 3 oocytes) is shown per individual condition. There was significant uptake of glucose, inhibited by the presence of fructose, by oocytes injected with GLUT7 mRNA derived from GLUT7pBF (**A**). Uptake of glucose and fructose, but not deoxy glucose, was observed by oocytes injected with GLUT7 mRNA derived from GLUT7pGEM-HE (**B**). ** $p \leq 0.01$

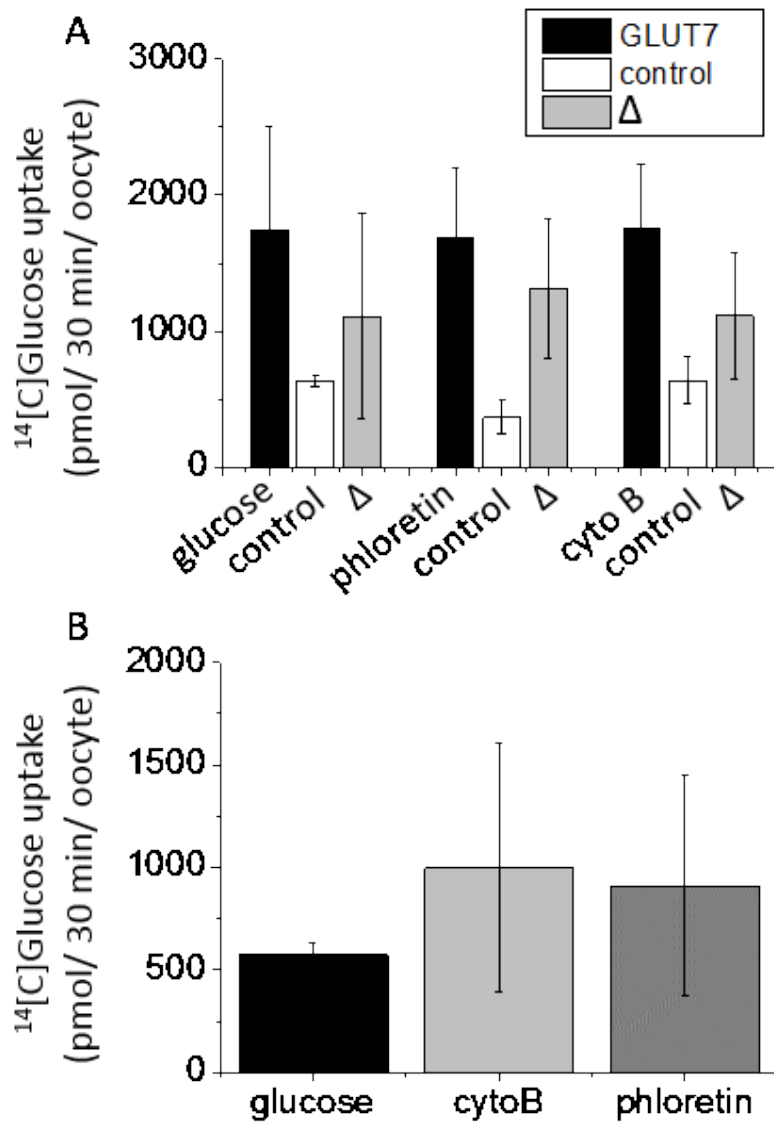


Figure 6-10 Inhibition of glucose uptake by GLUT7-expressing oocytes. Five days post GLUT7 mRNA microinjection oocytes were incubated in 0.1 mM glucose solution containing [¹⁴C] glucose for 30 min in the presence of 100 μM phloretin or 100 μM cytochalasin B (cytoB). Internalized sugar uptake was determined by scintillation spectrometry for GLUT7-expressing oocytes (black bars) and water injected controls (open bars) (**A**). Net change in uptake, Δ, (grey bars) was determined by normalizing the uptake observed by GLUT7 to control uptake. Neither cytochalasin B nor phloretin inhibited uptake of glucose by oocytes injected with GLUT7 mRNA derived from GLUT7pBF (**A**) or GLUT7 mRNA derived from GLUT7pGEM-HE (**B**). Each data point represents the mean of 6 replicates (of 3 oocytes), normalized to control for each condition, ± SEM.

6.4.2 Determination of expression of recombinant hGLUT7 on oocytes membrane extracts

Automated capillary Western blot, Wes (see Chapter 2 section 2.4.7), was used to investigate expression of GLUT7 on oocyte membranes. Membranes were extracted from 10 oocytes 5 days post-microinjection with GLUT7 mRNA or water. Cell lysate from TC7 cells was used as a positive control for the presence of GLUT7. Detection of GLUT7 was only successful in membranes extracted from oocytes microinjected with mRNA derived from the GLUT7pGEM-HE plasmid (Figure 6.11), with size comparable to protein detected in the TC7 cell lysate. Nevertheless, there was substantial non-specific binding from the antibody in the membrane extract samples, creating a much stronger signal than that observed for GLUT7 (Figure 6.12 A). The GLUT7 antibody used for protein detection targets the glycosylated epitope and so membrane extracts, as well as the TC7 cell lysate, were treated with the glycosidase PNGase before imaging with the aim to enhance detection. A shift in size was clearly observed between PNGase-treated and untreated membrane samples from GLUT7-microinjected oocyte membranes (shift from about ~ 59 kDa to about ~ 48 kDa after PNGase treatment), serving as further confirmation that the peak in question did in fact correspond to GLUT7 protein (Figure 6.12 B). Optimal GLUT7 antibody dilution of 1:10 for Wes experiments was determined by Dr. S. Tumova.

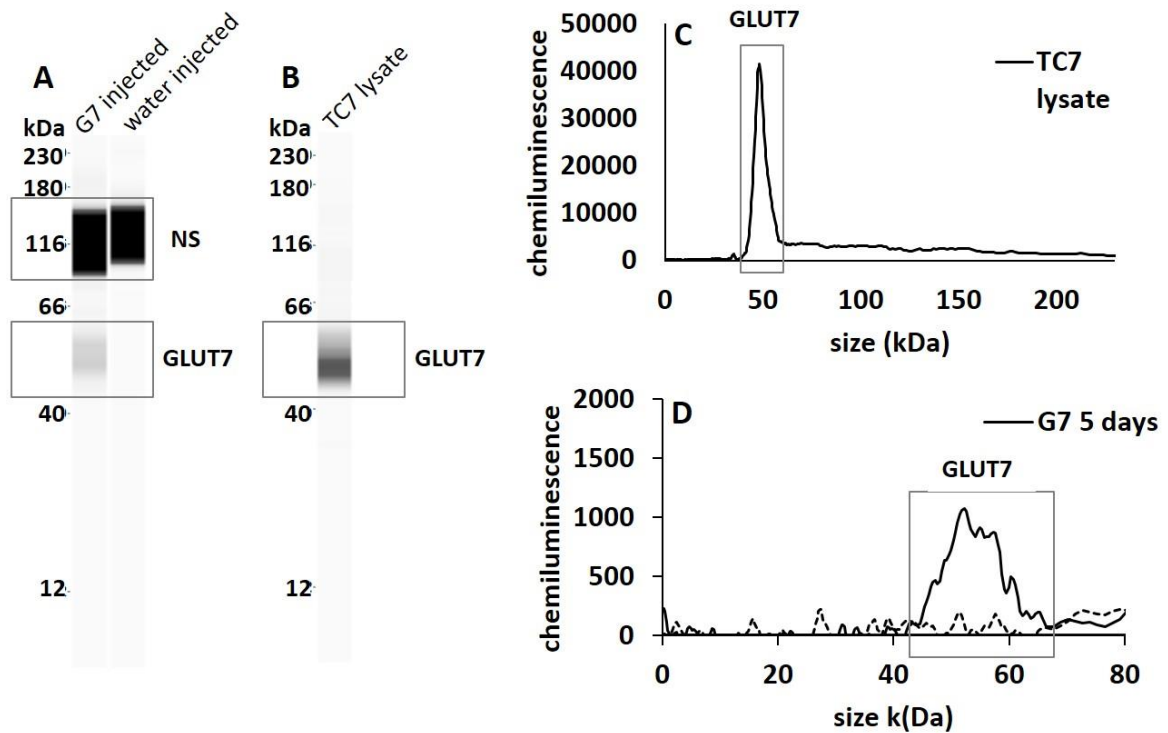


Figure 6-11 Confirmation of expression of GLUT7 on oocyte membrane extracts by Wes. Membranes extracted from ten oocytes five days post injection with GLUT7 mRNA, as well as water injected control membranes, were analysed using automated capillary Western blot (Wes). Analysis of membrane extracts of GLUT7 and control injected oocytes (**A**) and the positive control TC7 cell lysate shown as a gel-like image (**B**). The same TC7 cell lysate (**C**) and GLUT7, isolated and magnified from original image, and control injected membrane extracts (**D**) are shown as an electropherogram (**C**). Detected protein size for GLUT7 was 52 kDa for oocyte membrane extract and 50 kDa for TC7 cell lysate. Concentration of TC7 cell lysate loaded was 0.5 mg/ml; membrane extracts were loaded without dilution. Antibody dilution was 1:10.

The difficulty in obtaining a clear detection of GLUT7 on oocyte membrane samples could be explained by the fact that, in general, GLUT transporters are prone to aggregation. Although a treatment with detergent is performed on the membrane extract samples prior to protein analysis it is possible that the sample is not entirely digested and that the antibody binding site on the GLUT7 proteins is not fully accessible, causing not all the available protein to be detected. Another possibility

is that the unspecific binding sites are preferred by the antibody, decreasing the signal for GLUT7 even further. Nevertheless, the lower expression of this transporter on oocyte membranes, particularly when compared to other GLUTs and cell lysates, is the most likely cause of its weak detection.

A layer of follicular cells surrounds the oocytes, separating it from the external environment, has been reported to express ion channels as well as transporters (Miledi and Woodward, 1989a), (Miledi and Woodward, 1989b). Presence of this follicular cells interferes mostly with electrophysiological recordings, nevertheless, it is removed prior to microinjections by treatment with collagenase (Browne and Werner, 1984). This also facilitates the microinjection procedure by eliminating some of the resistance when piercing the oocyte cell membrane with the micropipette (Bianchi, 2006). Although unlikely, any remaining follicular cells present in the membrane extract samples could potentially lead to non-specific proteins being recognized by the GLUT7 antibody and contributing to the non-specific signal observed in these samples.

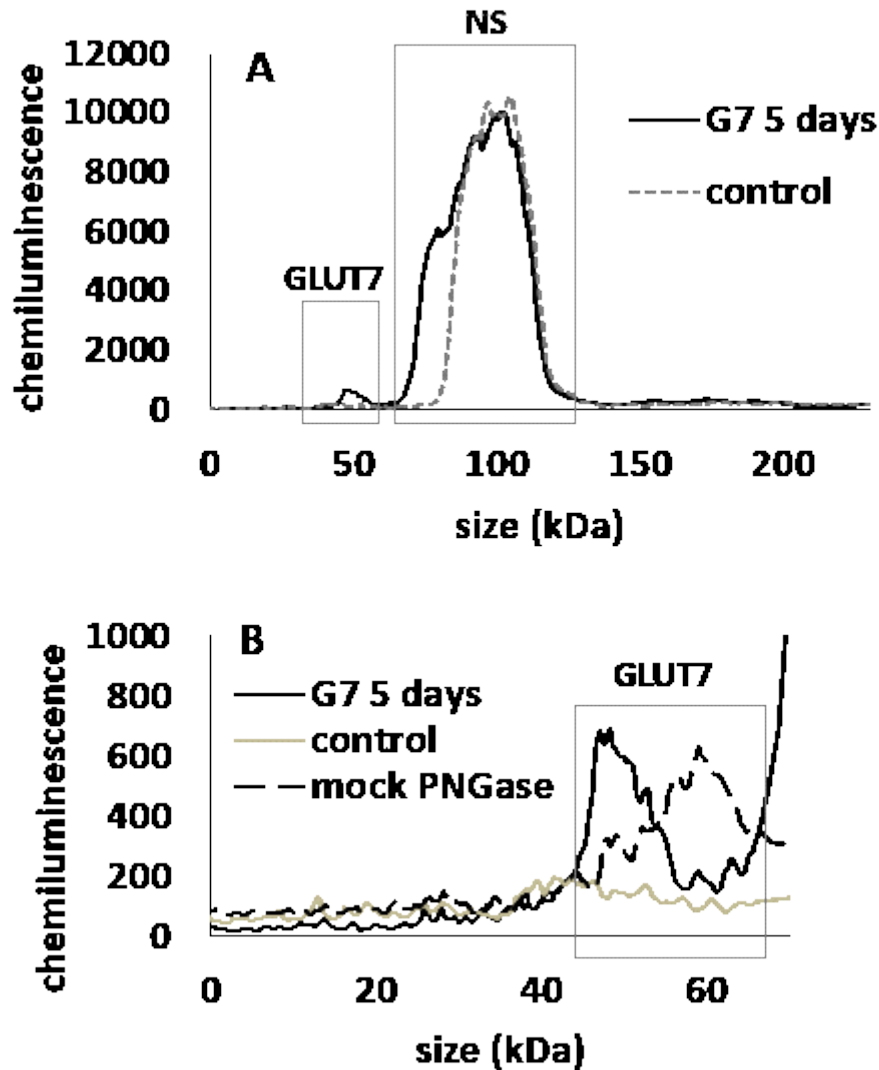


Figure 6-12 Confirmation of expression of GLUT7 on oocyte membranes. Membranes, extracted from ten oocytes five days post injection with GLUT7 mRNA, as well as water injected control membranes, were analysed using automated capillary Western blot (Wes). Electropherogram from analysis of membrane extracts of GLUT7 and control injected oocytes, displaying the antibody un-specific binding in relation to the GLUT7 signal (**A**). The same sample, isolated and magnified from original, compared to itself with (G7 5 days) and without (mock PNGase) PNGase digestion (**B**). The shift in size from untreated (59 kDa) to treated (48 kDa) confirms that this peak does in fact correspond to GLUT7 protein. Membrane extracts were un-diluted. Antibody dilution was 1:10.

6.5 Uptake experiment results and discussion

In order to attribute inhibition of GLUT7-mediated glucose/fructose transport by a specific compound or extract oocytes expressing this transporter were incubated in a sugar solution, containing ^{14}C -glucose/fructose, in the presence and absence of each compound/extract. Uptake inhibition experiments were conducted using two plant extracts and compounds also used in GLUT5 and GLUT2 uptake inhibition studies presented in the previous chapters (Chapter 4 and 5), with the aim to identify common inhibitors of all transporters. Furthermore, both plant extracts (German chamomile and green tea) were being used, or would in the future be used, in human studies conducted by other individuals in the research group (Villa-Rodriguez et al., 2017a), (Nyambe-Silavwe and Williamson, 2016). In other words, extract were chosen with the aim to validate results within the research group and to attribute inhibition to specific transporters. The pure compounds apigenin, EGCG and quercetin were also chosen to conduct concentration dependent GLUT7-mediated glucose and fructose uptake inhibition experiments for two of these compounds were shown to inhibit fructose uptake by GLUT5 (apigenin and EGCG, Chapter 4), and all three inhibited GLUT2-mediated glucose and fructose uptake (Chapter 5). Considering the research objective of investigating the inhibition profile of GLUT2, GLUT5 and GLUT7, and identifying novel inhibitors of these transporters, these compounds were thought to be good candidates. GLUT7 uptake inhibition studies were only conducted with the plant extracts and pure compounds mentioned above due to the amount of time required for oocyte microinjections and to perform inhibition studies. All extracts and compounds used in the uptake inhibition studies by GLUT7 described in this

chapter are listed in Table 6.1. Inhibition of GLUT7 fructose and glucose uptake was conducted with pure compounds as previously performed with GLUT2, which also transports both sugars (Chapter 5). Compounds used in concentration dependent GLUT7-mediated fructose and glucose uptake inhibition studies are marked in Table 6.1 with an asterisk.

Table 6-1 Compounds/extracts used in GLUT7-mediated glucose/fructose uptake inhibition studies described in this chapter

Compound/ extract	Inhibition of GLUT7 mediated sugar uptake
Apigenin *	Glucose and fructose
Cytochalasin B	Glucose
EGCG *	Glucose and fructose
German chamomile	Glucose
Green tea	Glucose
Phloretin	Glucose
Quercetin *	Glucose and fructose

* compounds for which a uptake inhibition experiments were carried out with two GLUT7 substrates.

6.5.1 Effect of extracts on glucose uptake by GLUT7

The effect of plant extracts on glucose uptake by GLUT7 was investigated by incubation of microinjected oocytes at 25 °C in a 0.1 mM glucose solution with radiolabelled glucose and increasing concentrations of a particular extract. Oocytes were microinjected with GLUT7 mRNA derived from either GLUT7pBF or GLUT7pGEM-HE in order to directly compare the quality of both mRNA products and their glucose uptake profiles. Presence of German chamomile or green tea extracts did not influence the uptake of glucose by GLUT7 in oocytes microinjected

with mRNA derived from GLUT7pBF (Figure 6.13 A and C) or GLUT7pGEM-HE (Figure 6.13 B and D).

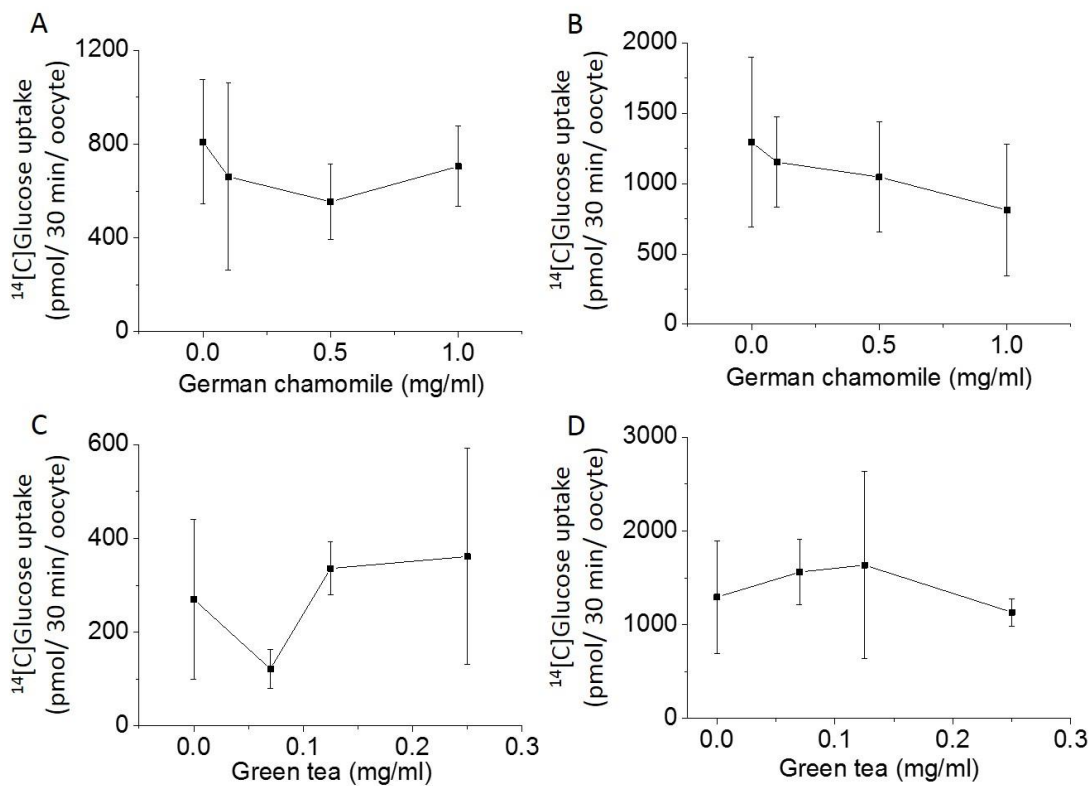


Figure 6-13 Effect of plant extracts on glucose uptake by GLUT7-expressing oocytes. Five days post GLUT7 mRNA microinjection oocytes were incubated in 0.1 mM glucose solution containing [¹⁴C] glucose for 30 min at 25 °C in the presence of increasing concentrations of German chamomile (0-1 mg/ml) (**A**, **B**) and green tea (0-0.25 mg/ml) (**C**, **D**) extracts. Neither German chamomile nor green tea extract had an impact on glucose uptake by oocytes microinjected with mRNA derived from GLUT7pBF plasmid (**A**, **B**) or GLUT7pGEM-HE plasmid (**C**, **D**). Each data point represents the mean of 6 replicates (of 3 oocytes), normalized to control for each condition, ± SEM.

Variation between replicates was again a substantial problem when it came to uptake experiments with GLUT7-expressing oocytes. This variability can be partially attributed to the biological differences in oocytes derived from different ovaries coming from varying females, as well as the previously discussed (refer to Chapter 4, section 4.5.1) seasonal component affecting the ability of oocytes to

express heterologous proteins (Delpire et al., 2011) (Conn, 1991). In addition, the quality of the mRNA microinjected into the oocytes may also contribute to the observed variability. As an example, GLUT7pBF plasmid produced two distinct mRNA products, and while only one could be translated into GLUT7 both contributed to the measurement of mRNA concentration. In other words, the precise amount of the translatable mRNA in the total mRNA sample was not determined and it is likely that only a fraction of the concentration of the total mRNA microinjected into oocytes corresponded to the translatable mRNA product. Furthermore, multiple products were also produced following IVT reaction with linear GLUT7pGEM-HE plasmid. Although this was highly likely leftover secondary structure it still represented a fraction of the overall mRNA concentration, meaning that less translational mRNA was injected into the oocytes, potentially leading to less protein expression on membrane of varying oocytes.

6.5.2 Effect of pure compounds on glucose and fructose uptake by GLUT7

The direct impact of pure compounds on glucose and fructose uptake by GLUT7 was measured using the same experimental conditions as for the extracts, namely oocytes were incubated in a 0.1 mM sugar solution for 30 min at 25 °C. Unlike previous uptake experiments with the GLUTs however, where 3 oocytes were homogenized together, here 10 oocytes were grouped and homogenized together in an effort to potentially decrease variability between replicates. Each data point represents the mean of 3 replicates \pm SEM. Oocytes were microinjected with either water, to serve as controls, or mRNA derived from GLUT7pGEM-HE plasmid. To

add to that, mRNA obtained from IVT reaction with GLUT7pBF plasmid linearized with either PmlI or MluI were used in oocyte microinjection, in order to rule out any potential mRNA quality differences products derived from DNA linearized with these enzymes. Uptake of glucose and fructose by GLUT7-expressing oocytes, by means of injection with all each individual mRNA product, was unchanged in the presence of 100 μ M quercetin (Figure 6.14 A and B). Similarly, there was no significant change in fructose uptake by GLUT7-expressing oocytes in the presence of 500 μ M EGCG (Figure 6.15 B). Interestingly, however, there was a significant change (46% reduction at 500 μ M, $p \leq 0.05$) observed in glucose uptake from oocytes microinjected with mRNA derived from IVT reaction or GLUT7pBF plasmid when it was linearized with MluI restriction enzyme (Figure 6.15 A). Only an uptake reduction trend was noted for the GLUT7-expressing oocytes by means of microinjection with the other two mRNA products; 39% reduction in uptake ($p = 0.06$) and 30% reduction in uptake ($p = 0.07$) for GLUT7pGEM-HE plasmid derived mRNA microinjected oocytes and oocytes injected with GLUT7pBF plasmid linearized with PmlI mRNA, respectively (Figure 6.15 A). Glucose transport by GLUT7-expressing oocytes was unaffected by the presence of 50 μ M apigenin (Figure 6.16 A). Nevertheless, there was a significant decrease in fructose transport by oocytes microinjected with mRNA derived from GLUT7pGEM-HE and oocytes injected with GLUT7pBF plasmid linearized with PmlI mRNA (53% and 45% reduction in uptake at 50 μ M for GLUT7pGEM-HE and GLUT7pBF mRNA injected oocytes, respectively, $p \leq 0.05$) (Figure 6.16 B). No significant change in fructose uptake by oocytes microinjected with mRNA derived from GLUT7pBF

plasmid linearized by MluI was observed. This was predominantly due to the large variability observed between the replicates for this particular sample and condition.

Additionally, a concentration dependent uptake experiment in the presence of apigenin was carried out with oocytes microinjected with mRNA derived from GLUT7pGEM-HE plasmid. Apigenin significantly, and concentration dependently, inhibited GLUT7-mediated fructose uptake ($IC_{50} = 16 \pm 12 \mu\text{M}$) (Figure 6.17 B). In this experiment, GLUT7-mediated glucose uptake was also significantly inhibited by apigenin, at its highest concentration ($IC_{50} = 38 \pm 2 \mu\text{M}$) (Figure 6.17 A). Differences in protein expression, brought about by biological variations between oocytes, and affinity of GLUT7 for glucose and fructose could help explain why fructose uptake by this protein was more prominently affected in the presence of apigenin. Similar experiments with GLUT2-expressing oocytes have observed significant differences in inhibition of glucose and fructose uptake with the same inhibitor (Kwon et al., 2007). For instance, the quercetin precursors isoquercitrin and spiraeoside were almost twice as effective at inhibiting GLUT2-mediated fructose uptake when compared to glucose uptake. To add to that, quercetin and phloretin almost completely inhibited GLUT2-mediated glucose uptake, being not as potent inhibitors of fructose uptake by this same transporter (Kwon et al., 2007). Uptake experiments in cells overexpressing GLUT7 could help determine if higher levels of protein expression are needed in order for an inhibition of glucose uptake by apigenin to be detectable.

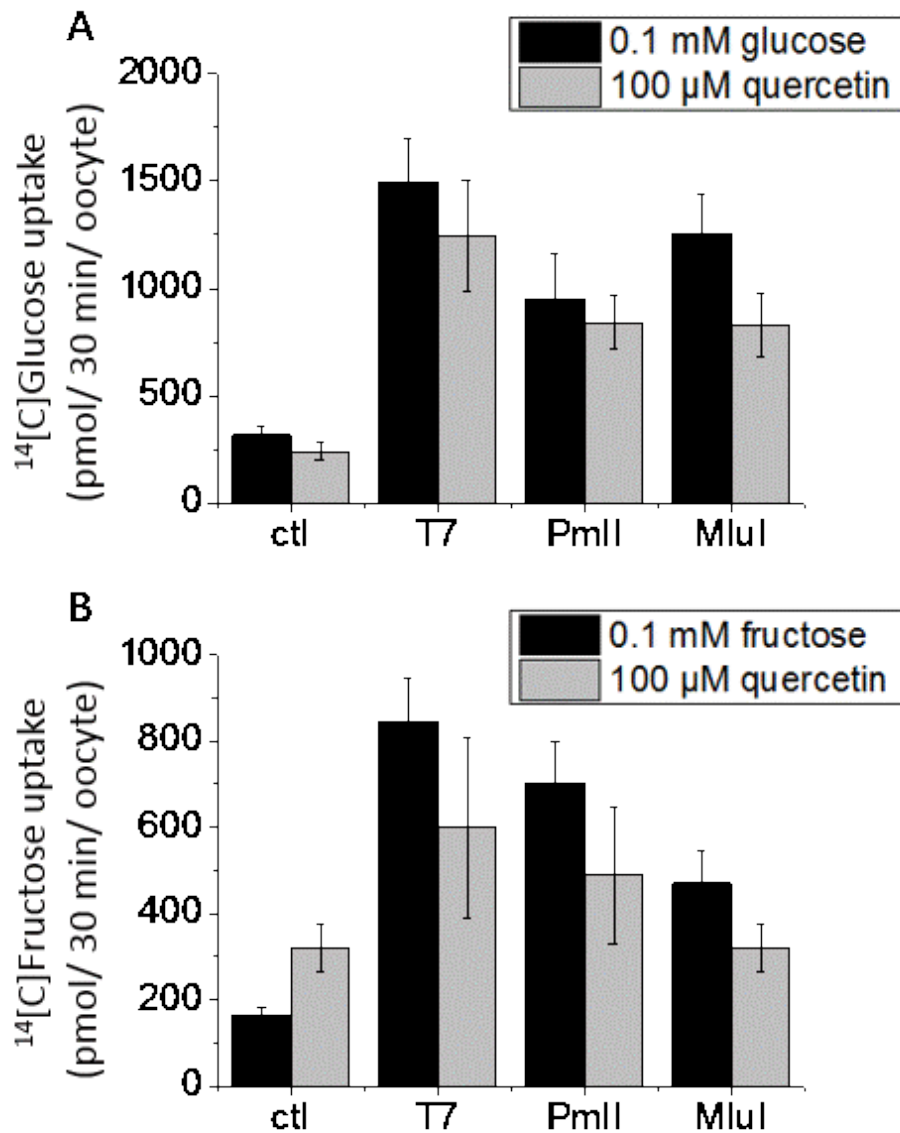


Figure 6-14 Effect of quercetin on sugar uptake by GLUT7-expressing oocytes. Five days post GLUT7 mRNA microinjection oocytes were incubated in 0.1 mM glucose/fructose solution containing the corresponding [¹⁴C] sugar for 30 min in the presence of 100 μM quercetin. Internalized sugar uptake was determined by scintillation spectrometry for protein expressing oocytes and control oocytes in sugar solution only (black bars) and in the presence of 100 μM quercetin (grey bars). Quercetin did not have an effect on either glucose uptake (**A**) or fructose uptake (**B**) by oocytes microinjected with mRNA derived from GLUT7pGEM-HE plasmid (T7) or mRNA derived from GLUT7pBF plasmid following linearization with PmlI or MluI restriction enzymes. Each data point represents the mean of 3 replicates (of 10 oocytes) ± SEM.

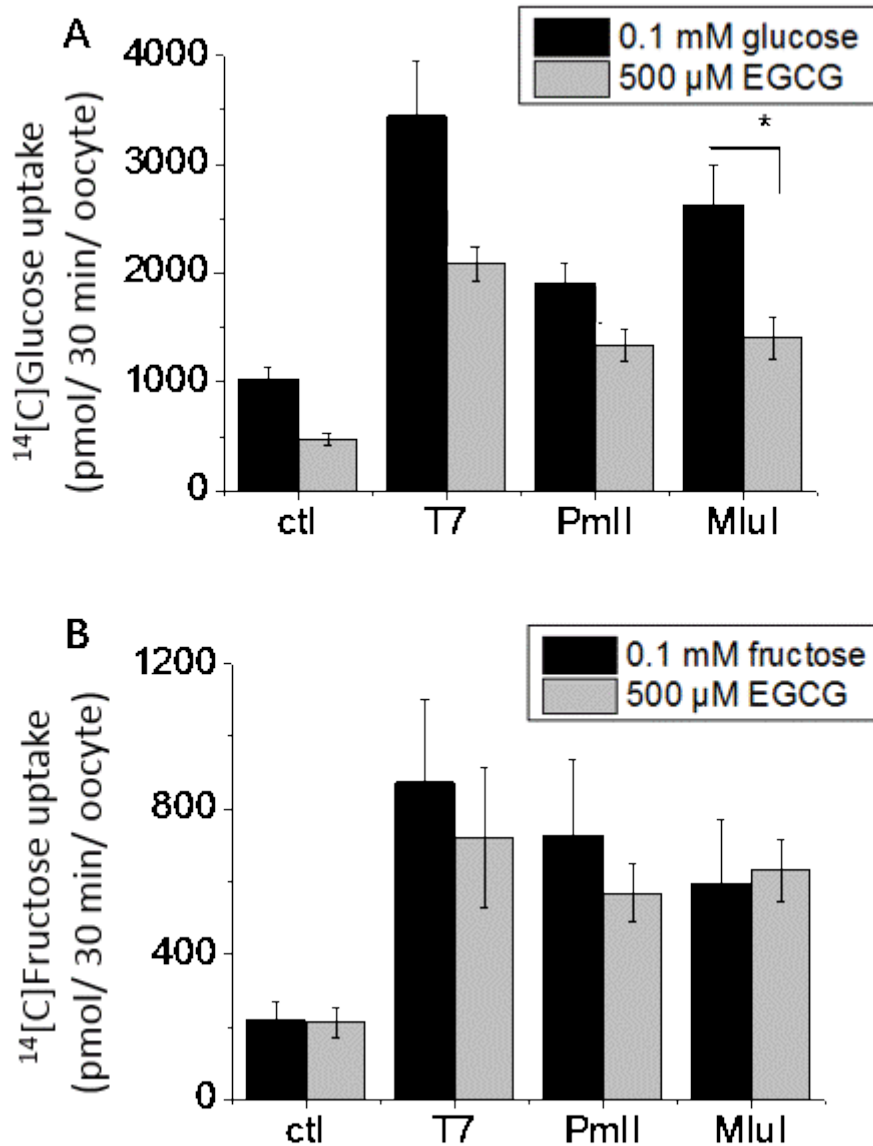


Figure 6-15 Effect of EGCG on sugar uptake by GLUT7-expressing oocytes. Five days post GLUT7 mRNA microinjection oocytes were incubated in 0.1 mM glucose/fructose solution containing the corresponding [¹⁴C] sugar for 30 min in the presence of 500 μM EGCG. Internalized sugar uptake was determined by scintillation spectrometry for protein expressing oocytes and control oocytes in sugar solution only (black bars) and in the presence of 500 μM EGCG (grey bars). EGCG significantly inhibited glucose uptake by oocytes microinjected with mRNA derived from GLUT7pBF linearized with MluI (46% reduction at 500 μM, $p \leq 0.05$) and an inhibition ‘trend’ was observed for the other mRNA samples (**A**). EGCG had no effect on fructose uptake by oocytes microinjected with mRNA derived from GLUT7pGEM-HE plasmid (T7) or mRNA derived from GLUT7pBF plasmid following linearization with PmlI or MluI restriction enzymes (**B**). Each data point represents the mean of 3 replicates (of 10 oocytes) \pm SEM. * $p \leq 0.05$

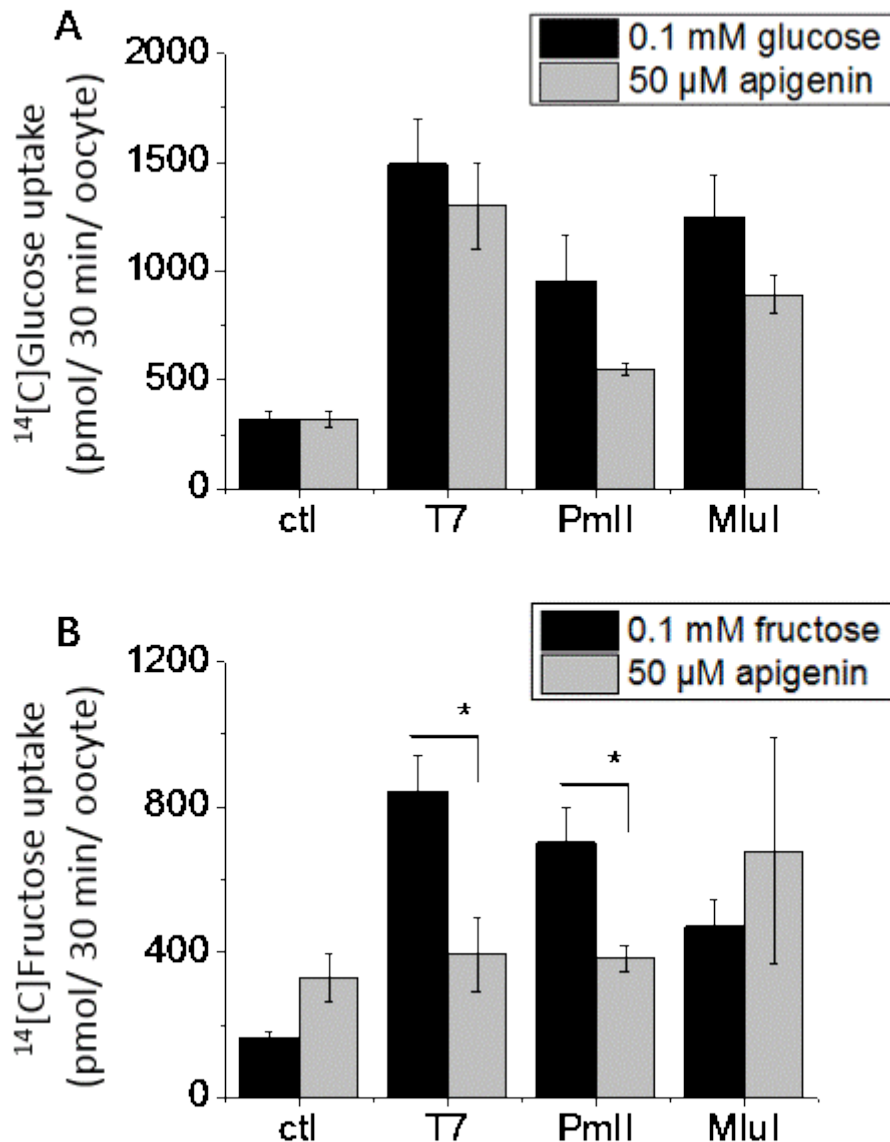


Figure 6-16 Effect of apigenin on sugar uptake by GLUT7-expressing oocytes. Five days post GLUT7 mRNA microinjection oocytes were incubated in 0.1 mM glucose/fructose solution containing the corresponding [¹⁴C] sugar for 30 min in the presence of 50 μM apigenin. Internalized sugar uptake was determined by scintillation spectrometry for protein expressing oocytes and control oocytes in sugar solution only (black bars) and in the presence of 50 μM apigenin (grey bars). Apigenin did not have an effect on glucose uptake or by oocytes microinjected with mRNA derived from GLUT7pGEM-HE plasmid (T7) or mRNA derived from GLUT7pBF plasmid following linearization with PmlI or MluI restriction enzymes (**A**). Apigenin significantly inhibited fructose uptake by oocytes microinjected with mRNA derived from GLUT7pGEM-HE (53% reduction in uptake at 50 μM) and oocytes injected with GLUT7pBF plasmid linearized with PmlI mRNA (45% reduction in uptake at 50 μM) (**B**). Each data point represents the mean of 3 replicates (of 10 oocytes) ± SEM. * $p \leq 0.05$

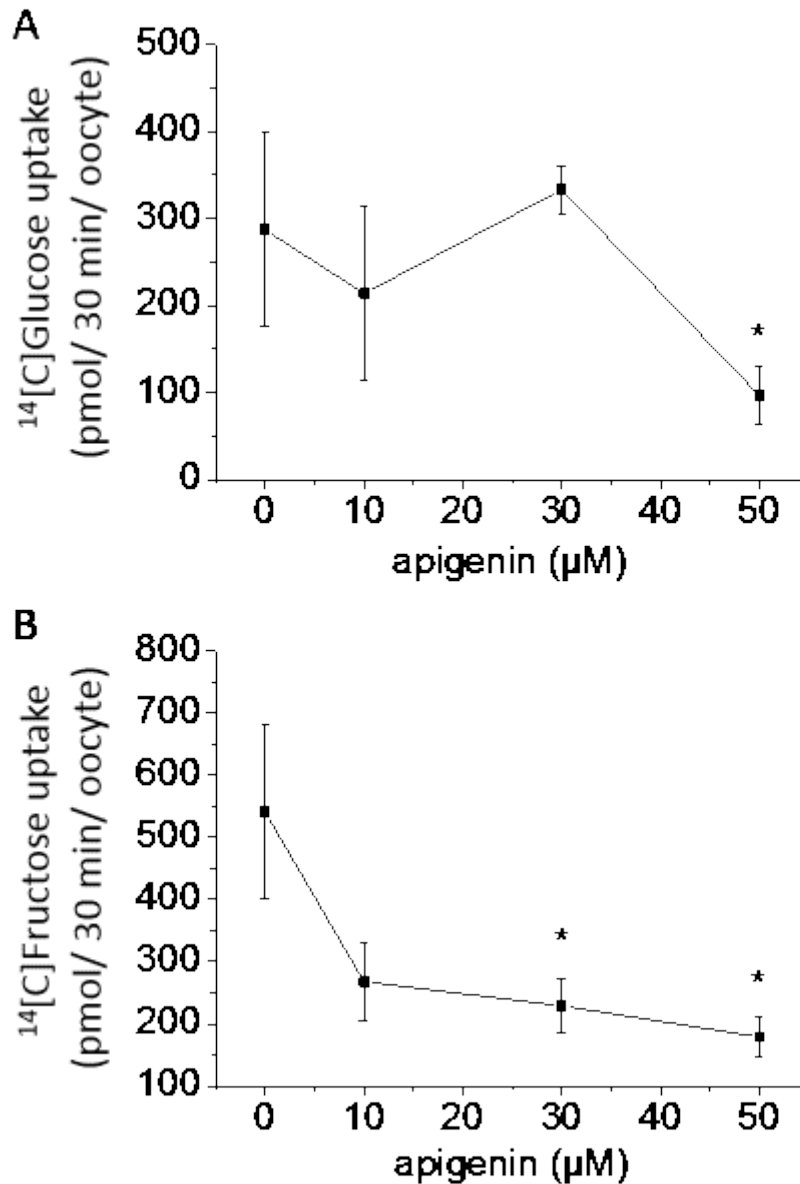


Figure 6-17 Effect of apigenin on sugar uptake by GLUT7-expressing oocytes. Five days post GLUT7 mRNA microinjection oocytes were incubated in 0.1 mM glucose/fructose solution containing the corresponding [^{14}C] sugar for 30 min in the presence of increasing concentrations of apigenin (0-50 μM). Apigenin significantly inhibited glucose uptake (66% inhibition at 50 μM) (**A**) and fructose uptake ($\text{IC}_{50} = 29 \pm 10 \mu\text{M}$) (**B**) by oocytes microinjected with mRNA derived from GLUT7pGEM-HE. Each data point represents the mean of 3 (**A**) or 6 replicates (**B**) (of 10 oocytes), normalized to control for each condition, \pm SEM. * $p \leq 0.05$

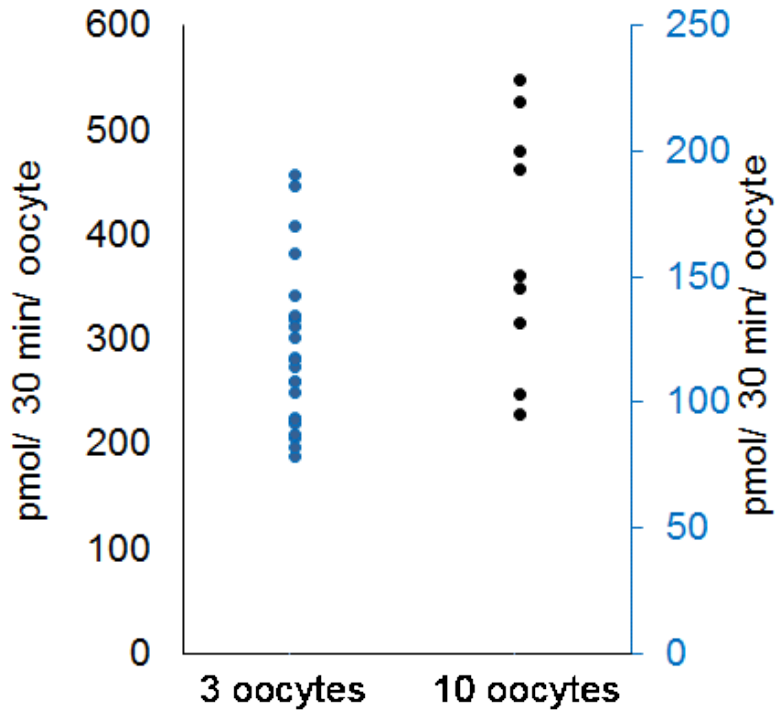


Figure 6-18 Dot plot representing values for uptake by control oocytes in single uptake experiments with 3 and 10 oocytes. This figure represents the uptake by water injected control oocytes after incubation in [¹⁴C] sugar, for 30 min, in the absence of any (poly)phenol or extract. Each individual dot represents one replicate. Uptake by samples containing 10 oocytes homogenized together was higher than that observed by samples of 3 oocytes only, as expected. Variation in uptake is similar for both groups.

A dot plot of the specific uptake by water-injected control oocytes in single sugar uptake experiments with 3 and 10 oocytes, in the absence of any (poly)phenol or extracts, is shown in Figure 6.18 above. Sugar uptake by individual samples containing 10 oocytes homogenized together was higher than that observed by samples of 3 oocytes only, as expected. Some biological variation is observed, however, this is relatively comparable between the two groups. It can be concluded, therefore, that the variation is an attribute of varying levels protein expression in the oocytes.

6.5.3 Summary of results from glucose and fructose uptake experiments

The results presented here show that GLUT7, when expressed in oocytes, is able to transport both glucose and fructose. This goes against previous findings by Ebert et al., where sugar uptake by oocytes expressing GLUT7 was not detected (Ebert et al., 2017). Nevertheless, experiments executed by this group were performed using oocytes microinjected with less GLUT7 mRNA (13.8 ng as opposed to 50 ng microinjected into oocytes used in the experiments above) and with a shorter expression period post-microinjection, namely, 4 days. To add to that, oocytes were incubated in a sugar solution of higher concentration (1 mM) for a shorter period of time of 10 min only. Other differences between experiment protocols include digested oocyte storage conditions, radiolabelled substrate concentration, and wash solution. Furthermore, non-injected oocytes, instead of water injected oocytes, were used as controls in experiments performed by this group, which does not properly control for the microinjection procedure itself and the oocyte pigmented ring scar caused by the micropipette prick (O'Connell et al., 2011). The quality of the oocytes could also have affected membrane protein expression, a problem which was faced when expressing the GLUTs during this project as well. An investigation of husbandry facilities by Delpire et al found that animals kept in static water facilities, as opposed to recirculating water facilities, led to a much more robust and reproducible expression of the heterologously expressed transporter of interest. In addition, oocytes isolated from females kept in recirculating facilities showed a significant deterioration during the summer months (April to August) (Delpire et al., 2011), an issue previously reported by

other researchers (Conn, 1991). To add to this, once the oocytes are extracted from the ovary they are susceptible to microbial contaminations, leading to black foci on the oocyte animal pole and deterioration in the health of the oocyte (O'Connell et al., 2011). This group found that bacteria, which become associated with oocytes are susceptible to amikacin and ciprofloxacin, which should be added to oocyte storage solution to avoid contamination of oocytes (O'Connell et al., 2011). Oocytes used for the experiments presented in this chapter were obtained by extraction from ovaries of females kept in a recirculating facility (European Xenopus Resource Centre, University of Portsmouth, UK), which most likely played a role in the variability seen between individual experiments, based on the observations discussed above. Moreover, oocyte storage solution contained amikacin and ciprofloxacin, however, contaminations did occasionally occur, in which case oocytes were not used for experiments and disposed of. Oocytes at stage V-VI of development were visually selected for uptake experiments as endogenous transporter activity is not only variable between batches of oocytes but in oocytes of different developmental stages. This has a particular impact on membrane permeability, intracellular ion concentrations and surface pattern of extracellular currents (Miller and Zhou, 2000). Nonetheless, as the method of selection is purely visual it is possible that oocytes in transition to or from stage V-VI were selected for uptake experiments, adding another factor that could contribute to variability between experiments. This again highlights the importance of a control from the same batch of eggs injected with a similar volume of water.

The concluding findings that GLUT7 does in fact transport glucose and fructose corroborated previous observations by Li et al, where GLUT7 microinjected oocytes were incubated at similar conditions to those applied to uptake experiments presented in this chapter, namely oocytes were incubated in 0.1 mM sugar solution for 30 min 5 days post-microinjections (Li et al., 2004). Furthermore, the determinations that GLUT7 is not inhibited by either phloretin or cytochalasin B, and that glucose uptake by the transporter is significantly inhibited in the presence of fructose are in agreement with previous observations by the same group (Li et al., 2004). By confirming that fructose is in fact transported by GLUT7 these results also fit with the hypothesis that a conserved isoleucine-containing motif present in GLUTs 2, 5 and 7 may be essential for the transport of fructose (Manolescu et al., 2005).

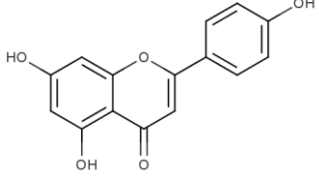
Detection of GLUT7 protein on oocyte membrane samples was only achieved in samples microinjected with mRNA derived from GLUT7pGEM-HE plasmid. Nevertheless, non-specific binding signal was high in both mRNA injected and water injected oocyte membrane samples. This suggests that the antibody used for protein detection recognises a particular protein(s) present in the oocyte membrane. It is also possible that this unspecific binding site is preferred by the antibody, meaning that effectively less GLUT7 than is available is detected. In other words, the antibody is 'used up' by the non-specific band. In addition, as GLUT transporters are prone to aggregation, the binding site of the antibody on GLUT7 could have not been fully accessible. These observations could explain why no GLUT7 was detected in oocyte membrane samples following microinjection with

GLUT7pBF plasmid derived mRNA. Nonetheless, the lower expression of this protein when expressed on oocytes membranes, particularly when compared to the other GLUTs, is likely to be the main cause of limited protein detection.

A novel finding from the GLUT7 uptake experiments in the presence of individual compounds was that apigenin significantly inhibited the uptake of fructose ($IC_{50} = 16 \pm 12 \mu\text{M}$) and glucose ($IC_{50} = 38 \pm 2 \mu\text{M}$) by this transporter. The structure of this compound is shown in Table 6.2. Initially, a reduction in GLUT7-mediated uptake was only observed for fructose, and not for glucose. Moreover, although there was a decrease in GLUT7-mediated glucose uptake by oocytes microinjected with PmlI linearized GLUT7pBF plasmid derived mRNA, this was not significant. In a subsequent concentration dependent uptake experiment, however, there was a significant decrease in glucose uptake by GLUT7 following oocyte microinjection with mRNA derived from GLUT7pGEM-HE plasmid. This occurrence could be explained by differences in protein expression, attributed to biological variations between oocytes, as well as the affinity of GLUT7 for glucose and fructose. The pure compound EGCG also demonstrated potential as an inhibitor of glucose uptake by GLUT7. Presence of quercetin had no impact on either glucose or fructose uptake by GLUT7. Although apigenin did not significantly inhibit fructose uptake by GLUT7-expressing oocytes following microinjection with MluI linearized GLUT7pBF plasmid derived mRNA, this was due to the high variability between the experimental replicates. In the same way, when microinjected with this same mRNA, oocytes incubated in the presence of EGCG demonstrated a significantly reduced uptake of glucose ($p \leq 0.05$), while only a trend ($p = 0.06$) was observed

for the other two mRNA products. Even though sugar uptake confirms GLUT7 expression on oocyte membranes following GLUT7pBF plasmid derived mRNA microinjection, regardless of which restriction enzyme was used in the linearization step, protein was not detectable by automated Western blotting (Wes). For this reason, the overall conclusions of the effect of pure compounds on GLUT7 sugar uptake were a consequence of the analysis of results obtained from oocytes microinjected with mRNA derived from GLUT7pGEM-HE plasmid. The plant extracts German chamomile and green tea did not have any effect on glucose uptake by GLUT7-expressing oocytes, although these experiments had a high variability between replicates which could have masked an inhibition by these extracts. Overall it can be concluded that the GLUT7 in *X. laevis* oocytes expression model was successful at determining the sugar transport capability of this protein as well as a novel inhibitor. The structure of apigenin could be considered in conjunction with sequence alignment results and point mutation studies for the further characterization of this transporter in terms of substrate-protein interactions and substrate binding.

Table 6-2 Structure of apigenin and its inhibition of GLUT7 sugar uptake

Compound	Substrate	Inhibition	Structure
Apigenin	Glucose and fructose	IC _{50G} = 38 ± 2 μM IC _{50F} = 16 ± 12 μM	

Chapter 7

Summary discussion, future perspectives and conclusions

7.1 Research rationale and objectives

7.1.1 The role of (poly)phenols in CVD and T2DM prevention

CVD is the number one cause of death worldwide, with coronary heart disease (CHD) alone being responsible for over 1 million deaths annually within the European Union (Nichols et al., 2014). Nonetheless, the rates of CVD progression in many developed European countries, including the UK, are in decline (Gale et al., 2012), (Threapleton et al., 2013). This reduction in CVD has been attributed to improvements in risk factors for CVD, particularly by means of lifestyle changes (Unal et al., 2004), (Jennings et al., 2009). One of the main risk factors associated with CVD is diabetes, with diabetic patients being classed as at high risk of CVD regardless of other potential risk factors (Jennings et al., 2009). Nearly 5% of the world's population is affected by diabetes, with T2DM accounting for 90-95% of cases worldwide (Hajjaghaalipour et al., 2015). According to the World Health Organisation's projections the number of people suffering from diabetes will reach more than 300 million by 2025 (Fayaz and Suvanish Kumar, 2014). Lifestyle intervention, risk factor management and cardioprotective drugs are able to significantly reduce morbidity and mortality in patients with established CVD and those at high risk of developing disease (Wood et al., 2008), (Jennings et al., 2009).

Nevertheless, pharmaceutical drugs used in the treatment of diabetes in many countries worldwide, such as acarbose and metformin, are commonly accompanied by side effects and discomfort, such as nausea, flatulence and diarrhoea (Chiasson, 2006), (Coniff et al., 1995), (Holman, 2007). Although the clinical benefits of metformin were confirmed in clinical trials, such as the UK Prospective Diabetes Study, up to 25% of patients suffered from metformin-associated gastrointestinal side effects, with approximately 5% not being able to tolerate the drug (McCreight et al., 2016), (Dujic et al., 2015). This has contributed to a rise in use of herbal medicine in the treatment of diseases in recent years, particularly due to their natural origin and reduced side effects (Modak et al., 2007). Dietary intake of (poly)phenols is estimated to be of ~ 1 g/day per person, with many of these compounds having a positive effect on reduction of disease risk factors associated with CVD and diabetes, as previously described in Chapter 1 (de Bock et al., 2012), (Lim et al., 2010). For instance, administration of green tea significantly reduced blood pressure after a three week period (Nantz et al., 2009), with a reduction in LDL-cholesterol also being attributed to compounds in this beverage (Maron et al., 2003). In addition, total and LDL-cholesterol were decreased after consumption of a controlled diet with black tea (Davies et al., 2003). Coffee has also been linked to T2DM reduction, possibly due to LDL-cholesterol and fasting glycaemia lowering properties (van Dam and Feskens, 2002), (Pimentel et al., 2009), (Manach et al., 2004). Furthermore, cocoa (poly)phenols have been shown to increase HDL-cholesterol, decrease blood pressure, as well as reduce relative risk of CVD (Buijsse et al., 2010), (Mellor et al., 2010).

7.1.2 Effect of (poly)phenols on carbohydrate uptake and digestion

Many (poly)phenols have been shown to have an effect on sugar digestion, as well as uptake and post-prandial distribution of glucose and fructose, as previously discussed in Chapter 1. For instance, (poly)phenol consumption has been shown to have a positive impact on glycaemic control in several meta-analysis studies, (Liu et al., 2014), (Hooper et al., 2012), (Zheng et al., 2013), (Shrime et al., 2011), (Palma-Duran et al., 2017), (Muraki et al., 2013). Furthermore, compounds present in green tea, strawberry, raspberry, blueberry and blackcurrant have been shown to be potent inhibitors of α -amylase and α -glucosidase (McDougall et al., 2005), (Nyambe-Silavwe et al., 2015). These enzymes, responsible for sugar production, are also the target of the anti-diabetic drug acarbose, meaning that a long-term consumption of (poly)phenols could have a comparable effect to this drug on reducing diabetes risk (Williamson, 2013). To add to that, certain compounds, such as quercetin, have been shown to lower glucose absorption by inhibiting GLUT2-mediated glucose uptake, in cell and oocyte models (Kwon et al., 2007), (Johnston et al., 2005). Expression of the facilitative sugar transporters GLUT2 and GLUT5 is elevated in the diabetic state, meaning that sugar metabolism is permanently increased in diabetic patients (Legeza et al., 2014), (Cohen et al., 2014). For this reason these transporters are possible targets for slowing down the rate of sugar absorption in the gut, and its associated responses (Williamson, 2013). *In vivo*, a (poly)phenol-rich intervention, with compounds that inhibit digestive enzymes and sugar transporters, was shown to have an impact on postprandial blood glucose by significantly reducing the area under the curve (Nyambe-Silavwe and Williamson, 2016). In this project, direct inhibition of transporters expressed in the gut, able to transport fructose, by specific (poly)phenols was investigated. This

research aspired to identify specific compounds or extracts that could potentially be added to interventions aimed at improving health markers, control of fructose uptake and post-prandial distribution of sugars in both healthy volunteers and patients with CVD or diabetes.

7.2 Discussion of research outcomes and novelty of findings

7.2.1 Characterization of hGLUT7

Expression of both GLUT2 and GLUT5 has been shown to be increased in the presence of glucose and fructose, respectively (Legeza et al., 2014), (Cohen et al., 2014), suggesting that expression of sugar transporters could be modulated by sugars. Glucose and fructose uptake by heterologously expressed GLUT7 in the *X. laevis* oocyte model has been previously observed (Li et al., 2004), and confirmed in this study through expression of GLUT7 mRNA derived from two distinct plasmids (Chapter 6). As fructose was identified as a substrate for this protein the effects of this sugar on the expression of GLUT7 was investigated in this project. There was a significant increase in mRNA and total protein expression when cells were grown in media supplemented with fructose, compared to glucose only. Nevertheless, increase in GLUT7 protein expression was more extreme than changes in mRNA levels. This suggests that perhaps the increase in protein expression is not a direct effect of the marginally elevated GLUT7 mRNA levels, but rather, due to post-translational modifications (PTMs). Chemical modifications brought about by PTMs may impact localization and activity of proteins, as well as their interactions with other cellular molecules (Lodish et al., 2008). There are over

300 different types of PTMs known, some occurring shortly after translation and impacting protein folding and stability, while others take place after folding and localization, thereby affecting the biological activity of the protein (Jensen, 2004). The dynamic activity of the human proteome in response to different stimuli is commonly mediated through PTMs, which aim at cellular activity regulation (Lodish et al., 2008), (IHGSC, 2004). Glycosylation, or the attachment of sugar moieties to proteins, is a PTM that can affect protein-protein interactions, due to the increase in size and 'bulkiness' of the protein, by facilitating or preventing protein binding to similar interaction domains (Rudd and Dwek, 1997). Changes in protein solubility are also correlated to glycosylation (Jensen, 2004). In the endoplasmic reticulum (ER), protein glycosylation ensures that only properly folded proteins are trafficked to the Golgi, serving as a quality control for the protein folding process (Wormald et al., 2002). Therefore, it is possible that in the presence of fructose, more GLUT7 protein is glycosylated, and hence, transported to the Golgi for secretion into the cytoplasm (Lodish et al., 2008). Another possibility is that GLUT7, stored in vesicles responsible for transport of proteins between the Golgi compartments, is more readily released in the presence of fructose, leading to higher expression levels of this protein being detected (Nelson and Cox, 2008), (Cooper, 2000). One of the most common types of glycosylation is N-glycosylation, where the glycan is attached to the carboxamido nitrogen on asparagine residues (Trombetta, 2003). GLUT7 protein, expressed in the oocytes and Caco-2/TC7 cell models, is N-glycosylated, as determined by a shift in size following treatment with the peptide:N-glycosidase (PNGase) F (Chapters 3 and 6). The interaction of lectins, glycan-binding proteins, with glycosylated proteins are a commonly used tool for glycoprotein identification and purification (Varki et al., 2009). To add to that, the

isotope-coded glycosylation-site-specific tagging (IGOT) technique, which is based on lectin column-mediated affinity binding with glycoproteins followed by specific incorporation of a stable isotope tag into the N-glycosylation site, allows for peptide identification by LC-MS. Differences in the absolute amounts of glycosylated GLUT7 following treatment with and without fructose, using imaging or LC-MS techniques, would help to further characterize the role that this sugar plays in the regulation of fructose uptake.

7.2.2 Sugar uptake experiments

Uptake of sugar by heterologously-expressed human proteins was successfully observed using the *X. laevis* oocyte model. This expression model targeted each individual GLUT transporter on their own, allowing for a precise characterization of inhibitors for each transporter. Biological variation between oocytes was expected, and changes in level of protein expression by this model are likely to be attributed to the seasonal variations and husbandry facilities, as discussed previously in Chapters 4-6 (Delpire et al., 2011), (Conn, 1991), (Miller and Zhou, 2000). Fructose-specific transporter, GLUT5 was significantly inhibited in the presence of sugar analogue inhibitors L-sorbose-Bn-OZO and 2,5-anhydro-D-mannitol, as expected (Girniene et al., 2003), (Yang et al., 2002), (Tatibouet et al., 2000). Inhibition of fructose uptake by this transporter was also achieved in the presence of EGCG, as previously reported (Slavic et al., 2009). In addition, through the expression model created and used for uptake experiments in this project, novel GLUT5 inhibitors were determined, namely, apigenin, hesperetin, and its glycoside

hesperidin. Sugar-free pomegranate and German chamomile plant extracts also significantly inhibited GLUT5-mediated fructose uptake in this model (Chapter 4).

Confirmation of hGLUT2 expression model functionality was achieved through observed inhibition of this transporter in the presence of known inhibitors phloretin, quercetin and cytochalasin B (Kwon et al., 2007), (Song et al., 2002), (Jung and Rampal, 1977), (Krupka, 1985). Using the oocyte expression model, novel inhibitors of GLUT2-mediated glucose uptake, in the form of plant extracts and pure compounds, were also determined. Inhibitors of GLUT2-mediated glucose uptake are as follows; German chamomile, green tea, sugar-free pomegranate, and oleuropein-rich (Bonolive) extracts, as well as pure compounds hesperetin and hesperidin. Furthermore, glucose and fructose uptake by this transporter was shown to be significantly inhibited in the presence of apigenin, EGCG and quercetin (Chapter 5).

Expression of hGLUT7 in oocytes has previously produced controversial results, with some groups being able to identify uptake of glucose and fructose by this transporter, while others observed no sugar uptake (Li et al., 2004), (Ebert et al., 2017). To date, there have been no reports of specific inhibitors of this proteins. In this project, uptake of fructose and glucose by hGLUT7 expressed in oocytes was observed with mRNA derived from two independent plasmid constructs. Furthermore, neither phloretin nor cytochalasin B were shown to inhibit GLUT7 sugar uptake, however, a competitive inhibition of glucose uptake by this transporter was associated with presence of fructose, as previously reported (Li et

al., 2004). In this project, an inhibition trend of GLUT7-glucose mediated uptake was observed in the presence of EGCG. Moreover, apigenin, at high concentrations, significantly decreased the uptake of fructose by GLUT7. These observations were comparable for the two individual hGLUT7 expression models, derived from microinjections with mRNA obtained from two separate hGLUT7-containing plasmids, used in the uptake experiments (Chapter 6). The observation that GLUT7 is able to transport fructose is in agreement with the hypothesis that a conserved isoleucine-containing motif in the sequence of GLUTs 2, 5 and 7 is responsible for the transport of this sugar (Manolescu et al., 2005). GLUT5 inhibition by the compounds identified in this research project are likely to act by competitive inhibition, through binding to the active site and/or binding-site cleft, where bulkier groups are able to bind and potentially lead to a stronger inhibition of this protein (Yang et al., 2002), (Girniene et al., 2003). Molecular docking analysis of well characterized GLUT2 inhibitors have shown that while phloretin binds extracellularly to this protein, where glucose also binds, cytochalasin B binds to an intracellular binding site (Salas-Burgos et al., 2004). Furthermore, reported K_M values for uptake of sugars by GLUT2 in the presence and absence of quercetin suggests that binding site for sugar and this compound are different (Kwon et al., 2007). A comparison of inhibition profiles, obtained from analysis of sugar uptake in the presence of different concentrations of these well-established inhibitors, could help identify the specific binding site of (poly)phenols and plant extracts shown to significantly inhibit sugar uptake by GLUT2 and GLUT5. In addition, a linear-regression analysis of data from uptake experiments with varying concentrations of sugars, as well as (poly)phenols, could help confirm the hypothesis that these compounds and extracts exert their effects through

competitive inhibition of these transporters. This would, of course, require optimization of uptake experiments as too high a sugar concentration might not lead to any inhibition being detected, as was the case for GLUT5 inhibition experiments with high fructose concentrations (refer to Chapter 4). Moreover, structure based molecular docking and molecular dynamics studies could also help identify the type of inhibition exerted by compounds tested in this research, as well as determine the stability of their interactions with the transporters (Garcia-Mora et al., 2017). Nevertheless, this would require a precise structure of the GLUT transporters to be identified, an extremely challenging task for membrane-bound proteins due to their flexibility, lack of stability and partially hydrophobic surfaces (Carpenter et al., 2008). Development of a photoaffinity probes for the systems of interaction between the GLUT transporters and their inhibitors, identified in this research, would also help to establish the molecular interactions of the compounds with the transporters (Smith and Collins, 2015), (Tatibouet et al., 2000). Moreover, probing of the structure and steric factors that manage the interactions of glucose and fructose with GLUT7 would provide invaluable information about the binding potential of these sugars, and offer a stepping stone for the development/discovery of new inhibitors of this transporter (Smith and Collins, 2015). The pure compounds apigenin, quercetin and EGCG were used in sugar uptake inhibition studies on GLUT2, GLUT5 and GLUT7. In addition, these three compounds were used in experiments with two substrates of GLUT2 and GLUT7, namely fructose and glucose. Table 7.1 summarizes the results of the sugar uptake inhibition studies conducted with these compounds on all three GLUTs. Uptake experiments carried out in Chapters 4 and 5 identified that fructose uptake by GLUT2 and GLUT5 was significantly inhibited by apigenin, EGCG, hesperidin, German chamomile extract,

and sugar-free pomegranate extract. Apigenin also significantly inhibited fructose uptake by GLUT7 (Chapter 6). The potential of an additive inhibition induced by these compounds could be identified through co-expression of proteins in the *X. laevis* oocyte model. Further investigations of the impact of these compounds and extracts using other models, including *in vivo* work, would help determine their direct impact on the responses associated with sugar absorption.

Table 7-1 Summary of inhibition of GLUT2-, GLUT5- and GLUT7-mediated sugar uptake by pure compounds apigenin, quercetin and EGCG

	GLUT2		GLUT5	GLUT7	
	glucose	fructose	fructose	glucose	fructose
Apigenin (μM)	27 \pm 4	28 \pm 10	40 \pm 4	38 \pm 2	16 \pm 12
Quercetin (μM)	7 \pm 1	8 \pm 2	NI	NI	NI
EGCG (μM)	72 \pm 13	93 \pm 16	72 \pm 13	NI	NI

* NI = no inhibition

The flavonoids listed in Table 7.1 above, investigated for their inhibitory potential on GLUT2, 5 and 7- mediated sugar uptake in this project, have been previously reported to have an inhibitory impact on other sugar transporters as well, with EGCG inhibiting GLUT1 and SGLT1 (Slavic et al., 2009), (Johnston et al., 2005) and apigenin downregulating GLUT1 mRNA and protein expression (Melstrom et al., 2008). Quercetin has been shown to inhibit GLUT1 sugar transport as well as insulin-mediated GLUT4 translocation in adipocytes (Xu et al., 2014), (Strobel et al., 2005), which like GLUT2, belong to class 1 in the GLUT classification (Mueckler

and Thorens, 2013). Together with the data presented here this suggests that flavonoids have the potential to be used as inhibitors of multiple GLUT transporters. The interaction of flavonoids with GLUTs is likely exerted through binding on a site that differs from the binding site of the sugar, and inhibitory potential could be additionally linked with the sequence similarities between GLUTs. For instance, quercetin has been shown to inhibit GLUTs 1, 2 and 4 (Xu et al., 2014), (Kwon et al., 2007), (Strobel et al., 2005), all of which belong to class 1. Furthermore, it was concluded from sugar uptake experiments presented in Chapter 6 that GLUT7 is able to transport both glucose and fructose, supporting the hypothesis that an isoleucine-containing motif present in GLUTs 2, 5 and 7 could be essential to fructose transport (Manolescu et al., 2005). Considering GLUT protein sequence may dictate which substrates are recognized by GLUT transporters, it could also be important in the potential binding and inhibitory effects of flavonoids.

7.3 Future research perspectives

7.3.1 Cell culture studies

Inhibition of GLUT2 and GLUT5-mediated sugar uptake by specific compounds is associated with binding at the same site as the substrates, as well as additional binding to other sites on the protein (Yang et al., 2002), (Girniene et al., 2003), (Salas-Burgos et al., 2004). Similarly, GLUT7-mediated glucose uptake was significantly inhibited by presence of fructose, likely due to competitive inhibition (Li et al., 2004), (Chapter 6). Although it is thought that (poly)phenols would exert inhibition of sugar uptake by this protein in the same manner, it is possible that

certain compounds also have an effect on protein expression levels. For this reason, analysis of GLUT7 protein and mRNA expression in cells grown in the presence of apigenin, shown to significantly inhibit fructose uptake by this protein (Chapter 6), would help to determine the mode by which this compound bestows inhibition. Trafficking of the protein to the membrane, or re-internalization of membrane bound protein, could also be a potential target for inhibitors. Therefore, quantitative analysis of cell surface GLUT7 expression, using the cell surface biotinylation technique, following treatment with apigenin would help provide further information as to the potential inhibitory mechanisms of this compound.

7.3.2 Human intervention studies

(Poly)phenols have been shown to impact carbohydrate digestion and sugar absorption by the intestine through their inhibition of digestive enzymes and sugar transporters, as previously discussed (Manzano and Williamson, 2010), (McDougall et al., 2005), (Hanhineva et al., 2010). To add to that, data has demonstrated that dietary (poly)phenols maybe have potential prebiotic effects, promoting the growth of particular bacteria in the gut that have been linked to improved glucose tolerance (Jin et al., 2012), (Vendrame et al., 2011), (Kim et al., 2016). This research project focused on identifying potential inhibitors of specific sugar transporters expressed in the gut with the aim to instigate human intervention studies that would then investigate the effects of the novel inhibitors identified *in vivo*, using concentrations achievable through the diet or supplementation. Intervention studies looking at the effects of long and short-term (poly)phenol exposure suggests a protective effect against many different conditions through

attenuation of risk factors (Arts and Hollman, 2005), (Williamson and Manach, 2005), (Shi and Williamson, 2016). A study looking at the effects of acute and chronic black tea consumption, for instance, showed a reversal of endothelial dysfunction in patients with coronary artery disease (Duffy et al., 2001). Furthermore, an investigation of the acute effects of a (poly)phenol-rich intervention on glycaemic response showed that (poly)phenols had an effect on postprandial blood glucose *in vivo*, by reducing the area under the curve (Nyambe-Silavwe and Williamson, 2016). Short and long-term administration of apigenin, shown in this study to inhibit three fructose transporters, in the form of a human intervention, would help determine the potential effect of this compound on postprandial glycaemic response. Isotopic tracer studies could be used to measure changes in fructose levels in the plasma following consumption of apigenin as a supplement or dietary form, eg. German chamomile extract (Sun and Empie, 2012b). In addition, analysis of faecal samples following interventions with apigenin could establish the presence of *Bifidobacteria*, a genus of bacteria associated with improved glucose tolerance and lowered inflammatory markers (Vendrame et al., 2011), (Cuervo et al., 2015). Investigating the potential effects of apigenin by different methods of delivery, namely through the diet or supplementation, would also provide valuable information about the functionality of this compound as a sugar absorption inhibitor *in vivo*.

7.4 Overall conclusion

One of the novel findings of this research was that expression of GLUT7 was significantly increased in the presence of fructose, as seen in the Caco-2/TC7 cell model. This project identified that only apical and basolateral fructose, and not the other sugars tested, induced both GLUT7 mRNA and total protein in differentiated Caco-2/TC7 cells. The increased protein concentration in the cell did not change the ratio between surface-expressed and total protein, implying that increases were due to more protein synthesis or less degradation, and not enhanced trafficking per se. This observation beckons for additional studies to further characterize the lesser known GLUT7, with the aim to establish the role it plays in the regulation of sugar uptake. Another overall objective of this project was to determine the direct impact of specific (poly)phenols and food extracts on fructose and glucose uptake by GLUT2 and GLUT7 transporters, as well as their effect on sugar uptake by the fructose specific transporter GLUT5. Differentiated Caco-2 and Caco-2/TC7 cell monolayers, as for the intestine *in vivo*, express a variety of GLUTs and other sugar transporters, which makes them unsuitable for determination of the role of individual transporters. Therefore the *Xenopus laevis* expression system was used to elucidate effects of (poly)phenols as inhibitors on individual functional GLUTs. A successful quantitative model was set up, through heterologous expression of human transporters present in the gut in *X. laevis* oocytes, with the outlook to quantify the inhibition of sugar transporters by polyphenols. Through this, novel inhibitors of GLUT2-mediated glucose and fructose transport, as well as GLUT5-mediated fructose transport, were established. Furthermore, one compound (apigenin), able to significantly inhibit fructose uptake by GLUT2, 5 and 7, was

identified. The results from uptake experiments using the *X. laevis* oocyte model obtained in this project can be used to validate cell culture and *in vivo* studies, as well as inspire future studies using these models. In addition, this research highlights the potential that (poly)phenols have to modulate sugar transport by inhibition of GLUT transporters, and that the specificity of inhibition could be exploited in mechanistic studies to examine the role of sugar transporters in cells.

References

- ADS 2014. Diagnosis and classification of diabetes mellitus. *Diabetes Care*, 37 Suppl 1, S81-90.
- AFFLECK, J. A., HELLIWELL, P. A. & KELLETT, G. L. 2003. Immunocytochemical detection of GLUT2 at the rat intestinal brush-border membrane. *J Histochem Cytochem*, 51, 1567-74.
- ALZAID, F., CHEUNG, H. M., PREEDY, V. R. & SHARP, P. A. 2013. Regulation of Glucose Transporter Expression in Human Intestinal Caco-2 Cells following Exposure to an Anthocyanin-Rich Berry Extract. *PLoS One*, 8, e78932.
- ANDÚJAR, I., RECIO, M. C. & GINER, R. M. R., J. L. 2012. Cocoa Polyphenols and Their Potential Benefits for Human Health. *Oxid Med Cell Longev*, 2012, 23.
- ANGELIS, I. D. & TURCO, L. 2011. Caco-2 cells as a model for intestinal absorption. *Curr Protoc Toxicol*, Chapter 20, Unit20.6.
- ARTS, I. C. & HOLLMAN, P. C. 2005. Polyphenols and disease risk in epidemiologic studies. *Am J Clin Nutr*, 81, 317s-325s.
- ASTON, L. M. 2006. Glycaemic index and metabolic disease risk. *Proc Nutr Soc*, 65, 125-34.
- BAHADORAN, Z., MIRMIRAN, P. & AZIZI, F. 2013. Dietary polyphenols as potential nutraceuticals in management of diabetes: a review. *J Diabetes Metab Disord*, 12, 43.
- BANIHANI, S., SWEDAN, S. & ALGURAAN, Z. 2013. Pomegranate and type 2 diabetes. *Nutr Res*, 33, 341-8.
- BANKS, W. A., COON, A. B., ROBINSON, S. M., MOINUDDIN, A., SHULTZ, J. M., NAKAOKE, R. & MORLEY, J. E. 2004. Triglycerides induce leptin resistance at the blood-brain barrier. *Diabetes*, 53, 1253-60.
- BANTLE, J. P. 2009. Dietary fructose and metabolic syndrome and diabetes. *J Nutr*, 139, 1263S-1268S.
- BARCLAY, A. W., PETOCZ, P., MCMILLAN-PRICE, J., FLOOD, V. M., PRVAN, T., MITCHELL, P. & BRAND-MILLER, J. C. 2008. Glycemic index, glycemic load, and chronic disease risk--a meta-analysis of observational studies. *Am J Clin Nutr*, 87, 627-37.
- BARONE, S., FUSSELL, S. L., SINGH, A. K., LUCAS, F., XU, J., KIM, C., WU, X., YU, Y., AMLAL, H., SEIDLER, U., ZUO, J. & SOLEIMANI, M. 2009. Slc2a5 (Glut5) is essential for the absorption of fructose in the intestine and generation of fructose-induced hypertension. *J Biol Chem*, 284, 5056-66.
- BASCIANO, H., FEDERICO, L. & ADELI, K. 2005. Fructose, insulin resistance, and metabolic dyslipidemia. *Nutr Metab (Lond)*, 2, 5.

- BASU, S., YOFFE, P., HILLS, N. & LUSTIG, R. H. 2013. The relationship of sugar to population-level diabetes prevalence: an econometric analysis of repeated cross-sectional data. *PLoS One*, 8, e57873.
- BATES, B., LENNOX, A., PRENTICE, A., BATES, C. & SWAN, G. 2012. National Diet and Nutrition Survey: Headline Results from Years 1, 2 and 3 (Combined) of the Rolling Programme (2008/2009–2010/11). London: Department of Health, Food Standards Agency.
- BAUD, G., RAVERDY, V., BONNER, C., DAOUDI, M., CAIAZZO, R. & PATTOU, F. 2016. Sodium glucose transport modulation in type 2 diabetes and gastric bypass surgery. *Surg Obes Relat Dis*, 12, 1206-12.
- BECKERT, B. & MASQUIDA, B. 2011. Synthesis of RNA by in vitro transcription. *Methods Mol Biol*, 703, 29-41.
- BENTLEY, P. A., SHAO, Y., MISRA, Y., MORIELLI, A. D. & ZHAO, F. Q. 2012. Characterization of bovine glucose transporter 1 kinetics and substrate specificities in *Xenopus* oocytes. *J Dairy Sci*, 95, 1188-97.
- BIALOSTOSKY, K., WRIGHT, J. D., KENNEDY-STEPHENSON, J., MCDOWELL, M. & JOHNSON, C. L. 2002. Dietary intake of macronutrients, micronutrients, and other dietary constituents: United States 1988-94. *Vital Health Stat* 11, 1-158.
- BIANCHI, L. A. D., M. 2006. Heterologous expression of *C. elegans* ion channels in *Xenopus* oocytes *WormBook*, The *C. elegans* Research Community, WormBook, doi/10.1895/wormbook.1.117.1, <http://www.wormbook.org>.
- BLAKEMORE, S. J., ALEDO, J. C., JAMES, J., CAMPBELL, F. C., LUCOCQ, J. M. & HUNDAL, H. S. 1995. The GLUT5 hexose transporter is also localized to the basolateral membrane of the human jejunum. *Biochem J*, 309 (Pt 1), 7-12.
- BOJAROVA, P. & KREN, V. 2011. Glycosidases in carbohydrate synthesis: when organic chemistry falls short. *Chimia (Aarau)*, 65, 65-70.
- BOJIC, M., DEBELJAK, Z., MEDIC-SARIC, M. & TOMICIC, M. 2012. Interference of selected flavonoid aglycons in platelet aggregation assays. *Clin Chem Lab Med*, 50, 1403-8.
- BORNET, F. R., JARDY-GENNETIER, A. E., JACQUET, N. & STOWELL, J. 2007. Glycaemic response to foods: impact on satiety and long-term weight regulation. *Appetite*, 49, 535-53.
- BRISKE-ANDERSON, M. J., FINLEY, J. W. & NEWMAN, S. M. 1997. The influence of culture time and passage number on the morphological and physiological development of Caco-2 cells. *Proc Soc Exp Biol Med*, 214, 248-57.
- BROER, S. 2010. *Xenopus laevis* Oocytes. *Methods Mol Biol*, 637, 295-310.
- BROWNE, C. L. & WERNER, W. 1984. Intercellular junctions between the follicle cells and oocytes of *Xenopus laevis*. *J Exp Zool*, 230, 105-13.
- BUDDINGTON, R. K. & DIAMOND, J. M. 1989. Ontogenetic development of intestinal nutrient transporters. *Annu Rev Physiol*, 51, 601-19.
- BUIJSSE, B., WEIKERT, C., DROGAN, D., BERGMANN, M. & BOEING, H. 2010. Chocolate consumption in relation to blood pressure and risk of cardiovascular disease in German adults. *European Heart Journal*, 31, 1616-1623.

- BURANT, C. F., TAKEDA, J., BROTH-LAROCHE, E., BELL, G. I. & DAVIDSON, N. O. 1992. Fructose transporter in human spermatozoa and small intestine is GLUT5. *J Biol Chem*, 267, 14523-6.
- BURCELIN, R. & THORENS, B. 2001. Evidence that extrapancreatic GLUT2-dependent glucose sensors control glucagon secretion. *Diabetes*, 50, 1282-9.
- BUSCEMI, S., VERGA, S., BATSIS, J. A., DONATELLI, M., TRANCHINA, M. R., BELMONTE, S., MATTINA, A., RE, A. & CERASOLA, G. 2010. Acute effects of coffee on endothelial function in healthy subjects. *Eur J Clin Nutr*, 64, 483-9.
- BUTT, M. S., IMRAN, A., SHARIF, M. K., AHMAD, R. S., XIAO, H., IMRAN, M. & RSOOL, H. A. 2014. Black tea polyphenols: a mechanistic treatise. *Crit Rev Food Sci Nutr*, 54, 1002-11.
- CARPENTER, E. P., BEIS, K., CAMERON, A. D. & IWATA, S. 2008. Overcoming the challenges of membrane protein crystallography. *Curr Opin Struct Biol*, 18, 581-6.
- CHA, J. Y., CHO, Y. S., KIM, I., ANNO, T., RAHMAN, S. M. & YANAGITA, T. 2001. Effect of hesperetin, a citrus flavonoid, on the liver triacylglycerol content and phosphatidate phosphohydrolase activity in orotic acid-fed rats. *Plant Foods Hum Nutr*, 56, 349-58.
- CHANTRET, I., RODOLOSSE, A., BARBAT, A., DUSSAULX, E., BROTH-LAROCHE, E., ZWEIBAUM, A. & ROUSSET, M. 1994. Differential expression of sucrase-isomaltase in clones isolated from early and late passages of the cell line Caco-2: evidence for glucose-dependent negative regulation. *J Cell Sci*, 107 (Pt 1), 213-25.
- CHEESEMAN, C. 2008. GLUT7: a new intestinal facilitated hexose transporter. *Am J Physiol Endocrinol Metab*, 295, E238-41.
- CHEESEMAN, C. I. 1993. GLUT2 is the transporter for fructose across the rat intestinal basolateral membrane. *Gastroenterology*, 105, 1050-6.
- CHIASSON, J. L. 2006. Acarbose for the prevention of diabetes, hypertension, and cardiovascular disease in subjects with impaired glucose tolerance: the Study to Prevent Non-Insulin-Dependent Diabetes Mellitus (STOP-NIDDM) Trial. *Endocr Pract*, 12 Suppl 1, 25-30.
- COHEN, M., KITSBERG, D., TSYTKIN, S., SHULMAN, M., AROETI, B. & NAHMIAS, Y. 2014. Live imaging of GLUT2 glucose-dependent trafficking and its inhibition in polarized epithelial cysts. *Open Biol*, 4.
- COLVILLE, C. A., SEATTER, M. J., JESS, T. J., GOULD, G. W. & THOMAS, H. M. 1993. Kinetic analysis of the liver-type (GLUT2) and brain-type (GLUT3) glucose transporters in *Xenopus* oocytes: substrate specificities and effects of transport inhibitors. *Biochem J*, 290 (Pt 3), 701-6.
- CONIFF, R. F., SHAPIRO, J. A., ROBBINS, D., KLEINFELD, R., SEATON, T. B., BEISSWENGER, P. & MCGILL, J. B. 1995. Reduction of glycosylated hemoglobin and postprandial hyperglycemia by acarbose in patients with NIDDM. A placebo-controlled dose-comparison study. *Diabetes Care*, 18, 817-24.
- CONN, P. M. 1991. *Electrophysiology and Microinjection*: , London, Academic Press Limited.
- COOPER, G. M. 2000. *The Cell: A Molecular Approach*, Sunderland, MA, Sinauer Associates.

- COORE, H. G. & RANDLE, P. J. 1964. Regulation of insulin secretion studied with pieces of rabbit pancreas incubated in vitro. *Biochem J*, 93, 66-78.
- CORDAIN, L., MILLER, J. B., EATON, S. B., MANN, N., HOLT, S. H. & SPETH, J. D. 2000. Plant-animal subsistence ratios and macronutrient energy estimations in worldwide hunter-gatherer diets. *Am J Clin Nutr*, 71, 682-92.
- CROZIER, A., DEL RIO, D. & CLIFFORD, M. N. 2010. Bioavailability of dietary flavonoids and phenolic compounds. *Mol Aspects Med*, 31, 446-67.
- CUERVO, A., HEVIA, A., LOPEZ, P., SUAREZ, A., SANCHEZ, B., MARGOLLES, A. & GONZALEZ, S. 2015. Association of polyphenols from oranges and apples with specific intestinal microorganisms in systemic lupus erythematosus patients. *Nutrients*, 7, 1301-17.
- CUI, X. L., SOTEROPOULOS, P., TOLIAS, P. & FERRARIS, R. P. 2004. Fructose-responsive genes in the small intestine of neonatal rats. *Physiol Genomics*, 18, 206-17.
- CURA, A. J. & CARRUTHERS, A. 2012. Role of monosaccharide transport proteins in carbohydrate assimilation, distribution, metabolism, and homeostasis. *Compr Physiol*, 2, 863-914.
- DANAEI, G., FINUCANE, M. M., LU, Y., SINGH, G. M., COWAN, M. J., PACIOREK, C. J., LIN, J. K., FARZADFAR, F., KHANG, Y. H., STEVENS, G. A., RAO, M., ALI, M. K., RILEY, L. M., ROBINSON, C. A. & EZZATI, M. 2011. National, regional, and global trends in fasting plasma glucose and diabetes prevalence since 1980: systematic analysis of health examination surveys and epidemiological studies with 370 country-years and 2.7 million participants. *Lancet*, 378, 31-40.
- DAVID, E. S., CINGARI, D. S. & FERRARIS, R. P. 1995. Dietary induction of intestinal fructose absorption in weaning rats. *Pediatr Res*, 37, 777-82.
- DAVIES, M. J., JUDD, J. T., BAER, D. J., CLEVIDENCE, B. A., PAUL, D. R., EDWARDS, A. J., WISEMAN, S. A., MUESING, R. A. & CHEN, S. C. 2003. Black tea consumption reduces total and LDL cholesterol in mildly hypercholesterolemic adults. *J Nutr*, 133, 3298s-3302s.
- DAY, A. J., CANADA, J. F., DIAZ, J. C., KROON, P. A., MCLAUCHLAN, R., FAULDS, C. B., PLUMB, G. W., MORGAN, M. R. A. & WILLIAMSON, G. 2000. Dietary flavonoid and isoflavone glycosides are hydrolysed by the lactase site of lactase phlorizin hydrolase. *FEBS Lett*, 468, 166-170.
- DE BOCK, M., DERRAIK, J. G. & CUTFIELD, W. S. 2012. Polyphenols and glucose homeostasis in humans. *J Acad Nutr Diet*, 112, 808-15.
- DEACON, N. J. & EBRINGER, A. 1979. Post-translational modification of rat immunoglobulins synthesized in the *Xenopus* oocyte translation system. *Immunology*, 38, 137-44.
- DEBOSCH, B. J., CHI, M. & MOLEY, K. H. 2012. Glucose transporter 8 (GLUT8) regulates enterocyte fructose transport and global mammalian fructose utilization. *Endocrinology*, 153, 4181-91.
- DEL RIO, D., RODRIGUEZ-MATEOS, A., SPENCER, J. P., TOGNOLINI, M., BORGES, G. & CROZIER, A. 2013. Dietary (poly)phenolics in human health: structures, bioavailability, and evidence of protective effects against chronic diseases. *Antioxid Redox Signal*, 18, 1818-92.
- DELIE, F. & RUBAS, W. 1997. A human colonic cell line sharing similarities with enterocytes as a model to examine oral absorption: advantages and

- limitations of the Caco-2 model. *Crit Rev Ther Drug Carrier Syst*, 14, 221-86.
- DELPIRE, E., GAGNON, K. B., LEDFORD, J. J. & WALLACE, J. M. 2011. Housing and husbandry of *Xenopus laevis* affect the quality of oocytes for heterologous expression studies. *J Am Assoc Lab Anim Sci*, 50, 46-53.
- DENG, D., SUN, P., YAN, C., KE, M., JIANG, X., XIONG, L., REN, W., HIRATA, K., YAMAMOTO, M., FAN, S. & YAN, N. 2015. Molecular basis of ligand recognition and transport by glucose transporters. *Nature*, 526, 391-6.
- DESMET, T., SOETAERT, W., BOJAROVA, P., KREN, V., DIJKHUIZEN, L., EASTWICK-FIELD, V. & SCHILLER, A. 2012. Enzymatic glycosylation of small molecules: challenging substrates require tailored catalysts. *Chemistry*, 18, 10786-801.
- DICK, W. R., FLETCHER, E. A. & SHAH, S. A. 2016. Reduction of Fasting Blood Glucose and Hemoglobin A1c Using Oral Aloe Vera: A Meta-Analysis. *J Altern Complement Med*, 22, 450-7.
- DOBLADO, M. & MOLEY, K. H. 2009. Facilitative glucose transporter 9, a unique hexose and urate transporter. *Am J Physiol Endocrinol Metab*, 297, E831-5.
- DOEGE, H., BOCIANSKI, A., SCHEEPERS, A., AXER, H., ECKEL, J., JOOST, H. G. & SCHURMANN, A. 2001. Characterization of human glucose transporter (GLUT) 11 (encoded by SLC2A11), a novel sugar-transport facilitator specifically expressed in heart and skeletal muscle. *Biochem J*, 359, 443-9.
- DONG, X. C., COPPS, K. D., GUO, S., LI, Y., KOLLIPARA, R., DEPINHO, R. A. & WHITE, M. F. 2008. Inactivation of hepatic Foxo1 by insulin signaling is required for adaptive nutrient homeostasis and endocrine growth regulation. *Cell Metab*, 8, 65-76.
- DOUARD, V. & FERRARIS, R. P. 2008. Regulation of the fructose transporter GLUT5 in health and disease. *Am J Physiol Endocrinol Metab*, 295, E227-37.
- DOUARD, V. & FERRARIS, R. P. 2013. The role of fructose transporters in diseases linked to excessive fructose intake. *J Physiol*, 591, 401-14.
- DROZDOWSKI, L. A. & THOMSON, A. B. 2006. Intestinal sugar transport. *World J Gastroenterol*, 12, 1657-70.
- DU, L. & HEANEY, A. P. 2012. Regulation of adipose differentiation by fructose and GluT5. *Mol Endocrinol*, 26, 1773-82.
- DUFFY, S. J., KEANEY, J. F., JR., HOLBROOK, M., GOKCE, N., SWERDLOFF, P. L., FREI, B. & VITA, J. A. 2001. Short- and long-term black tea consumption reverses endothelial dysfunction in patients with coronary artery disease. *Circulation*, 104, 151-6.
- DUJIC, T., ZHOU, K., DONNELLY, L. A., TAVENDALE, R., PALMER, C. N. & PEARSON, E. R. 2015. Association of Organic Cation Transporter 1 With Intolerance to Metformin in Type 2 Diabetes: A GoDARTS Study. *Diabetes*, 64, 1786-93.
- DYER, J., WOOD, I. S., PALEJWALA, A., ELLIS, A. & SHIRAZI-BEECHEY, S. P. 2002. Expression of monosaccharide transporters in intestine of diabetic humans. *Am J Physiol Gastrointest Liver Physiol*, 282, G241-8.
- EBERT, K., LUDWIG, M., GEILLINGER, K. E., SCHOBERTH, G. C., ESSENWANGER, J., STOLZ, J., DANIEL, H. & WITT, H. 2017.

- Reassessment of GLUT7 and GLUT9 as Putative Fructose and Glucose Transporters. *J Membr Biol*, 250, 171-182.
- ELLIOTT, S. S., KEIM, N. L., STERN, J. S., TEFF, K. & HAVEL, P. J. 2002. Fructose, weight gain, and the insulin resistance syndrome. *Am J Clin Nutr*, 76, 911-22.
- FANG, R., VEITCH, N. C., KITE, G. C., PORTER, E. A. & SIMMONDS, M. S. 2013. Enhanced profiling of flavonol glycosides in the fruits of sea buckthorn (*Hippophae rhamnoides*). *J Agric Food Chem*, 61, 3868-75.
- FAYAZ, S. M. & SUVANISH KUMAR, V. S. R., K. G. 2014. Finding Needles in a Haystack: Application of Network Analysis and Target Enrichment Studies for the Identification of Potential Anti-Diabetic Phytochemicals. *PLoS One*, 9.
- FERRARIS, R. P. 2001. Dietary and developmental regulation of intestinal sugar transport. *Biochem J*, 360, 265-76.
- FERRELL, J. E., JR. 1999. Building a cellular switch: more lessons from a good egg. *Bioessays*, 21, 866-70.
- FORESTER, S. C., GU, Y. & LAMBERT, J. D. 2012. Inhibition of starch digestion by the green tea polyphenol, (-)-epigallocatechin-3-gallate. *Mol Nutr Food Res*, 56, 1647-54.
- FOROUHI, N. G. & WAREHAM, N. J. 2014. The EPIC-InterAct Study: A Study of the Interplay between Genetic and Lifestyle Behavioral Factors on the Risk of Type 2 Diabetes in European Populations. *Curr Nutr Rep*, 3, 355-363.
- FUKE, H. & OHNO, M. 2008. Role of poly (A) tail as an identity element for mRNA nuclear export. *Nucleic Acids Res*, 36, 1037-49.
- GALE, C. P., CATTLE, B. A., WOOLSTON, A., BAXTER, P. D., WEST, T. H., SIMMS, A. D., BLAXILL, J., GREENWOOD, D. C., FOX, K. A. & WEST, R. M. 2012. Resolving inequalities in care? Reduced mortality in the elderly after acute coronary syndromes. The Myocardial Ischaemia National Audit Project 2003-2010. *Eur Heart J*, 33, 630-9.
- GANTT, R. W., PELTIER-PAIN, P. & THORSON, J. S. 2011. Enzymatic methods for glyco(diversification/randomization) of drugs and small molecules. *Nat Prod Rep*, 28, 1811-53.
- GAO, X., QI, L., QIAO, N., CHOI, H. K., CURHAN, G., TUCKER, K. L. & ASCHERIO, A. 2007. Intake of added sugar and sugar-sweetened drink and serum uric acid concentration in US men and women. *Hypertension*, 50, 306-12.
- GARCIA-MORA, P., MARTIN-MARTINEZ, M., ANGELES BONACHE, M., GONZALEZ-MUNIZ, R., PENAS, E., FRIAS, J. & MARTINEZ-VILLALUENGA, C. 2017. Identification, functional gastrointestinal stability and molecular docking studies of lentil peptides with dual antioxidant and angiotensin I converting enzyme inhibitory activities. *Food Chem*, 221, 464-472.
- GEE, J. M., DUPONT, M. S., DAY, A. J., PLUMB, G. W., WILLIAMSON, G. & JOHNSON, I. T. 2000. Intestinal transport of quercetin glycosides in rats involves both deglycosylation and interaction with the hexose transport pathway. *J Nutr*, 130, 2765-71.
- GIRNIENE, J., TATIBOUET, A., SACKUS, A., YANG, J., HOLMAN, G. D. & ROLLIN, P. 2003. Inhibition of the D-fructose transporter protein GLUT5

- by fused-ring glyco-1,3-oxazolidin-2-thiones and -oxazolidin-2-ones. *Carbohydr Res*, 338, 711-9.
- GORAN, M. I., ULIJASZEK, S. J. & VENTURA, E. E. 2013. High fructose corn syrup and diabetes prevalence: a global perspective. *Glob Public Health*, 8, 55-64.
- GORBOULEV, V., SCHURMANN, A., VALLON, V., KIPP, H., JASCHKE, A., KLESSEN, D., FRIEDRICH, A., SCHERNECK, S., RIEG, T., CUNARD, R., VEYHL-WICHMANN, M., SRINIVASAN, A., BALEN, D., BRELJAK, D., REXHEPAJ, R., PARKER, H. E., GRIBBLE, F. M., REIMANN, F., LANG, F., WIESE, S., SABOLIC, I., SENDTNER, M. & KOEPESELL, H. 2012. Na(+)-D-glucose cotransporter SGLT1 is pivotal for intestinal glucose absorption and glucose-dependent incretin secretion. *Diabetes*, 61, 187-96.
- GOTO, T., HORITA, M., NAGAI, H., NAGATOMO, A., NISHIDA, N., MATSUURA, Y. & NAGAOKA, S. 2012. Tiliroside, a glycosidic flavonoid, inhibits carbohydrate digestion and glucose absorption in the gastrointestinal tract. *Mol Nutr Food Res*, 56, 435-45.
- GOUYON, F., ONESTO, C., DALET, V., PAGES, G., LETURQUE, A. & BROTLAROCHE, E. 2003. Fructose modulates GLUT5 mRNA stability in differentiated Caco-2 cells: role of cAMP-signalling pathway and PABP (polyadenylated-binding protein)-interacting protein (Paip) 2. *Biochem J*, 375, 167-74.
- GREENWOOD, D. C., THREAPLETON, D. E., EVANS, C. E., CLEGHORN, C. L., NYKJAER, C., WOODHEAD, C. & BURLEY, V. J. 2014. Association between sugar-sweetened and artificially sweetened soft drinks and type 2 diabetes: systematic review and dose-response meta-analysis of prospective studies. *Br J Nutr*, 112, 725-734.
- GREFNER, N. M., GROMOVA, L. V., GRUZDKOV, A. A. & KOMISSARCHIK, I. 2014. The interaction between SGLT1 or GLUT2 glucose transporter and the cytoskeleton in the enterocyte as well as Caco2 cell during hexose absorption. *Tsitologija*, 56, 749-57.
- GROSSO, G., STEPANIAK, U., TOPOR-MADRY, R., SZAFRANIEC, K. & PAJAK, A. 2014. Estimated dietary intake and major food sources of polyphenols in the Polish arm of the HAPIEE study. *Nutrition*, 30, 1398-403.
- GRUNDY, S. M. 1998. Multifactorial causation of obesity: implications for prevention. *Am J Clin Nutr*, 67, 563s-72s.
- GURDON, J. B., LANE, C. D., WOODLAND, H. R. & MARBAIX, G. 1971. Use of frog eggs and oocytes for the study of messenger RNA and its translation in living cells. *Nature* 233, 177-182.
- GURDON, J. B., LINGREL, J. B. & MARBAIX, G. 1973. Message stability in injected frog oocytes: long life of mammalian alpha and beta globin messages. *J Mol Biol*, 80, 539-551.
- GUZMAN-MALDONADO, H. & PAREDES-LOPEZ, O. 1995. Amylolytic enzymes and products derived from starch: a review. *Crit Rev Food Sci Nutr*, 35, 373-403.
- HAJDUCH, E., DARAKHSHAN, F. & HUNDAL, H. S. 1998. Fructose uptake in rat adipocytes: GLUT5 expression and the effects of streptozotocin-induced diabetes. *Diabetologia*, 41, 821-8.

- HAIAGHAALIPOUR, F., KHALILPOURFARSHBAFI, M. & ARYA, A. 2015. Modulation of Glucose Transporter Protein by Dietary Flavonoids in Type 2 Diabetes Mellitus. *Int J Biol Sci*, 11, 508-524.
- HALLEY-STOTT, R. P., PASQUE, V., ASTRAND, C., MIYAMOTO, K., SIMEONI, I., JULLIEN, J. & GURDON, J. B. 2010. Mammalian nuclear transplantation to Germinal Vesicle stage *Xenopus* oocytes - a method for quantitative transcriptional reprogramming. *Methods*, 51, 56-65.
- HANHINEVA, K., TORRONEN, R., BONDIA-PONS, I., PEKKINEN, J., KOLEHMAINEN, M., MYKKANEN, H. & POUTANEN, K. 2010. Impact of dietary polyphenols on carbohydrate metabolism. *Int J Mol Sci*, 11, 1365-402.
- HEDIGER, M. A., COADY, M. J., IKEDA, T. S. & WRIGHT, E. M. 1987. Expression cloning and cDNA sequencing of the Na⁺/glucose co-transporter. *Nature*, 330, 379-81.
- HELLIWELL, P. A. & KELLETT, G. L. 2002. The active and passive components of glucose absorption in rat jejunum under low and high perfusion stress. *J Physiol*, 544, 579-89.
- HELLIWELL, P. A., RICHARDSON, M., AFFLECK, J. & KELLETT, G. L. 2000. Stimulation of fructose transport across the intestinal brush-border membrane by PMA is mediated by GLUT2 and dynamically regulated by protein kinase C. *Biochem J*, 350, 149-154.
- HELLIWELL, P. A., RUMSBY, M. G. & KELLETT, G. L. 2003. Intestinal sugar absorption is regulated by phosphorylation and turnover of protein kinase C beta11 mediated by phosphatidylinositol 3-kinase- and mammalian target of rapamycin-dependent pathways. *J Biol Chem*, 278, 28644-50.
- HENDERSON, P. J. & BALDWIN, S. A. 2012. Structural biology: Bundles of insights into sugar transporters. *Nature*, 490, 348-50.
- HIGDON, J. V. & FREI, B. 2003. Tea catechins and polyphenols: health effects, metabolism, and antioxidant functions. *Crit Rev Food Sci Nutr*, 43, 89-143.
- HOKAYEM, M., BLOND, E., VIDAL, H., LAMBERT, K., MEUGNIER, E., FEILLET-COUDRAY, C., COUDRAY, C., PESENTI, S., LUYTON, C., LAMBERT-PORCHERON, S., SAUVINET, V., FEDOU, C., BRUN, J. F., RIEUSSET, J., BISBAL, C., SULTAN, A., MERCIER, J., GOUDABLE, J., DUPUY, A. M., CRISTOL, J. P., LAVILLE, M. & AVIGNON, A. 2013. Grape polyphenols prevent fructose-induced oxidative stress and insulin resistance in first-degree relatives of type 2 diabetic patients. *Diabetes Care*, 36, 1454-61.
- HOLLANDS, W., VOORSPOELS, S., JACOBS, G., AABY, K., MEISLAND, A., GARCIA-VILLALBA, R., TOMAS-BARBERAN, F., PISKULA, M., MAWSON, D. & VOVK, I. 2017. Development, validation and evaluation of an analytical method for the determination of monomeric and oligomeric procyanidins in apple extracts. *J Chromatogr A*, 1495, 46-56.
- HOLMAN, R. 2007. Metformin as first choice in oral diabetes treatment: the UKPDS experience. *Journ Annu Diabetol Hotel Dieu*, 13-20.
- HOOPER, L., KAY, C., ABDELHAMID, A., KROON, P. A., COHN, J. S., RIMM, E. B. & CASSIDY, A. 2012. Effects of chocolate, cocoa, and flavan-3-ols on cardiovascular health: a systematic review and meta-analysis of randomized trials. *Am J Clin Nutr*, 95, 740-51.

- HU, F. B., MANSON, J. E., STAMPFER, M. J., COLDITZ, G., LIU, S., SOLOMON, C. G. & WILLETT, W. C. 2001. Diet, lifestyle, and the risk of type 2 diabetes mellitus in women. *N Engl J Med*, 345, 790-7.
- IHGSC 2004. Finishing the euchromatic sequence of the human genome. *Nature*, 431, 931-45.
- IMPELLIZZERI, D., ESPOSITO, E., MAZZON, E., PATERNITI, I., DI PAOLA, R., MORITTU, V. M., PROCOPIO, A., BRITTI, D. & CUZZOCREA, S. 2011. Oleuropein aglycone, an olive oil compound, ameliorates development of arthritis caused by injection of collagen type II in mice. *J Pharmacol Exp Ther*, 339, 859-69.
- JAFRI, M. A., ASLAM, M., JAVED, K. & SINGH, S. 2000. Effect of *Punica granatum* Linn. (flowers) on blood glucose level in normal and alloxan-induced diabetic rats. *J Ethnopharmacol*, 70, 309-14.
- JEN, K. L., ROCHON, C., ZHONG, S. B. & WHITCOMB, L. 1991. Fructose and sucrose feeding during pregnancy and lactation in rats changes maternal and pup fuel metabolism. *J Nutr*, 121, 1999-2005.
- JENKINS, D. J., KENDALL, C. W., AUGUSTIN, L. S., FRANCESCHI, S., HAMIDI, M., MARCHIE, A., JENKINS, A. L. & AXELSEN, M. 2002. Glycemic index: overview of implications in health and disease. *Am J Clin Nutr*, 76, 266s-73s.
- JENNINGS, C., MEAD, A., JONES, J., HOLDEN, A., CONNOLLY, S., KOTSEVA, K. & WOOD, D. 2009. *Preventive Cardiology - a practical manual* Oxford, Oxford University Press.
- JENSEN, O. N. 2004. Modification-specific proteomics: characterization of post-translational modifications by mass spectrometry. *Curr Opin Chem Biol*, 8, 33-41.
- JIN, J. S., TOUYAMA, M., HISADA, T. & BENNO, Y. 2012. Effects of green tea consumption on human fecal microbiota with special reference to *Bifidobacterium* species. *Microbiol Immunol*, 56, 729-39.
- JOHNSON, R. J., PEREZ-POZO, S. E., SAUTIN, Y. Y., MANITIUS, J., SANCHEZ-LOZADA, L. G., FEIG, D. I., SHAFIU, M., SEGAL, M., GLASSOCK, R. J., SHIMADA, M., RONCAL, C. & NAKAGAWA, T. 2009. Hypothesis: could excessive fructose intake and uric acid cause type 2 diabetes? *Endocr Rev*, 30, 96-116.
- JOHNSON, R. J., SEGAL, M. S., SAUTIN, Y., NAKAGAWA, T., FEIG, D. I., KANG, D. H., GERSCH, M. S., BENNER, S. & SANCHEZ-LOZADA, L. G. 2007. Potential role of sugar (fructose) in the epidemic of hypertension, obesity and the metabolic syndrome, diabetes, kidney disease, and cardiovascular disease. *Am J Clin Nutr*, 86, 899-906.
- JOHNSTON, K., SHARP, P., CLIFFORD, M. & MORGAN, L. 2005. Dietary polyphenols decrease glucose uptake by human intestinal Caco-2 cells. *FEBS Lett*, 579, 1653-7.
- JUNG, C. Y. & RAMPAL, A. L. 1977. Cytochalasin B binding sites and glucose transport carrier in human erythrocyte ghosts. *J Biol Chem*, 252, 5456-63.
- JUNG, H. S., LIM, Y. & KIM, E. K. 2014. Therapeutic phytochemicals for obesity and diabetes. *Int J Mol Sci*, 15, 21505-37.
- JUNG, U. J., LEE, M. K., PARK, Y. B., KANG, M. A. & CHOI, M. S. 2006. Effect of citrus flavonoids on lipid metabolism and glucose-regulating enzyme mRNA levels in type-2 diabetic mice. *Int J Biochem Cell Biol*, 38, 1134-45.

- KANE, S., SEATTER, M. J. & GOULD, G. W. 1997. Functional studies of human GLUT5: effect of pH on substrate selection and an analysis of substrate interactions. *Biochem Biophys Res Commun*, 238, 503-5.
- KATO, A., MINOSHIMA, Y., YAMAMOTO, J., ADACHI, I., WATSON, A. A. & NASH, R. J. 2008. Protective effects of dietary chamomile tea on diabetic complications. *J Agric Food Chem*, 56, 8206-11.
- KELLETT, G. L. & BROT-LAROCHE, E. 2005. Apical GLUT2: a major pathway of intestinal sugar absorption. *Diabetes*, 54, 3056-62.
- KELLETT, G. L., BROT-LAROCHE, E., MACE, O. J. & LETURQUE, A. 2008. Sugar absorption in the intestine: the role of GLUT2. *Annu Rev Nutr*, 28, 35-54.
- KELLETT, G. L. & HELLIWELL, P. A. 2000. The diffusive component of intestinal glucose absorption is mediated by the glucose-induced recruitment of GLUT2 to the brush-border membrane. *Biochem J*, 350 Pt 1, 155-62.
- KERIMI, A., NYAMBE-SILAVWE, H., GAUER, J. S., TOMAS-BARBERAN, F. A. & WILLIAMSON, G. 2017. Pomegranate juice, but not an extract, confers a lower glycemic response on a high-glycemic index food: randomized, crossover, controlled trials in healthy subjects. *Am J Clin Nutr*.
- KIM, H. M. & KIM, J. 2013. The effects of green tea on obesity and type 2 diabetes. *Diabetes Metab J*, 37, 173-5.
- KIM, Y., KEOGH, J. & CLIFTON, P. 2016. Polyphenols and Glycemic Control. *Nutrients*, 8.
- KIPP, H., KHOURSANDI, S., SCHARLAU, D. & KINNE, R. K. 2003. More than apical: Distribution of SGLT1 in Caco-2 cells. *Am J Physiol Cell Physiol*, 285, C737-49.
- KONNER, M. & EATON, S. B. 2010. Paleolithic nutrition: twenty-five years later. *Nutr Clin Pract*, 25, 594-602.
- KRAUT, N. 2014. *Human Study on the Intra- and Interindividual Variation in Absorption and Metabolism of Coffee Chlorogenic Acids and Effects on Biomarkers of Health in Humans*. PhD thesis, University of Leeds.
- KRUPKA, R. M. 1985. Asymmetrical binding of phloretin to the glucose transport system of human erythrocytes. *J Membr Biol*, 83, 71-80.
- KWON, O., ECK, P., CHEN, S., CORPE, C. P., LEE, J. H., KRUHLAK, M. & LEVINE, M. 2007. Inhibition of the intestinal glucose transporter GLUT2 by flavonoids. *FASEB J*, 21, 366-77.
- LACOMBE, V. A. 2014. Expression and regulation of facilitative glucose transporters in equine insulin-sensitive tissue: from physiology to pathology. *ISRN Vet Sci*, 2014, 409547.
- LAIRSON, L. L., HENRISSAT, B., DAVIES, G. J. & WITHERS, S. G. 2008. Glycosyltransferases: structures, functions, and mechanisms. *Annu Rev Biochem*, 77, 521-55.
- LAVILLE, M. & NAZARE, J. A. 2009. Diabetes, insulin resistance and sugars. *Obes Rev*, 10 Suppl 1, 24-33.
- LE, M. T., FRYE, R. F., RIVARD, C. J., CHENG, J., MCFANN, K. K., SEGAL, M. S., JOHNSON, R. J. & JOHNSON, J. A. 2012. Effects of high-fructose corn syrup and sucrose on the pharmacokinetics of fructose and acute metabolic and hemodynamic responses in healthy subjects. *Metabolism*, 61, 641-51.

- LEGEZA, B., BALAZS, Z. & ODERMATT, A. 2014. Fructose promotes the differentiation of 3T3-L1 adipocytes and accelerates lipid metabolism. *FEBS Lett*, 588, 490-6.
- LI, J., INOUE, J., CHOI, J. M., NAKAMURA, S., YAN, Z., FUSHINOBU, S., KAMADA, H., KATO, H., HASHIDUME, T., SHIMIZU, M. & SATO, R. 2015. Identification of the Flavonoid Luteolin as a Repressor of the Transcription Factor Hepatocyte Nuclear Factor 4alpha. *J Biol Chem*, 290, 24021-35.
- LI, Q., MANOLESCU, A., RITZEL, M., YAO, S., SLUGOSKI, M., YOUNG, J. D., CHEN, X. Z. & CHEESEMAN, C. I. 2004. Cloning and functional characterization of the human GLUT7 isoform SLC2A7 from the small intestine. *Am J Physiol Gastrointest Liver Physiol*, 287, G236-42.
- LIM, J. S., MIETUS-SNYDER, M., VALENTE, A., SCHWARZ, J. M. & LUSTIG, R. H. 2010. The role of fructose in the pathogenesis of NAFLD and the metabolic syndrome. *Nat Rev Gastroenterol Hepatol*, 7, 251-64.
- LIN, S. T., TU, S. H., YANG, P. S., HSU, S. P., LEE, W. H., HO, C. T., WU, C. H., LAI, Y. H., CHEN, M. Y. & CHEN, L. C. 2016. Apple Polyphenol Phloretin Inhibits Colorectal Cancer Cell Growth via Inhibition of the Type 2 Glucose Transporter and Activation of p53-Mediated Signaling. *J Agric Food Chem*, 64, 6826-37.
- LITHERLAND, G. J., HAJDUCH, E., GOULD, G. W. & HUNDAL, H. S. 2004. Fructose transport and metabolism in adipose tissue of Zucker rats: diminished GLUT5 activity during obesity and insulin resistance. *Mol Cell Biochem*, 261, 23-33.
- LIU, R. H. 2013. Dietary bioactive compounds and their health implications. *J Food Sci*, 78 Suppl 1, A18-25.
- LIU, Y. J., ZHAN, J., LIU, X. L., WANG, Y., JI, J. & HE, Q. Q. 2014. Dietary flavonoids intake and risk of type 2 diabetes: a meta-analysis of prospective cohort studies. *Clin Nutr*, 33, 59-63.
- LODISH, H., BERK, A., KAISER, C., KREIGER, M., SCOTT, M., BRETSCHER, A., PLOEGH, H. & MATSUDAIRA, P. 2008. *Molecular Cell Biology*, New York, NY, Freeman and Company.
- LORENZ, T. C. 2012. Polymerase Chain Reaction: Basic Protocol Plus Troubleshooting and Optimization Strategies. *J Vis Exp*, 63.
- LUDWIG, D. S. 2002. The glycemic index: physiological mechanisms relating to obesity, diabetes, and cardiovascular disease. *Jama*, 287, 2414-23.
- MAHRAOUI, L., RODOLOSSE, A., BARBAT, A., DUSSAULX, E., ZWEIBAUM, A., ROUSSET, M. & BROT-LAROCHE, E. 1994. Presence and differential expression of SGLT1, GLUT1, GLUT2, GLUT3 and GLUT5 hexose-transporter mRNAs in Caco-2 cell clones in relation to cell growth and glucose consumption. *Biochem J*, 298 Pt 3, 629-33.
- MANACH, C., SCALBERT, A., MORAND, C., REMESY, C. & JIMENEZ, L. 2004. Polyphenols: food sources and bioavailability. *Am J Clin Nutr*, 79, 727-47.
- MANOLESCU, A., SALAS-BURGOS, A. M., FISCHBARG, J. & CHEESEMAN, C. I. 2005. Identification of a hydrophobic residue as a key determinant of fructose transport by the facilitative hexose transporter SLC2A7 (GLUT7). *J Biol Chem*, 280, 42978-83.
- MANOLESCU, A. R., AUGUSTIN, R., MOLEY, K. & CHEESEMAN, C. 2007a. A highly conserved hydrophobic motif in the exofacial vestibule of fructose

- transporting SLC2A proteins acts as a critical determinant of their substrate selectivity. *Mol Membr Biol*, 24, 455-63.
- MANOLESCU, A. R., WITKOWSKA, K., KINNAIRD, A., CESSFORD, T. & CHEESEMAN, C. 2007b. Facilitated hexose transporters: new perspectives on form and function. *Physiology (Bethesda)*, 22, 234-40.
- MANZANO, S. & WILLIAMSON, G. 2010. Polyphenols and phenolic acids from strawberry and apple decrease glucose uptake and transport by human intestinal Caco-2 cells. *Mol Nutr Food Res*, 54, 1773-80.
- MARON, D. J., LU, G. P., CAI, N. S., WU, Z. G., LI, Y. H., CHEN, H., ZHU, J. Q., JIN, X. J., WOUTERS, B. C. & ZHAO, J. 2003. Cholesterol-lowering effect of a theaflavin-enriched green tea extract: a randomized controlled trial. *Arch Intern Med*, 163, 1448-53.
- MARSH, K., BARCLAY, A., COLAGIURI, S. & BRAND-MILLER, J. 2011. Glycemic index and glycemic load of carbohydrates in the diabetes diet. *Curr Diab Rep*, 11, 120-7.
- MARTIN-PELAEZ, S., COVAS, M. I., FITO, M., KUSAR, A. & PRAVST, I. 2013. Health effects of olive oil polyphenols: recent advances and possibilities for the use of health claims. *Mol Nutr Food Res*, 57, 760-71.
- MARTY, N., DALLAPORTA, M. & THORENS, B. 2007. Brain glucose sensing, counterregulation, and energy homeostasis. *Physiology (Bethesda)*, 22, 241-51.
- MATHEWS, M. J., LIEBENBERG, L. & MATHEWS, E. H. 2015. How do high glycemic load diets influence coronary heart disease? *Nutr Metab (Lond)*, 12, 6.
- MCCREIGHT, L. J., BAILEY, C. J. & PEARSON, E. R. 2016. Metformin and the gastrointestinal tract. *Diabetologia*, 59, 426-35.
- MCDERMOTT, G. P., DO, D., LITTERST, C. M., MAAR, D., HINDSON, C. M., STEENBLOCK, E. R., LEGLER, T. C., JOUVENOT, Y., MARRS, S. H., BEMIS, A., SHAH, P., WONG, J., WANG, S., SALLY, D., JAVIER, L., DINIO, T., HAN, C., BRACKBILL, T. P., HODGES, S. P., LING, Y., KLITGORD, N., CARMAN, G. J., BERMAN, J. R., KOEHLER, R. T., HIDDESEN, A. L., WALSE, P., BOUSSE, L., TZONEV, S., HEFNER, E., HINDSON, B. J., CAULY, T. H., 3RD, HAMBLY, K., PATEL, V. P., REGAN, J. F., WYATT, P. W., KARLIN-NEUMANN, G. A., STUMBO, D. P. & LOWE, A. J. 2013. Multiplexed target detection using DNA-binding dye chemistry in droplet digital PCR. *Anal Chem*, 85, 11619-27.
- MCDOUGALL, G. J., SHPIRO, F., DOBSON, P., SMITH, P., BLAKE, A. & STEWART, D. 2005. Different polyphenolic components of soft fruits inhibit alpha-amylase and alpha-glucosidase. *J Agric Food Chem*, 53, 2760-6.
- MCKAY, D. L. & BLUMBERG, J. B. 2006. A review of the bioactivity and potential health benefits of chamomile tea (*Matricaria recutita* L.). *Phytother Res*, 20, 519-30.
- MELLOR, D. D., SATHYAPALAN, T., KILPATRICK, E. S., BECKETT, S. & ATKIN, S. L. 2010. High-cocoa polyphenol-rich chocolate improves HDL cholesterol in Type 2 diabetes patients. *Diabet Med*, 27, 1318-21.
- MELSTROM, L. G., SALABAT, M. R., DING, X. Z., MILAM, B. M., STROUCH, M., PELLING, J. C. & BENTREM, D. J. 2008. Apigenin inhibits the GLUT-1

- glucose transporter and the phosphoinositide 3-kinase/Akt pathway in human pancreatic cancer cells. *Pancreas*, 37, 426-31.
- MEYER, K. A., KUSHI, L. H., JACOBS, D. R., JR., SLAVIN, J., SELLERS, T. A. & FOLSOM, A. R. 2000. Carbohydrates, dietary fiber, and incident type 2 diabetes in older women. *Am J Clin Nutr*, 71, 921-30.
- MILEDI, R. & WOODWARD, R. M. 1989a. Effects of defolliculation on membrane current responses of *Xenopus* oocytes. *J Physiol*, 416, 601-21.
- MILEDI, R. & WOODWARD, R. M. 1989b. Membrane currents elicited by prostaglandins, atrial natriuretic factor and oxytocin in follicle-enclosed *Xenopus* oocytes. *J Physiol*, 416, 623-43.
- MILLER, A. J. & ZHOU, J. J. 2000. *Xenopus* oocytes as an expression system for plant transporters. *Biochim Biophys Acta*, 1465, 343-58.
- MODAK, M., DIXIT, P., LONDHE, J., GHASKADBI, S. & DEVASAGAYAM, T. P. 2007. Indian herbs and herbal drugs used for the treatment of diabetes. *J Clin Biochem Nutr*, 40, 163-73.
- MORGAN, E., MACE, O. J. A., J. & KELLETT, G. 2007. Apical GLUT2 and Cav1.3: regulation of rat intestinal glucose and calcium absorption. *J Physiol* 580, 593-604.
- MUECKLER, M., CARUSO, C., BALDWIN, S. A., PANICO, M., BLENCH, I., MORRIS, H. R., ALLARD, W. J., LIENHARD, G. E. & LODISH, H. F. 1985. Sequence and structure of a human glucose transporter. *Science*, 229, 941-5.
- MUECKLER, M. & THORENS, B. 2013. The SLC2 (GLUT) family of membrane transporters. *Mol Aspects Med*, 34, 121-38.
- MURAKI, I., IMAMURA, F., MANSON, J. E., HU, F. B., WILLETT, W. C., VAN DAM, R. M. & SUN, Q. 2013. Fruit consumption and risk of type 2 diabetes: results from three prospective longitudinal cohort studies. *Bmj*, 347, f5001.
- MUROTA, K., MATSUDA, N., KASHINO, Y., FUJIKURA, Y., NAKAMURA, T., KATO, Y., SHIMIZU, R., OKUYAMA, S., TANAKA, H., KODA, T., SEKIDO, K. & TERAOKA, J. 2010. alpha-Oligoglucosylation of a sugar moiety enhances the bioavailability of quercetin glucosides in humans. *Arch Biochem Biophys*, 501, 91-7.
- NANTZ, M. P., ROWE, C. A., BUKOWSKI, J. F. & PERCIVAL, S. S. 2009. Standardized capsule of *Camellia sinensis* lowers cardiovascular risk factors in a randomized, double-blind, placebo-controlled study. *Nutrition*, 25, 147-54.
- NELSON, D. & COX, M. 2008. *Lehninger Principles of Biochemistry*, New York, NY, Freeman and Company.
- NGUYEN, S., CHOI, H. K., LUSTIG, R. H. & HSU, C. Y. 2009. Sugar-sweetened beverages, serum uric acid, and blood pressure in adolescents. *J Pediatr*, 154, 807-13.
- NICHOLS, M., TOWNSEND, N., SCARBOROUGH, P. & RAYNER, M. 2014. Cardiovascular disease in Europe 2014: epidemiological update. *Eur Heart J*, 35, 2950-9.
- NIELSEN, S. J. & POPKIN, B. M. 2004. Changes in beverage intake between 1977 and 2001. *Am J Prev Med*, 27, 205-10.
- NISHIMURA, H., PALLARDO, F. V., SEIDNER, G. A., VANNUCCI, S., SIMPSON, I. A. & BIRNBAUM, M. J. 1993. Kinetics of GLUT1 and GLUT4

- glucose transporters expressed in *Xenopus* oocytes. *J Biol Chem*, 268, 8514-20.
- NOBIGROT, T., CHASALOW, F. I. & LIFSHITZ, F. 1997. Carbohydrate absorption from one serving of fruit juice in young children: age and carbohydrate composition effects. *J Am Coll Nutr*, 16, 152-8.
- NYAMBE-SILAVWE, H., VILLA-RODRIGUEZ, J., ILFIE, I., HOLMES, M., AYDIN, E., JENSEN, J. & WILLIAMSON, G. 2015. Inhibition of human α -amylase by dietary polyphenols. *J Funct Foods*, 19, 723-732.
- NYAMBE-SILAVWE, H. & WILLIAMSON, G. 2016. Polyphenol- and fibre-rich dried fruits with green tea attenuate starch-derived postprandial blood glucose and insulin: a randomised, controlled, single-blind, cross-over intervention. *Br J Nutr*, 116, 443-50.
- NYAMBE, H. 2016. *Effects of carbohydrase inhibiting polyphenols on glycaemic response in vivo*. PhD thesis, University of Leeds.
- O'CONNELL, D., MRUK, K., ROCHELEAU, J. M. & KOBERTZ, W. R. 2011. *Xenopus laevis* oocytes infected with multi-drug-resistant bacteria: implications for electrical recordings. *J Gen Physiol*, 138, 271-7.
- OCHOA, M., LALLES, J. P., MALBERT, C. H. & VAL-LAILLET, D. 2015. Dietary sugars: their detection by the gut-brain axis and their peripheral and central effects in health and diseases. *Eur J Nutr*, 54, 1-24.
- PAFFENBARGER, R. O., E. 1996. *LifeFit: An Effective Exercise Program for Optimal Health and a Longer Life – part II*, Human Kinetics Publishers.
- PALMA-DURAN, S. A., VLASSOPOULOS, A., LEAN, M., GOVAN, L. & COMBET, E. 2017. Nutritional intervention and impact of polyphenol on glycohemoglobin (HbA1c) in non-diabetic and type 2 diabetic subjects: Systematic review and meta-analysis. *Crit Rev Food Sci Nutr*, 57, 975-986.
- PANDEY, K. B. & RIZVI, S. I. 2009. Plant polyphenols as dietary antioxidants in human health and disease. *Oxid Med Cell Longev*, 2, 270-8.
- PARK, Y. K. & YETLEY, E. A. 1993. Intakes and food sources of fructose in the United States. *Am J Clin Nutr*, 58, 737s-747s.
- PARMAR, H. S. & KAR, A. 2008. Medicinal values of fruit peels from *Citrus sinensis*, *Punica granatum*, and *Musa paradisiaca* with respect to alterations in tissue lipid peroxidation and serum concentration of glucose, insulin, and thyroid hormones. *J Med Food*, 11, 376-81.
- PEREZ-JIMENEZ, J., NEVEU, V., VOS, F. & SCALBERT, A. 2010. Identification of the 100 richest dietary sources of polyphenols: an application of the Phenol-Explorer database. *Eur J Clin Nutr*, 64 Suppl 3, S112-20.
- PIMENTEL, G., ZEMDEGS, J., THEORODO, J. & MOTA, J. 2009. Does long-term coffee intake reduce type 2 diabetes mellitus risk? *Diabetol Metab Syndr*, 1.
- POPKIN, B. M. & NIELSEN, S. J. 2003. The sweetening of the world's diet. *Obes Res*, 11, 1325-32.
- RAO, S. S., ATTALURI, A., ANDERSON, L. & STUMBO, P. 2007. Ability of the normal human small intestine to absorb fructose: evaluation by breath testing. *Clin Gastroenterol Hepatol*, 5, 959-63.
- REINICKE, K., SOTOMAYOR, P., CISTERNA, P., DELGADO, C., NUALART, F. & GODOY, A. 2012. Cellular distribution of Glut-1 and Glut-5 in benign and malignant human prostate tissue. *J Cell Biochem*, 113, 553-62.

- ROBBINS, R. J., LEONCZAK, J., JOHNSON, J. C., LI, J., KWIK-URIBE, C., PRIOR, R. L. & GU, L. 2009. Method performance and multi-laboratory assessment of a normal phase high pressure liquid chromatography-fluorescence detection method for the quantitation of flavanols and procyanidins in cocoa and chocolate containing samples. *J Chromatogr A*, 1216, 4831-40.
- ROBBINS, R. J., LEONCZAK, J., LI, J., JOHNSON, J. C., COLLINS, T., KWIK-URIBE, C. & SCHMITZ, H. H. 2012. Determination of flavanol and procyanidin (by degree of polymerization 1-10) content of chocolate, cocoa liquors, powder(s), and cocoa flavanol extracts by normal phase high-performance liquid chromatography: collaborative study. *J AOAC Int*, 95, 1153-60.
- RODER, P. V., GEILLINGER, K. E., ZIETEK, T. S., THORENS, B., KOEPESELL, H. & DANIEL, H. 2014. The role of SGLT1 and GLUT2 in intestinal glucose transport and sensing. *PLoS One*, 9, e89977.
- RODRIGUEZ-MATEOS, A., VAUZOUR, D., KRUEGER, C. G., SHANMUGANAYAGAM, D., REED, J., CALANI, L., MENA, P., DEL RIO, D. & CROZIER, A. 2014. Bioavailability, bioactivity and impact on health of dietary flavonoids and related compounds: an update. *Arch Toxicol*, 88, 1803-53.
- RUDD, P. M. & DWEK, R. A. 1997. Glycosylation: heterogeneity and the 3D structure of proteins. *Crit Rev Biochem Mol Biol*, 32, 1-100.
- SALAS-BURGOS, A., ISEROVICH, P., ZUNIGA, F., VERA, J. C. & FISCHBARG, J. 2004. Predicting the three-dimensional structure of the human facilitative glucose transporter glut1 by a novel evolutionary homology strategy: insights on the molecular mechanism of substrate migration, and binding sites for glucose and inhibitory molecules. *Biophys J*, 87, 2990-9.
- SAMBROOK, J. & RUSSELL, D. 2001. *Molecular Cloning a Laboratory Manual*, New York, Cold Spring Harbor Laboratory Press.
- SAMBUY, Y., DE ANGELIS, I., RANALDI, G., SCARINO, M. L., STAMMATI, A. & ZUCCO, F. 2005. The Caco-2 cell line as a model of the intestinal barrier: influence of cell and culture-related factors on Caco-2 cell functional characteristics. *Cell Biol Toxicol*, 21, 1-26.
- SAMUEL, V. T. & SHULMAN, G. I. 2012. Mechanisms for insulin resistance: common threads and missing links. *Cell*, 148, 852-71.
- SCALBERT, A., MANACH, C., MORAND, C., REMESY, C. & JIMENEZ, L. 2005. Dietary polyphenols and the prevention of diseases. *Crit Rev Food Sci Nutr*, 45, 287-306.
- SCALBERT, A., MORAND, C., MANACH, C. & REMESY, C. 2002. Absorption and metabolism of polyphenols in the gut and impact on health. *Biomed Pharmacother*, 56, 276-82.
- SCALBERT, A. & WILLIAMSON, G. 2000. Dietary intake and bioavailability of polyphenols. *J Nutr*, 130, 2073S-85S.
- SCHEEPERS, A., SCHMIDT, S., MANOLESCU, A., CHEESEMAN, C. I., BELL, A., ZAHN, C., JOOST, H. G. & SCHURMANN, A. 2005. Characterization of the human SLC2A11 (GLUT11) gene: alternative promoter usage, function, expression, and subcellular distribution of three isoforms, and lack of mouse orthologue. *Mol Membr Biol*, 22, 339-51.

- SCHULZE, M. B., MANSON, J. E., LUDWIG, D. S., COLDITZ, G. A., STAMPFER, M. J., WILLETT, W. C. & HU, F. B. 2004. Sugar-sweetened beverages, weight gain, and incidence of type 2 diabetes in young and middle-aged women. *Jama*, 292, 927-34.
- SHI, Y. & WILLIAMSON, G. 2016. Quercetin lowers plasma uric acid in pre-hyperuricaemic males: a randomised, double-blinded, placebo-controlled, cross-over trial. *Br J Nutr*, 115, 800-6.
- SHRESTHA, S., EHLERS, S. J., LEE, J. Y., FERNANDEZ, M. L. & KOO, S. I. 2009. Dietary green tea extract lowers plasma and hepatic triglycerides and decreases the expression of sterol regulatory element-binding protein-1c mRNA and its responsive genes in fructose-fed, ovariectomized rats. *J Nutr*, 139, 640-5.
- SHRIME, M. G., BAUER, S. R., MCDONALD, A. C., CHOWDHURY, N. H., COLTART, C. E. & DING, E. L. 2011. Flavonoid-rich cocoa consumption affects multiple cardiovascular risk factors in a meta-analysis of short-term studies. *J Nutr*, 141, 1982-8.
- SLAVIC, K., DERBYSHIRE, E. T., NAFTALIN, R. J., KRISHNA, S. & STAINES, H. M. 2009. Comparison of effects of green tea catechins on apicomplexan hexose transporters and mammalian orthologues. *Mol Biochem Parasitol*, 168, 113-116.
- SMITH, E. & COLLINS, I. 2015. Photoaffinity labeling in target- and binding-site identification. *Future Med Chem*, 7, 159-83.
- SONG, J., KWON, O., CHEN, S., DARUWALA, R., ECK, P., PARK, J. B. & LEVINE, M. 2002. Flavonoid inhibition of sodium-dependent vitamin C transporter 1 (SVCT1) and glucose transporter isoform 2 (GLUT2), intestinal transporters for vitamin C and Glucose. *J Biol Chem*, 277, 15252-60.
- SPENCER, J. P., ABD EL MOHSEN, M. M., MINIHANE, A. M. & MATHERS, J. C. 2008. Biomarkers of the intake of dietary polyphenols: strengths, limitations and application in nutrition research. *Br J Nutr*, 99, 12-22.
- STANHOPE, K. L., SCHWARZ, J. M., KEIM, N. L., GRIFFEN, S. C., BREMER, A. A., GRAHAM, J. L., HATCHER, B., COX, C. L., DYACHENKO, A., ZHANG, W., MCGAHAN, J. P., SEIBERT, A., KRAUSS, R. M., CHIU, S., SCHAEFER, E. J., AI, M., OTOKOZAWA, S., NAKAJIMA, K., NAKANO, T., BEYSEN, C., HELLERSTEIN, M. K., BERGLUND, L. & HAVEL, P. J. 2009. Consuming fructose-sweetened, not glucose-sweetened, beverages increases visceral adiposity and lipids and decreases insulin sensitivity in overweight/obese humans. *J Clin Invest*, 119, 1322-34.
- STROBEL, P., ALLARD, C., PEREZ-ACLE, T., CALDERON, R., ALDUNATE, R. & LEIGHTON, F. 2005. Myricetin, quercetin and catechin-gallate inhibit glucose uptake in isolated rat adipocytes. *Biochem J*, 386, 471-8.
- STUART, C. A., HOWELL, M. E. & YIN, D. 2007. Overexpression of GLUT5 in diabetic muscle is reversed by pioglitazone. *Diabetes Care*, 30, 925-31.
- SUGIMOTO, K., HOSOTANI, T., KAWASAKI, T., NAKAGAWA, K., HAYASHI, S., NAKANO, Y., HIROSHI INUI, H. & YAMANOUCHI, T. 2010. Eucalyptus Leaf Extract Suppresses the Postprandial Elevation of Portal, Cardiac and Peripheral Fructose Concentrations after Sucrose Ingestion in Rats. *J Clin Biochem Nutr*, 46, 205-211.

- SUGIMOTO, K., SUZUKI, J., NAKAGAWA, K., HAYASHI, S., ENOMOTO, T., FUJITA, T., YAMAJI, R., INUI, H. & NAKANO, Y. 2005. Eucalyptus leaf extract inhibits intestinal fructose absorption, and suppresses adiposity due to dietary sucrose in rats. *Br J Nutr*, 93, 957-63.
- SUN, S. Z. & EMPIE, M. W. 2012a. Fructose metabolism in humans - what isotopic tracer studies tell us. *Nutr Metab (Lond)*, 9, 89.
- SUN, S. Z. & EMPIE, M. W. 2012b. Fructose metabolism in humans – what isotopic tracer studies tell us. *Nutr Metab (Lond)*, 9.
- TAGUCHI, C., FUKUSHIMA, Y., KISHIMOTO, Y., SUZUKI-SUGIHARA, N., SAITA, E., TAKAHASHI, Y. & KONDO, K. 2015. Estimated Dietary Polyphenol Intake and Major Food and Beverage Sources among Elderly Japanese. *Nutrients*, 7, 10269-81.
- TANASOVA, M., PLUTSCHACK, M., MUROSKI, M. E., STURLA, S. J., STROUSE, G. F. & MCQUADE, D. T. 2013. Fluorescent THF-based fructose analogue exhibits fructose-dependent uptake. *Chembiochem*, 14, 1263-70.
- TATIBOUET, A., YANG, J., MORIN, C. & HOLMAN, G. D. 2000. Synthesis and evaluation of fructose analogues as inhibitors of the D-fructose transporter GLUT5. *Bioorg Med Chem*, 8, 1825-33.
- TEFF, K. L., ELLIOTT, S. S., TSCHOP, M., KIEFFER, T. J., RADER, D., HEIMAN, M., TOWNSEND, R. R., KEIM, N. L., D'ALESSIO, D. & HAVEL, P. J. 2004. Dietary fructose reduces circulating insulin and leptin, attenuates postprandial suppression of ghrelin, and increases triglycerides in women. *J Clin Endocrinol Metab*, 89, 2963-72.
- THOMPSON, A., IANCU, C., NGUYEN, T., KIM, D. & CHOE, J. 2015. Inhibition of human GLUT1 and GLUT5 by plant carbohydrate products; insights into transport specificity. *Sci Rep*, 5.
- THOMPSON, A., URSU, O., BABKIN, P., IANCU, C., WHANG, A., OPREA, T. & CHOEB, J. 2016. Discovery of a specific inhibitor of human GLUT5 by virtual screening and in vitro transport evaluation. *Sci Rep*, 6.
- THORENS, B. 2001. GLUT2 in pancreatic and extra-pancreatic gluco-detection (review). *Mol Membr Biol*, 18, 265-73.
- THORENS, B. & MUECKLER, M. 2010. Glucose transporters in the 21st Century. *Am J Physiol Endocrinol Metab*, 298, E141-5.
- THORSEN, K., DRENGSTIG, T. & RUOFF, P. 2014. Transepithelial glucose transport and Na⁺/K⁺ homeostasis in enterocytes: an integrative model. *Am J Physiol Cell Physiol*, 307, C320-37.
- THREAPLETON, D. E., GREENWOOD, D. C., BURLEY, V. J., ALDWAIRJI, M. & CADE, J. E. 2013. Dietary fibre and cardiovascular disease mortality in the UK Women's Cohort Study. *Eur J Epidemiol*, 28, 335-46.
- TOBIN, V., LE GALL, M., FIORAMONTI, X., STOLARCZYK, E., BLAZQUEZ, A. G., KLEIN, C., PRIGENT, M., SERRADAS, P., CUIF, M. H., MAGNAN, C., LETURQUE, A. & BROT-LAROCHE, E. 2008. Insulin internalizes GLUT2 in the enterocytes of healthy but not insulin-resistant mice. *Diabetes*, 57, 555-62.
- TODA, M., KAWABATA, J. & KASAI, T. 2001. Inhibitory effects of ellagi- and gallotannins on rat intestinal alpha-glucosidase complexes. *Biosci Biotechnol Biochem*, 65, 542-7.

- TORRES, P., POVEDA, A., JIMENEZ-BARBERO, J., PARRA, J. L., COMELLES, F., BALLESTEROS, A. O. & PLOU, F. 2011. Enzymatic synthesis of α -glucosides of resveratrol with surfactant activity. *Adv Synth Catal*, 1077-1086.
- TROMBETTA, E. S. 2003. The contribution of N-glycans and their processing in the endoplasmic reticulum to glycoprotein biosynthesis. *Glycobiology*, 13, 77r-91r.
- TSAO, R. 2010. Chemistry and biochemistry of dietary polyphenols. *Nutrients*, 2, 1231-46.
- TURCO, L., CATONE, T., CALONI, F., DI CONSIGLIO, E., TESTAI, E. & STAMMATI, A. 2011. Caco-2/TC7 cell line characterization for intestinal absorption: how reliable is this in vitro model for the prediction of the oral dose fraction absorbed in human? *Toxicol In Vitro*, 25, 13-20.
- ULDRY, M., IBBERSON, M., HOSOKAWA, M. & THORENS, B. 2002. GLUT2 is a high affinity glucosamine transporter. *FEBS Lett*, 524, 199-203.
- ULDRY, M. & THORENS, B. 2004. The SLC2 family of facilitated hexose and polyol transporters. *Pflugers Arch*, 447, 480-9.
- UNAL, B., CRITCHLEY, J. A. & CAPEWELL, S. 2004. Explaining the decline in coronary heart disease mortality in England and Wales between 1981 and 2000. *Circulation*, 109, 1101-7.
- VAN DAM, R. M. & FESKENS, E. J. 2002. Coffee consumption and risk of type 2 diabetes mellitus. *Lancet*, 360, 1477-8.
- VARKI, A., CUMMINGS, R. D., ESKO, J. D., FREEZE, H. H., STANLEY, P., BERTOZZI, C. R., HART, G. W. & ETZLER, M. E. 2009. *Essentials of Glycobiology*, Cold Spring Harbor, NY, Cold Spring Harbor Laboratory Press.
- VENDRAME, S., GUGLIELMETTI, S., RISO, P., ARIOLI, S., KLIMIS-ZACAS, D. & PORRINI, M. 2011. Six-week consumption of a wild blueberry powder drink increases bifidobacteria in the human gut. *J Agric Food Chem*, 59, 12815-20.
- VILLA-RODRIGUEZ, J., AYDIN, E., GAUER, J. S., PYNER, P., WILLIAMSON, G. & KERIMI, A. 2017a. Green tea and chamomile teas, but not acarbose, attenuate glucose and fructose transport via inhibition of GLUT2 and GLUT5. *Mol Nutr Food Res*, Accepted
- VILLA-RODRIGUEZ, J. A., AYDIN, E., GAUER, J. S., PYNER, A., WILLIAMSON, G. & KERIMI, A. 2017b. Green and Chamomile Teas, but not Acarbose, Attenuate Glucose and Fructose Transport via Inhibition of GLUT2 and GLUT5. *Mol Nutr Food Res*.
- VIUDA-MARTOS, M., FERNANDEZ-LOPEZ, J. & PEREZ-ALVAREZ, J. A. 2010. Pomegranate and its Many Functional Components as Related to Human Health: A Review. *Comprehensive Reviews in Food Science and Food Safety*, 9, 635-654.
- VOZZO, R., BAKER, B., WITTERT, G. A., WISHART, J. M., MORRIS, H., HOROWITZ, M. & CHAPMAN, I. 2002. Glycemic, hormone, and appetite responses to monosaccharide ingestion in patients with type 2 diabetes. *Metabolism*, 51, 949-57.
- WELSH, J. A., SHARMA, A. J., GRELLINGER, L. & VOS, M. B. 2011. Consumption of added sugars is decreasing in the United States. *Am J Clin Nutr*, 94, 726-34.

- WILDER-SMITH, C., LI, X., HO, S., LEONG, S. M., WONG, R. K., KOAY, E. & FERRARIS, R. P. 2014. Fructose transporters GLUT5 and GLUT2 expression in adult patients with fructose intolerance. *United European Gastroenterol J.*, 2, 14-21.
- WILLIAMSON, G. 2013. Possible effects of dietary polyphenols on sugar absorption and digestion. *Mol Nutr Food Res*, 57, 48-57.
- WILLIAMSON, G. & MANACH, C. 2005. Bioavailability and bioefficacy of polyphenols in humans. II. Review of 93 intervention studies. *Am J Clin Nutr*, 81, 243S-255S.
- WOLEVER, T. M., JENKINS, D. J., JENKINS, A. L. & JOSSE, R. G. 1991. The glycemic index: methodology and clinical implications. *Am J Clin Nutr*, 54, 846-54.
- WOOD, D. A., KOTSEVA, K., CONNOLLY, S., JENNINGS, C., MEAD, A., JONES, J., HOLDEN, A., DE BACQUER, D., COLLIER, T., DE BACKER, G. & FAERGEMAN, O. 2008. Nurse-coordinated multidisciplinary, family-based cardiovascular disease prevention programme (EUROACTION) for patients with coronary heart disease and asymptomatic individuals at high risk of cardiovascular disease: a paired, cluster-randomised controlled trial. *Lancet*, 371, 1999-2012.
- WORMALD, M. R., PETRESCU, A. J., PAO, Y. L., GLITHERO, A., ELLIOTT, T. & DWEK, R. A. 2002. Conformational studies of oligosaccharides and glycopeptides: complementarity of NMR, X-ray crystallography, and molecular modelling. *Chem Rev*, 102, 371-86.
- WRIGHT, E. M., HIRAYAMA, B. A. & LOO, D. F. 2007. Active sugar transport in health and disease. *J Intern Med*, 261, 32-43.
- XU, M., HU, J., ZHAO, W., GAO, X., JIANG, C., LIU, K., LIU, B. & HUANG, F. 2014. Quercetin differently regulates insulin-mediated glucose transporter 4 translocation under basal and inflammatory conditions in adipocytes. *Mol Nutr Food Res*, 58, 931-41.
- YANG, J., DOWDEN, J., TATIBOUET, A., HATANAKA, Y. & HOLMAN, G. D. 2002. Development of high-affinity ligands and photoaffinity labels for the D-fructose transporter GLUT5. *Biochem J*, 367, 533-9.
- ZEMESTANI, M., RAFRAF, M. & ASGHARI-JAFARABADI, M. 2016. Chamomile tea improves glycemic indices and antioxidants status in patients with type 2 diabetes mellitus. *Nutrition*, 32, 66-72.
- ZEYMER, U. 2006. Cardiovascular benefits of acarbose in impaired glucose tolerance and type 2 diabetes. *I J Cardiol*, 107, 11-20.
- ZHENG, X. X., XU, Y. L., LI, S. H., HUI, R., WU, Y. J. & HUANG, X. H. 2013. Effects of green tea catechins with or without caffeine on glycemic control in adults: a meta-analysis of randomized controlled trials. *Am J Clin Nutr*, 97, 750-62.
- ZIEGLER, K., KERIMI, A., POQUET, L. & WILLIAMSON, G. 2016. Butyric acid increases transepithelial transport of ferulic acid through upregulation of the monocarboxylate transporters SLC16A1 (MCT1) and SLC16A3 (MCT4). *Arch Biochem Biophys*, 599, 3-12.

Appendix A pBF plasmid sequence

```
1 cggctacaattaatacataaccttatgtatcatcacatagcattttaggtgacaactataaataacaagcttgcttgtctttttgagaagctcagaataaacgctcaactttggcagggatccgggccccggg
135 ttaactagcctagaattcatcgatatccatggctogacgagctcogagatctgcagctggtaaccggttaccactaaaccagcctcaagaacaccggaaatggagctcttaagctacataataccaacttacacttta
269 caaaatgtgtgtcccccaaatgtagccattcgtatctgctcctaataaaaaagaaagtcttcttcacattctaaaaaaaaaaaaaaaaaaaaaaaaaaaaaaaaaaaaaaaaaaaaaaaaaaaaaaaaaaaa
403 aaaaaaaaaaaaaaaaaaaaaaaaaaaaaaaaaaaaaaaaaaaaaaaaaaaaaaaaaaaaaaaaaaaaaaaaaaaaaaaaaaaaaaaaaaaaaaaaaaaaaaaaaaaaaaaaaaaaaaaaaaaaaaaaaaaaa
537 ctgaatggcgaatggcgcgacgcccctgtagcggcgcattaagcgcggcgggtgtggtggttacgcgcagcgtgacccgtacacttgccagcgcctagcggccgctcctttcgctttctcccttcccttct
671 cgccacgttcgcccgtttcccccgtcaagctcctaaatcgggggctcccttttaggggttccgatttagtgctttacggcacctcgacccccaaaaaacttgattagggatgaggttccagtagtggccatcgccct
805 gatagacgggtttttcgccctttgacgttggagtcacagcttcttaaatagtggaactcttgttccaaactggaaacaactcaaccctatctcoggtctattcttttgattataagggattttgcgatttcggcc
939 tattggttaaaaaatgagctgatttaacaaaaatttaacgogaattttaacaaaaatattaacgtttacaatttcccaggtggcacttttcggggaaatgtgcgaggaaacccctatttggttattttctaaata
1073 cattcaaatatgtatccgctcatgagacaataaacctgataaatgcttcaataatattgaaaaaggaagatgatgagatattcaacatttccgtgtcgccttattcccttttttggggcattttgccttccgtgt
1207 ttttgcaccagaaacgctggtgaaagttaaagatgctgaagatcagttgggtgcacgagtggtttacatcgaactggatctcaacagcggtaagatccttgagagttttcgccccgaagaacgttttccaa
1341 tgatgagcacttttaagttctgctatgtggcgcggtattatcccgtattgacgcccggcaagagcaactcoggtcgcgcacatacactattctcagaatgacttggttgagtaactcaccagtcacagaaaagcat
1475 cttacggatggcatgacagtaagagaattatgcagtgctgccataaccatgagtgataaacactgcggcacaacttacttctgacaacgatcggaggaccgaaggagctaaccgctttttgcaacaactggggga
1609 tcatgtaactcgccttgatcggttgggaaccggagctgaatgaagccataccaaaacgacgagcgtgacaccacgatgcctgtagcaatggcaacaacgttgccgaaactattaactggcgaactacttactctag
1743 cttcccggcaacaattaatagactggatggaggcggataaagtgcaggaccacttctgcgctcggcccttccggctgggtggtttattgctgataaaactggagccgggtgagcgtgggtctcggggtatcatt
1877 gcagcactggggccagatggtaagccctcccgtatcgtagttatctacacgacggggagtcaggcaactatggatgaacgaaatagacagatcgctgagataggtgcctcactgattaagcatggtaactgtc
2011 agaccaagtttactcatatatacttttagattgatttaaaacttcaatttttaaaaggatctaggtgaagatcctttttgataatctcatgacaaaaatcccttaacgtgagtttctgttccactgagcgt
2145 cagaccccgtagaaaagatcaaaggatcttcttgagatccttttttctgcgctaactctgctgcttgcaaaaaaaaccacgctaccagcgggtggtttgtttgcccggatcaagagctaccaactcctttt
2279 ccgaaggtaactggcttcagcagagcgcagataccaaatactgtccttctagtgtagccgtagtttagggccaccactcaagaactctgtagcaccgcctacatacctcgtctgctaatcctgttaccagtggc
2413 tgctgccagtgccgataaagtctgtcttaccgggttggactcaagacgatagttaccggataaggcgcagcgggtcgggctgaacggggggttcgtgcacacagcccagcttggagcgaacgacctacaccgaac
2547 tgagatacctacagcgtgagctatgagaaaagcgcacgcttcccgaaggagaaaaggcggacaggtatccggtaagcggcagggctcggaaacaggagagcgcacgagggagcttccagggggaacgcctggtat
2681 ctttatagtcctgtcgggtttcggccactctgacttgagcgtcgatttttgtgatgctcgtcaggggggggagcctatggaaaaacgacgcaacgcggcctttttacgggttctcggccttttgccttgcctt
2815 tgctcacatgttcttctcgtggttatcccctgattctgtggataaccgtattaccgctttgagtgagctgataccgctcgcgcgacggaaacgacccgagcgcagcagctcagtgagcagggaagcgggaagagc
2949 gcccaatacgaacccgctctccccgcgcttggccgattcattaatgcagccg
```

XbaI restriction site PolyA tail SP6 promoter

Appendix C GLUT2pBF sequence

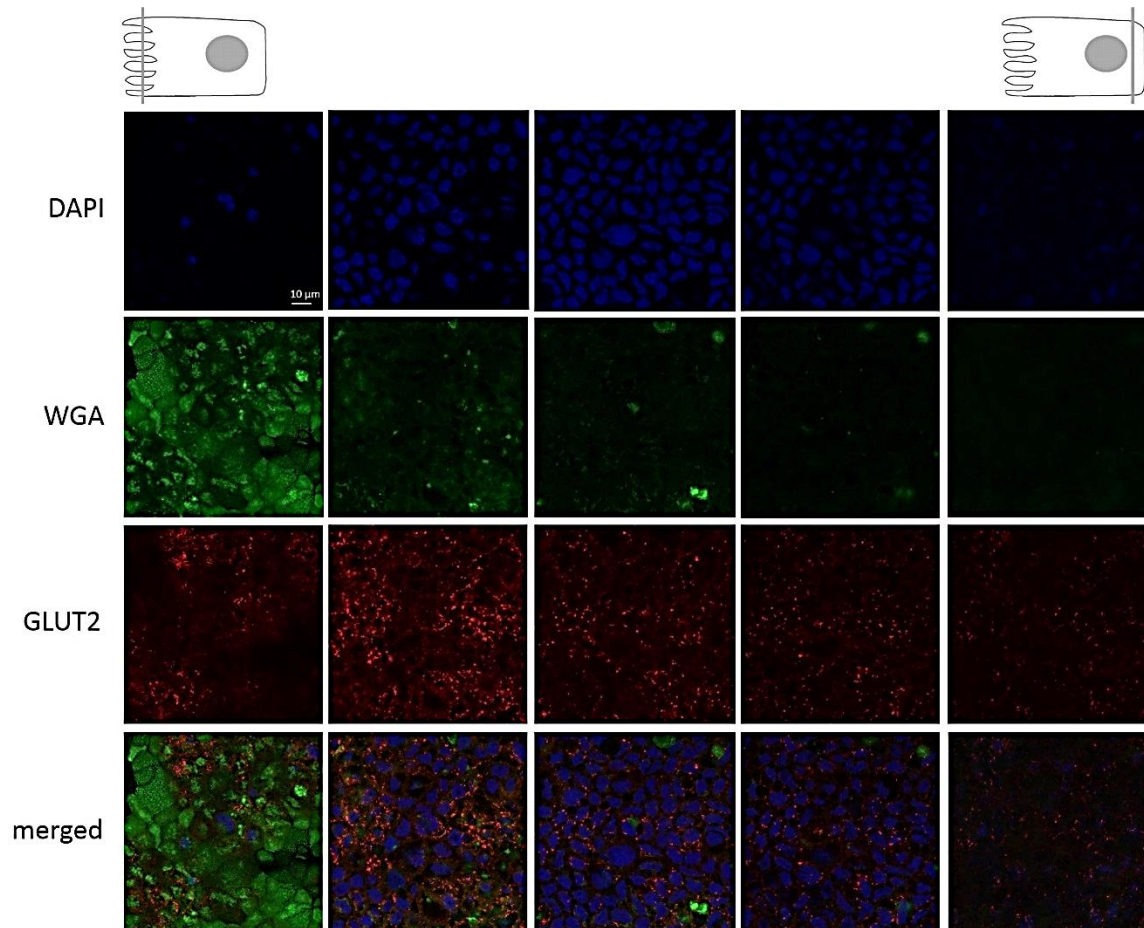
```

1 Cggctacaattaatacacaaccttatgtatcacacacacacgctttaggggagcactatgaataacaagcttgctgttctttttgcagaagctcagaataaacgctcaactttggcagggatccggggc
130 cgggttaactagtcCCACTGCTTACTGGCTTATCGAAATTAATACGACTCACTATAGGGAGACCCAAGCTGGCTAGTTAAGCTATCAACAAGTTTGTACAAAAAGCAGGCTCCGCGGCCGCCCTT
259 CACCATGACAGAAGATAAAGGTCACCTGGGACCCCTGGTTTTCTACTGTCTACTGCTGTGCTGGGTTCCCTCCAGTTTGGATATGACATTGGTGTGATCAATGCACCTCAACAGGTAATAATCTCACA
388 TAGACATGTTTTGGGTGTTCCACTGGATGACCGAAAAGCTATCAACAATGTTTCAACAGTACAGATGAAGTCCCAACAATCTCATACTCAATGAACCCAAAACCAACCCCTTGGGCTGAGGAAGA
517 GACTGTGGCAGCTGCTCAACTAATCACCATGCTCTGGTCCCTGTCTGTATCCAGCTTTCAGTGTGGTGAATGACTGCAITCATTCTTTGGTGGGTGGCTTGGGGACACACTTGGAAAGAAATCAAAGCCAT
646 GITAGTAGCAAACTTCTGTCAATTAGTTGGAGCTCTCTGTATGGGGTTTTCAAATTTGGGACCACTCTCATATACTTATAATTGCTGGAAGAAGCATATCAGGACTATATTGTGGGCTAATTTCAGGCCT
775 GGTTCCTATGTATATCGGTGAAATTGTCCAAACCCCTCTCAGGGGAGCAGCTTGGCAGCTTTTCAICAGCTGGCCATCGTCACGGGCATTCTTATTAGTCAGATTATTGGTCTTGAATTTATCTTGGGC
904 TTATGATCTGTGGCACAATCCTGCTTGGCCGTCTGGTGTGGCAGCCATCCTTCAGTCTCTGCTACTCTTTTTCTGTCCAGAAAAGCCCCAGATACCTTTACATCAAGTTAGATGAGGAAGTCAAAAGCAA
1033 ACAAAGCTTGAAGAAGCTCAGAGGATATGATGATGTCACCAAGATATTAATGAAATGAGAAAAAGAAAGAGAAGAAGCATCGAGTGAAGCAGAAAAGTCTCTATAATTGAGCTCTTCAACCAATTCAGCTA
1162 CCGACAGCCCTATTCTAGTGGCAGTGTCTGATGCTGGCTCAGCAATTTCCGGAATCAATGGCATTTTTACTACTCAACCAAGCATTTTTTCAGACGGCTGGTATCAGCAAACTGTTTATGCAACCAT
1291 TGGAGTTGGCGCTGTAACATGGTTTTCTACTGCTGTCTGTATTCTTGTGGAGAAGGCAGGGCGCAGCTTCTCTCTTCAATTGGAATGAGTGGGATGTTGTTTGTGCCATCTTCAITGTCAGTGGG
1420 ACTTGTGCTGCTGAATAAGTTCTCTTGGATGAGTTATGTGAGCATGATAGCCATCTTCTCTTGTGCTGCTTCTTGAATTTGGGCCAGGCCGATCCCTGGTTCATGGTGGCTGAGTTTTCTGAGTCA
1549 AGGACCACGCTCTGCTGCTTTAGCAATAGCTGCAATTCAGCAATTTGACCTGCAATTTCAITGTAGCTCTGTGTTCCAGTACATTGCGGACTTCTGTGGACCTTATGTGTTTTCTCTTGTCTGGAGT
1678 GCTCCTGGCCTTACCCTGTTACATTTTTTAAAGTCCAGAAAACCAAGGAAAGTCTTTTGGAGAAATGCTGAGAAATCCAAAAGAAAGAGTGGCTCAGCCCACAGGCCAAAAGCTGCTGTAGAAAT
1807 GAAATTCCTAGGAGCTACAGAGACTGTGTAAGGGTGGGCGCGCCGACCCAGCTTTCTTGTACAAGTGGTTGATCTAGAGGGGGCCGCGGTTCAAGGTAAGCCTATCCCTAACCCCTCTCCTCGTCTCG
1936 ATTCTACGCGTACCGGTTAGTAATGAGTTTAAACGGGGAGGCTAACTGAAACACGGAAGGAGCAATACCGGAAGGAACTGATAGAATTTCATCGATtccatggctgcagcagctcgagatctgcag
2065 ctggtaccggttaccactaaaccagcctcaagaacaccggaatggagctctctaagctacataataaccaacttacactttacaanaatggttcccccaaaaatgtagccattcgtatctgctcctaataaaa
2194 aagaaagtcttctcacattctaaaaaaaaaaaaaaaaaaaaaaaaaaaaaaaaaaaaaaaaaaaaaaaaaaaaaaaaaaaaaaaaaaaaaaaaaaaaaaaaaaaaaaaaaaaaaaaaaaaaaaaaaaaaa
2323 aaaaaaaaaaaaaaaaaaaaaaacgctttagcgtccctggcgtaatagcgaagaggccgcaccgctgccttcccaacagttgcgcagcctgaatggcgaatggcgcgacgcgcctgtagcggcga
2452 ttaagcgcggcgggtgtggtggttacgcgcagcgtgaccgctacacttgcagcgccttagcgcgcctcctttogcttcttcccttcccttctcgccacgcttgcgggcttccccgctcaagctcta
2581 aatcgggggctccctttagggttccgatttagtgctttagcgcacctcgacccccaaaaaacttgattaggggtgatggttcaagtagtgggcatcgccctgatagacggttttccgoccttgacgcttg
2710 gagtccaagcttcttaaatagtgactcttgttccaaactggaacaacactcaaccctatctcgttctattcttttgattataagggatgttgcgacttccggcctattggttaaaaaatgagctgatt
2839 taacaaaaatttaacgcgaatttaacaaaaatataacgtttacaatttcccaggtggcacttttccgggaaatgtgcgcggaaccctatttgtttattttctaaatacattcaaatatgtatccgc
2968 tcatgagacaataaccctgataaatgcttcaataatattgaaaaaggaagatgatgattcaacatttccggtgcgccttattcccttttttgcggcatttgccttctggttttggctcaccag
3097 aacgcgtggtgaaagttaaagatgctgaagatcagttgggtgcaagagtggttacaatcgaactggatctcaacagcggtaagatccttgagagtttgcgcccgaagaacgttttcaatgatgagca
3226 cttttaaagtctctgctatgtggcgcggtattatcccgatttagcgcgggcaagagcaactcggctgcgcgcatataactattctcagaatgacttgggtgagtaactcaccagctcacagaaaaatcctta
3355 cggatggcatgacagtaagagaattatgcatgctgccaataaccatgagtgataaacactgcccgaacttacttctgacaacgatcggaggaccgaaggagctaacccgctttttgcaacaatggggg
3484 atcatgtaactcgccttgatcgttgggaaccggagctgaatgaagccataccaaacgcagcagcgtgacaccaagatgctgtagcaatggcaacaacgttgcgcaaacatttaactggcgaactactta
3613 ctctagcttcccggcaacaataatagactggatggagcgggataaagttgacaggaccacttctgcgctcggcccttccggctggtggtttattgctgataaatctggagccggtgagcgtgggtctc
3742 gcggtatcattgcagcactggggccagatggtaagccctcccgtatcgtagttatctacacgacggggagtcaggcaactatggatgaacgaaatagacagatcgctgagataggtgcctcactgatta
3871 agcattggttaactgtcagaccaagtttactcatatatacttttagattgatttaaaacttcaattttaatttaaaaggatctaggtgaaagatccttttgataatctcatgaccaaaatcccttaacgtg
4000 agtttctgcttccactgagcgtcagaccccgtagaaaagatcaaaagatcttcttgagatcctttttctgcgctaatctgctgcttgcgaacaaaaaaaccacccgctaccagcgggtggtttgttgc
4129 cggatcaagagctaccaactcttttccgaaggttaactggctcagcagagcgcagataccaaatactgctcctctagtgctgctggttaggttaggccaccacttcaagaactctgtagcaacgctacat
4258 accctcctctgtaaatcctgttaaccagtggtgctgccaagtggtgctgcttcaacgggttggactcaagcagatagttaccggataaaggcgcagcggctcgggctgaacggggggtctgtgca
4387 cacagcccagcttggagcgaacgacctacaccgaactgagatacctacagcgtgagctatgagaaagcgcacgcttccggaaggagaaaggcggacaggtatccggttagcggcagggtcggaaacag
4516 gagagcgcagagggagcttccagggggaacgcctggtatctttatagtcctgtcgggtttccgcccctctgacttgagcgtcgattttgtgatgctcgtcagggggggcggagcctatgaaaaaacg
4645 ccagcaacgcggccttttaccggttctctggccttttctgctcactgttcttctctgcttattccctgattctgtggataaacggtattaccgctttagtgagctgataaccgctcggc
4774 gcagccgaacgacccgagcgcagcagtcagtgagcgggaagcgggaagcggcccaatacgcgaacccgcttccccgcgcgcttggccgattcattaatgcagccg

```

PmlI restriction site PolyA tail GLUT2 gene SP6 promoter Forward and reverse primers

Appendix F Confocal images of GLUT2 with WGA



Appendix G Confocal images of GLUT7 with WGA

